Table of Contents

2.0 STRUCTURAL EVALUATION **2-1**

2.1 Structural Design 2.1-1
2.1.1 Discussion 2.1-1
2.1.1.1 Universal Transport Cask 2.1-1
2.1.1.2 Transportable Storage Canister 2.1-3
2.1.1.3 Fuel Basket 2.1-4
2.1.1.4 Impact Limiters 2.1-6
2.1.1.5 GTCC Waste Canister and Basket 2.1-6
2.1.2 Design Criteria 2.1-7
2.1.2.1 Codes and Standards 2.1-7
2.1.2.2 Exceptions to Codes and Standards 2.1-8
2.1.2.3 Load Combinations 2.1-9
2.1.2.4 Allowable Stress Limits - Ductile Failure 2.1-10
2.1.2.5 Miscellaneous Structural Failure Modes 2.1-18

2.2 Weights and Centers of Gravity 2.2-1

2.3 Mechanical Properties of Materials 2.3-1
2.3.1 Summary of Materials 2.3-1
2.3.2 Austenitic Stainless Steels 2.3-3
2.3.3 Precipitation-Hardened Stainless Steel 2.3-9
2.3.4 Carbon Steel 2.3-11
2.3.5 Bolting Materials 2.3-13
2.3.6 Aluminum Alloys 2.3-17
2.3.7 Shielding Material 2.3-19
2.3.8 Impact Limiter Materials 2.3-22

2.4 General Standards for All Packages 2.4-1
2.4.1 Minimum Package Size 2.4-1
2.4.2 Tamper-Indication Feature 2.4-1
2.4.3 Positive Closure 2.4-1

Table of Contents (Continued)

2.4.4 Chemical, Galvanic, or Other Reactions 2.4-2
2.4.4.1 Component Operating Environment 2.4-2
2.4.4.2 Component Material Categories 2.4-3
2.4.4.3 General Effects of Identified Reactions 2.4-7
2.4.4.4 Adequacy of Cask Operating Procedures 2.4-7
2.4.4.5 Effects of Reaction Products 2.4-7
2.4.5 Conformance to Cask Design Requirements 2.4-9
2.4.6 Continuous Venting 2.4-9

2.5 Lifting and Tiedown Standards 2.5-1
2.5.1 Lifting Devices 2.5-1
2.5.1.1 Lifting Trunnion Analysis 2.5-1
2.5.1.2 Cask Lid Lifting Analysis 2.5-30
2.5.2 Tiedown Devices 2.5-31
2.5.2.1 Tiedown Component Loading 2.5-32
2.5.2.2 Rear Support 2.5-42
2.5.2.3 Front Support 2.5-50
2.5.2.4 Overload 2.5-51

2.6 Normal Conditions of Transport 2.6-1
2.6.1 Heat 2.6-1
2.6.1.1 Summary of Pressures and Temperatures 2.6-3
2.6.1.2 Thermal Expansion Evaluation 2.6-3
2.6.1.3 Stress Calculations and Comparison to Allowable Stresses 2.6-4
2.6.2 Cold 2.6-14
2.6.2.1 Summary of Pressures and Temperatures 2.6-14
2.6.2.2 Thermal Expansion Evaluation 2.6-14
2.6.2.3 Stress Calculations and Comparison to Allowable Stresses 2.6-14
2.6.3 Reduced External Pressure 2.6-23
2.6.4 Increased External Pressure 2.6-23

Table of Contents (Continued)

2.6.5 Vibration 2.6-23
2.6.6 Water Spray 2.6-25
2.6.7 Free Drop (1-Foot): Cask Body Analysis 2.6-26
2.6.7.1 One-Foot End Drop 2.6-27
2.6.7.2 One-Foot Side Drop 2.6-40
2.6.7.3 One-Foot Corner Drop 2.6-47
2.6.7.4 One-Foot Oblique Drop 2.6-60
2.6.7.5 Impact Limiters 2.6-61
2.6.7.6 Closure Analysis 2.6-104
2.6.7.7 Neutron Shield Analysis 2.6-109
2.6.7.8 Upper Ring/Outer Shell Intersection Analysis 2.6-121
2.6.8 Corner Drop 2.6-125
2.6.9 Compression 2.6-125
2.6.10 Penetration 2.6-125
2.6.11 Fabrication Stresses 2.6-126
2.6.11.1 Lead Pour 2.6-127
2.6.11.2 Cooldown 2.6-128
2.6.11.3 Lead Creep 2.6-132
2.6.12 PWR Transportable Storage Canister Analysis - Normal Conditions of Transport 2.6-136
2.6.12.1 Analysis Description 2.6-136
2.6.12.2 Finite Element Model Description - PWR Canister 2.6-139
2.6.12.3 Thermal Expansion and Thermal Stresses Evaluation of Canister for PWR Fuel 2.6-148
2.6.12.4 Stress Evaluation of PWR Canister for 1-Foot End-Drop Load Condition 2.6-154
2.6.12.5 Stress Evaluation of PWR Canister for Combined Thermal and 1-Foot End-Drop Load Condition 2.6-162
2.6.12.6 Stress Evaluation of PWR Canister for 1-Foot Side-Drop Load Condition 2.6-168
2.6.12.7 Stress Evaluation of PWR Canister for Combined Thermal and 1-Foot Side-Drop Load Condition 2.6-173

Table of Contents (Continued)

2.6.12.8 Stress Evaluation of PWR Canister for 1-Foot Corner-Drop Load Condition 2.6-177
2.6.12.9 Stress Evaluation of PWR Canister for Combined Thermal and 1-Foot Corner-Drop Load Conditions 2.6-183
2.6.12.10 Shear Stresses for 1-Foot Drops 2.6-189
2.6.12.11 Canister Bearing Stresses for 1-Foot Side Drop 2.6-189
2.6.12.12 Canister Buckling Evaluation for 1-Foot End Drop 2.6-191
2.6.13 PWR Basket Analysis - Normal Conditions of Transport 2.6-195
2.6.13.1 Analysis Description 2.6-199
2.6.13.2 Finite Element Model Description - PWR Basket 2.6-199
2.6.13.3 Thermal Conditions and Expansion Evaluation for PWR Support Disks 2.6-211
2.6.13.4 Stress Evaluation of PWR Support Disks for 1-Foot End-Drop Load Condition 2.6-212
2.6.13.5 Stress Evaluation of PWR Support Disks for Combined Thermal and 1-Foot End Drop Conditions 2.6-216
2.6.13.6 Stress Evaluation of PWR Support Disk for 1-Foot Side-Drop Load Conditions 2.6-219
2.6.13.7 Stress Evaluation of PWR Support Disk for Combined Thermal and 1-Foot Side-Drop Load Condition 2.6-242
2.6.13.8 Stress Evaluation of PWR Support Disk for 1-Foot Off-Angle Load Conditions 2.6-247
2.6.13.9 Stress Evaluation of Support Disk for Combined Thermal and 1-Foot Off-Angle Conditions 2.6-247
2.6.13.10 Stress Evaluation of Tie Rods and Spacers for 1-Foot End-Drop Load Condition 2.6-248
2.6.13.11 Support Disk Shear Stresses for 1-Foot Drops 2.6-249
2.6.13.12 Bearing Stress - Basket Contact with Canister Shell 2.6-250
2.6.13.13 Basket Weldment Analysis for 1-Foot End-Drop 2.6-250
2.6.13.14 Support Disk Buckling Evaluation 2.6-255

Table of Contents (Continued)

2.6.14 BWR Transportable Storage Canister Analysis - Normal Conditions of Transport 2.6-261
2.6.14.1 Analysis Description 2.6-264
2.6.14.2 Finite Element Model Description - BWR Canister 2.6-264
2.6.14.3 Thermal Expansion and Thermal Stress Evaluation of Canister for BWR Fuel 2.6-273
2.6.14.4 Stress Evaluation of BWR Canister for 1-Foot End-Drop Load Condition 2.6-278
2.6.14.5 Stress Evaluation of BWR Canister for Combined Thermal and 1-Foot End-Drop Load Condition 2.6-286
2.6.14.6 Stress Evaluation of the BWR Canister for 1-Foot Side-Drop Load Condition 2.6-292
2.6.14.7 Stress Evaluation of BWR Canister for Combined Thermal and 1-Foot Side-Drop Load Conditions 2.6-297
2.6.14.8 Stress Evaluation of BWR Canister for 1-Foot Corner-Drop Load Condition 2.6-301
2.6.14.9 Stress Evaluation of BWR Canister for Combined Thermal and 1-Foot Corner-Drop Load Conditions 2.6-307
2.6.14.10 Shear Stresses for 1-Foot Drops 2.6-313
2.6.14.11 Canister Bearing Stresses for 1-Foot Side-Drop 2.6-313
2.6.14.12 Canister Buckling Evaluation for 1-Foot End-Drop 2.6-313
2.6.15 BWR Basket Analysis - Normal Conditions of Transport 2.6-317
2.6.15.1 Analysis Description 2.6-322
2.6.15.2 Finite Element Model Description - BWR Basket 2.6-322
2.6.15.3 Thermal Condition and Expansion Evaluation of BWR Support-Disks 2.6-326
2.6.15.4 Stress Evaluation of BWR Support Disk for 1-Foot End-Drop Load Condition 2.6-327
2.6.15.5 Stress Evaluation of BWR Support Disk for Combined Thermal and 1-Foot End Drop Load Conditions 2.6-331

Table of Contents (Continued)

2.6.15.6 Stress Evaluation of BWR Support Disk for 1-Foot Side-Drop Load Condition 2.6-334
2.6.15.7 Stress Evaluation of BWR Support Disk for Combined Thermal and 1-Foot Side-Drop Load Conditions 2.6-375
2.6.15.8 Stress Evaluation of BWR Support Disk for 1-Foot Corner-Drop Load Conditions 2.6-381
2.6.15.9 Stress Evaluation of BWR Support Disk for Combined Thermal and 1-Foot Corner-Drop Load Conditions 2.6-381
2.6.15.10 Stress Evaluation of Tie Rods and Spacers for 1-Foot End-Drop Load Condition 2.6-381
2.6.15.11 Support Disk Shear Stresses for 1-Foot Drops 2.6-382
2.6.15.12 Bearing Stress - Basket Contact with Inner Shell 2.6-382
2.6.15.13 Basket Weldment Analysis for 1-Foot End-Drop 2.6-383
2.6.15.14 Support Disk Buckling Evaluation 2.6-387
2.6.16 Universal Transport Cask Cavity Spacers 2.6-396
2.6.16.1 PWR Cask Cavity Spacers 2.6-396
2.6.16.2 BWR Cask Cavity Spacers 2.6-400

2.7 Hypothetical Accident Conditions 2.7-1
2.7.1 Free Drop (30 ft) - Cask Body Analysis 2.7-1
2.7.1.1 30-Foot End Drop 2.7-3
2.7.1.2 30-Foot Side Drop 2.7-11
2.7.1.3 30-Foot Corner Drop 2.7-15
2.7.1.4 30-Foot Oblique Drop 2.7-22
2.7.1.5 Lead Slump Resulting from a Cask Drop Accident 2.7-29
2.7.1.6 Impact Limiter Analysis - Hypothetical Accident Conditions 2.7-30
2.7.1.7 Closure Analysis 2.7-33
2.7.2 Puncture 2.7-40
2.7.2.1 Puncture - Cask Side Midpoint 2.7-41
2.7.2.2 Puncture - Lid Center 2.7-48
2.7.2.3 Puncture - Center of Cask Bottom 2.7-52
2.7.2.4 Puncture - Port Cover 2.7-60

Table of Contents (Continued)

2.7.2.5 Puncture Accident - Shielding Consequences 2.7-61
2.7.3 Thermal 2.7-62
2.7.3.1 Summary of Pressures and Temperatures 2.7-62
2.7.3.2 Differential Thermal Expansion Stress 2-7-62
2.7.4 Crush 2.7-66
2.7.5 Immersion - Fissile Material 2.7-66
2.7.6 Immersion - All Packages 2.7-66
2.7.6.1 Membrane Stresses in Cask Outer Shell (away from ends) 2.7-69
2.7.6.2 Bending Stress in the Bottom Forging (at center) 2.7-69
2.7.6.3 Bending Stress in the Cask Lid (at center) 2.7-70
2.7.6.4 Bending Stress in the Cask Bottom (at center) 2.7-70
2.7.6.5 Bending Stress in the Port Cover Plate (at center) 2.7-71
2.7.7 PWR Transportable Storage Canister Analysis - Accident Conditions 2.7-73
2.7.7.1 Analysis Description 2.7-74
2.7.7.2 Analysis Results - PWR Canister 2.7-74
2.7.7.3 Canister Buckling Evaluation for 30-Foot End Drop 2.7-88
2.7.8 PWR Basket Analysis - Accident Conditions 2.7-91
2.7.8.1 Stress Evaluation of Support Disk 2.7-91
2.7.8.2 Stress Evaluation of Tie Rods and Spacers 2.7-116
2.7.8.3 Buckling Evaluation of Support Disk 2.7-119
2.7.8.4 Fuel Tube Analysis 2.7-125
2.7.8.5 Basket Weldment Analysis for 30-Foot End Drop 2.7-132
2.7.9 BWR Transportable Storage Canister Analysis - Accident Conditions 2.7-136
2.7.9.1 Analysis Description 2.7-137
2.7.9.2 Analysis Results - BWR Canister 2.7-137
2.7.9.3 Canister Buckling Evaluation for 30-Foot End Drop 2.7-151
2.7.10 BWR Basket Analysis - Accident Conditions 2.7-153
2.7.10.1 Stress Evaluation of Support Disk 2.7-154
2.7.10.2 Stress Evaluation of Tie Rods and Spacers 2.7-181
2.7.10.3 Buckling Evaluation of Support Disk 2.7-183
2.7.10.4 Fuel Tube Analysis 2.7-189
2.7.10.5 Basket Weldment Analysis for 30-Foot End-Drop 2.7-194

Table of Contents (Continued)

2.7.11 Summary of Damage to Cask Due to Hypothetical Accident Conditions .. 2.7-198
2.7.12 Cask Inner Shell Buckling Analysis 2.7-201
2.7.12.1 Analysis Methodology 2.7-201
2.7.12.2 Analysis Results 2.7-202
2.7.12.3 Detailed Code Case N-284-1 Buckling Evaluation 2.7-202

2.8 Special Form 2.8-1

2.9 Fuel Rods 2.9-1
2.9.1 PWR Fuel Rod Buckling Assessment 2.9-1
2.9.1.1 Overview of Analysis Methodology 2.9-1
2.9.1.2 Fuel Rod Mode Shapes and Buckling Evaluation 2.9-3
2.9.2 BWR Fuel Rod Buckling Assessment 2.9-4

2.10 Appendices 2.10-1
2.10.1 Computer Program Descriptions 2.10.1-1
2.10.1.1 ANSYS 2.10.1-1
2.10.1.2 RBCUBED 2.10.1-2
2.10.2 Finite Element Model - Universal Transport Cask 2.10.2-1
2.10.2.1 Load Application and Boundary Conditions 2.10.2-5
2.10.2.2 Post-Processing of Results 2.10.2-13
2.10.3 Confirmatory Testing Program – UMS® Impact Limiters and Attachments 2.10.3-1
2.10.3.1 Confirmatory Testing Program Results Summary 2.10.3-1
2.10.3.2 Description of the UMS® Cask Scale Model for the 30-Foot Drop Tests 2.10.3-3
2.10.3.3 Acceptance Criteria for Model Performance 2.10.3-6
2.10.3.4 Equipment and Instrumentation 2.10.3-6
2.10.3.5 Filter Frequency Identification for the Accelerometer Data 2.10.3-9
2.10.3.6 Results/Evaluation for the 30-Foot Top End Drop Test 2.10.3-13
2.10.3.7 Static Crush Test for the End Drop Orientation 2.10.3-18
2.10.3.8 Results/Evaluation for the 30-Foot Side Drop Test 2.10.3-22
2.10.3.9 Evaluation of a 30-Foot Oblique Drop 2.10.3-28

Table of Contents (Continued)

2.10.3.10 Results/Evaluation for the 30-Foot Top Corner Drop Test 2.10.3-29
2.10.3.11 Scale Model Drawings 2.10.3-31
2.10.4 Dynamic Load Factor (DLF) Evaluation for PWR and BWR Support Disks 2.10.4-1
2.10.4.1 1-Foot End Drop Analysis 2.10.4-1
2.10.4.2 Side Drop Analysis 2.10.4-7

2.11 Site Specific Contents Structural Evaluations 2.11-1
2.11.1 Site Specific Spent Fuel 2.11-1
2.11.1.1 Maine Yankee Site Specific Spent Fuel 2.11.1-1
2.11.2 Site Specific Greater Than Class C Waste 2.11.2-1
2.11.2.1 Maine Yankee Greater Than Class C Waste 2.11.2-1

2.12 References 2.12-1

List of Figures

Figure 2.5.1.1-1 Primary Lifting Trunnion Geometry 2.5-27
Figure 2.5.1.1-2 Secondary Lifting Trunnion Geometry 2.5-28
Figure 2.5.2.1-1 Front Support and Tiedown Geometry 2.5-37
Figure 2.5.2.1-2 Shear Ring Geometry 2.5-38
Figure 2.5.2.1-3 Free-Body Diagram of Cask Subjected to Lateral Load 2.5-39
Figure 2.6.7.5-1 Universal Transport Cask with Impact Limiters 2.6-80
Figure 2.6.7.5-2 Cross Section of Lower Impact Limiter 2.6-81
Figure 2.6.7.5-3 Crush Stress-Strain Curves for Redwood (Crush Strength Parallel to Grain) 2.6-82
Figure 2.6.7.5-4 Crush Stress-Strain Curves for Redwood (Crush Strength Perpendicular to Grain) 2.6-83
Figure 2.6.7.5-5 Crush Stress-Strain Curves for Balsa Wood (Crush Strength Parallel to Grain) 2.6-84
Figure 2.6.7.5-6 Variation of Crush Strength of Redwood and Balsa Wood with Impact Angle at 40 Percent Strain 2.6-85
Figure 2.6.7.5-7 Cask Side-Drop Geometry 2.6-86
Figure 2.6.7.5-8 Cask End-Drop Geometry 2.6-87
Figure 2.6.7.5-9 Cask Oblique-Drop Geometry 2.6-88
Figure 2.6.7.5-10 Accelerometer Time History at the Bottom of the NAC-STC 1/4-Scale Model Cask (75° Oblique Drop) 2.6-89
Figure 2.6.7.5-11 Accelerometer Time History at the Top of the NAC-STC 1/4-Scale Model Cask (75° Oblique Drop) 2.6-90
Figure 2.6.7.5-12 Force-Deformation Curve - Lower Impact Limiter (Bottom End Impact, 0 Degrees) 2.6-91
Figure 2.6.7.5-13 Force-Deformation Curve - Lower Impact Limiter (Bottom Corner Impact, 24 Degrees) 2.6-92
Figure 2.6.7.5-14 Force-Deformation Curve - Lower Impact Limiter (Bottom Oblique Impact, 75 Degrees) 2.6-93
Figure 2.6.7.5-15 Force-Deformation Curve - Upper Impact Limiter (Top End Impact, 0 Degrees) 2.6-94
Figure 2.6.7.5-16 Force-Deformation Curve - Upper Impact Limiter (Top Corner Impact, 24 Degrees) 2.6-95

List of Figures (Continued)

Figure 2.6.7.5-17 Force-Deformation Curve - Upper Impact Limiter (Top Oblique Impact, 75 Degrees) 2.6-96
Figure 2.6.7.5-18 Force-Deformation Curve - Side Impact (90 Degrees) 2.6-97
Figure 2.6.7.5-19 Impact Limiter Attachment Geometry 2.6-98
Figure 2.6.7.7-1 Neutron Shield Geometry 2.6-112
Figure 2.6.12-1 PWR Transportable Storage Canister 2.6-137
Figure 2.6.12-2 PWR Transportable Storage Canister Shell and Lids 2.6-138
Figure 2.6.12.2-1 PWR Canister Assembly Finite Element Model 2.6-143
Figure 2.6.12.2-2 Canister Structural and Shield Lid Finite Element Mesh 2.6-144
Figure 2.6.12.2-3 Structural and Shield Lid Weld Regions Finite Element Mesh 2.6-145
Figure 2.6.12.2-4 Canister Bottom Plate Finite Element Mesh 2.6-146
Figure 2.6.12.3-1 Identification of Sections for Evaluating Linearized Stresses in Canister (in) 2.6-151
Figure 2.6.13-1 PWR Fuel Assembly Basket 2.6-196
Figure 2.6.13-2 Support Disk Cross Section Configuration 2.6-197
Figure 2.6.13-3 PWR Fuel Tube Configuration 2.6-198
Figure 2.6.13.2-1 PWR Basket for Side-Drop 2.6-204
Figure 2.6.13.2-2 Side Drop Orientation 2.6-205
Figure 2.6.13.2-3 Location of the Section to Obtain Linearized Stresses (Left half of support disk) 2.6-206
Figure 2.6.13.2-4 Location of the Section to Obtain Linearized Stresses (Right half of support disk) 2.6-207
Figure 2.6.13.4-1 Locations of Maximum P_m+P_b Stresses —1-Foot End Drop, Thermal Case A 2.6-213
Figure 2.6.13.5-1 Locations of Maximum P+Q Stresses —1-Foot End Drop, Thermal Case A 2.6-217
Figure 2.6.13.6-1 Support Disk Side-Drop Orientations 2.6-221
Figure 2.6.13.6-2 Locations of Maximum P_m+P_b Intensities—0° Side Drop Orientation, Thermal Case A 2.6-222
Figure 2.6.13.6-3 Locations of Maximum P_m+P_b Stresses—18.22° Side Drop Orientation, Thermal Case A 2.6-223
Figure 2.6.13.6-4 Locations of Maximum P_m+P_b Stresses—26.28° Side Drop Orientation, Thermal Case A 2.6-224

List of Figures (Continued)

Figure 2.6.13.6-5 Locations of Maximum P_m+P_b Stresses —45° Side Drop Orientation, Thermal Case A 2.6-225

Figure 2.6.13.13-1 Finite Element Model of the Top Weldment Plate 2.6-252
Figure 2.6.13.13-2 Finite Element Model of the Bottom Weldment Plate 2.6-253
Figure 2.6.14-1 BWR Transportable Storage Canister 2.6-262
Figure 2.6.14-2 BWR Transportable Storage Canister Shell and Lids 2.6-263
Figure 2.6.14.2-1 BWR Canister Assembly Finite Element Mesh (with 45° Basket orientation) 2.6-268
Figure 2.6.14.2-2 Canister Structural and Shield Lid Finite Element Mesh 2.6-269
Figure 2.6.14.2-3 Structural and Shield Lid Weld Regions Finite Element Mesh 2.6-270
Figure 2.6.14.2-4 Canister Bottom Plate Finite Element Mesh 2.6-271
Figure 2.6.14.3-1 Identification of the Sections for Evaluating the Linearized Stresses in the Canister 2.6-275
Figure 2.6.15-1 BWR Fuel Assembly Basket 2.6-319
Figure 2.6.15-2 Support Disk Cross Section Configuration 2.6-320
Figure 2.6.15-3 BWR Fuel Tube Configuration 2.6-321
Figure 2.6.15.2-1 ANSYS Model of BWR Basket for Side-Drop 2.6-324
Figure 2.6.15.2-2 Close-up of the Ligaments and the Interface with the Canister Shell and the Cask Inner Shell 2.6-325
Figure 2.6.15.4-1 Locations of Maximum Primary Nodal Stress Intensities for 1-Foot End Drop 2.6-328
Figure 2.6.15.5-1 Locations of Maximum Primary and Secondary Nodal Stress Intensities for 1-Foot End-Drop 2.6-332
Figure 2.6.15.6-1 Support Disk Side-Drop Orientations 2.6-337
Figure 2.6.15.6-2 Locations of the Sections Used to Obtain Linearized Stresses for the Support Disk for the 1st Quadrant (X>0,Y>0) 2.6-338
Figure 2.6.15.6-3 Locations of the Sections Used to Obtain Linearized Stresses for the Support Disk for the 2nd Quadrant (X<0,Y<0) 2.6-339
Figure 2.6.15.6-4 Locations of the Sections Used to Obtain Linearized Stresses for the Support Disk for the 3rd Quadrant (X<0,Y<0) 2.6-340

List of Figures (Continued)

Figure 2.6.15.6-5 Locations of the Sections Used to Obtain Linearized Stresses for the Support Disk for the 4th Quadrant (X>0,Y<0) 2.6-341
Figure 2.6.15.6-6 Locations of Maximum Linearized Stress Intensities - 0° Drop Orientation 2.6-342
Figure 2.6.15.6-7 Locations of Maximum Linearized Stress Intensities - 31.82° Drop Orientation 2.6-343
Figure 2.6.15.6-8 Locations of Maximum Linearized Stress Intensities - 49.46° Drop Orientation 2.6-344
Figure 2.6.15.6-9 Locations of Maximum Linearized Stress Intensities - 77.92° Drop Orientation 2.6-345
Figure 2.6.15.6-10 Locations of Maximum Linearized Stress Intensities - 90° Drop Orientation 2.6-346
Figure 2.6.15.13-1 Finite Element Model of the Top Weldment Plate 2.6-384
Figure 2.6.15.13-2 Finite Element Model of the Bottom Weldment Plate 2.6-385
Figure 2.7.1.5-1 Radial Lead Slump Model 2.7-31
Figure 2.7.2.1-1 Cask Body Model for Puncture Analysis 2.7-44
Figure 2.7.2.1-2 Location of Sections for Evaluation 2.7-45
Figure 2.7.2.2-1 ANSYS Model for Cask Lid 2.7-51
Figure 2.7.2.3-1 Bottom Puncture Finite Element Model and Boundary Conditions 2.7-56
Figure 2.7.2.3-2 Location of Sections for Evaluation 2.7-57
Figure 2.7.6-1 Cross Section of Cask Body 2.7-72
Figure 2.7.7.2-1 Identification of the Sections for Evaluating the Linearized Stresses in the PWR Canister 2.7-76
Figure 2.7.9.2-1 Identification of Sections for Evaluating Linearized Stresses in BWR Canister 2.7-139

Figure 2.9-1 Typical Fuel Rod Finite Element Model and Boundary Conditions 2.9-5
Figure 2.9-2 Typical First Lateral Mode Shape Plot for Fuel Rod 2.9-6
Figure 2.9-3 Typical First Buckling Mode Shape for Fuel Rod 2.9-7
Figure 2.10.2-1 Primary Components of the Universal Transport Cask 2.10.2-3
Figure 2.10.2-2 Universal Transport Cask 3-D Model 2.10.2-4

List of Figures (Continued)

Figure 2.10.2.1-1 Cask Body Loading for Side-Drop Conditions 2.10.2-11
Figure 2.10.2.1-2 View of Cask Model Showing Pressure Distribution for Side-Drop Analysis 2.10.2-12
Figure 2.10.2.2-1 Lower Cask Body Section Locations 2.10.2-14
Figure 2.10.2.2-2 Sections Through Cask Body Ligaments 2.10.2-14
Figure 2.10.2.2-3 Cask Body Sections at Center 2.10.2-15
Figure 2.10.2.2-4 Cask Body Sections in Upper Cask 2.10.2-15
Figure 2.10.3-1 Typical Unfiltered Acceleration Time History for the UMS® Quarter-Scale Model Top End Drop 2.10.3-32
Figure 2.10.3-2 Typical Filtered Acceleration Time History for the UMS® Quarter-Scale Model Top End Drop, Overlayed with the Unfiltered Data 2.10.3-33
Figure 2.10.3-3 Force-Deflection Curve for Static Test 1 for a 45° Section of the UMS® Quarter-Scale Model Upper Impact Limiter 2.10.3-34
Figure 2.10.3-4 Force-Deflection Curve for Static Test 2 for a 45° Section of the UMS® Quarter-Scale Model Upper Impact Limiter 2.10.3-35
Figure 2.10.3-5 Typical Unfiltered Acceleration Time History for the UMS® Quarter-Scale Model Side Drop 2.10.3-36
Figure 2.10.3-6 Typical Filtered Acceleration Time History for the UMS® Quarter-Scale Model Side Drop, Overlayed with the Unfiltered Data 2.10.3-37
Figure 2.10.3-7 Typical Unfiltered Acceleration Time History for the UMS® Quarter-Scale Model Top Corner Drop 2.10.3-38
Figure 2.10.3-8 Typical Filtered Acceleration Time History for the UMS® Quarter-Scale Model Top Corner Drop, Overlayed with the Unfiltered Data 2.10.3-39

List of Figures (Continued)

Figure 2.10.4.1-1 ANSYS Finite Element Model of PWR Support Disk for End Drop Analysis 2.10.4-3
Figure 2.10.4.1-2 ANSYS Finite Element Model of BWR Support Disk for End Drop Analysis 2.10.4-3
Figure 2.10.4.1-3 1-Foot End-Drop Acceleration Time History 2.10.4-4
Figure 2.10.4.1-4 1-Foot End-Drop Frequency Response Spectrum 2.10.4-4
Figure 2.10.4.2-1 ANSYS Finite Element Model of PWR Support Disk for Side Drop Analysis 2.10.4-9
Figure 2.10.4.2-2 ANSYS Finite Element Model of BWR Support Disk for Side Drop Analysis 2.10.4-9
Figure 2.10.4.2-3 LS-DYNA Finite Element Model for Side Drop Analysis 2.10.4-10
Figure 2.10.4.2-4 1-Foot Side-Drop Acceleration Time History 2.10.4-11
Figure 2.10.4.2-5 PWR Support Disk Acceleration Time History for 1-Foot Side-Drop 2.10.4-11
Figure 2.10.4.2-6 BWR Support Disk Acceleration Time History for 1-Foot Side-Drop 2.10.4-12
Figure 2.10.4.2-7 PWR Support Disk Frequency Response Spectrum for 1-Foot Side Drop 2.10.4-12
Figure 2.10.4.2-8 BWR Support Disk Frequency Response Spectrum for 1-Foot Side Drop 2.10.4-13
Figure 2.11.1.1-1 PWR Basket Drop Orientations and Case Study Loading Positions for Maine Yankee Consolidated Fuel 2.11.1-4
Figure 2.11.2.1-1 Maine Yankee GTCC Basket Finite Element Model 2.11.2-22
Figure 2.11.2.1-2 Maine Yankee GTCC Basket Finite Element Model Pressure Loading Locations 2.11.2-23
Figure 2.11.2.1-3 Maine Yankee GTCC Basket Finite Element Model Section Locations for Stress Evaluation 2.11.2-24
Figure 2.11.2.1-4 Finite Element Model for Maine Yankee GTCC Basket Support Wall 2.11.2-25
Figure 2.11.2.1-5 Finite Element Model for Maine Yankee GTCC Basket Separator Plate 2.11.2-26

List of Tables

Table 2.1.2-1 Exceptions to Codes and Standards 2.1-12
Table 2.1.2-2 Load Combinations: Normal and Hypothetical Accident Conditions 2.1-15
Table 2.1.2-3 Allowable Stress Limits for Containment Structures 2.1-16
Table 2.1.2-4 Allowable Stress Limits for Noncontainment Structures 2.1-17
Table 2.2-1 Calculated Weights and Centers of Gravity: Cask with Canister Containing PWR Fuel 2.2-2
Table 2.2-2 Calculated Weights and Centers of Gravity: Cask with Canister Containing BWR Fuel 2.2-3
Table 2.2-3 Calculated Weights and Centers of Gravity: Cask with Canister Containing Greater Than Class C (GTCC) Waste 2.2-4
Table 2.3.2-1 Mechanical Properties of SA-240, Type 304 Stainless Steel 2.3-4
Table 2.3.2-2 Mechanical Properties of SA-479, Type 304 Stainless Steel 2.3-5
Table 2.3.2-3 Mechanical Properties of SA-240, Type 304L Stainless Steel 2.3-6
Table 2.3.2-4 Mechanical Properties of SA-336, Type 304 Stainless Steel 2.3-7
Table 2.3.2-5 Mechanical Properties of Type XM-19 Stainless Steel 2.3-8
Table 2.3.3-1 Mechanical Properties of SA-564 and SA-693, Type 630, 17-4 PH Stainless Steel 2.3-10
Table 2.3.4-1 Mechanical Properties of SA-533, Type B, Class 2 Carbon Steel 2.3-12
Table 2.3.5-1 Mechanical Properties of SB-637, Grade N07718 Nickel Alloy Steel Bolting Material 2.3-14
Table 2.3.5-2 Mechanical Properties of SA-193, Grade B6, High Alloy Steel Bolting Material 2.3-15
Table 2.3.5-3 Mechanical Properties of SA-193, Grade B8S, High Alloy Steel Bolting Material 2.3-16
Table 2.3.6-1 Mechanical Properties of 6061-T651 Aluminum Alloy 2.3-18
Table 2.3.7-1 Static Mechanical Properties of Chemical Copper Lead 2.3-20
Table 2.3.7-2 Mechanical Properties of NS-4-FR 2.3-21
Table 2.4.4.2-1 Summary of Universal Transport Cask Materials Categories and Operating Environments 2.4-8
Table 2.5.1.1-1 Primary Trunnion/Top Forging Intersection Analysis Results 2.5-29
Table 2.5.2.1-1 Reactions Caused by Tiedown Devices (from 10 CFR 71.45(b)) 2.5-40
Table 2.5.2.1-2 Reactions Caused by Tiedown Devices (from AAR Field Manual Rule 88) 2.5-41

List of Tables (Continued)

Table 2.6.1.1-1 Maximum Component Temperatures – Normal Conditions of Transport, Maximum Decay Heat, Maximum Ambient Temperature 2.6-7
Table 2.6.1.1-2 Summary of Canister Pressures During Normal Conditions of Transport 2.6-8
Table 2.6.1.1-3 Summary of Cask Pressures During Normal Conditions of Transport 2.6-8
Table 2.6.1.3-1 P_m Stresses – 150 psig Internal Pressure*, Heat (100°F) 2.6-9
Table 2.6.1.3-2 $P_m + P_b$ Stresses – 150 psig Internal Pressure*, Heat (100°F) 2.6-10
Table 2.6.1.3-3 Thermal (Q) Stresses – Heat (100°F) 2.6-11
Table 2.6.1.3-4 P_m Stresses – 1-*g* Gravity Load*, Heat (100°F) 2.6-12
Table 2.6.1.3-5 $P_m + P_b$ Stresses – 1-*g* Gravity Load*, Heat (100°F) 2.6-13
Table 2.6.2.1-1 Minimum Component Temperatures – Normal Conditions of Transport, Maximum Decay Heat, Minimum Ambient Temperature (Thermal Cold) 2.6-17
Table 2.6.2.3-1 P_m Stresses – 150 psig Internal Pressure*, Cold (-40°F) 2.6-18
Table 2.6.2.3-2 $P_m + P_b$ Stresses – 150 psig Internal Pressure*, Cold (-40°F) 2.6-19
Table 2.6.2.3-3 Thermal (Q) Stresses – Cold (-40°F) 2.6-20
Table 2.6.2.3-4 P_m Stresses – 1-*g* Gravity Load*, Cold (-40°F) 2.6-21
Table 2.6.2.3-5 $P_m + P_b$ Stresses – 1-*g* Gravity Load*, Cold (-40°F) 2.6-22
Table 2.6.7.1-1 P_m Stresses - 1-Foot Top End-Drop, Bolt Preload, Internal Pressure 2.6-28
Table 2.6.7.1-2 $P_m + P_b$ Stresses - 1-Foot Top End-Drop Bolt Preload, Internal Pressure 2.6-29
Table 2.6.7.1-3 $P_m + P_b + Q$ Stresses - 1-Foot Top End-Drop, Bolt Preload, Internal Pressure, Thermal Hot 2.6-30
Table 2.6.7.1-4 $P_m + P_b + Q$ Stresses - 1-Foot Top End-Drop, Bolt Preload, Internal Pressure, Thermal Cold 2.6-31
Table 2.6.7.1-5 Critical P_m Stress Summary (ksi)- 1-Foot Top End-Drop, Bolt Preload, Internal Pressure 2.6-32
Table 2.6.7.1-6 Critical $P_m + P_b$ Stress Summary (ksi) - 1-Foot Top End-Drop, Bolt Preload, Internal Pressure 2.6-32
Table 2.6.7.1-7 Critical $P_m + P_b + Q$ Stress Summary (ksi) - 1-Foot Top End-Drop, Bolt Preload, Internal Pressure, Impact, Thermal Hot 2.6-33

List of Tables (Continued)

Table 2.6.7.1-8 Critical $P_m + P_b + Q$ Stress Summary (ksi) - 1-Foot Top End-Drop, Bolt Preload, Internal Pressure, Impact, Thermal Cold 2.6-33
Table 2.6.7.1-9 P_m Stresses - 1-Foot Bottom End-Drop, Bolt Preload, Internal Pressure 2.6-34
Table 2.6.7.1-10 $P_m + P_b$ Stresses - 1-Foot Bottom End-Drop, Bolt Preload, Internal Pressure 2.6-35
Table 2.6.7.1-11 $P_m + P_b + Q$ Stresses - 1-Foot Bottom End-Drop, Bolt Preload, Internal Pressure, Impact, Thermal Hot 2.6-36
Table 2.6.7.1-12 $P_m + P_b + Q$ Stresses - 1-Foot Bottom End-Drop, Bolt Preload, Internal Pressure, Impact, Thermal Cold 2.6-37
Table 2.6.7.1-13 Critical P_m Stress Summary (ksi) - 1-Foot Bottom End-Drop, Bolt Preload, Internal Pressure 2.6-38
Table 2.6.7.1-14 Critical $P_m + P_b$ Stress Summary (ksi) - 1-Foot Bottom End-Drop Bolt Preload, Internal Pressure 2.6-38
Table 2.6.7.1-15 Critical $P_m + P_b + Q$ Stress Summary (ksi) - 1-Foot Bottom End-Drop Bolt Preload, Internal Pressure, Thermal Hot 2.6-39
Table 2.6.7.1-16 Critical $P_m + P_b + Q$ Stress Summary (ksi) - 1-Foot Bottom End-Drop Bolt Preload, Internal Pressure, Thermal Cold 2.6-39
Table 2.6.7.2-1 P_m Stresses - 1-Foot Side-Drop, Bolt Preload, Internal Pressure 2.6-41
Table 2.6.7.2-2 $P_m + P_b$ Stresses - 1-Foot Side-Drop, Bolt Preload, Internal Pressure 2.6-42
Table 2.6.7.2-3 $P_m + P_b + Q$ Stresses - 1-Foot Side-Drop, Bolt Preload, Internal Pressure, Thermal Hot 2.6-43
Table 2.6.7.2-4 $P_m + P_b + Q$ Stresses - 1-Foot Side-Drop, Bolt Preload, Internal Pressure, Thermal Cold 2.6-44
Table 2.6.7.2-5 Critical P_m Stress Summary (ksi) - 1-Foot Side-Drop, Bolt Preload, Internal Pressure 2.6-45
Table 2.6.7.2-6 Critical $P_m + P_b$ Stress Summary (ksi) - 1-Foot Side-Drop Bolt Preload, Internal Pressure 2.6-45
Table 2.6.7.2-7 Critical $P_m + P_b + Q$ Stress Summary (ksi) - 1-Foot Side-Drop Bolt Preload, Internal Pressure, Thermal Hot 2.6-46

List of Tables (Continued)

Table 2.6.7.2-8 Critical $P_m + P_b + Q$ Stress Summary (ksi) - 1-Foot Side-Drop, Bolt Preload, Internal Pressure, Thermal Cold 2.6-46

Table 2.6.7.3-1 P_m Stresses - 1-Foot Top Corner-Drop, Bolt Preload, Internal Pressure 2.6-48

Table 2.6.7.3-2 $P_m + P_b$ Stresses - 1-Foot Top Corner-Drop Bolt Preload, Internal Pressure 2.6-49

Table 2.6.7.3-3 $P_m + P_b + Q$ Stresses - 1-Foot Top Corner-Drop, Bolt Preload, Internal Pressure, Thermal Hot 2.6-50

Table 2.6.7.3-4 $P_m + P_b + Q$ Stresses - 1-Foot Top Corner-Drop, Bolt Preload, Internal Pressure, Thermal Cold 2.6-51

Table 2.6.7.3-5 Critical P_m Stress Summary (ksi) - 1-Foot Top Corner-Drop, Bolt Preload, Internal Pressure 2.6-52

Table 2.6.7.3-6 Critical $P_m + P_b$ Stress Summary (ksi) - 1-Foot Top Corner-Drop, Bolt Preload, Internal Pressure 2.6-52

Table 2.6.7.3-7 Critical $P_m + P_b + Q$ Stress Summary (ksi) - 1-Foot Top Corner-Drop, Bolt Preload, Internal Pressure, Thermal Hot 2.6-53

Table 2.6.7.3-8 Critical $P_m + P_b + Q$ Stress Summary (ksi) - 1-Foot Top Corner-Drop, Bolt Preload, Internal Pressure, Thermal Cold 2.6-53

Table 2.6.7.3-9 P_m Stresses - 1-Foot Bottom Corner-Drop, Bolt Preload, Internal Pressure 2.6-54

Table 2.6.7.3-10 $P_m + P_b$ Stresses - 1-Foot Bottom Corner-Drop, Bolt Preload, Internal Pressure 2.6-55

Table 2.6.7.3-11 $P_m + P_b + Q$ Stresses - 1-Foot Bottom Corner-Drop, Bolt Preload, Internal Pressure, Thermal Hot 2.6-56

Table 2.6.7.3-12 $P_m + P_b + Q$ Stresses - 1-Foot Bottom Corner-Drop, Bolt Preload, Internal Pressure, Thermal Cold 2.6-57

Table 2.6.7.3-13 Critical P_m Stress Summary (ksi) - 1-Foot Bottom Corner-Drop, Bolt Preload, Internal Pressure 2.6-58

Table 2.6.7.3-14 Critical $P_m + P_b$ Stress Summary (ksi) - 1-Foot Bottom Corner-Drop Bolt Preload, Internal Pressure 2.6-58

List of Tables (Continued)

Table 2.6.7.3-15 Critical $P_m + P_b + Q$ Stress Summary (ksi) - 1-Foot Bottom Corner-Drop Bolt Preload, Internal Pressure, Thermal Hot 2.6-59
Table 2.6.7.3-16 Critical $P_m + P_b + Q$ Stress Summary (ksi) - 1-Foot Bottom Corner-Drop Bolt Preload, Internal Pressure, Thermal Cold 2.6-59
Table 2.6.7.5-1 Summary of Results - Impact Limiter Analysis for 1-Foot Free Drop 2.6-99
Table 2.6.7.5-2 Summary of Results - Impact Limiter Analysis for 30-Foot Free Drop 2.6-101
Table 2.6.7.5-3 Summary of Cask Drop Equivalent *g*-Load Factors 2.6-103
Table 2.6.7.5-4 Summary of Results of RBCUBED Impact Limiter Analysis for 30-Foot Drop for Wood Properties at 70°F 2.6-103
Table 2.6.7.8-1 Resultant Stress Intensity Values in the Equivalent Ring 2.6-124
Table 2.6.11.2-1 Stress Analysis Results for Uniform Pressure Loading of Inner Shell Due to Lead Pouring 2.6-133
Table 2.6.12.2-1 Gap and Element Type Definition - Canister Model 2.6-147
Table 2.6.12.2-2 Material Definition - Canister Model 2.6-147
Table 2.6.12.3-1 PWR Canister Linearized Q Stresses - Thermal Only (Hot 1) 2.6-152
Table 2.6.12.3-2 Linearized Stresses - Thermal Only (Cold 2) 2.6-153
Table 2.6.12.4-1 PWR Canister Critical Sections for the Pressure Only and 1-Foot End-Drop Load Condition 2.6-155
Table 2.6.12.4-2 PWR Canister P_m Stresses - Internal Pressure 2.6-156
Table 2.6.12.4-3 PWR Canister $P_m + P_b$ Stresses - Internal Pressure 2.6-157
Table 2.6.12.4-4 PWR Canister P_m Stresses - 1-Foot Top End-Drop 2.6-158
Table 2.6.12.4-5 PWR Canister $P_m + P_b$ Stresses - 1-Foot Top End-Drop 2.6-159
Table 2.6.12.4-6 PWR Canister P_m Stresses - 1-Foot Bottom End-Drop, Internal Pressure 2.6-160
Table 2.6.12.4-7 PWR Canister $P_m + P_b$ Stresses - 1-Foot Bottom End-Drop, Internal Pressure 2.6-161
Table 2.6.12.5-1 PWR Canister Critical Sections for the Combined 1-Foot End-Drop and Thermal Load Condition 2.6-163

List of Tables (Continued)

Table 2.6.12.5-2 PWR Canister $P_m + P_b + Q$ Stresses - 1-Foot Top End-Drop, Thermal Cold 2.6-164
Table 2.6.12.5-3 PWR Canister $P_m + P_b + Q$ Stresses - 1-Foot Top End-Drop, Thermal Heat 2.6-165
Table 2.6.12.5-4 PWR Canister $P_m + P_b + Q$ Stresses - 1-Foot Bottom End-Drop, Thermal Cold 2.6-166
Table 2.6.12.5-5 PWR Canister $P_m + P_b + Q$ Stresses - 1-Foot Bottom End-Drop, Thermal Heat 2.6-167
Table 2.6.12.6-1 PWR Canister Critical Sections for the 1-Foot Side-Drop Load Condition 2.6-170
Table 2.6.12.6-2 PWR Canister: P_m Stresses - 1-Foot Side-Drop 2.6-171
Table 2.6.12.6-3 PWR Canister $P_m + P_b$ Stresses - 1-Foot Side-Drop, Internal Pressure 2.6-172
Table 2.6.12.7-1 PWR Canister Critical Sections for Combined 1-Foot Side-Drop and Thermal Load Condition 2.6-174
Table 2.6.12.7-2 PWR Canister $P_m + P_b + Q$ Stresses - 1-Foot Side-Drop, Thermal Cold 2.6-175
Table 2.6.12.7-3 PWR Canister $P_m + P_b + Q$ Stresses - 1-Foot Side-Drop, Thermal Heat 2.6-176
Table 2.6.12.8-1 PWR Canister Critical Sections for the 1-Foot Corner-Drop Load Condition 2.6-178
Table 2.6.12.8-2 PWR Canister P_m Stresses 1-Foot Top Corner-Drop, Internal Pressure 2.6-179
Table 2.6.12.8-3 PWR Canister $P_m + P_b$ Stresses - 1-Foot Top Corner-Drop 2.6-180
Table 2.6.12.8-4 PWR Canister P_m Stresses - 1-Foot Bottom Corner-Drop 2.6-181
Table 2.6.12.8-5 PWR Canister $P_m + P_b$ Stresses - 1-Foot Bottom Corner-Drop 2.6-182
Table 2.6.12.9-1 PWR Canister Critical Sections for the Combined 1-Foot Corner-Drop and Thermal Load Condition 2.6-184
Table 2.6.12.9-2 PWR Canister $P_m + P_b + Q$ Stresses - 1-Foot Top Corner-Drop, Thermal Cold 2.6-185
Table 2.6.12.9-3 PWR Canister $P_m + P_b + Q$ Stresses - 1-Foot Top Corner-Drop, Thermal Heat 2.6-186
Table 2.6.12.9-4 PWR Canister $P_m + P_b + Q$ Stresses - 1-Foot Bottom Corner-Drop, Internal Pressure, Thermal Cold 2.6-187

List of Tables (Continued)

Table 2.6.12.9-5 PWR Canister $P_m + P_b + Q$ Stresses - 1-Foot Bottom Corner-Drop, Internal Pressure, Thermal Heat 2.6-188
Table 2.6.12.12-1 Geometry Parameters for the PWR Canister 2.6-193
Table 2.6.12.12-2 Buckling Evaluation Results for the PWR Canister for 1-Foot End Drop 2.6-194
Table 2.6.13.2-1 Listing of Cross Sections for Stress Evaluation of Support Disk 2.6-208
Table 2.6.13.4-1 $P_m + P_b$ Stresses for Support Disk -1-Foot End-Drop, Thermal Case A 2.6-214
Table 2.6.13.4-2 $P_m + P_b$ Stresses for Support Disk -1-Foot End-Drop, Thermal Case B 2.6-215
Table 2.6.13.5-1 $P_m + P_b + Q$ Stresses for Support Disk—1-Foot End-Drop, Thermal Case A 2.6-218
Table 2.6.13.6-2 P_m Stresses for Support Disk—1-Foot Side-Drop, 0° Orientation, Thermal Case A 2.6-226
Table 2.6.13.6-3 $P_m + P_b$ Stresses for Support Disk—1-Foot Side-Drop, 0° Orientation, Thermal Case A 2.6-227
Table 2.6.13.6-4 P_m Stresses for Support Disk—1-Foot Side-Drop, 0° Orientation, Thermal Case B 2.6-228
Table 2.6.13.6-5 $P_m + P_b$ Stresses for Support Disk—1-Foot Side-Drop, 0° Orientation, Thermal Case B 2.6-229
Table 2.6.13.6-6 P_m Stresses for Support Disk—1-Foot Side-Drop, 18.22° Orientation, Thermal Case A 2.6-230
Table 2.6.13.6-7 $P_m + P_b$ Stresses for Support Disk—1-Foot Side-Drop, 18.22° Orientation, Thermal Case A 2.6-231
Table 2.6.13.6-8 P_m Stresses for Support Disk—1-Foot Side-Drop, 18.22° Orientation, Thermal Case B 2.6-232
Table 2.6.13.6-9 $P_m + P_b$ Stresses for Support Disk—1-Foot Side-Drop, 18.22° Orientation, Thermal Case B 2.6-233
Table 2.6.13.6-10 P_m Stresses for Support Disk—1-Foot Side-Drop, 26.28° Orientation, Thermal Case A 2.6-234

List of Tables (Continued)

Table 2.6.13.6-11 $P_m + P_b$ Stresses for Support Disk—1-Foot Side-Drop, 26.28° Orientation, Thermal Case A 2.6-235
Table 2.6.13.6-12 P_m Stresses for Support Disk—1-Foot Side-Drop, 26.28° Orientation, Thermal Case B 2.6-236
Table 2.6.13.6-13 $P_m + P_b$ Stresses for Support Disk—1-Foot Side-Drop, 26.28° Orientation, Thermal Case B 2.6-237
Table 2.6.13.6-14 P_m Stresses for Support Disk—1-Foot Side-Drop, 45° Orientation, Thermal Case A 2.6-238
Table 2.6.13.6-15 $P_m + P_b$ Stresses for Support Disk—1-Foot Side-Drop, 45° Orientation, Thermal Case A 2.6-239
Table 2.6.13.6-16 P_m Stresses for Support Disk—1-Foot Side-Drop, 45° Orientation, Thermal Case B 2.6-240
Table 2.6.13.6-17 $P_m + P_b$ Stresses for Support Disk —1-Foot Side-Drop, 45° Orientation, Thermal Case B 2.6-241
Table 2.6.13.7-1 $P_m + P_b + Q$ Stresses for Support Disk—1-Foot Side-Drop, 0° Orientation, Thermal Case A 2.6-243
Table 2.6.13.7-2 $P_m + P_b + Q$ Stresses for Support Disk—1-Foot Side-Drop, 18.22° Orientation, Thermal Case A 2.6-244
Table 2.6.13.7-3 $P_m + P_b + Q$ Stresses for Support Disk—1-Foot Side-Drop, 26.28° Orientation, Thermal Case A 2.6-245
Table 2.6.13.7-4 $P_m + P_b + Q$ Stresses for Support Disk—1-Foot Side-Drop, 45° Orientation, Thermal Case A 2.6-246
Table 2.6.13.13-1 Minimum Margins of Safety for the Top/Bottom Weldments for 1-Foot End-Drop 2.6-254
Table 2.6.13.14-1 Minimum Margins of Safety from Buckling Evaluation of PWR Support Disk 2.6-260

Table 2.6.14.2-1 Real Constant Sets Defined in Canister Model 2.6-272
Table 2.6.14.2-2 Material Sets Defined in Canister Model 2.6-272
Table 2.6.14.3-1 BWR Canister Linearized Q Stresses - Thermal Only (Hot 1) 2.6-276
Table 2.6.14.3-2 BWR Canister Linearized Q Stresses - Thermal Only (Cold 2) 2.6-277
Table 2.6.14.4-1 BWR Canister Critical Sections for the 1-Foot End-Drop Condition . 2.6-279
Table 2.6.14.4-2 BWR Canister P_m Stresses - Internal Pressure 2.6-280

List of Tables (Continued)

Table 2.6.14.4-3 BWR Canister $P_m + P_b$ Stresses - Internal Pressure 2.6-281
Table 2.6.14.4-4 BWR Canister P_m Stresses - 1-Foot Top End-Drop 2.6-282
Table 2.6.14.4-5 BWR Canister $P_m + P_b$ Stresses - 1-Foot Top End-Drop 2.6-283
Table 2.6.14.4-6 BWR Canister P_m Stresses - 1-Foot Bottom End-Drop, Internal Pressure 2.6-284
Table 2.6.14.4-7 BWR Canister $P_m + P_b$ Stresses - 1-Foot Bottom End-Drop, Internal Pressure 2.6-285
Table 2.6.14.5-1 BWR Canister Critical Sections for the Combined 1-Foot End-Drop and Thermal Load Condition 2.6-287
Table 2.6.14.5-2 BWR Canister $P_m + P_b + Q$ Stresses - 1-Foot Top End-Drop, Thermal Cold 2.6-288
Table 2.6.14.5-3 BWR Canister $P_m + P_b + Q$ Stresses - 1-Foot Top End-Drop, Thermal Heat 2.6-289
Table 2.6.14.5-4 BWR Canister $P_m + P_b + Q$ Stresses - 1-Foot Bottom End-Drop, Thermal Cold 2.6-290
Table 2.6.14.5-5 BWR Canister $P_m + P_b + Q$ Stresses - 1-Foot Bottom End-Drop, Thermal Heat 2.6-291
Table 2.6.14.6-1 BWR Canister Critical Sections for the 1-Foot Side-Drop Load Condition 2.6-294
Table 2.6.14.6-2 BWR Canister P_m Stresses - 1-Foot Side-Drop 2.6-295
Table 2.6.14.6-3 BWR Canister $P_m + P_b$ Stresses - 1-Foot Side-Drop, Internal Pressure 2.6-296
Table 2.6.14.7-1 BWR Canister Critical Sections for the Combined 1-Foot Side-Drop and Thermal Load Condition 2.6-298
Table 2.6.14.7-2 BWR Canister $P_m + P_b + Q$ Stresses - 1-Foot Side-Drop, Thermal Cold 2.6-299
Table 2.6.14.7-3 BWR Canister $P_m + P_b + Q$ Stresses - 1-Foot Side-Drop, Thermal Heat 2.6-300
Table 2.6.14.8-1 BWR Canister Critical Sections for the 1-Foot Corner-Drop Load Condition 2.6-302
Table 2.6.14.8-2 BWR Canister P_m Stresses - 1-Foot Top Corner-Drop, Internal Pressure 2.6-303

List of Tables (Continued)

Table 2.6.14.8-3 BWR Canister $P_m + P_b$ Stresses - 1-Foot Top Corner Drop 2.6-304
Table 2.6.14.8-4 BWR Canister P_m Stresses - 1-Foot Bottom Corner-Drop, Internal Pressure 2.6-305
Table 2.6.14.8-5 BWR Canister $P_m + P_b$ Stresses - 1-Foot Bottom Corner-Drop..... 2.6-306
Table 2.6.14.9-1 BWR Canister Critical Sections for the Combined 1-Foot Corner-Drop and Thermal Load Condition 2.6-308
Table 2.6.14.9-2 BWR Canister $P_m + P_b + Q$ Stresses - 1-Foot Top Corner-Drop, Thermal Cold 2.6-309
Table 2.6.14.9-3 BWR Canister $P_m + P_b + Q$ Stresses - 1-Foot Top Corner-Drop, Thermal Heat..... 2.6-310
Table 2.6.14.9-4 BWR Canister $P_m + P_b + Q$ Stresses - 1-Foot Bottom Corner Drop, Internal Pressure, Thermal Cold 2.6-311
Table 2.6.14.9-5 BWR Canister $P_m + P_b + Q$ Stresses - 1-Foot Bottom Corner Drop, Thermal Heat..... 2.6-312
Table 2.6.14.12-1 Geometry Parameters for the BWR Canister 2.6-315
Table 2.6.14.12-2 Buckling Evaluation Results for the BWR Canister for 1-Foot End-Drop 2.6-316
Table 2.6.15.4-1 $P_m + P_b$ Stresses for Support Disk 1-Foot End-Drop, Thermal Case 1 ..... 2.6-329
Table 2.6.15.4-2 $P_m + P_b$ Stresses for Support Disk 1-Foot End-Drop, Thermal Case 4 ..... 2.6-330
Table 2.6.15.5-1 $P_m + P_b + Q$ Stresses for Support Disk 1-Foot End-Drop, Thermal Case 4 ..... 2.6-333
Table 2.6.15.6-1 Listing of Cross Sections for the Stress Evaluation of Support Disk 2.6-347
Table 2.6.15.6-2 P_m Stresses for Support Disk—1-Foot Side-Drop, 0° Orientation, Thermal Case 1 ..... 2.6-355
Table 2.6.15.6-3 $P_m + P_b$ Stresses for Support Disk—1-Foot Side-Drop, 0° Orientation, Thermal Case 1 ..... 2.6-356
Table 2.6.15.6-4 P_m Stresses for Support Disk—1-Foot Side-Drop, 0° Orientation, Thermal Case 2 ..... 2.6-357
Table 2.6.15.6-5 $P_m + P_b$ Stresses for Support Disk—1-Foot Side-Drop, 0° Orientation, Thermal Case 2 ..... 2.6-358

List of Tables (Continued)

Table 2.6.15.6-6 P_m Stresses for Support Disk—1-Foot Side-Drop, 31.82° Orientation, Thermal Case 1 ..... 2.6-359
Table 2.6.15.6-7 $P_m + P_b$ Stresses for Support Disk—1-Foot Side-Drop, 31.82° Orientation, Thermal Case 1 ..... 2.6-360
Table 2.6.15.6-8 P_m Stresses for Support Disk—1-Foot Side-Drop, 31.82° Orientation, Thermal Case 2 ..... 2.6-361
Table 2.6.15.6-9 $P_m + P_b$ Stresses for Support Disk—1-Foot Side-Drop, 31.82° Orientation, Thermal Case 2 ..... 2.6-362
Table 2.6.15.6-10 P_m Stresses for Support Disk—1-Foot Side-Drop, 49.46° Orientation, Thermal Case 1 ..... 2.6-363
Table 2.6.15.6-11 $P_m + P_b$ Stresses for Support Disk—1-Foot Side-Drop, 49.46° Orientation, Thermal Case 1 ..... 2.6-364
Table 2.6.15.6-12 P_m Stresses for Support Disk—1-Foot Side-Drop, 49.46° Orientation, Thermal Case 2 ..... 2.6-365
Table 2.6.15.6-13 $P_m + P_b$ Stresses for Support Disk—1-Foot Side-Drop, 49.46° Orientation, Thermal Case 2 ..... 2.6-366
Table 2.6.15.6-14 P_m Stresses for Support Disk—1-Foot Side-Drop, 77.92° Orientation, Thermal Case 1 ..... 2.6-367
Table 2.6.15.6-15 $P_m + P_b$ Stresses for Support Disk—1-Foot Side-Drop, 77.92° Orientation, Thermal Case 1 ..... 2.6-368
Table 2.6.15.6-16 P_m Stresses for Support Disk—1-Foot Side-Drop, 77.92° Orientation, Thermal Case 2 ..... 2.6-369
Table 2.6.15.6-17 $P_m + P_b$ Stresses for Support Disk—1-Foot Side-Drop, 77.92° Orientation, Thermal Case 2 ..... 2.6-370
Table 2.6.15.6-18 P_m Stresses for Support Disk—1-Foot Side-Drop, 90° Orientation, Thermal Case 1 ..... 2.6-371
Table 2.6.15.6-19 $P_m + P_b$ Stresses for Support Disk—1-Foot Side-Drop, 90° Orientation, Thermal Case 1 ..... 2.6-372
Table 2.6.15.6-20 P_m Stresses for Support Disk—1-Foot Side-Drop, 90° Orientation, Thermal Case 2 ..... 2.6-373
Table 2.6.15.6-21 $P_m + P_b$ Stresses for Support Disk—1-Foot Side-Drop, 90° Orientation, Thermal Case 2 ..... 2.6-374

List of Tables (Continued)

Table 2.6.15.7-1 $P_m + P_b + Q$ Stresses for Support Disk -1-Foot Side-Drop, 0° Orientation, Thermal Case 2 ..... 2.6-376
Table 2.6.15.7-2 $P_m + P_b + Q$ Stresses for Support Disk -1-Foot Side-Drop, 31.82° Orientation, Thermal Case 2 ..... 2.6-377
Table 2.6.15.7-3 $P_m + P_b + Q$ Stresses for Support Disk -1-Foot Side-Drop, 49.46° Orientation, Thermal Case 2 ..... 2.6-378
Table 2.6.15.7-4 $P_m + P_b + Q$ Stresses for Support Disk -1-Foot Side-Drop, 77.92° Orientation, Thermal Case 2 ..... 2.6-379
Table 2.6.15.7-5 $P_m + P_b + Q$ Stresses for Support Disk -1-Foot Side-Drop, 90° Orientation, Thermal Case 2 ..... 2.6-380
Table 2.6.15.13-1 Minimum Margins of Safety for the Top/Bottom Weldments for a 1-Foot End-Drop With and Without Thermal Stresses 2.6-386
Table 2.6.15.14-1 Minimum Margins of Safety from Buckling Evaluation of BWR Support Disk (Weak Axis) 2.6-394
Table 2.6.15.14-2 Minimum Margins of Safety from Buckling Evaluation of BWR Support Disk (Strong Axis) 2.6-395
Table 2.7.1.1-1 P_m Stresses—30-Foot Top End-Drop, Thermal Condition 1 ..... 2.7-5
Table 2.7.1.1-2 $P_m + P_b$ Stresses—30-Foot Top End-Drop, Thermal Condition 1 ..... 2.7-6
Table 2.7.1.1-3 Critical P_m Stress Summary—30-Foot Top End-Drop, Thermal Condition 1 ..... 2.7-7
Table 2.7.1.1-4 Critical $P_m + P_b$ Stress Summary—30-Foot Top End-Drop, Thermal Condition 1 ..... 2.7-7
Table 2.7.1.1-5 P_m Stresses—30-Foot Bottom End-Drop, Thermal Condition 1 ..... 2.7-8
Table 2.7.1.1-6 $P_m + P_b$ Stresses—30-Foot Bottom End-Drop, Thermal Condition 1 ..... 2.7-9
Table 2.7.1.1-7 Critical P_m Stress Summary—30-Foot Bottom End-Drop, Thermal Condition 1 ..... 2.7-10
Table 2.7.1.1-8 Critical $P_m + P_b$ Stress Summary—30-Foot Bottom End-Drop, Thermal Condition 1 ..... 2.7-10
Table 2.7.1.2-1 P_m Stresses—30-Foot Side-Drop, Thermal Condition 1 ..... 2.7-12
Table 2.7.1.2-2 $P_m + P_b$ Stresses—30-Foot Side-Drop, Thermal Condition 1 ..... 2.7-13
Table 2.7.1.2-3 Critical P_m Stress Summary—30-Foot Side-Drop, Thermal Condition 1 ..... 2.7-14

List of Tables (Continued)

Table 2.7.1.2-4 Critical $P_m + P_b$ Stress Summary—30-Foot Side-Drop, Thermal Condition 1 ..... 2.7-14
Table 2.7.1.3-1 P_m Stresses—30-Foot Top Corner-Drop, Thermal Condition 1 ..... 2.7-16
Table 2.7.1.3-2 $P_m + P_b$ Stresses—30-Foot Top Corner-Drop, Thermal Condition 1 ..... 2.7-17
Table 2.7.1.3-3 Critical P_m Stress Summary—30-Foot Top Corner-Drop, Thermal Condition 1 ..... 2.7-18
Table 2.7.1.3-4 Critical $P_m + P_b$ Stress Summary—30-Foot Top Corner-Drop, Thermal Condition 1 ..... 2.7-18
Table 2.7.1.3-5 P_m Stresses—30-Foot Bottom Corner-Drop, Thermal Condition 1 ..... 2.7-19
Table 2.7.1.3-6 $P_m + P_b$ Stresses—30-Foot Bottom Corner-Drop, Thermal Condition 1 ..... 2.7-20
Table 2.7.1.3-7 Critical P_m Stress Summary—30-Foot Bottom Corner-Drop, Thermal Condition 1 ..... 2.7-21
Table 2.7.1.3-8 Critical $P_m + P_b$ Stress Summary—30-Foot Bottom Corner-Drop, Thermal Condition 1 ..... 2.7-21
Table 2.7.1.4-1 P_m Stresses—30-Foot Top 75° Oblique-Drop, Thermal Condition 1 ... 2.7-23
Table 2.7.1.4-2 $P_m + P_b$ Stresses—30-Foot Top 75° Oblique-Drop, Thermal Condition 1 ..... 2.7-24
Table 2.7.1.4-3 Critical P_m Stress Summary—30-Foot Top 75° Oblique-Drop, Thermal Condition 1 ..... 2.7-25
Table 2.7.1.4-4 Critical $P_m + P_b$ Stress Summary—30-Foot Top 75° Oblique-Drop, Thermal Condition 1 ..... 2.7-25
Table 2.7.1.4-5 P_m Stresses—30-Foot Bottom 75° Oblique-Drop, Thermal Condition 1 ..... 2.7-26
Table 2.7.1.4-6 $P_m + P_b$ Stresses—30-Foot Bottom 75° Oblique-Drop, Thermal Condition 1 ..... 2.7-27
Table 2.7.1.4-7 Critical P_m Stress Summary—30-Foot Bottom 75° Oblique-Drop, Thermal Condition 1 ..... 2.7-28
Table 2.7.1.4-8 Critical $P_m + P_b$ Stress Summary—30-Foot Bottom 75° Oblique-Drop, Thermal Condition 1 ..... 2.7-28
Table 2.7.1.5-1 Lead Slump Calculation Parameters 2.7-32
Table 2.7.2.1-1 Local Membrane Stresses - Puncture Cask Side 2.7-46
Table 2.7.2.1-2 Stress Evaluation - Puncture Cask Side 2.7-47

List of Tables (Continued)

Table 2.7.2.3-1 Cask Bottom Puncture Stresses 2.7-58
Table 2.7.2.3-2 Puncture Stress Evaluation Results 2.7-59
Table 2.7.3.1-1 Maximum Component Temperatures - Hypothetical Accident Conditions Fire Accident (PWR Cask) 2.7-63
Table 2.7.3.1-2 Maximum Component Temperatures—Hypothetical Accident Conditions Fire Accident (BWR Cask) 2.7-64
Table 2.7.3.1-3 Summary of Maximum Canister Pressures During Hypothetical Accident Conditions 2.7-65
Table 2.7.3.1-4 Summary of Maximum Cask Cavity Pressures During Hypothetical Accident Conditions 2.7-65
Table 2.7.7.2-1 PWR Canister P_m Stresses - 30-Foot Side-Drop - 45° Basket Orientation 2.7-77
Table 2.7.7.2-2 PWR Canister $P_m + P_b$ Stresses - 30-Foot Side-Drop - 45° Basket Orientation 2.7-78
Table 2.7.7.2-3 PWR Canister P_m Stresses - 30-Foot Bottom End-Drop - Internal Pressure 2.7-79
Table 2.7.7.2-4 PWR Canister $P_m + P_b$ Stresses - 30-Foot Bottom End-Drop - Internal Pressure 2.7-80
Table 2.7.7.2-5 PWR Canister P_m Stresses - 30-Foot Top End-Drop 2.7-81
Table 2.7.7.2-6 PWR Canister $P_m + P_b$ Stresses - 30-Foot Top End-Drop 2.7-82
Table 2.7.7.2-7 PWR Canister P_m Stresses - 30-Foot Bottom Corner-Drop 2.7-83
Table 2.7.7.2-8 PWR Canister $P_m + P_b$ Stresses - 30-Foot Bottom Corner-Drop 2.7-84
Table 2.7.7.2-9 PWR Canister P_m Stresses - 30-Foot Top Corner- Drop 2.7-85
Table 2.7.7.2-10 PWR Canister $P_m + P_b$ Stresses - 30-Foot Top Corner-Drop 2.7-86
Table 2.7.7.2-11 Summary of Minimum Margins of Safety for PWR Canister - 30-Foot Drops 2.7-87
Table 2.7.7.3-1 Buckling Evaluation Results for the PWR Canister for 30-Foot End Drop 2.7-90
Table 2.7.8.1-1 Summary of Stress Evaluation of Support Disk—30-Foot Side-Drop 2.7-95
Table 2.7.8.1-2 P_m Stresses for Support Disk—30-Foot Side-Drop, 0° Orientation, Thermal Case A 2.7-96

List of Tables (Continued)

Table 2.7.8.1-3 $P_m + P_b$ Stresses for Support Disk—30-Foot Side-Drop, 0° Orientation, Thermal Case A 2.7-97
Table 2.7.8.1-4 P_m Stresses for Support Disk—30-Foot Side-Drop, 0° Orientation, Thermal Case B 2.7-98
Table 2.7.8.1-5 $P_m + P_b$ Stresses for Support Disk—30-Foot Side-Drop, 0° Orientation, Thermal Case B 2.7-99
Table 2.7.8.1-6 P_m Stresses for Support Disk—30-Foot Side-Drop, 18.22° Orientation, Thermal Case A 2.7-100
Table 2.7.8.1-7 $P_m + P_b$ Stresses for Support Disk—30-Foot Side-Drop, 18.22° Orientation, Thermal Case A 2.7-101
Table 2.7.8.1-8 P_m Stresses for Support Disk—30-Foot Side-Drop, 18.22° Orientation, Thermal Case B 2.7-102
Table 2.7.8.1-9 $P_m + P_b$ Stresses for Support Disk—30-Foot Side-Drop, 18.22° Orientation, Thermal Case B 2.7-103
Table 2.7.8.1-10 P_m Stresses for Support Disk—30-Foot Side-Drop, 26.28° Orientation, Thermal Case A 2.7-104
Table 2.7.8.1-11 $P_m + P_b$ Stresses for Support Disk—30-Foot Side-Drop, 26.28° Orientation, Thermal Case A 2.7-105
Table 2.7.8.1-12 P_m Stresses for Support Disk—30-Foot Side-Drop, 26.28° Orientation, Thermal Case B 2.7-106
Table 2.7.8.1-13 $P_m + P_b$ Stresses for Support Disk—30-Foot Side-Drop, 26.28° Orientation, Thermal Case B 2.7-107
Table 2.7.8.1-14 P_m Stresses for Support Disk—30-Foot Side-Drop, 45° Orientation, Thermal Case A 2.7-108
Table 2.7.8.1-15 $P_m + P_b$ Stresses for Support Disk—30-Foot Side-Drop, 45° Orientation, Thermal Case A 2.7-109
Table 2.7.8.1-16 P_m Stresses for Support Disk—30-Foot Side-Drop, 45° Orientation, Thermal Case B 2.7-110
Table 2.7.8.1-17 $P_m + P_b$ Stresses for Support Disk—30-Foot Side-Drop, 45° Orientation, Thermal Case B 2.7-111
Table 2.7.8.1-18 Summary of Stress Evaluation of Support Disk—30-Ft End-Drop 2.7-112

List of Tables (Continued)

Table 2.7.8.1-19 $P_m + P_b$ Stresses for Support Disk—30-Ft End-Drop, Thermal Case A 2.7-113
Table 2.7.8.1-20 $P_m + P_b$ Stresses for Support Disk—30-Foot End-Drop, Thermal Case B 2.7-114
Table 2.7.8.1-21 Summary of Stress Evaluation of Support Disk—30-Ft Oblique Drop 2.7-115

Table 2.7.9.2-1 BWR Canister P_m Stresses - 30-Foot Side Drop 2.7-140
Table 2.7.9.2-2 BWR Canister $P_m + P_b$ Stresses - 30-Foot Side Drop 2.7-141
Table 2.7.9.2-3 BWR Canister P_m Stresses - 30-Foot Bottom End-Drop, Internal Pressure 2.7-142
Table 2.7.9.2-4 BWR Canister $P_m + P_b$ Stresses - 30-Foot Bottom End-Drop, Internal Pressure 2.7-143
Table 2.7.9.2-5 BWR Canister P_m Stresses - 30-Foot Top-End Drop 2.7-144
Table 2.7.9.2-6 BWR Canister $P_m + P_b$ Stresses - 30-Foot Top-End Drop 2.7-145
Table 2.7.9.2-7 BWR Canister P_m Stresses - 30-Foot Bottom-Corner Drop 2.7-146
Table 2.7.9.2-8 BWR Canister $P_m + P_b$ Stresses - 30-Foot Bottom-Corner Drop 2.7-147
Table 2.7.9.2-9 BWR Canister P_m Stresses - 30-Foot Top-Corner Drop, Internal Pressure 2.7-148
Table 2.7.9.2-10 BWR Canister $P_m + P_b$ Stresses - 30-Foot Top-Corner Drop 2.7-149
Table 2.7.9.2-11 Summary of Minimum Margins of Safety for BWR Canister - 30-Foot Drops 2.7-150
Table 2.7.9.3-1 Buckling Evaluation Results for the BWR Canister for 30-Foot End-Drop 2.7-152
Table 2.7.10.1-1 Summary of Stress Evaluation of Support Disk - 30-Foot Side-Drop 2.7-157
Table 2.7.10.1-2 P_m Stresses for Support Disk 30-Foot Side-Drop, 0° Orientation, Thermal Case 1 ..... 2.7-158
Table 2.7.10.1-3 $P_m + P_b$ Stresses for Support Disk 30-Foot Side-Drop, 0° Orientation, Thermal Case 1 ..... 2.7-159
Table 2.7.10.1-4 P_m Stresses for Support Disk 30-Foot Side-Drop, 0° Orientation, Thermal Case 2 ..... 2.7-160

List of Tables (Continued)

Table 2.7.10.1-5 $P_m + P_b$ Stresses for Support Disk 30-Foot Side-Drop, 0° Orientation, Thermal Case 2 ..... 2.7-161
Table 2.7.10.1-6 P_m Stresses for Support Disk 30-Foot Side-Drop, 31.82° Orientation, Thermal Case 1 ..... 2.7-162
Table 2.7.10.1-7 $P_m + P_b$ Stresses for Support Disk 30-Foot Side-Drop, 31.82° Orientation, Thermal Case 1 ..... 2.7-163
Table 2.7.10.1-8 P_m Stresses for Support Disk 30-Foot Side-Drop, 31.82° Orientation, Thermal Case 2 ..... 2.7-164
Table 2.7.10.1-9 $P_m + P_b$ Stresses for Support Disk 30-Foot Side-Drop, 31.82° Orientation, Thermal Case 2 ..... 2.7-165
Table 2.7.10.1-10 P_m Stresses for Support Disk 30-Foot Side-Drop, 49.46° Orientation, Thermal Case 1 ..... 2.7-166
Table 2.7.10.1-11 $P_m + P_b$ Stresses for Support Disk 30-Foot Side-Drop, 49.46° Orientation, Thermal Case 1 ..... 2.7-167
Table 2.7.10.1-12 P_m Stresses for Support Disk 30-Foot Side-Drop, 49.46° Orientation, Thermal Case 2 ..... 2.7-168
Table 2.7.10.1-13 $P_m + P_b$ Stresses for Support Disk 30-Foot Side-Drop, 49.46° Orientation, Thermal Case 2 ..... 2.7-169
Table 2.7.10.1-14 P_m Stresses for Support Disk 30-Foot Side-Drop, 77.92° Orientation, Thermal Case 1 ..... 2.7-170
Table 2.7.10.1-15 $P_m + P_b$ Stresses for Support Disk 30-Foot Side-Drop, 77.92° Orientation, Thermal Case 1 ..... 2.7-171
Table 2.7.10.1-16 P_m Stresses for Support Disk 30-Foot Side-Drop, 77.92° Orientation, Thermal Case 2 ..... 2.7-172
Table 2.7.10.1-17 $P_m + P_b$ Stresses for Support Disk 30-Foot Side-Drop, 77.92° Orientation, Thermal Case 2 ..... 2.7-173
Table 2.7.10.1-18 P_m Stresses for Support Disk 30-Foot Side-Drop, 90° Orientation, Thermal Case 1 ..... 2.7-174
Table 2.7.10.1-19 $P_m + P_b$ Stresses for Support Disk 30-Foot Side-Drop, 90° Orientation, Thermal Case 1 ..... 2.7-175
Table 2.7.10.1-20 P_m Stresses for Support Disk 30-Foot Side-Drop, 90° Orientation, Thermal Case 2 ..... 2.7-176

List of Tables (Continued)

Table 2.7.10.1-21 $P_m + P_b$ Stresses for Support Disk 30-Foot Side-Drop, 90° Orientation, Thermal Case 2 ..... 2.7-177
Table 2.7.10.1-22 Summary of Stress Evaluation of Support Disk - 30-Foot End-Drop 2.7-178
Table 2.7.10.1-23 $P_m + P_b$ Stresses for Support Disk 30-Foot End-Drop, Thermal Case 1 ..... 2.7-179
Table 2.7.10.1-24 $P_m + P_b$ Stresses for Support Disk -30-Foot End-Drop, Thermal Case 4 ..... 2.7-180
Table 2.7.10.3-1 Minimum Margins of Safety from Buckling Evaluation of BWR Support Disk (Weak Axis) 2.7-187
Table 2.7.10.3-2 Minimum Margins of Safety from Buckling Evaluation of BWR Support Disk (Strong Axis) 2.7-188
Table 2.7.11-1 Summary of Maximum Calculated Stresses in Cask 30-Foot Free Drop 2.7-199
Table 2.7.11-2 Summary of Maximum Calculated Stresses in Cask—Puncture 2.7-200
Table 2.7.12-1 Buckling Evaluation Load Cases and Results for the Universal Transport Cask 2.7-210
Table 2.7.12-2 Geometry Parameters for the Universal Transport Cask 2.7-211
Table 2.9-1 Location of Lateral Constraints – PWR Fuel Rods 2.9-8
Table 2.9-2 PWR Fuel Rod Analysis Summary 2.9-8
Table 2.9-3 Location of Lateral Constraint for BWR Fuel Rods 2.9-9
Table 2.9-4 BWR Fuel Rod Analysis Summary 2.9-9
Table 2.10.2.2-1 Component Section and Temperature Definition 2.10.2-16
Table 2.10.2.2-2 Stress Section Locations 2.10.2-17
Table 2.10.4.1-1 Response Acceleration for PWR Support Disk for 1-Foot End Drop 2.10.4-5
Table 2.10.4.1-2 Response Acceleration for BWR Support Disk for 1-Foot End Drop 2.10.4-6
Table 2.10.4.2-1 Response Acceleration for PWR Support Disk for 1-Foot Side Drop 2.10.4-14
Table 2.10.4.2-2 Response Acceleration for BWR Support Disk for 1-Foot Side Drop 2.10.4-15

List of Tables (Continued)

Table 2.11.1.1-1 Normalized Stress Ratios – UMS® PWR Basket Support Disk Sectional Stresses Due to Maine Yankee Consolidated Fuel to the Design Basis PWR Fuel Basket Maximum Stresses (Base Case) 2.11.1-5

Table 2.11.1.1-2 P_m Stresses for Support Disk—1-Foot Side Drop, 45° Orientation, Thermal Case B, Structural Case 1 ..... 2.11.1-6

Table 2.11.1.1-3 $P_m + P_b$ Stresses for Support Disk—1-Foot Side Drop, 45° Orientation, Thermal Case B, Structural Case 1 ..... 2.11.1-7

Table 2.11.2.1-1 Maine Yankee GTCC Basket Weldment Sectional Stresses for Normal Condition Side Drop (ksi) 2.11.2-27

Table 2.11.2.1-2 Maine Yankee GTCC Basket Weldment Sectional Stresses for Accident Condition Side Drop (ksi) 2.11.2-27

Table 2.11.2.1-3 Summary of Maine Yankee GTCC Basket Weldment Side Drop Stress Evaluation 2.11.2-28

Table 2.11.2.1-4 Evaluation of the Weld Between the Shield Cylinder and Support Disk 2.11.2-28

2.0 STRUCTURAL EVALUATION

This chapter presents the structural analyses of the Universal Transport Cask. The results of the analyses demonstrate that the package satisfies the requirements of 10 CFR 71 [1], specifically, Subpart E, "Package Approval Standards," and Subpart F, "Package and Special Form Tests." The results show that containment is not breached under any of the normal conditions of transport or the hypothetical accident conditions specified in 10 CFR 71 (April 1, 1996). Since 10 CFR 71 includes essentially all of the IAEA Safety Series No. 6 requirements [2], only minor additional analyses were required to demonstrate that the packaging also complies with the IAEA Safety Series No. 6 requirements. These analyses were performed.

In the structural analyses presented herein, state-of-the-art methods are used to calculate stresses in large structures subject to steady-state and transient loadings. The evaluation of the structural characteristics of the containment boundary is based on a conservative interpretation of the requirements of Section III of the ASME Boiler and Pressure Vessel Code, Nuclear Power Plant Components. The ASME Boiler and Pressure Vessel Code is the recognized standard for pressure vessel analysis, mechanical properties of materials, and allowable stress values.

Analyses are performed for the principal structural components of the Universal Transport Cask under normal conditions of transport and hypothetical accident conditions specified in 10 CFR 71.

THIS PAGE INTENTIONALLY LEFT BLANK

2.1 Structural Design

2.1.1 Discussion

The transportation component of the Universal MPC System® consists of a Universal Transport Cask containing a welded Transportable Storage Canister . The canister assembly includes a canister and a basket loaded with PWR or BWR spent fuel **or Greater Than Class C (GTCC) waste.** The impact limiters attached to the top and bottom of the cask protect the cask and contents from damage resulting from impacts that could occur during transport. These principal components **of the Universal MPC System are described in this section.**

2.1.1.1 Universal Transport Cask

The Universal Transport Cask is a cylindrical, multiwalled cask designed to safely transport a canister containing 24 PWR fuel assemblies, 56 BWR fuel assemblies **or GTCC waste.** The primary components of the cask are **the**:

1. Cask body (inner shell, outer shell, lead gamma shielding, and cask bottom)
2. Cask lid, bolts, and O-rings
3. Port covers, port coverplates, bolts, and O-rings
4. Neutron shield
5. Lifting trunnions and rotation pockets
6. Impact limiters (upper and lower)

The cask primary containment boundary consists of the (1) inner shell; (2) bottom forging; (3) top forging; (4) cask lid, and lid inner O-ring; (5) vent port coverplate, and vent port coverplate inner O-ring; (6) drain port coverplate, and drain port coverplate inner O-ring. A detailed discussion of the containment boundary is presented in Chapter 4.0. The geometry and materials of fabrication of the cask components are described in Section 1.2.1 and **are** shown on the License Drawings presented in Section 1.3.4.

The Universal Transport Cask body supports and protects the cask cavity contents for the normal conditions of transport and the hypothetical accident conditions. The lead located between the cask inner and outer shells provides the primary gamma radiation shielding for the cask in the radial direction. The bottom plate closes the cask bottom end and provides axial gamma radiation shielding. The bottom plate traps a layer of NS-4-FR, which provides neutron radiation shielding in the axial direction. The cask lid, bolts, and O-rings are the primary closure components of the cask.

The vent port is located in the cask lid and the drain port is located in the bottom forging. Each port is protected by a port coverplate. The primary containment boundary at the vent port and at the drain port is the port coverplate and its inner O-ring. The O-ring is located on the bottom surface of the port coverplate. A second O-ring is also located on the bottom surface of the port coverplate outside of, and concentric with, the primary containment inner O-ring. Each port cover has a test port that penetrates the region between the O-rings to enable leak testing of the O-rings using the interseal region. The inner O-ring is tested by pressurizing the cask cavity with helium and using a helium leak detector at the test ports in the cask lid and in the port coverplates. The outer O-rings are tested by pressurizing the interseal regions with helium and using a helium leak detector around the edge of the cask lid and the two port coverplates.

The cask lid, bolts, and outer O-ring provide the primary containment boundary. The lid is secured to the top forging by 48 bolts (2–8 UN-2A bolts) preloaded by an installation torque to restrain rotation of the edge of the lid and to maintain a containment seal for the critical load condition. The critical load condition is a uniformly distributed pressure resulting from the impact of the canister and cavity contents on the inner surface of the lid during a top-end or top-corner impact.

The neutron shielding material, NS-4-FR, is installed in the annulus that surrounds the cask outer shell along the length of the cask cavity and between the bottom forging and the bottom plate. NS-4-FR is a solid, synthetic polymer that absorbs the neutron radiation emitted by the cask contents.

Four lifting trunnions, two primary and two secondary, are provided on the outside of the top forging at 90-degree intervals. Two diametrically opposed primary trunnions are welded into 2.0-in. deep recesses in the top forging. The two secondary trunnions are bolted to the top

forging when redundant lifts are performed. The purpose of the trunnions is to enable lifting and handling of the cask. Two types of lifting systems may be used: redundant (four trunnions) or nonredundant (two trunnions). The lifting trunnions are designed to satisfy the heavy lifting requirements of NUREG-0612 [3] and attendant standard ANSI N14.6 [4] for a nonredundant lift using the two primary lifting trunnions or a redundant lift using all four of the lifting trunnions, as well as the requirements of 10 CFR 71.45(a) and Paragraph 506 of IAEA Safety Series No. 6. Analyses show that overload failure of the trunnions will not impair the ability of the cask body to continue to perform its function.

Two rotation pockets are welded to the outer shell near the bottom of the cask. Neutron shield material is displaced to accommodate the placement of the rotation pockets, which are used to support the bottom of the cask on the shipping frame and also, as a pivot point to rotate the cask from the vertical lifting position to the horizontal position and vice versa. The rotation pocket design prevents lateral and rearward movement of the cask. The pocket welds are designed to fail in shear before the outer shell fails, thereby enabling the cask to continue to perform its primary function.

Forward movement of the cask is prevented by the shear ring welded to the top forging of the cask. In the transport configuration, forward axial loads from the cask are passed through to the support frame where the shear ring contacts the frame. The shear ring welds are designed to fail in shear before the top forging, minimizing the damage to the cask, enabling the cask body to perform its primary function.

2.1.1.2 Transportable Storage Canister

The Transportable Storage Canister Assembly consists of a stainless steel canister shell assembly, a shield lid, and a structural lid. The shell assembly is a cylindrical shell welded to a bottom plate and a shield lid support ring welded to the interior of the canister shell. The shell assembly with both the shield and structural lid welded in place provides a double welded canister closure system for the fuel assemblies loaded in the basket. The canister assembly provides confinement for the spent fuel during storage. No credit is taken for the canister containment function during transport operations.

A basket assembly, as described in Section 2.1.1.3, is positioned inside the shell assembly. The basket structure locates and supports the basket contents. There are two basket designs, each of which is designed to accommodate either intact PWR or BWR fuel assemblies. The transportable storage canister assembly is moved in a transfer cask during fuel-loading operations. The shield and structural lids are welded to the canister shell while the loaded canister is in the transfer cask.

In the spent fuel pool, the fuel is loaded into the basket/canister assembly positioned in the transfer cask. Upon completion of fuel loading, the shield lid is lowered into the top of the canister. The shield lid assembly is a 7-in.-thick Type 304 stainless steel disk positioned on the shield lid support ring above the basket assembly. Then the loaded canister assembly is moved to a decontamination pit for the remaining canister closure operations, including installation of the drain pipe.

Two penetrations through the shield lid are provided for draining, vacuum drying, and backfilling the canister with helium. The drain penetration is threaded on the top to accept the drain pipe. The pipe extends to within 1/8 in. of the bottom of the canister to facilitate draining water from the inside of the canister.

The vent port is used to pressurize the canister or as a vent/discharge port during cask operations. Both the drain and vent ports have a cover welded over the quick disconnect prior to installation of the structural lid.

The structural lid is a 3-in. thick Type 304L stainless steel disk positioned on top of the shield lid and welded to the shell after the shield lid is welded in place and the canister is drained, dried, and backfilled with helium. The structural lid is designed with removable hoist rings so that the loaded canister can be lifted. The canister design parameters for the transport of different classes of PWR and BWR fuel are provided in Chapter 1.0.

2.1.1.3 Fuel Basket

The fuel basket assembly structure is located inside the canister shell assembly. The basket and canister shell assemblies are handled as one unit. The basket provides the fuel assemblies with lateral support, decay heat removal capability, and criticality control during all storage and

transportation normal conditions of transport and hypothetical accident conditions. The basket can be loaded with up to 24 intact PWR fuel assemblies or up to 56 intact BWR fuel assemblies. Some design features are common to both the PWR and BWR fuel baskets and some features are unique to each basket, as described in the following paragraphs.

The common design features between the PWR and BWR basket structure designs are the top and bottom weldments, support disks, heat transfer disks, fuel tubes, tie rods and nuts, and split spacers. When complete, the basket structure is a rigid cylindrical structure. The base of the structure is the stainless steel bottom weldment.

Either 8 (PWR) or 6 (BWR) stainless steel tie rods are welded to the bottom weldment. The tie rods are used to mechanically join the bottom weldment with the top weldment and hold in place all layers of the support disks and heat transfer disks. Each weldment is designed to support the entire basket structure for all loads. The axial loads are bounded by hypothetical accident condition top/bottom-end drop loads. The fuel assemblies are self-supporting in the axial direction.

The basket structure is assembled by stacking the support disks and the heat transfer disks over the tie rods, each separated by either a spacer or split spacer and washer. The system of multiple support disks is designed to support the fuel assemblies and fuel tubes for all lateral loads. The lateral loads are bounded by hypothetical accident condition side-drop loads. The heat transfer disks do not transmit structural loads (other than self-weight) for any load condition.

The support disks satisfy structural design criteria requirements at temperatures that result from either the normal conditions of transport or hypothetical accident. The aluminum heat transfer disks enhance thermal performance of the basket structure by augmenting its overall heat the conduction properties.

The support disks in the PWR basket are separated and supported at 4.92-in. center-to-center intervals by tie rods and spacer nuts at eight locations. The heat transfer disks are located in the central region of the basket and supported by the eight tie rods and spacer nuts. The number of support disks and heat transfer disks in the PWR basket varies depending upon the class of fuel (Class 1, 2, or 3 PWR fuel) the basket is designed to contain. The PWR fuel tubes are encased by BORAL poison plates on each of the four sides.

The support disks in the BWR basket are separated and supported at 3.83-in. center-to-center intervals by tie rods and spacer nuts at six locations. The heat transfer disks are located in the central region of the basket and supported by the six tie rods and spacer nuts. As is the case for the PWR basket, the number of support disks and heat transfer disks in the BWR basket varies depending upon the class of fuel (Class 4 or Class 5 BWR fuel) the basket is designed to contain. Three types of tubes are designed to contain BWR fuel: tubes with BORAL on two sides, tubes with BORAL one side, and tubes with no BORAL.

2.1.1.4 Impact Limiters

The Universal Transport Cask packaging includes two removable, cup-shaped impact limiters, which absorb the energy of a cask drop impact through the crushing of redwood and balsa wood.

Prior to shipment, the upper impact limiter is bolted to the top forging with 16 retaining rods, washers, and nuts. Likewise, the lower impact limiter is bolted to the bottom plate with 16 retaining rods, washers, and nuts. Both impact limiters are designed to limit impact loads on the cask and its contents resulting from either the normal conditions of transport or hypothetical accident drop scenarios. The impact limiters are fabricated from redwood and balsa wood wedge-shaped sections glued together to form a cylindrical shape. The wood impact-absorbing medium is completely enclosed in a stainless steel shell that is fabricated from 0.25-in. stainless steel plate.

The maximum normal condition of transport (1-ft free drop) impact load is calculated to be 17.1g in the bottom end drop orientation. The design load used in all normal conditions of transport impact calculations is 20g. The maximum hypothetical accident condition (30-ft free drop) impact load is calculated to be 54.9g in the oblique-drop orientation. A design load of 60g is used in all hypothetical accident condition impact calculations except the 30-foot end-drop evaluation of the BWR basket, where a design load of 55g is used.

2.1.1.5 GTCC Waste Canister and Basket

The GTCC waste canister is identical in design to the spent fuel transportable storage canister described in Section 2.1.1.2. The GTCC waste basket is designed to ASME Code, Section III, Subsection NF and conforms to the applicable load combinations and buckling criteria of Regulatory Guide 7.8, and NUREG/CR-6322, respectively. Exceptions to applicable code requirements for these components are shown in Table 2.1.2-1.

2.1.2 Design Criteria

2.1.2.1 Codes and Standards

The structural design of the Universal Transport Cask incorporates criteria based on the following codes and standards.

General Criteria (Assembled Components)

- 10 CFR 71, "Packaging and Transportation of Radioactive Material," April 1, 1996. [1]
- 10 CFR 72, "Licensing Requirements for the Independent Storage of Spent Nuclear Fuel and High Level Radioactive Waste," April 1, 1996. [5]
- IAEA Safety Series No. 6, "Regulations for the Safe Transport of Radioactive Materials," 1985 Edition, as amended 1990. [2]

Cask Structural Design

- ASME Boiler and Pressure Vessel Code, Section III, Division I, Subsection NB, 1995 Edition, with 1995 Addenda. [6]
- NUREG/CR-3019, "Recommended Welding Criteria for Use in the Fabrication of Shipping Containers for Radioactive Materials," dated March 1984. [7]
- NUREG/CR-3854, "Fabrication Criteria for Shipping Containers," dated March 1985. [8]
- NUREG/CR-6007, "Stress Analysis of Closure Bolts for Shipping Casks," dated January 1993. [9]
- Regulatory Guide 7.6, "Design Criteria for the Structural Analysis of Shipping Cask Containment Vessels," Revision 1, March 1978. [10]
- Regulatory Guide 7.8, "Load Combinations for the Structural Analysis of Shipping Casks for Radioactive Material," Revision 1, March 1989. [11]

Cask Inner Shell and Canister Buckling

- ASME Boiler and Pressure Vessel Code Cases, Nuclear Components, Case N-284-1, "Metal Containment Shell Buckling Design Methods," Approved March 1995. [12]

Cask Structural Materials Fracture Toughness

- Regulatory Guide 7.11, "Fracture Toughness Criteria of Base Material for Ferritic Steel Shipping Cask Containment Vessels with a Maximum Wall Thickness of 4 in. (0.1 m)," dated June 1991. [13]
- Regulatory Guide 7.12, "Fracture Toughness Criteria of Base Material for Ferritic Steel Shipping Cask Containment Vessels with a Wall Thickness Greater than 4 in. (0.1 m) But Not Exceeding 12 in. (0.3m)," dated June 1991. [14]

Cask-Lifting Trunnions

- NUREG-0612, "Control of Heavy Loads at Nuclear Power Plants," dated July 1980. [3]
- ANSI N14.6, "Special Lifting Devices for Shipping Containers Weighing 10,000 Pounds or More," dated June 1993. [4]

Basket Structural Design

- ASME Boiler and Pressure Vessel Code, Section III, Division I, Subsection NG, 1995 Edition, with 1995 Addenda. [15]
- Regulatory Guide 7.8, "Load Combinations for the Structural Analysis of Shipping Casks for Radioactive Material," Revision 1, March 1989. [11]
- NUREG/CR-6322, "Buckling Analysis of Spent Fuel Baskets," dated May 1995. [16]

2.1.2.2 Exceptions to Codes and Standards

Specific exceptions to the above codes and standards (Section 2.1.2.1) are identified in Table 2.1.2-1. These exceptions are justified based on other requirements for the design and analysis of the Universal Transport Cask and the Transportable Storage Canister, as well as based upon standard industry practice for the storage and transport of spent nuclear fuel.

2.1.2.3 Load Combinations

The load conditions that must be considered for the design of a spent-fuel transport cask are defined in 10 CFR 71 and Regulatory Guide 7.8 [11] and summarized in Table 2.1.2-2. The stresses in the containment structure and the noncontainment structures satisfy the stress limits defined in Regulatory Guide 7.6, "Design Criteria for the Structural Analysis of Shipping Cask Containment Vessels." [10] These limits are essentially the same as those in the "ASME Boiler and Pressure Vessel Code," Section III, Division 1, Subsection NB, for Class 1 Components. [6]

The Universal Transport Cask is analyzed as a pressure vessel, whose containment boundary is not breached during any loading condition. The cask design allows for well-defined load paths that are analyzed by using straightforward, proven structural analysis methods. The structural analysis of the cask is a linear elastic analysis. In those cases where loadings are open to analytical interpretation, several load condition analyses are performed to bound the actual load conditions.

Each normal condition of transport and each hypothetical accident condition is characterized by a combination of various loading types. These load type combinations define the total load criteria for each condition. The loading types that must be considered include ambient thermal, decay heat, external and internal pressures, bolt preload, inertia, and cask drop impacts. The cask is analyzed for normal conditions of transport in Section 2.6 and for hypothetical accident conditions in Section 2.7.

The total stresses in the cask components are calculated as the combination of stresses that results from each of the various load types (thermal, pressure, and mechanical) associated with a given load condition. For those load conditions and components analyzed by using classical hand-calculational methods, the total stress components are obtained by summing the individual stress components for each type of load associated with the load condition. This summation is appropriate because the individual and total stress components are linear, elastic stresses.

The evaluation of lead-pour fabrication stress is presented in Section 2.6.11. Since the residual stress in the inner shell induced by shrinkage of the lead after pouring is relieved because of the low creep strength of the lead, the stresses are not combined with other loads. The evaluations of "Heat" (100°F) and "Cold" conditions (-40°F) are presented in Sections 2.6.1 and 2.6.2, respectively. The cask free drop conditions are evaluated in Sections 2.6.7 and 2.7.1. The

loading conditions used (bolt pre-load, internal pressure, inertia load and thermal load) are described in Section 2.10.2.

2.1.2.4 Allowable Stress Limits - Ductile Failure

Allowable stress limits are established for the cask containment structures, noncontainment structures, lifting trunnions, rotation pockets, bolts, and impact limiters. Regulatory Guide 7.6 and the ASME Code Section III, Subsection NB, are used to establish the allowable stress limits for the Universal Transport Cask primary containment boundary for both normal conditions of transport and hypothetical accident conditions. Material property data used in calculating the allowable stress limits correspond to the design stress intensities (S_m), yield strengths (S_y), and ultimate strengths (S_u) presented in Section 2.3.

The cask primary containment boundary includes the following elements:

- 4.25 in.-thick cup-shaped bottom forging (Type 304 stainless steel),
- 67.61 in. ID, 2 in.-thick inner shell (Type 304 stainless steel), to which the bottom forging is welded,
- Top forging (Type 304 stainless steel), to which the top end of the inner shell is welded,
- 6.5 in. thick cask lid (Type 304 stainless steel), its inner O-ring and 48 lid bolts (SB-637, Grade N07718 nickel alloy steel).

The vent port coverplate, inner O-rings coverplate, bolts, drain port coverplate, inner O-ring, and coverplate bolts are also part of the primary containment boundary. The allowable stress criteria used for containment structures and bolting materials are summarized in Table 2.1.2-3. These criteria are consistent with Regulatory Guide 7.6 and applicable parts of Article NB-3000 and Appendix F of the ASME Boiler and Pressure Vessel Code. [17] Analysis section locations on the cask are identified in Section 2.10.2 to aid in the evaluations of the various load conditions.

In the evaluation of the cask primary containment boundary, no credit is taken for the Transportable Storage Canister, although the canister is designed as a confinement boundary to satisfy 10 CFR 72 [5] spent fuel storage requirements.

The noncontainment structural members are shown to satisfy essentially the same structural criteria as the containment structure, even though Regulatory Guide 7.6 applies only to containment structures. Noncontainment structures include all structural members other than the

primary containment boundary components, but exclude the lifting trunnions, rotation pockets, and impact limiters. Allowable stresses for the noncontainment structures and noncontainment bolting materials are presented in Table 2.1.2-4.

The allowable stresses for the lifting and handling components of the Universal Transport Cask are based on the requirements of 10 CFR 71.45(a) [1] which requires use of material yield strength with a load factor of 3.0. The lifting and handling components of the cask also satisfy the structural requirements of NUREG-0612 [3] and ANSI N14.6 [4]: the maximum allowable stress is the material yield strength with a load factor of 6.0 or the material ultimate strength with a load factor of 10.0, whichever is less.

The lead (gamma-shielding material) is enclosed between the inner and outer cask shells and the top forging and bottom plate. The lead does not perform a structural function. However, the weight and low yield strength of the lead is considered, where appropriate, in the analyses of cask shell components.

The impact limiters are not stress-limited. While performing their intended function during a free-drop impact, the impact limiters crush and thereby absorb the energy of the impact. The crushing of the redwood and balsa wood contained in the limiter dissipates the kinetic energy of the cask while limiting the deceleration forces applied to the cask.

The Transportable Storage Canister is analyzed as a containment structure. The canister is structurally sound, criticality safe and contains a thermally efficient basket. The canister, which has a double welded closure, serves as a second enclosure of the spent fuel with the fuel cladding being the first enclosure. The basket provides the lateral structural support for the fuel assemblies and maintains the subcritical configuration during all normal conditions of transport and hypothetical accident conditions.

Table 2.1.2-1 Exceptions to Codes and Standards

Code Section	ASME SECTION III, SUBSECTION NB CODE EXCEPTIONS
	Transport Cask
Article NB-8000: Nameplates, Stamping, and Reports	The Code requirements for this article are not met for the Transport Cask as it is not N-stamped and code data reports are not required. However, the Cask is marked as required by 10 CFR 71.
	Transportable Storage Canister
NB-1100 Code Stamping of Components	The canister is designed and fabricated in accordance with Subsection NB of the Code to the maximum practical extent. However, code stamping of canister components is not required and canister components are not code stamped and there is no involvement of an Authorized Inspection Agency.
NB-2000 ASME Approved Material Supplier	Materials will be supplied by NAC-approved suppliers with Certified Material Test Reports in accordance with NB-2000 requirements.
Subparagraph NB-3352.3 Joints of Category C	The structural lid-to-shell weld joint does not comply with the allowable joint configurations (NB4243 - full penetration joint). The weld joint design ensures protection of the lid in side impacts.
NB-4243 Full Penetration Welds Required for Category C joints	The shield lid and structural lid welds are not full penetration welds. These welds are field installed after the canister is loaded with spent fuel and access to the inside of the canister to complete a full penetration weld with a weld build-up is not possible (i.e. t=0"). However, the thickness of the groove weld is 0.88 inch, which is greater than the required thickness of 0.3125 inch.
Paragraph NB-4421 Removal of Backing Rings	In accordance with NB-4243 (Category C) corner joints welded from one side with the backing ring removed are acceptable. The UMS® structural lid to shell weld design uses a backing ring for the joint that is not removed. The backing ring permits completion of the partial depth groove weld. It is not considered in any analyses and has no detrimental effect on canister function.

Table 2.1.2-1 Exceptions to Codes and Standards (Continued)

Code Section	ASME SECTION III, SUBSECTION NB CODE EXCEPTIONS (Continued)
	Transportable Storage Canister (Continued)
Paragraph NB-5230 Radiographic or Ultrasonic Weld Examination (Structural Lid to Canister Shell)	The structural lid to canister shell weld will be verified by either ultrasonic examination (UT) or by progressive liquid penetrant examination (PT). If progressive PT examination is used, it must include the root and final layers, and each intermediate (approximately) 3/8-inch of weld depth. If UT is used, it will be followed by a final surface PT examination. For either examination, the maximum, undetectable flaw size is demonstrated to be smaller than the critical flaw size. The critical flaw size is determined in accordance with ASME Code, Section XI methods. The examination of the weld will be performed by qualified personnel per ASME Code Section V, Articles 5 (UT) and 6 (PT) with acceptance per ASME Code Section III, NB-5332 (UT) per 1997 Addenda, and NB-5350 for (PT).
Paragraph NB-5230 Radiographic or Ultrasonic Weld Examination (Shield Lid to Canister Shell and Port Covers to Shield Lid)	A root and final liquid penetrant examination has been specified because a radiographic examination cannot be performed since the canister is loaded with spent fuel and ultrasonic examination of these weld joints is not indicated because of the joint configuration. In addition, ultrasonic examination would require close proximity to the canister shield lid, which would expose personnel to high dose rates. Two welds close all leak paths through the canister shield and structural lids. In addition, the shield lid weld is pressure tested and helium leak tested to confirm its integrity.
Article NB-6111 Pressure Testing	A hydrostatic or pneumatic test of the Transportable Storage Canister is not performed at the time of fabrication because the canister (pressure vessel) is not closed until it is loaded with the spent fuel or radioactive waste that it holds for storage and transport. The canister is leak tested and pressure tested (following fuel loading) during the canister closure operations.
Article NB-7000 Overpressure Protection	No overpressure protection is provided since the function of the canister is to confine radioactive material. The canister is designed to withstand an internal pressure that considers 100% fuel rod failure and the maximum accident temperature.
Article NB-8000 Nameplates, Stamping and Reports	The Transportable Storage Canister is not Code stamped and no reports are completed that are associated with these activities.

Table 2.1.2-1 Exceptions to Codes and Standards (Continued)

Code Section	ASME SECTION III, SUBSECTION NG CODE EXCEPTIONS
	Spent Fuel Basket Assembly
NG-2000 ASME Approved Material Supplier	Materials will be supplied by NAC-approved suppliers with Certified Material Test Reports in accordance with NB-2000 requirements.
Article NG-8000 Nameplates, Stamping and Reports	The Internal Fuel Basket Assembly is not Code stamped and no reports are completed that are associated with these activities.

Code Section	ASME SECTION III, SUBSECTION NF CODE EXCEPTIONS
	GTCC Waste Basket Assembly
NB-2000 ASME Approved Material Supplier	Materials will be supplied by NAC approved suppliers with Certified Material Test Reports in accordance with NB-2000 requirements.
Article NF-8000 Nameplates, Stamping and Reports	The Internal GTCC Waste Basket Assembly is not Code stamped and no reports are completed that are associated with these activities.

Table 2.1.2-2 Load Combinations: Normal and Hypothetical Accident Conditions

	Applicable Initial Conditions								
	Ambient Temperature		Solar Insolation		Decay Heat		Internal Pressure		Fabrication
Load Conditions – Apply Separately	100°F	-20°F	Maximum	Minimum (Zero)	Maximum	Minimum (Zero)	Maximum	Minimum	Stresses
Normal Conditions of Transport:									
Hot Environment (100° F Ambient Temperature)			X		X		X		X
Cold Environment (-40° F Ambient Temperature)				X		X		X	X
Increased External Pressure 20 psia		X		X		X		X	X
Minimum External Pressure 3.5 psia	X		X		X		X		X
Vibration and Shock	X		X		X		X		X
		X		X		X		X	X
Free Drop (1-foot)	X		X		X		X		X
		X		X		X		X	X
Hypothetical Accident Conditions:									
Free Drop (30-foot)	X		X		X		X		X
		X		X		X		X	X
Puncture	X		X		X		X		X
		X		X		X		X	X
Thermal Fire Accident	X		X		X		X		X
200 Meter Immersion (290 psi external pressure)	X		X		X		X		X
		X		X		X		X	X

Table 2.1.2-3 Allowable Stress Limits for Containment Structures

Stress Intensity Category	Allowable Stress Intensity		Bolt Allowable Stress Intensity*	
	Normal Conditions	Accident Conditions	Normal Conditions	Accident Conditions
Primary membrane	$1.0S_m$	Lesser of: $2.4\ S_m$ and $0.7\ S_u$	$2.0(S_m)_{BM}$	Lesser of: $1.0\ S_y$ and $0.7\ S_u$
Primary membrane + Primary bending	$1.5\ S_m$	Lesser of: $3.6\ S_m$ and $1.0\ S_u$	$3.0(S_m)_{BM}$	$1.0\ S_y$
Range of primary + secondary	$3.0\ S_m$	N/A	-----	-----
Shear	$0.6\ S_m$	$0.42\ S_u$	-----	-----
Bearing	$1.0\ S_y$ or $1.5\ S_y$**	$1.0\ S_u$	-----	-----
Buckling	Inner shell: ASME Code Case N-284-1 [12]		----	----

*Neglecting stress concentrations.

**Distance to edge > distance over which bearing load is applied.

S_u = material ultimate strength.

S_y = material yield strength.

S_m = material design stress intensity.

= lesser of: $S_u/3$ and $2S_y/3$.

(S_m) bolting material = $S_y/3$.

Table 2.1.2-4 Allowable Stress Limits for Noncontainment Structures

Stress Intensity Category	Allowable Stress Intensity		Bolt Allowable Stress Intensity*		Basket Allowable Stress**	
	Normal Conditions	Accident Conditions	Normal Conditions	Accident Conditions	Normal Conditions	Accident Conditions
Primary membrane	1.0 S_m	0.7 S_u	2.0$(S_m)_{BM}$	*Lesser of : 1.0 S_y and 0.7 S_u	1.0 S_m	0.7 S_u
Primary membrane + Primary Bending	1.5 S_m	1.0 S_u	3.0$(S_m)_{BM}$	1.0 S_y	1.5 S_m	1.0 S_u
Range of Primary + Secondary	3.0 S_m	N/A			3.0 S_m	N/A
Shear	Greater of: 0.6 S_m or 0.6 S_y	0.5 S_u			0.6 S_m	0.42 S_u
Bearing	1.0 S_y or 1.5 S_y***	1.0 S_u			1.0 S_y	1.0 S_u
Buckling					NUREG/CR-6322	

*Neglecting stress concentrations.
**ASME Boiler & Pressure Vessel Code, Section III, Subsection NG.
***Distance to edge > distance over which bearing load is applied.
S_u = material ultimate strength.
S_y = material yield strength.
S_m = material design stress intensity.
= lesser of: $S_u/3$ and $2S_y/3$.
(S_m) bolting material = $S_y/3$.

2.1.2.5 Miscellaneous Structural Failure Modes

2.1.2.5.1 Brittle Fracture

The primary structural material of the Universal Transport Cask is Type 304 stainless steel. The outer shell, inner shell, top forging, bottom forging, neutron shield shell, cask bottom plate, and port coverplates are fabricated from Type 304 stainless steel. The Transportable Storage Canister shield lid and the tie rods in the PWR and BWR baskets are also fabricated from Type 304 stainless steel. The canister shell, structural lid, and bottom plate are fabricated from Type 304L stainless steel. The support disks in the PWR basket are constructed from 17-4-PH, Type 630, stainless steel. The support disks in the BWR basket are constructed from SA-533, Type B, Class 2 carbon steel.

Type 304 and 304L stainless steel are austenitic stainless steels and, therefore, do not undergo a ductile-to-brittle transition in the temperature range of interest for a spent-fuel transport cask. Therefore, brittle fracture is not a concern.

Regulatory Guide 7.11, "Fracture Toughness Criteria of Base Material for Ferritic Steel Shipping Cask Containment Vessels with a Maximum Wall Thickness of 4 Inches (0.1 m)," [13] which identifies fracture toughness criteria, references the criteria contained in NUREG/CR-1815, "Recommendations for Protecting Against Failure by Brittle Fracture in Ferritic Steel Shipping Containers Up to Four Inches Thick" [18]. The cask lid bolts are made of SB-637, Grade N07718 nickel alloy steel bolting material. The port coverplate bolts are made of SA-193, Grade B6, Type 410 stainless steel. According to Section 5 of NUREG/CR-1815, bolts generally are not considered fracture-critical components because multiple load paths exist and because bolted systems are designed to be redundant. Therefore, brittle fracture evaluation of the bolts is not required. Nonetheless, the bolt materials possess a level of resistance to brittle fracture that is comparable to the other cask component materials.

The support disks in the PWR basket are made of 17-4-PH, Type 630 stainless steel plate that is 0.5 in. thick. The BWR basket support disks are made from SA533, Type B, Class 2 plate that is 0.625 in. thick.

Paragraph NG-2311 of the ASME B&PV Code [15] states that materials 0.625 in. thick and less need not be impact tested. Therefore, no nil-ductility or brittle fracture concerns are associated with either the PWR or BWR support disks.

2.1.2.5.2 Fatigue

Universal Transport Cask

The Universal Transport Cask - containment structure is evaluated for the effects of fatigue in accordance with the criteria contained in ASME Code, Section III, NB-3222.4 for cyclic operation. NB-3222.4(a) states that cyclical service analysis is not required when the six criteria of NB-3222.4(d) are satisfied. Justification for exemption from a detailed cyclic analysis is provided below.

A normal operating cycle of the transport cask consists of: 1) loading an empty cask at ambient temperature with a canister containing maximum heat load; 2) transporting the contents to a destination; and 3) unloading the contents and letting the cask return to ambient temperature. The anticipated number of normal operating cycles for the cask is not expected to exceed 1200 cycles (24 cycles per year x 50 years).

The following is a summary of the application of the six NB-3222.4(d) criteria to the Universal Transport Cask.

1. Atmospheric Pressure Cycle. Since the cask normally operates at atmospheric pressure, the normal operation process for the cask includes one evacuation cycle and one pressurization cycle for the total of two pressure changes. This results in 2,400 (2 x 1200) pressure cycles. This is significantly lower than the value of 20,000 corresponding to $3S_m$ for the cask material (56.1 ksi at 400°F).

2. Normal Pressure Service Fluctuations. The normal operating pressure for the cask is 50 psig, but the pressure boundary is designed for 75 psig. S_a for 10^6 cycles is determined to be 26.5 ksi and S_m is 18.7 ksi. The significant range of normal pressure changes is 1/3 x design pressure x (S/S_m) = 35.4 psi. The only pressure fluctuations during normal operations occur due to changes in ambient condition and are calculated to be below 3 psi. Therefore, these fluctuations are insignificant and do not need to be considered.

3. Temperature Difference - Startup and Shutdown. As discussed above, not more than 1,200 startup-shutdown cycles are expected during the lifetime of the cask. The corresponding S_m determined from the fatigue curves is 120 ksi. Therefore, taking the material properties from Section 2.3, the value of $S_a/2\alpha$ is calculated to be 245°F—substantially higher than the temperature difference between any two adjacent points on the cask.

4. Temperature Difference - Normal Service. Similar to (2) above, S_a is determined to be 26.5 ksi and $S/2E\alpha$ is calculated to be 54°F. Clearly, this is substantially higher than the change in temperature difference between any two adjacent points on the cask during normal service.

5. Temperature Difference - Dissimilar Materials. The cask components are fabricated from austenitic stainless steel except for the lid bolts which are ASME SB 637 Grade N07718 and the coverplate bolts which are SA193 Grade B6. The quantity of $S/2(E_1\alpha_1 - E_2\alpha_2)$ is calculated to be 192°F for the coverplate bolts and 349°F for the lid bolts. This is substantially higher than the temperature difference between any adjacent points of the basket.

6. Mechanical Loads. The fluctuations due to mechanical loads are considered significant only when they exceed the S_a quantity corresponding to 10^6 cycles. This value is determined to be 26.5 ksi. From the results in Section 2.6.7, the maximum cask stress for normal conditions of transport is 21.5 ksi when the 1-ft. drop is included.

Therefore, the Universal Transport Cask structural components meet the exemption criteria of NB-3222.4(d) and do not require a detailed cyclic service analysis. **However, a fatigue evaluation is performed for the cask closure lid bolts as shown in Section 2.6.7.6.1.**

Transportable Storage Canister

The Transportable Storage Canister is not evaluated for effects of fatigue. A normal operating cycle for a canister consists of (1) loading an empty canister/basket at the spent fuel pool (assumed to be ambient temperature) with a full load of fuel assemblies generating the maximum allowable heat load, (2) storage of the canister for 5 years or more, and (3) loading the canister into the transport cask in which is be shipped to a destination for unloading. The canister may be exposed to one hypothetical accident, after which the canister is taken out of service. A typical canister is not exposed to significant cycling during its design life.

2.1.2.5.3 Buckling

The Universal Transport Cask inner shell and the canister are evaluated for structural stability by using Code Case N-284-1 (Metal Containment Shell Buckling Design Methods) of the ASME Code [12]. The PWR and BWR basket structures, without the support of the canister, are evaluated for buckling effects by using the criteria defined in NUREG/CR-6322 [16], which is based on the ASME Code, Section III, Division 1, Subsection NF [19]. The code or standard used to evaluate structural stability of the containment shell, canister shell, and basket is described in the following paragraphs.

Structural stability ensures that the shell does not buckle during fabrication, for normal conditions of transport, or hypothetical accident conditions. The buckling evaluation requirements of Regulatory Guide 7.6, Paragraph C.5, are shown to be satisfied by the results of the interaction equation calculations of Code Case N-284-1. This section discusses the Code Case N-284-1 methodology for the calculation of the Universal Transport Cask inner shell buckling. The detailed buckling evaluation of the cask is provided in Section 2.7.12 of this report. The basket evaluation for the normal conditions of transport and hypothetical accident conditions is presented in Sections 2.6.13, 2.6.15, 2.7.8, and 2.7.10.

Code Case N-284-1

The ASME Boiler and Pressure Vessel Code sets forth service limits that are analogous to load conditions found in 10 CFR 71. As stated in Regulatory Guide 7.6, the normal conditions of transport correspond to Level A Service Limits, and the hypothetical accident conditions correspond to Level D Service Limits. A buckling safety factor at 2.0 is used in Level A (normal transport) conditions. A buckling safety factor of 1.34 is used in Level D (accident) conditions. Code Case N-284-1 addresses both elastic and inelastic buckling.

Interaction equations are used to combine the largest hoop compressive, axial compressive, and in-plane shear loadings calculated in each load case (cask body or canister) analyzed. Appendix F of the ASME Boiler and Pressure Vessel Code, (for Level D Service Loadings) [17] specifically identifies the use of a Code Case for metal containment shell buckling as an acceptable means of addressing buckling issues.

Buckling of the inner shell, which is the primary component of containment, is evaluated as follows:

1. Use classical theory to determine the theoretical elastic buckling stresses.
2. Apply the appropriate factors of safety and interaction equations to elastic and inelastic buckling cases and establish the worst-case compressive and in-plane shear stresses.
3. Calculate and apply capacity reduction factors, which account for differences between classical theory and predicted instability stress for fabricated shells.
4. Calculate plasticity reduction factors and apply them in cases where elastically determined buckling stresses are above the proportional limit.

Theoretical Elastic Buckling Stresses

Cask inner shell geometric parameters and material properties are used in the elastic buckling evaluation. The theoretical elastic buckling stresses for the inner shell are calculated by using the equations of Code Case N-284-1, the inner shell geometric parameters, and the material yield strength and elastic modulus. Code Case N-284-1 provides elastic stress formulas for unstiffened cylindrical shells.

Capacity Reduction Factors

Capacity reduction factors compensate for differences between classically determined and predicted instability stresses for fabricated shells. The capacity reduction factors are determined by using methods described in Section-1500 of Code Case N-284-1. To directly use the capacity reduction factors, the tolerance requirements of NE-4220 of the ASME Boiler and Pressure Vessel Code, Subsection NE [20] must be satisfied. NE-4221.1 and NE-4221.2 set forth the maximum difference in cross-section diameters and maximum deviation from true theoretical form for external pressure.

Plasticity Reduction Factors

Plasticity reduction factors account for nonlinear material behavior, which occurs when buckling stresses exceed the proportional limit of the material. Plasticity reduction factors are dependent upon the magnitude of the applied compressive or in-plane shear stress, S_i. Because values for S_i are not directly calculated, the equations used to determine the reduction factors for axial compression, hoop compression, and shear (Section-1600 of Code Case N-284-1) are used.

Upper Bound Magnitudes for Compressive Stresses and In-Plane Shear Stresses

From Section-1600 of Code Case N-284-1, as an upper limit, the compressive stresses, S_i ($i = \phi$ or θ), must be less than the yield strength, S_y, divided by the appropriate factor of safety ($S_i < S_y/FS$). Similarly, for shear, $S_{\phi\theta}$, must be less than or equal to 0.6 S_y divided by the appropriate factor of safety ($S_{\phi\theta} < 0.6\ S_y/FS$). As discussed earlier in this section, the factor of safety is 2.0 for normal transport and 1.34 for hypothetical accident conditions. Under no circumstances may the values for the upper bound magnitudes of compressive stresses and in-plane shear stresses be exceeded. However, satisfying these limits alone is not sufficient to demonstrate that buckling does not occur; the interaction equations must also be satisfied.

Interaction Equations

Elastic and inelastic interaction equations must be satisfied for all states of compressive and in-plane shear stress. The interaction equations for cylindrical shells are directly available from Paragraph 1713.1.1 and Paragraph 1713.2.1 of Code Case N-284-1. Once a stress state is established for a specific shell, plasticity reduction factors can be determined and all appropriate interaction equations checked. Elastic interaction equations must be satisfied and, if any of the uniaxial critical stress values exceed the proportional limit of the fabricated material, the inelastic interaction equations must also be satisfied.

2.1.2.5.4 Creep Considerations at Elevated Temperatures

Structural components of the Universal Transport Cask and the canister are fabricated from stainless steel, which does not experience creep below temperatures of 700°F. The canister is the package structural component exposed to the highest temperatures, which remain below 700°F. Therefore, the potential for creep is essentially zero. Design considerations relative to the creep failure mode are therefore satisfied.

2.1.2.5.5 Impact Limiter Deformation Limits

The Universal Transport Cask impact limiters are designed to crush and, thereby, absorb the kinetic energy of the cask acquired during a free-drop accident. The geometry of the impact limiters and the crush characteristics of the energy-absorbing material are designed to limit the deceleration forces applied to the cask.

The Universal Transport Cask impact limiters limit the maximum deceleration experienced by the cask body to less than 54.9 g for all impact conditions. The deceleration force is a function of the crush strength of the energy-absorbing material in the impact limiter and the area of crush. The impact limiter must provide a sufficient depth of energy-absorbing material so that all of the kinetic energy of the package is absorbed (cask is stopped) before the limiter is crushed to its solid "stacked" height (approximately 30% of the initial depth).

2.2 Weights and Centers of Gravity

The calculated weights of the major components of the Universal Transport Cask containing PWR and BWR fuel are presented in Table 2.2-1 and Table 2.2-2, respectively. **The calculated weight of the Transport Cask with Greater Than Class C (GTCC) waste is provided in Table 2.2-3.** These tables also summarize the weights and center of gravity locations of the cask for the three cask configurations most likely to occur: empty, under-the-hook loaded with fuel, and loaded with fuel/ready for transport. In the tables, the term "Empty" implies the absence of the canister or fuel in the cask cavity, although the spacers do remain in the cask cavity. "Under-the-hook weight" includes the cask with lid, spacer, and yoke. "Transport-ready weight" includes the loaded cask with upper and lower impact limiters. The cask under-the-hook and the transport-ready design weights are 250,000 and 260,000 lb, respectively.

The axial locations of the centers of gravity are measured from the bottom outer surface of the cask body. The centers of gravity are on the axial centerline of the cask because the cask is symmetric about that axis.

Table 2.2-1 Calculated Weights and Centers of Gravity: Cask with Canister Containing PWR Fuel

Component Description	Class 1 Fuel		Class 2 Fuel		Class 3 Fuel	
	Wt. (lb)	C.G. (in.)[1]	Wt. (lb)	C.G. (in.)[1]	Wt. (lb)	C.G. (in.)[1]
Fuel	37,608	—	38,448	—	35,520	—
Basket	14,957	—	15,994	—	16,489	—
Canister without lids	8,388	—	8,733	—	9,022	—
Canister structural lid + backing ring	2,927	—	2,927	—	2,927	—
Canister shield lid	6,825	—	6,825	—	6,825	—
Loaded/Closed Canister[6]	70,705	89.98	72,927	93.74	70,783	98.45
Spacers	1,714	—	975	—	0	—
Cask Cavity Contents Weight	72,419	—	73,902	—	70,783	—
Top impact limiters	8,846	—	8,846	—	8,846	—
Bottom impact limiters	8,846	—	8,846	—	8,846	—
Cask lid	8,869	—	8,869	—	8,869	—
Transport cask without lid	151,029	—	151,029	—	151,029	—
Transport cask with lid[1]	159,898	104.22	159,898	104.22	159,898	104.22
Transport cask with cask lid + spacer	161,612	—	160,873	—	159,898	—
Water weight	12,893	—	14,668	—	15,637	—
Yoke[2]	8,000	—	8,000	—	8,000	—
Under-the-hook weight (dry)[3]	240,317	—	241,800	—	238,681	—
Under-the-hook weight (wet)[4]	244,893	—	247,104	—	244,122	—
Transport ready weight[1, 5]	250,009	107.99	251,492	106.79	248,373	106.30
Design transport weight	260,000	—	260,000	—	260,000	—

1. Measured from bottom outer surface of cask body.
2. Yoke is used for lifting purposes only. Therefore, yoke is not included in transport cask analysis and center of gravity is not calculated.
3. Under-the-hook weight: cask with lid, spacer, loaded canister, and yoke.
4. Under the hook weight cask without lid, loaded canister without structural lid, spacer, and with water in the canister and cask annulus.
5. Transport-ready weight: loaded cask with impact limiters.
6. Measured from bottom outer surface of canister body.

Table 2.2-2 Calculated Weights and Centers of Gravity: Cask with Canister Containing BWR Fuel

Component Description	Class 4 Fuel		Class 5 Fuel	
	Wt. (lb)	C.G. (in.)	Wt. (lb)	C.G. (in.)
Fuel	38,976	—	38,976	—
Basket	17,845	—	18,199	—
Canister without lids	8,786	—	8,969	—
Canister structural lid + backing ring	2,927	—	2,927	—
Canister shield lid	6,825	—	6,825	—
Loaded/Closed Canister[6]	75,359	93.75	75,896	97.22
Spacers	2,073	—	518	—
Cask Cavity Contents Weight	77,432	—	76,414	—
Top impact limiters	8,846	—	8,846	—
Bottom impact limiters	8,846	—	8,846	—
Cask lid	8,869	—	8,869	—
Transport cask without lid	151,029	—	151,029	—
Transport cask with lid[1]	159,898	104.22	159,898	104.22
Transport cask with cask lid + spacer	161,971	—	160,416	—
Water weight	15,038	—	15,407	—
Yoke[2]	8,000	—	8,000	—
Under-the-hook weight (dry)[3]	245,330	—	244,312	—
Under-the-hook weight (wet)[4]	250,185	—	249,507	—
Transport ready weight[1,5]	255,022	105.94	254,004	106.23
Design transport weight	260,000	—	260,000	—

1. Measured from bottom outer surface of cask body.
2. Yoke is used for lifting purposes only. Therefore, yoke is not included in transport cask analysis and center of gravity is not calculated.
3. Under-the-hook weight: cask with lid, spacer, loaded canister, and yoke.
4. Under the hook weight cask without lid, loaded canister without structural lid, spacer, and with water in the canister and cask annulus.
5. Transport-ready weight:loaded cask with impact limiters.
6. Measured from bottom outer surface of canister body.

Table 2.2-3 Calculated Weights and Centers of Gravity: Cask with Canister Containing Greater Than Class C (GTCC) Waste

Component Description	Maine Yankee GTCC Waste	
	Weight (lb)	Center of Gravity (inches)
GTCC Waste	20,000	—
Basket	32,314	—
Canister without lids	8,388	—
Canister structural lid + backing ring	2,927	—
Canister shield lid	6,825	—
Loaded/Closed Canister[5]	70,454	93.84
Spacers	1,714	—
Cask Cavity Contents Weight	72,168	—
Top impact limiter	8,846	—
Bottom impact limiter	8,846	—
Cask lid	8,869	—
Transport cask without lid	151,029	—
Transport cask with lid[1]	159,898	104.22
Transport cask with cask lid + spacer	161,612	—
Yoke[2]	8,000	—
Under-the-hook weight[3]	240,066	—
Transport ready weight[1, 4]	249,758	108.54
Design transport weight	260,000	—

1. Measured from bottom outer surface of cask body.
2. Yoke is used for lifting purposes only. Therefore, yoke is not included in transport cask analysis and center of gravity is not calculated.
3. Under-the-hook weight: cask with lid, spacer, loaded canister, and yoke.
4. Transport-ready weight: loaded cask with impact limiters.
5. Measured from bottom outer surface of canister body.

2.3 Mechanical Properties of Materials

The material mechanical properties corresponding to the calculated material temperatures of the Universal Transport Cask are used in the structural analyses for the normal conditions of transport and the hypothetical accident load conditions. The mechanical properties at the applicable temperature are also used in calculating the allowable stresses in each component analysis. The cask materials and their mechanical properties are described in the following sections.

2.3.1 Summary of Materials

A summary list of the materials from which the Universal Transport Cask and other major components are fabricated is presented here. The mechanical properties of these materials are presented in tables in Sections 2.3.2 through 2.3.8. The effects of temperature on the mechanical properties are shown. The coefficients of thermal expansion presented in this section represent the mean value for the temperature range from 70°F to the indicated temperature.

Cask Component	Material
Cask inner shell	ASME SA-240, Type 304 stainless steel
Cask outer shell	ASTM A-240, Type 304 stainless steel
Cask bottom plate	ASTM A-240, Type 304 stainless steel
Bottom forging	ASME SA-336, Type 304 stainless steel
Top forging	ASME SA-336, Type 304 stainless steel
Neutron shield shell	ASTM A-240 Type 304 stainless steel
Neutron shield	NS-4-FR
Neutron shield heat transfer fins	Explosively bonded ASTM B-152 copper/ASTM A-240 Type 304 stainless steel
Gamma shield	ASTM B-29, chemical **copper grade** lead
Cask lid	ASME SA-336, Type 304 stainless steel
Lid bolts	ASME SB-637, Grade N07718, nickel alloy
Port coverplates	ASME SA-240/SA-479 Type 304 stainless steel
Port coverplate bolts	ASME SA-193, Grade B6 (Type 410) stainless steel
Lifting trunnions	ASME SA-564, TYPE 630, 17-4PH stainless steel
Rotation pockets	ASTM A-182, XM-19 stainless steel
Canister spacers - PWR cask	ASTM A240 Type 304 stainless steel
- BWR Cask	ASTM SB-209, Type 6061-T6 aluminum alloy
Canister shell	ASME SA-240, Type 304L stainless steel
Canister bottom plate	ASME SA-240, Type 304L stainless steel
Canister shield lid	ASTM A-240, Type 304 stainless steel
Canister structural lid	ASME SA-240, Type 304L stainless steel
Support disks-PWR basket	ASME SA-693, Type 630, 17-4 PH stainless steel
Support disks-BWR basket	ASME SA-533, Type B class 2 carbon steel
Heat transfer disks	ASME SB-209, Type 6061-**T651** aluminum alloy
Spacer nuts	ASME SA-479, Type 304 stainless steel
Tie rods	ASME SA-479, Type 304 stainless steel
Basket end weldments	ASME SA-240, Type 304 stainless steel
Fuel tubes	ASTM A-240 Type 304 stainless steel
Impact limiters	Redwood/balsa wood encased in ASTM A-240, Type 304 stainless steel
Retaining Rod	**ASME SA-193, Grade B8S, austenitic stainless steel**

2.3.2 Austenitic Stainless Steels

As discussed previously, most of the primary structural components of the Universal Transport Cask body are fabricated from Type 304 stainless steel. In addition to the cask body components, the Transportable Storage Canister shield lid, fuel tubes, basket top and bottom weldment plates, and tie rods in the baskets are also fabricated from Type 304 stainless steel. The canister shell, bottom plate, and structural lid are fabricated from Type 304L stainless steel. Type XM-19 stainless steel is used in the fabrication of the rotation pockets. These materials are selected because of their strength, ductility, and high resistance to corrosion and brittle fracture over a broad temperature range.

The mechanical properties of the stainless steels used to fabricate the Universal Transport Cask body are presented in Tables 2.3.2-1 through 2.3.2-5.

Table 2.3.2-1 Mechanical Properties of SA-240, Type 304 Stainless Steel

Property	**Value**							
Temperature (°F)	**-40**	**-20**	**70**	**200**	**300**	**400**	**500**	**750**
Ultimate Tensile Stress, S_u (ksi) [21]	75.0	75.0	75.0	71.0	66.0	64.4	63.5	63.1
Yield Stress, S_y (ksi) [21]	30.0	30.0	30.0	25.0	22.5	20.7	19.4	17.3
Design Stress Intensity, S_m (ksi) [21]	20.0	20.0	20.0	20.0	20.0	18.7	17.5	15.6
Modulus of Elasticity, E (ksi) [21]	28.7E+03	28.7E+03	28.3E+03	27.6E+03	27.0E+03	26.5E+03	25.8E+03	24.4E+03
Alternating Stress @ 10 cycles (ksi) [17]	718.0	718.0	708.0	690.5	675.5	663.0	645.5	610.4
Alternating Stress@ 10^6 cycles (ksi) [17]	28.7	28.7	28.3	27.6	27.0	26.5	25.8	24.4
Coefficient of Thermal Expansion, α (in/in/°F) [21]	8.13E-06	8.19E-06	8.46E-06	8.79E-06	9.00E-06	9.19E-06	9.37E-06	9.76E-06
Poisson's Ratio [21]	← 0.31 →							
Density [21]	← 503 lbm/ft^3 (0.291 lbm/in^3) →							

Note: Reference [17] Appendix I.

Table 2.3.2-2 Mechanical Properties of SA-479, Type 304 Stainless Steel

Property	**Value**							
Temperature (°F)	**-40**	**-20**	**70**	**+200**	**+300**	**+400**	**+500**	**+750**
Ultimate Tensile Stress, S_u, (ksi) *	No Value Given	75.0	75.0	71.0	66.0	64.4	63.5	63.1
Yield Stress, S_y, (ksi) *	No Value Given	30.0	30.0	25.0	22.5	20.7	19.4	17.3
Design Stress Intensity, S_m (ksi) [21]	20.0	20.0	20.0	20.0	20.0	18.7	17.5	15.6
Modulus of Elasticity (ksi) [21]	28.8E+03	28.7E+03	28.3E+03	27.6E+03	27.0E+03	26.5E+03	25.8E+03	24.4E+03
Coefficient of Thermal Expansion, α (in/in/° F) [21]	No Value Given		8.46E-06	8.79E-06	9.00E-06	9.19E-06	9.37E-06	9.76E-06
Alternating Stress @ 10 cycles (ksi) [17]	720	718	708	683	675	663	645	610
Alternating Stress @ 10^6 cycles (ksi) [17]	28.8	28.7	28.3	27.6	27.0	26.5	25.8	24.4
Poisson's Ratio [21]	← 0.275 @ 275°F →							
Density [21]	← 497 lbm/ft^3 (0.288 lbm/in^3) @ 300°F →							

Note: Reference [17] Appendix I.
Reference [21] ASME Section II, Part D, Material Properties.
* Calculated based on Design Stress Intensity:

$$\left(\frac{S_{m-temp}}{S_{m70}}\right) S_{u70} = S_{u-temp}$$

Table 2.3.2-3 Mechanical Properties of SA-240, Type 304L Stainless Steel

Property	**Value**							
Temperature (°F)	**-40**	**-20**	**70**	**200**	**300**	**400**	**500**	**750**
Ultimate Tensile Stress, S_u (ksi) [21]	70.0	70.0	70.0	66.2	60.9	58.5	57.8	55.9
Yield Stress, S_y (ksi) [21]	25.0	25.0	25.0	21.4	19.2	17.5	16.4	14.7
Design Stress Intensity, S_m (ksi) [21]	16.7	16.7	16.7	16.7	16.7	15.8	14.8	13.3
Modulus of Elasticity (ksi) [21]	28.7E+03	28.7E+03	28.3E+03	27.6E+03	27.0E+03	26.5E+03	25.8E+03	24.4E+03
Alternating Stress @ 10 cycles (ksi) [17]	718.0	718.0	708.0	690.5	675.5	663.0	645.5	610.4
Alternating Stress @ 10^6 cycles (ksi) [17]	28.7	28.7	28.3	27.6	27.0	26.5	25.8	24.4
Coefficient of Thermal Expansion, α (in/in/°F) [21]	8.13E-06	8.19E-06	8.46E-06	8.79E-06	9.00E-06	9.19E-06	9.37E-06	9.76E-06
Poisson's Ratio [21]	← 0.31 →							
Density [21]	← 503 lbm/ft^3(0.291 lbm/in^3) →							

Note: Reference [17] Appendix I.
Reference [21] ASME Section II, Part D, Material Properties.

Table 2.3.2-4 Mechanical Properties of SA-336, Type 304 Stainless Steel

Property	**Value**							
Temperature (°F)	**-40**	**-20**	**70**	**200**	**300**	**400**	**500**	**750**
Ultimate Tensile Stress, S_u (ksi) [21]	70.0	70.0	70.0	66.2	61.5	60.0	59.3	58.9
Yield Stress, S_y (ksi) [21]	30.0	30.0	30.0	25.0	22.5	20.7	19.4	17.3
Design Stress Intensity, S_m (ksi) [21]	20.0	20.0	20.0	20.0	20.0	18.7	17.5	15.6
Modulus of Elasticity, E (ksi) [21]	28.7E+03	28.7E+03	28.3E+03	27.6E+03	27.0E+03	26.5E+03	25.8E+03	24.4E+03
Alternating Stress @ 10 cycles (ksi) [17]	718.0	718.0	708.0	690.5	675.5	663.0	645.5	610.4
Alternating Stress @ 10^6 cycles (ksi) [17]	28.7	28.7	28.3	27.6	27.0	26.5	25.8	24.4
Coefficient of Thermal Expansion, α (in/in/°F) [21]	8.13E-06	8.19E-06	8.46E-06	8.79E-06	9.00E-06	9.19E-06	9.37E-06	9.76E-06
Poisson's Ratio [21]	← 0.31 →							
Density [21]	← 503 lbm/ft^3(0.291 lbm/in^3) →							

Note: Reference [17] Appendix I.
Reference [21] ASME Section II, Part D, Material Properties.

Table 2.3.2-5 Mechanical Properties of Type XM-19 Stainless Steel

Property	**Value**							
Temperature (°F)	**-40**	**-20**	**70**	**200**	**300**	**400**	**500**	**750**
Ultimate Tensile Stress, S_u (ksi) [21]	100.0	100.0	100.0	99.5	94.3	90.7	89.1	85.7
Yield Stress, S_y (ksi) [21]	55.0	55.0	55.0	47.0	43.4	40.8	38.8	35.8
Design Stress Intensity, S_m (ksi) [21]	33.3	33.3	33.3	33.2	31.4	30.2	29.7	28.5
Modulus of Elasticity, E (ksi) [21]	28.3E+03	28.3E+03	28.3E+03	27.6E+03	27.0E+03	26.5E+03	25.8E+03	24.5E+03
Alternating Stress @ 10 cycles (ksi) [17]	708.0	708.0	708.0	690.5	675.5	663.0	645.5	610.4
Alternating Stress @ 10^6 cycles (ksi) [17]	28.3	28.3	28.3	27.6	27.0	26.5	25.8	24.4
Coefficient of Thermal Expansion, α (in/in/°F) [21]	8.13E-06	8.19E-06	8.46E-06	8.79E-06	9.00E-06	9.19E-06	9.37E-06	9.76E-06
Thermal Conductivity, (Btu/hr-in °F) [21]	No Value Given		0.683	0.733	0.775	0.817	0.850	0.950
Poisson's Ratio [21]	← 0.31 →							
Density [21]	← 503 lbm/ft³ (0.291 lbm/in³) →							

Note: Reference [17] Appendix I.

2.3.3 Precipitation-Hardened Stainless Steel

SA-693, Type 630, 17-4 PH stainless steel is selected for the fabrication of support disks in the PWR basket because of its high strength combined with good corrosion and brittle fracture resistance. The primary and secondary lifting trunnions are fabricated of SA-564, Type 630, 17-4 PH stainless steel. 17-4 PH Type 630 is a chrome/nickel steel with 17% chromium and 4% nickel as compared with Type 304 austenitic steel, which has 18% chromium and 8% nickel. Both materials are considered to be stainless steel by the metals industry. The mechanical properties of this precipitation-hardened stainless steel are presented in Table 2.3.3-1.

Table 2.3.3-1 Mechanical Properties of SA-564 and SA-693, Type 630, 17-4 PH Stainless Steel

Property	**Value**							
Temperature (°F)	**-40**	**-20**	**70**	**200**	**300**	**400**	**500**	**650**
Ultimate Tensile Stress, S_u (ksi) [21]	135.0	135.0	135.0	135.0	135.0	131.4	128.5	125.7
Yield Stress, S_y (ksi) [21]	105.0	105.0	105.0	97.1	93.0	89.5	87.0	83.6
Design Stress Intensity, S_m (ksi) [21]	45.0	45.0	45.0	45.0	45.0	43.8	42.8	41.9
Modulus of Elasticity, (ksi) [21]	28.7E+03	28.7E+03	28.3E+03	27.6E+03	27.0E+03	26.5E+03	25.8E+03	**25.1E+03**
Alternating Stress @ 10 cycles (ksi) [17]	401.8	401.8	396.2	386.4	378.0	371.0	361.2	341.6
Alternating Stress @ 10^6 cycles (ksi) [17]	19.1	19.1	18.9	18.4	18.0	17.7	17.2	16.3
Coefficient of Thermal Expansion, α (in/in/°F) [21]	No Value Given	No Value Given	5.89E-06	5.90E-06	5.90E-06	5.91E-06	5.91E-06	5.93E-06
Thermal Conductivity,* (Btu/hr-in °F) [21]	No Values Given		0.824	0.883	0.933	0.975	1.017	1.117
Poisson's Ratio [21]	← 0.31 →							
Density [21]	← 503 lbm/ft³ (0.291 lbm/in³) →							

Note: Reference [17] Appendix I.

2.3.4 Carbon Steel

The support disks in the BWR fuel basket are made of SA-533, Type B, Class 2 carbon steel. This material is selected because of its high strength and resistance to corrosion and high levels of radiation. The mechanical properties of this material are provided in Table 2.3.4-1.

Table 2.3.4-1 Mechanical Properties of SA-533, Type B, Class 2 Carbon Steel

Property	**Value**						
Temperature (°F)	**-20**	**70**	**200**	**300**	**400**	**500**	**750**
Ultimate Tensile Stress, S_u (ksi) [21]	90.0	90.0	90.0	90.0	90.0	90.0	87.2
Yield Stress, S_y (ksi) [21]	70.0	70.0	65.5	64.5	63.2	62.3	59.3
Design Stress Intensity, S_m (ksi) [21]	30.0	30.0	30.0	30.0	30.0	30.0	No Value Given
Modulus of Elasticity, E (ksi) [21]	29.9E+03	29.2E+03	28.5E+03	28.0E+03	27.4E+03	27.0E+03	24.6E+03
Alternating Stress @ 10 cycles (ksi) [17]	465.0	465.0	453.8	435.0	436.3	429.9	391.7
Alternating Stress @ 10^6 cycles (ksi [17])	15.8	15.8	15.4	15.2	14.8	14.6	13.3
Coefficient of Thermal Expansion, α (in/in/°F) [21]	No Value Given	7.02E-06	7.25E-06	7.43E-06	7.58E-06	7.70E-06	8.00E-06
Thermal Conductivity (BTU/hr-in-°F) [21]	No Value Given	1.85	1.95	1.98	1.98	1.95	1.83
Poisson's Ratio [21]	← 0.31 →						
Density [21]	← 503 lbm/ft^3 (0.291 lbm/in^3) →						

Note: Reference [17] Appendix I.

2.3.5 Bolting Materials

The bolting materials for the Universal Transport Cask are selected to provide high strength, good resistance to corrosion and coefficients of thermal expansion similar to those of the components being joined.

The cask lid bolts are made of SB-637, Grade N07718 nickel alloy bolting material. The mechanical properties of this material are presented in Table 2.3.5-1. The mechanical properties for the port coverplate bolts, which are fabricated of SA-193, Grade B6 stainless steel, are presented in Table 2.3.5-2.

Table 2.3.5-1 Mechanical Properties of SB-637, Grade N07718 Nickel Alloy Steel Bolting Material

Property	**Value**							
Temperature (°F)	**-40**	**-20**	**70**	**200**	**300**	**400**	**500**	**750**
Ultimate Strength Stress, S_u *	No Value Given	185.0	185.0	177.6	173.5	170.6	168.7	165.0
Yield Stress, S_y (ksi) *	No Value Given	150.0	150.0	144.0	140.7	138.3	136.8	133.8
Maximum Allowable Stress, S (ksi) [21]	No Value Given	37.0	37.0	36.0	35.2	34.6	34.2	33.5
Design Stress Intensity, S_m (ksi) [21]	No Value Given	50.0	50.0	48.0	46.9	46.1	45.6	44.6
Modulus of Elasticity, E (ksi) [21]	29.6E+03	29.5E+03	29.0E+03	28.3E+03	27.8E+03	27.6E+03	27.1E+03	26.1E+03
Alternating Stress @ 10 cycles (ksi) [17]	13.3	13.7	13.1	12.7	12.5	12.4	12.2	11.7
Coefficient of Thermal Expansion, α (in/in/°F) [21]	No Value Given		7.05E-06	7.22E-06	7.33E-06	7.45E-06	7.57E-06	7.82E-06
Poisson's Ratio [21]	← 0.31 →							
Density [21]	← 503 lbm/ft³ (0.291 lbm/in³) →							

Note: Reference [17] Appendix I.

* Calculated based on Design Stress Intensity:

$$\left(\frac{S_{m\ temp}}{S_{m\ 70}}\right) S_{u70} = S_{u\ temp}$$

Table 2.3.5-2 Mechanical Properties of SA-193, Grade B6, High Alloy Steel Bolting Material

Property	**Value**							
Temperature (°F)	**-40**	**-20**	**70**	**200**	**300**	**400**	**500**	**600**
Ultimate Stress, S_u (ksi) *	No Value Given	110.0	110.0	104.9	101.5	98.3	95.6	92.9
Yield Stress, S_y (ksi) *	No Value Given	85.0	85.0	81.1	78.1	76.0	73.9	71.8
Design Stress Intensity, S_m (ksi) [21]	28.3	28.3	28.3	27.0	26.1	25.3	24.6	23.9
Modulus of Elasticity, E (ksi) [21]	30.1E+ 03	30.1E+ 03	29.2E+ 03	28.5E+ 03	27.9E+ 03	27.3E+ 03	26.7E+ 03	26.1E+03
Alternating Stress @ 10 cycles (ksi) [17]	1104.4	1100.0	1085.0	1058.0	1035.0	1015.0	989.0	935.3
Alternating Stress @ 10^6 cycles (ksi) [17]	13.0	12.9	12.7	12.4	12.2	11.9	11.6	11.0
Coefficient of Thermal Expansion, α (in/in/°F) [21]	5.73E-06	5.76E-06	5.92E-06	6.15E-06	6.30E-06	6.40E-06	6.48E-06	6.53E-06
Poisson's Ratio [21]	← 0.31 →							
Density [21]	← 503 lbm/ft^3 (0.291 lbm/in^3) →							

Note: Reference [17] Appendix I.

* Calculated based on Design Stress Intensity:

$$\left(\frac{S_{m-temp}}{S_{m70}}\right) S_{u70} = S_{u-temp}$$

Table 2.3.5-3 Mechanical Properties of SA-193, Grade B8S, High Alloy Steel Bolting Material

Property	Value							
Temperature (°F)	**-40**	**-20**	**70**	**200**	**300**	**400**	**500**	**600**
Ultimate Stress, S_u (ksi) [1]	No Value Given	95	95	93.7	87.3	82.0	79.2	78.0
Yield Stress, S_y (ksi) [2]	No Value Given	50	50	39.8	33.1	29.6	27.7	26.4
Design Stress Intensity, S_m (ksi) [21][3]	No Value Given	16.7	16.7	13.0	11.0	9.9	9.2	8.8
Modulus of Elasticity, E (ksi) [21]	28.8E+03	28.7E+03	28.3E+03	27.6E+03	27.0E+03	26.5E+03	25.8E+03	25.3E+03
Alternating Stress @ 10 cycles (ksi) [17]	720.5	718	708	690.5	675.5	663	645.5	632.9
Alternating Stress @ 10^6 cycles (ksi) [17]	28.8	28.7	28.3	27.6	27.0	26.5	25.8	25.3
Coefficient of Thermal Expansion, α (in/in/°F) [21]	8.27E-06	8.38E-06	8.55E-06	8.79E-06	9.00E-06	9.19E-06	9.37E-06	9.53E-06
Poisson's Ratio [21]	← 0.31 →							
Density [21]	← 501 lbm/ft^3(0.29 lbm/in^3) →							

1. Section II, Table U, page 444, Alloy S21800.
2. Section II, Table Y-1, page 536, Alloy S21800.
3. Section II, Table 4, page 416, B8S.

2.3.6 Aluminum Alloys

SB-209, Type 6061-**T651**, aluminum alloy is used to fabricate the heat transfer disks in the basket and the spacers used to locate the BWR canisters in the cask. The heat transfer disks are included in the basket to enhance heat transfer performance of the fuel support structure and are not safety-related load path components. The spacers are designed to locate the Transportable Storage Canisters axially in the transport cask cavity. The Type 6061-**T651** material is selected for its high thermal conductivity relative to material weight, high strength, and ASME recognition.

The mechanical properties of SB-209, Type 6061-**T651** aluminum alloy are presented in Table 2.3.6-1. These material properties are provided for information only and are not intended as documentation for the structural performance of the cask package.

Table 2.3.6-1 Mechanical Properties of 6061-**T651** Aluminum Alloy

Property	**Value**						
Temperature (°F)	**70**	**100**	**200**	**300**	**400**	**500**	**600**
Ultimate Tensile Stress, S_u (ksi) [22]	42.0	40.7	38.2	31.5	17.2	6.7	3.4
Yield Stress, Sy (ksi) [22]	35.0	33.9	32.2	26.9	14.0	5.3	2.5
Design Stress Intensity S_m (ksi) [22]	10.5	10.5	10.5	8.4	4.4	No Values Given	
Modulus of Elasticity, E (ksi) [21]	10.0E+03	9.9E+03	9.6E+03	9.2E+03	8.7E+03	8.1E+03	7.0E+03
Coefficient of Thermal Expansion, α (in/in/°F) [21]	No Value Given	12.6E-06	12.91E-06	13.22E-06	13.52E-06	13.7E-06	14.3E-06
Poisson's Ratio [21]	← 0.33 →						
Density [21]	← 0.098 lbm/in³ →						

2.3.7 Shielding Material

Gamma radiation shielding for the Universal Transport Cask is provided by the steel cask body and the lid and by the lead in the cask wall. The primary radial gamma radiation shielding for the cask is provided by a cylinder of chemical lead, which fills the annulus between the inner and outer shells. The lead will not experience large deformation or volume change because it is completely enclosed and is essentially incompressible. The coefficient of thermal expansion for lead is of particular significance because it is approximately twice that of stainless steel. The static mechanical properties of chemical copper lead are presented in Table 2.3.7-1.

Neutron radiation shielding for the cask is provided by a solid synthetic polymer, NS-4-FR, located in the bottom of the cask and around the outside of the outer shell. The solid neutron shield material eliminates leakage and maintenance concerns associated with liquid neutron shields. The NS-4-FR neutron-shielding function requires no strength and none is assumed for the structural evaluations. The mechanical properties of NS-4-FR are presented in Table 2.3.7-2.

Table 2.3.7-1 Static Mechanical Properties of Chemical Copper Lead

Property	**Value**					
Temperature (°F)	**-40**	**-20**	**70**	**200**	**300**	**600**
Tensile Yield Strength, S_y (ksi) [23]	0.700	0.680	0.640	0.490	0.380	**0.200**
Modulus of Elasticity, E (ksi) [24]	2.45E+03	2.42E+03	2.28E+03	2.06E+03	1.94E+03	1.5E+03
Coefficient of Thermal Expansion, α (in/in/°F) [24]	15.6E-06	15.7E-06	16.1E-06	16.6E-06	17.2E-06	20.2E-06
Poisson's Ratio [25]	← 0.40 →					
Density [25]	← 708 lbm/ft^3 (0.41 lbm/in^3) →					

Table 2.3.7-2 Mechanical Properties of NS-4-FR

Property	**Value**			
Temperature (°F)	**86**	**158**	**212**	**302**
Compressive Modulus, E_c (ksi) [26]	561	561	561	561
Coefficient of Thermal Expansion, α (in/in/°F) [26]	2.22E-05	4.72E-05	5.88E-05	5.741E-05
Density, (lbm/in^3) [26]	0.0607	0.0607	0.0607	0.0607

2.3.8 Impact Limiter Materials

The transport impact limiters for the Universal Transport Cask are fabricated from redwood and balsa wood that is encased in stainless steel shells. The impact limiters absorb the kinetic energy of the loaded cask in a drop impact by crushing the redwood and balsa wood. The energy dissipated, or absorbed by crushing the wood, for a given increment of time, is equal to the integral of the area (i.e., area of impact limiter engaged in crushing) times the crush strength of the wood. The area under the force-deflection curve is equal to the amount of energy absorbed by crushing of the redwood, balsa wood, and the impact limiter shell.

The force-deformation curves for the Universal Transport Cask upper and lower impact limiters for end, corner, 75° oblique, and side impact orientations are presented in Figures 2.6.7.5-**12** through 2.6.7.5-**18**. The crush stress–strain curves for the redwood and the balsa wood used in the design evaluation of the impact limiters are presented in Figures 2.6.7.5-3 through 2.6.7.5-5.

2.4 General Standards for All Packages

This section demonstrates that the design of the Universal Transport Cask complies with the general standards for all packages as specified in Paragraphs (a) through (h) of 10 CFR 71.43. A packaging is defined as an assembly of components necessary to ensure compliance with the packaging requirements of 10 CFR 71 for the transportation of radioactive contents.

2.4.1 Minimum Package Size

The transverse dimension of the Universal Transport Cask is 92.11 in., and the longitudinal dimension is 209.25 in. Both of these dimensions are greater than 10 cm; therefore, the requirements of 10 CFR 71.43(a) are satisfied.

2.4.2 Tamper-Indication Feature

Crimped wire seals are used on the Universal Transport Cask as tamper-indicators. A numbered crimped wire seal is looped through a hole in the end flange of the lifting trunnion and through a hole in an adjacent corner of the upper impact limiter. The upper impact limiter must be removed to obtain access to the cask closure assembly (lid and bolts); thus, a severed seal will indicate purposeful tampering. This feature satisfies the tamper-indication requirement of 10 CFR 71.43(b).

The drain port located in the cask bottom is protected by a bolted coverplate. The drain port is covered by the lower impact limiter, which must be removed for access to the coverplate. A numbered seal similar to the one discussed above is crimped onto a seal wire between the lower impact limiter and the rear cask support to satisfy the requirements of 10 CFR 71.43(b).

2.4.3 Positive Closure

Inadvertent opening of the cask lid or port coverplates from the combined effects of shock, vibration, thermal expansion, internal loads, or external loads cannot occur because of the large preload applied to the lid bolts. Loosening of these bolts is resisted by friction from the large clamping forces produced by the bolt installation torque. A written cask operations procedure is followed to ensure that each bolt is torqued. To open the cask lid, the bolts must be deliberately loosened with a wrench. Tamper-indicating features (Section 2.4.2) provide

evidence of attempted unauthorized operation of the cask closure. Therefore, the Universal Transport Cask containment system cannot be opened unintentionally and evidence of attempted unauthorized operation is provided. Thus, the requirements of 10 CFR 71.43(c) are satisfied.

2.4.4 Chemical, Galvanic, or Other Reactions

The materials used in the fabrication and operation of the Universal Transport Cask—including coatings, lubricants, and cleaning agents—have been evaluated to determine whether chemical, galvanic, or other reactions among the materials, contents, and environments can occur. All phases of cask operation—loading, unloading, handling, and transportation—have been considered for the environments that may be encountered under normal or accident conditions.

The evaluation identified no potential reactions that could adversely affect the overall integrity of the cask, the Transportable Storage Canister , or the structural integrity and retrievability of the canister from the cask. The evaluation conforms to the guidelines of NRC Bulletin 96-04, "Chemical, Galvanic, or Other Reactions in Spent Fuel Storage and Transportation Casks," [27], and demonstrates that the cask meets the requirements of 10 CFR 71.43(d).

2.4.4.1 Component Operating Environment

The Universal Transport Cask is loaded and handled dry. The component materials of the cask and canister are exposed to an operating environment in which the cask cavity contains either helium or air but transport cask external surroundings could be air, rain water/snow/ice, and/or marine (salty) water/air.

The exposed surfaces of the Universal Transport Cask and the Transportable Storage Canister are all stainless steel, except for the containment boundary o-ring seals of the transport cask.

Some of the cask component materials are completely enclosed and are exposed to an unchanging environment that is permanently sealed. These components include shielding materials in the cask body and the energy-absorbing materials in the impact limiters that are exposed only to the temperature effects of the operating environment. The sealed shielding material regions are typically evacuated and backfilled with helium, and the impact limiter shells are leak tested following fabrication.

Each of the categories of cask component materials is evaluated for potential reactions in each of the operating environments to which these materials are exposed. These exposures may occur during cask loading or unloading, handling, or transport, and normal and accident conditions.

The operating environments to which the cask component materials can be exposed do not provide the conditions necessary for a reaction (corrosion), because both moisture and oxygen must be present for corrosion to occur. Since the transport cask and canister are both dry at the time of loading, corrosion of the transport cask cavity shell and canister exterior surface do not occur. Loading of the canister in the transport cask occurs in air. During closing and sealing of the transport cask, the air is evacuated and the cask cavity is backfilled with helium. The displacement of oxygen in the cavity by helium effectively precludes corrosion. Galvanic corrosion (between dissimilar metals that are in contact) does not occur because the transport cask cavity and the canister are both fabricated from stainless steel.

The third of the operating environments involves those materials that are completely enclosed (permanently sealed) within another material, e.g., the primary shield materials (lead and NS-4-FR), or the energy-absorbing materials (wood) in the impact limiters. The metals oxidize any oxygen trapped in the sealed region until thermodynamic equilibrium is reached, i.e., a thin oxide layer develops on the lead . Similarly, the hydrogen in the NS-4-FR material captures any oxygen present until thermodynamic equilibrium is reached. Because the quantity of oxygen present, if any, is very small, equilibrium is reached very quickly and active corrosion in sealed regions does not occur.

2.4.4.2 Component Material Categories

The component materials evaluated are categorized on the basis of similarity of physical and chemical properties or similarity of component functions. The categories of materials that are considered are: (1) stainless/nickel alloy steels; (2) nonferrous metals; (3) shielding materials; (4) energy-absorbing materials; (5) cellular foams and insulations; (6) lubricants and greases; and (7) seals . These categories are evaluated on the basis of the environment to which they could be exposed during operation or use of the transport cask. The material categories and exposure environments are summarized in Table 2.4.4.2-1.

The cask component materials are not reactive among themselves, with the cask contents (the transportable storage canister), nor with the cask's dry operating environment during any phase of normal or accident condition loading, unloading, handling, or transportation operations. Because no reactions occur, no gases or other corrosion by-products are generated.

2.4.4.2.1 Stainless/Nickel Alloy Steels

No reaction of the cask component steels (stainless or nickel alloy) is expected in any environment except for the external marine (salt air) environment, where chloride-containing salt spray might initiate pitting of the exterior surface if the chlorides are allowed to concentrate and stay wet for extended periods of time (weeks). Only the external cask surface could be so exposed to the marine environment. The corrosion rate is, however, so low that no detectable corrosion products or gases are generated. Additionally to minimize the collection of such materials as salts, the cask has smooth external surfaces, and ridges and crevices are limited. The cask exterior is cleaned each time it is decontaminated to eliminate any collection of such chloride-containing salts or other corrosive agents.

Galvanic corrosion between the stainless steels, inconel, and the nickel alloy steels does not occur because no effective electrochemical potential difference exists between these metals. No coatings are applied to the stainless, or nickel alloy, steels.

Copper cooling fins in the neutron shield material and the lead gamma radiation shield material are in contact with the transport cask stainless steel shells but only in the completely enclosed (permanently sealed) gamma or neutron shield regions, where no water is present. Therefore, no reaction with stainless steel occurs.

No potential exists for a reaction between stainless steel and any silicone products, fluorocarbon elastomers, dry film lubricants, or EPDM (ethylene propolyene rubber) .

Therefore, there is no potential for reactions associated with the transport cask stainless steel components.

2.4.4.2.2 Nonferrous Metals

The nonferrous metals used in the Universal Transport Cask are copper and lead. As discussed in the previous section, these nonferrous metals do not react in contact with stainless steel. Copper fins embedded in the neutron shield (NS-4-FR) region do not react with the NS-4-FR because no electrochemical driving potential exists between the materials. Reactions of lead are described in Section 2.4.4.2.3.

There are no significant potential reactions associated with the nonferrous metal components of the transport cask.

2.4.4.2.3 Shielding Materials

The primary shielding materials used in the cask are lead and NS-4-FR [26]. These materials are completely enclosed and sealed in stainless steel during transport cask fabrication. These materials do not react with the stainless steel or with the copper fins. The lead oxidizes any oxygen trapped in the sealed region until thermodynamic equilibrium is reached, i.e., a thin oxide layer develops on the lead. Similarly, the hydrogen in the NS-4-FR material captures any oxygen present until thermodynamic equilibrium is reached. Because the quantity of oxygen present, if any, is very small, equilibrium is reached very quickly and active corrosion in sealed regions does not occur.

Therefore, no potential reactions are associated with the cask shielding materials.

2.4.4.2.4 Energy Absorbing Material

Redwood and balsa woods are used for energy absorption in the transport cask impact limiters. The wood is completely enclosed (sealed) in a stainless steel shell and no potential reactions occur between the wood and the stainless steel shells. The wood is coated with a preservative prior to installation in the impact limiter shell and blocks of wood may be glued together with an epoxy adhesive. A 0.125 in. thick layer of Fire Block® insulating material is affixed to the

interior surfaces of the impact limiter shell that are in direct contact with the transport cask surface. These are standard applications of preservatives and adhesives, and no post application reaction occurs.

No potential reactions are associated with the energy-absorbing or insulating material.

2.4.4.2.5 Cellular Foam and Insulation

Layers of expansion foam and strips of insulation are used in the solid neutron shield regions of the cask. The expansion foam permits thermal expansion of the solid neutron shield material during normal operation and the insulation protects the expansion foam during final closure welding of the neutron shield shell to the end plate. The foam and the insulation are nonflammable, nontoxic, and noncorrosive silicone products that are used in the cask in a standard design application.

No potential reactions are associated with the silicone expansion foam or insulation.

2.4.4.2.6 Lubricant and Grease

The dry film lubricants used in the cask meet the performance and general compositional requirements of the nuclear power industry. NEVER-SEEZ® lubricant is used primarily on rotating bearing surfaces. Neolube® is used primarily on threaded/mechanical connection surfaces. In addition, Dow Corning High Vacuum Grease is used as an adherent/lubricant to lubricate and retain the O-ring seals in their grooves. None of these lubricants contains elements or compounds prohibited by the NRC. NEVER-SEEZ® is a superior, high-temperature, antiseize and extreme pressure lubricant that contains flake particles of pure nickel, graphite, and other additives in a special grease carrier. It is used on the trunnion surfaces of the cask. Neolube® is 99% pure furnace graphite particles in isopropanol. It has excellent radiation resistance and high chemical purity. It dries as a thin, noncorrosive film with excellent adhesion, does not migrate, and is nonfreezable. Dow Corning High Vacuum Grease is a stiff, nonmelting, nonoxidizing, nongumming silicone lubricating material that is insoluble in most solutions.

No potential reactions are associated with these lubricants or grease.

2.4.4.2.7 Seals

O-ring seals formed from silicone rubber, ethylene propylene rubber (EPDM), and Viton compounds are used in the Universal Transport Cask. Viton is a silicon elastomer. EPDM or elastomer O-rings are used for transport cask applications because of their excellent short-term sealing capabilities and ease of handling. The components of all of the seal and gasket materials are stable and nonreactive.

No potential reactions are associated with the cask seal materials.

2.4.4.3 General Effects of Identified Reactions

No potential chemical, galvanic, or other reactions have been identified for the Universal Transport Cask. Therefore, no adverse conditions—such as the generation of flammable or explosive quantities of combustible gases , —can result during any phase of cask operations for normal, or accident conditions.

2.4.4.4 Adequacy of Cask Operating Procedures

Because this evaluation identifies no reactions between or among cask components, the Universal Transport Cask operating controls and procedures presented in Chapter 7.0 are adequate to minimize the occurrence of hazardous conditions.

2.4.4.5 Effects of Reaction Products

No potential chemical, galvanic, or other reactions have been identified for the cask. Therefore, the overall integrity of the cask and the structural integrity and retrievability of the spent fuel is not adversely affected for any cask operations throughout the design basis life of the cask. **No reactions occur between or among cask components that results in a change in thermal properties, changes in basket clearances, the binding of mechanical surfaces or the degrading of safety components, either directly or indirectly.**

Table 2.4.4.2-1 Summary of Universal Transport Cask Materials Categories and Operating Environments

ITEM	MATERIAL	ENVIRONMENT
Stainless Steels/Alloys	304, 304L, XM-19, 17-4PH, Nickel Alloy, 410	Sealed Internal Open Internal/ External
Nonferrous Metals	ASTM B152 Cu,	Sealed Internal
Shielding Materials	NS-4-FR, Chemical Copper Lead	Enclosed
Energy Absorbing Materials	Balsa Wood, Redwood	Enclosed
Cellular Foam/Insulation	Fire Block® HT-800® Silicone Foam	Enclosed
Lubricants and Greases	Never-Seeze® Neolube® High Vacuum Grease® by Dow Corning	Sealed Internal Open Internal
Seals and Gaskets	Silicone Rubber, EPDM, Viton	Sealed Internal Open Internal/ External

2.4.5 Conformance to Cask Design Requirements

The Universal Transport Cask is designed to meet the design requirements of 10 CFR 71. Criticality, shielding, radiological, thermal, and structural requirements of 10 CFR 71 are satisfied as shown analytically in this report. The cask is an exclusive-use package designed for transport in a 100°F environment such that personnel barrier or other accessible surface temperatures do not exceed 122°F. Therefore, the cask design, construction, and preparation for transport are in conformance with the requirements of 10 CFR 71.43(g).

2.4.6 Continuous Venting

The neutron shield is the only vented component of the Universal Transport Cask. It contains a solid synthetic polymer (NS-4-FR), which has been shown by manufacturers' testing to give off small amounts of water vapor at the temperatures that occur during the thermal (fire) accident. Two relief valves are provided in the bottom end plate to prevent a pressure build-up in the neutron shield (under hypothetical fire accident conditions) and to minimize recovery from an overpressure condition. Prior to the NS-4-FR being poured into each shell chamber, a release agent is applied to two of the interior metal surfaces of the neutron shield shell. The release agent will prevent the NS-4-FR from bonding with the metal surfaces, allowing the NS-4-FR to separate from the metal surfaces as it shrinks during curing. The small crack that results will be sufficient to allow the pressure at the top of the neutron shield tank to equalize with the bottom of the tank. The relief valves do not provide a safety function. No venting of the neutron shield or any of the cask component occurs during normal operations conditions; thus, the requirements of 10 CFR 71.43(h) are met.

THIS PAGE INTENTIONALLY LEFT BLANK

2.5 Lifting and Tiedown Standards

2.5.1 Lifting Devices

The Universal Transport Cask has two types of lifting devices: lifting trunnions and hoist rings. These lifting devices are designed to satisfy the requirements of 10 CFR 71.45(a), NUREG-0612, [3] and ANSI N14.6 [4]. NUREG-0612 defines specific design criteria to ensure the safe handling of heavy loads in critical regions of nuclear power plants and ANSI N14.6 defines very similar lifting criteria. The design criteria in NUREG-0612 and ANSI N14.6 equal or exceed those of 10 CFR 71.

The cask is equipped with two primary and two secondary lifting trunnions located on the top forging near the top of the cask, spaced at 90° intervals. The primary lifting trunnions are welded to the top forging, and the secondary lifting trunnions are bolted to the top forging. Two rotation pockets on the outer shell near the bottom of the cask permit rotation of the cask to the horizontal position and also provide longitudinal tiedown restraint in the aft direction during transport.

A single two-arm yoke (non-redundant, but designed to the critical load requirements), or a four-point combination of two yokes (redundant) may be used to lift and handle the cask. The two-arm yoke attaches to the primary lifting trunnions only. An overhead crane is used to lift the cask and yoke(s). No impact limiter is attached to the cask during lifting and handling. The lid hoist-rings are used for lifting the lid during installation or removal.

2.5.1.1 Lifting Trunnion Analysis

The Universal Transport Cask primary lifting trunnions are designed to meet the heavy lifting requirements of NUREG-0612 and ANSI N14.6 for a non-redundant lifting system, that is, a two-trunnion lift. The two primary lifting trunnions are capable of supporting a maximum load, defined as six times the design weight of the cask without producing stresses in the cask or trunnions greater than the material yield strength or ten times the design weight without producing stresses in the cask or trunnions exceeding the material ultimate strength.

The design weight of the cask, 260,000 lb, is used for the lifting analysis. The loads on each primary lifting trunnion for a non-redundant lift are as follows:

$$(F_y)_p = \frac{260{,}000 \times 6}{2} = 780{,}000 \text{ lb} \quad \text{(yield strength criteria)}$$

$$(F_u)_p = \frac{260{,}000 \times 10}{2} = 1{,}300{,}000 \text{ lb} \quad \text{(ultimate strength criteria)}$$

In addition to the primary lifting trunnions, the cask has the capability of being equipped with two additional, secondary lifting trunnions to accommodate a redundant (four-trunnion) lift. The two secondary lifting trunnions are capable of supporting a maximum load, defined as three times the design weight of the cask without producing stresses in the cask greater than the material yield strength or five times the design weight without producing stresses in the cask exceeding the material ultimate strength.

The loads on each lifting trunnion for a redundant lift are as follows:

$$(F_y)_s = \frac{260{,}000 \times 3}{2} = 390{,}000 \text{ lb} \quad \text{(yield strength criteria)}$$

$$(F_u)_s = \frac{260{,}000 \times 5}{2} = 650{,}000 \text{ lb} \quad \text{(ultimate strength criteria)}$$

The primary lifting trunnions are welded to the top forging and the secondary lifting trunnions are bolted to the top forging using twelve 1 1/8-12 UNF bolts.

The properties of the materials used in the lifting trunnion analysis are as follows at the conservatively high temperature of 350°F:

1. Trunnions — SA-564, Type 630

   $S_y = 91.25$ ksi

   $S_u = 133.25$ ksi

2. Top Forging — SA-336, Type 304

   $S_y = 21.60$ ksi

   $S_u = 60.75$ ksi

3. Filler Material — AWS E309

$S_y = 30.4$ ksi

$S_u = 80.0$ ksi

4. Bolting Material SB-637, Gr N07718

$S_y = 139.5$ ksi

$S_u = 172.1$ ksi

2.5.1.1.1 Primary Lifting Trunnions

Trunnion Shank

Per ANSI N14.6, the shear stress is taken as an average value over the cross section.

YIELD STRENGTH CRITERIA:

The shear stress is

$$\tau_{sy} = \frac{(F_y)_p}{A} = \frac{780{,}000}{(\pi/4)(6.50)^2} = 23{,}470 \text{ psi}$$

By applying the lifting force at the middle of the shank, the bending moment, M_y, is:

$$M_y = 780{,}000 \times 1.5 = 1{,}170{,}000 \text{ in} \cdot \text{lb}$$

and, the bending stress is

$$\sigma_{sy} = \frac{M_y}{S} = \frac{1{,}170{,}000}{(\pi/32)(6.50)^3} = 43{,}296 \text{ psi}$$

The combined stress is

$$\sigma_{evy} = \left[\left(\sigma_{sy}^2\right) + \left(3\tau_{sy}^2\right)\right]^{0.5} = 59{,}428 \text{ psi}$$

The margin of safety is

$$MS = \frac{S_y}{\sigma_{evy}} - 1 = +0.53$$

ULTIMATE STRENGTH CRITERIA

Trunion Shank

The shear stress is

$$\tau_{su} = \frac{(F_u)_p}{A} = \frac{1{,}300{,}000}{(\pi/4)(6.50)^2} = 39{,}116 \text{ psi}$$

By applying the lifting force at the middle of the shank, the bending moment, M_{su}, is:

$$M_{su} = 1{,}300{,}000 \times 1.5 = 1{,}950{,}000 \text{ in} \cdot \text{lb}$$

and, the bending stress is

$$\sigma_{su} = \frac{M_u}{S} = \frac{1{,}950{,}000}{(\pi/32)(6.50)^3} = 72{,}159 \text{ psi}$$

The combined stress is

$$\sigma_{evu} = \left[\left(\sigma_{su}^2\right) + \left(3\tau_{su}^2\right)\right]^{0.5} = 99{,}110 \text{ psi}$$

The margin of safety is

$$MS = \frac{S_u}{\sigma_{evu}} - 1 = +0.34$$

Primary Trunnion Base Weld

The primary trunnions are welded to the top forging of the cask body. The geometry of the weld at extreme locations conforms to the following configuration.

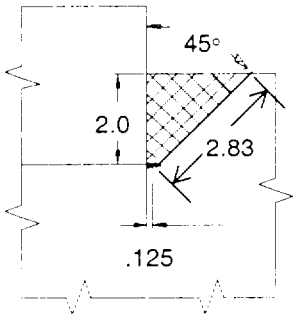

Point A

Vessel Longitudinal Plane

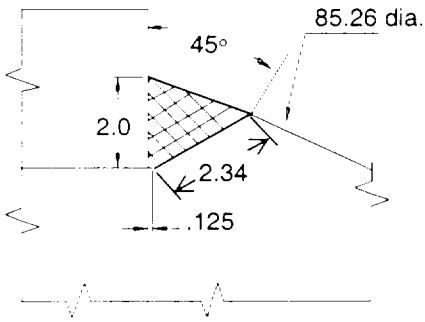

Point B

Vessel Cross Section

Sections Through Trunnion Welds

The welded connection is evaluated both at the trunnion/weld interface and at the weld/forging interface.

Primary Trunnion / Weld Interface

YIELD STRENGTH CRITERIA

The bending moment produces, at the trunnion/weld interface, a pattern of unit shear force as shown in the following diagram.

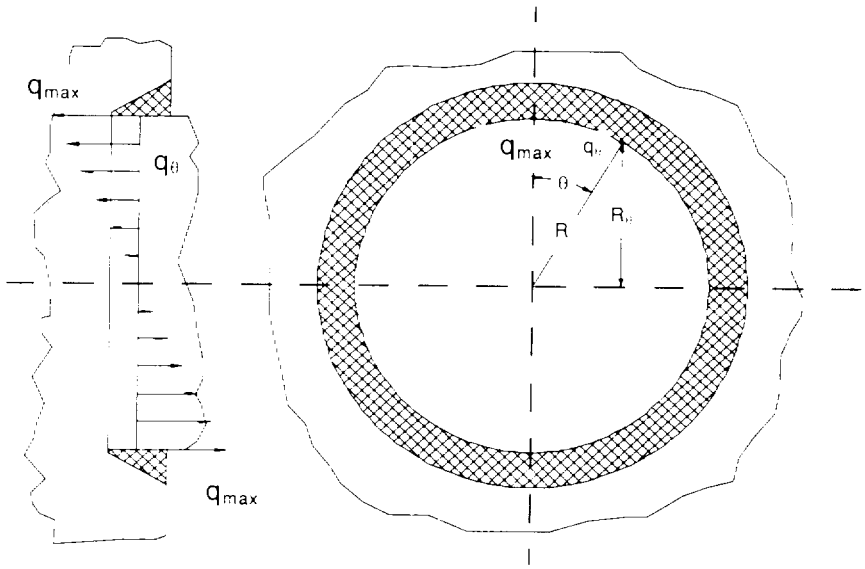

The differential bending moment, dM_y, due to the unit shear force $q_{y\theta}$, at an angular position θ, is

$$dM_y = \left(q_{y\theta} R d\theta\right)\left(R_\theta\right) = q_{ymax} R^2 \cos^2\theta \, d\theta$$

The value of q_{max} is

$$M_y = 4\int_0^{\frac{\pi}{2}} q_{ymax} R^2 \cos^2\theta d\theta$$

where $M_y = (F_y)(4) = 780{,}000 \times 4 = 3{,}120{,}000$ in·lb.

Then

$$q_{ymax} = \frac{M_y}{R^2\pi} = \frac{3.12 \times 10^6}{6^2\pi} = 27{,}587 \text{ lb/in.}$$

The maximum shear stress, τ_{ymax}, is

$$\tau_{ymax} = \frac{q_{ymax}}{t} = \frac{27{,}587}{2} = 13{,}794 \text{ psi}$$

where the weld depth, t, is 2 in.

The normal stress, σ_{by}, is

$$\sigma_{by} = \frac{F_y}{A_w} = \frac{780{,}000}{(\pi)(12)(2)} = 10{,}345 \text{ psi},$$

with the lower half of the weld in tension and the upper half in compression.

The weld material, with its lower yield strength, is used for the evaluation.

The combined stress is

$$\sigma_{evy} = \left[\left(\sigma_{by}^2\right) + \left(3\tau_{ymax}^2\right)\right]^{0.5} = 26{,}067 \text{ psi}$$

The margin of safety is

$$MS = \frac{S_y}{\sigma_{evy}} - 1 = \frac{30{,}400}{26{,}067} - 1 = +0.16$$

ULTIMATE STRENGTH CRITERIA

Using the same procedure as for the yield strength criteria, the maximum unit shear force, q_{umax}, is

$$q_{umax} = \frac{M_u}{R^2\pi} = \frac{5.2 \times 10^6}{6^2\pi} = 45{,}978 \text{ lb/in.}$$

where $M_u = (F_u)(4) = 1{,}300{,}000 \times 4 = 5.2 \times 10^6$ in·lb.

The maximum shear stress, τ_{umax}, is

$$\tau_{umax} = \frac{q_{umax}}{t} = \frac{45{,}978}{2} = 22{,}989 \text{ psi}$$

where the weld depth, t, is 2 in.

The normal stress, σ_{bu}, is

$$\sigma_{bu} = \frac{F_u}{A_w} = \frac{1{,}300{,}000}{(\pi)(12)(2)} = 17{,}242 \text{ psi}$$

with the lower half of the weld in tension and the upper half in compression.

The weld material, with its lower ultimate strength, is used for the evaluation.

The combined stress is

$$\sigma_{evu} = \left[\left(\sigma_{bu}^2\right) + \left(3\tau_{umax}^2\right)\right]^{0.5} = 43{,}412 \text{ psi}$$

The margin of safety is

$$MS = \frac{S_u}{\sigma_{evu}} - 1 = \frac{80{,}000}{43{,}412} - 1 = +0.84.$$

Weld / Forging Interface

The weld/forging interface consists of the 1/8 in. root around the trunnion and the surface on the 90° apex angle truncated cone.

The weld/forging interface varies from a maximum on the vessel longitudinal plane, to a minimum on the vessel cross-section plane. A weld mean section is taken for the analysis; its perimeter consists of the vertical height, 2.0 in.; the weld root, 0.125 in.; the slant height (mean between the maximum, 2.83 in. and the minimum, 2.34 in. values), 2.59 in.

The analysis section is taken as the surface of the cylinder, with radius R, concentric with the trunnion, where R is

$$R = 6 + 0.125 + (0.5)(2.59)(\sin 45°) = 7.04 \text{ in.}$$

The height of the cylinder is taken as

$$t = 2.59 \cos 45° = 1.83 \text{ in.}$$

YIELD STRENGTH CRITERIA

Shear Stress

The maximum unit shear force, q_{ymax}, is

$$q_{ymax} = \frac{M_y}{R^2\pi} = \frac{3.12\times10^6}{7.04^2\pi} = 20{,}038 \text{ lb/in.}$$

The maximum shear stress, $\tau_{y\,max}$, is

$$\tau_{y\,max} = \frac{q_{ymax}}{t} = \frac{20{,}038}{2.59\cos(45°)} = 10{,}941 \text{ psi}$$

where the weld depth, t, is 2.59·cos(45°) in.

The normal stress, σ_{by}, is

$$\sigma_{by} = \frac{F_y}{A_w} = \frac{780{,}000}{(\pi)(2)(7.04)(2.59)\cos 45°} = 9{,}628 \text{ psi}$$

with the lower half of the weld in tension and the upper half in compression. The forging material, with its lower ultimate strength, is used for the evaluation.

The combined stress is

$$\sigma_{evy} = \left[\left(\sigma_{by}^2\right) + \left(3\tau_{ymax}^2\right)\right]^{0.5} = 21{,}256 \text{ psi}$$

The margin of safety is

$$MS = \frac{S_y}{\sigma_{evy}} - 1 = \frac{21{,}600}{21{,}256} - 1 = +0.01$$

ULTIMATE STRENGTH CRITERIA

Shear Stress

The maximum unit shear force, q_{umax}, is

$$q_{umax} = \frac{M_u}{R^2 \pi} = \frac{5.2 \times 10^6}{7.04^2 \pi} = 33{,}397 \text{ lb/in.}$$

The maximum shear stress, τ_{umax}, is

$$\tau_{umax} = \frac{q_{umax}}{t} = \frac{33{,}397}{2.59 \cos(45°)} = 18{,}236 \text{ psi}$$

where the weld depth, t, is 2.59cos·(45°) in.

The normal stress, σ_{bu}, is

$$\sigma_{bu} = \frac{F_u}{A_w} = \frac{1{,}300{,}000}{(\pi)(2)(7.04)(2.59)\cos 45°} = 16{,}047 \text{ psi},$$

with the lower half of the weld in tension and the upper half in compression.

The forging material, with its lower ultimate strength, is used for the evaluation.

The combined stress is

$$\sigma_{evu} = \left[\left(\sigma_{bu}^2\right) + \left(3\tau_{umax}^2\right)\right]^{0.5} = 35{,}428 \text{ psi}$$

The margin of safety is

$$MS = \frac{S_u}{\sigma_{evu}} - 1 = \frac{60{,}750}{35{,}428} - 1 = +0.71$$

Trunnion Base Plate

The trunnion base plate is analyzed, conservatively, as a flat circular plate with its outer edge fixed according to the method in Roark [28]. The maximum bending (radial) stress in the trunnion base plate (upper and lower surface), occurs at the outer edge of the trunnion shank in the plane of the bending moment and is determined as follows.

$$\sigma_r = \frac{\beta M}{a t^2}$$

Where $\beta =$ a variable depending on the ratio b/a

b = radius of the trunnion = 3.25 in.

a = radius of the base plate = 6 in.

then, b/a = 0.542, and β =0.9793.

M = M_y or M_u

t = base plate thickness = 3.5 in.

YIELD STRENGTH CRITERIA

$$\sigma_{ry} = \frac{\beta\ M_y}{at^2} = \frac{0.9793\left(3.12 \times 10^6\right)}{6(3.5)^2} = 41{,}570 \text{ psi}$$

The margin of safety is

$$MS = \frac{Sy}{\sigma_{evy}} - 1 = \frac{91{,}250}{41{,}570} - 1 = +1.20$$

ULTIMATE STRENGTH CRITERIA

$$\sigma_{ru} = \frac{\beta\ M_u}{at^2} = \frac{0.9793\left(5.2 \times 10^6\right)}{6(3.5)^2} = 69{,}290 \text{ psi}$$

The margin of safety is

$$MS = \frac{Su}{\sigma_{ru}} - 1 = \frac{133{,}250}{69{,}290} - 1 = +0.92$$

Primary Trunnion Overload

10 CFR 71.45(a) requires any lifting attachment that is a structural part of a package to be designed so that failure under excessive load would not impair the ability of the package to meet other 10 CFR 71 requirements.

Lifting Trunnion Shank

Lifting trunnion shank (Ultimate Shear Strength):

$$F_u = \frac{\pi \cdot d^2}{4}(0.5S_u) = 1.75\times10^6 \text{ lb}$$

where

d = 6.5 in.

S_u = 133.25 ksi (ultimate tensile strength of the trunnion)

Trunnion/weld interface

The ultimate shear strength of the trunnion/weld interface is governed by the shear strength of the weld:

$$F_u = A_w \cdot (0.5S_u) = 2.40 \text{ x } 10^6 \text{ lbs}$$

where

A_w = trunnion/weld interface area, $(2)(12)(\pi) = 75.4 \text{ in}^2$

S_u = 80.0 ksi (ultimate tensile strength of the weld material)

Weld/forging interface

The weld/forging interface area, A_f, is taken as the mean of the weld/forging interface width at points A and B times the circumference at the mean radius of the weld/forging interface plus the area of the 1/8-in. root weld:

$$A_f = 2(\pi)(R_{mean})(h_{mean}) + \pi(6.125^2 - 6.0^2) = 119.3 \text{ in}^2.$$

Where

$$R_{mean} = \frac{[6.0 + 0.125 + (0.5)(2.0 \tan 45°)] + [6.0 + 0.125 + (0.5)(2.34 \sin 45°)]}{2} = 7.04 \text{ in.}$$

$$h_{mean} = \frac{2.83 + 2.34}{2} = 2.59 \text{ in.}$$

Then, the ultimate shear strength, F_{uf}, of the weld forging interface is:

$$F_{uf} = (A_f)(0.5)(S_u) = 3.62 \times 10^6 \text{ lbs.}$$

where

S_u = **60,750 psi** (ultimate tensile strength of the forging).

Thus, the lifting trunnion will fail in shear before the weld or the forging, ensuring that failure caused by excessive overload on the lifting trunnions will not impair the ability of the cask to meet other 10 CFR 71 requirements.

Primary Trunnion/Top Forging Intersection Analysis

Bending stresses are induced in the top forging and outer shell intersection when the cask is lifted at the lifting trunnions. These stresses are evaluated using a closed form ring solution described by Blake [29].

An equivalent ring is considered as representative for the region. See Figure 2.5.1.1-1.

The loading of the equivalent ring, is defined as follows:

F = lifting force = (0.5)**(260,000) = 130,000 lb**.

q = dead weight load per unit length

$$q = \frac{260{,}000}{(\pi)(76.435)} = 1083 \text{ lb/in.}$$

T_o = torque due to the lifting force = **(130,000)(8.91-1.5) = 963,300 in lb.**

The actual load case is a combination of two cases presented by Blake [29]: (1) Ring under toroidal moments and, (2) Ring under transverse uniform load. The combined bending and twisting moments on the equivalent ring, as a function of the angular position, are given by:

$$M = \frac{T_o \sin\theta}{2} - qr^2\left(1 - \frac{\pi}{2}\sin\theta\right)$$

$$T = \frac{T_o \cos\theta}{2} + qr^2\left(\theta + \frac{\pi}{2}\cos\theta - \frac{\pi}{2}\right)$$

The bending moment, M, produces bending (normal) stresses, that are obtained by,

$$\sigma = \frac{My}{I}$$

where $y = 11.66/2 = 5.83$ in.

and $I = (8.84)(11.66^3)/12 = 1167.8$ in^4.

The twisting moment, T, produces shear stresses. The locations for evaluation are the upper and lower sides of the ring cross section. The shear stresses at those positions are, from Spotts [30]:

$$\tau = \frac{T}{\alpha_2 bc^2}$$

where $b = 11.66$ in.

$c = 8.84$ in.

α_2 depends on the ratio b/c,

for this case, $\alpha_2 = 0.249$.

For evaluation, the Tresca failure criteria is selected. The category of stresses at the points selected is $P_L + P_b$. The corresponding allowable stress is 1.5 S_m, where $S_m = 19{,}350$ psi for the forging material, SA-336 Type 304.

The computation of stresses and the evaluation at angular positions 0° to 90°, is summarized in Table 2.5.1.1-1. The minimum calculated margin of safety is + 1.10.

2.5.1.1.2 Secondary Lifting Trunnions

The secondary lifting trunnions, together with the primary lifting trunnions, constitute the redundant load path arrangement for the lifting of the cask. The structural adequacy of the secondary lifting trunnions is evaluated in the following sections.

Secondary Lifting Trunnion Bolts

The two secondary lifting trunnions are bolted to the upper forging, with their axes in the same plane as the primary lifting trunnions.

The geometry of the secondary lifting trunnion is shown in Figure 2.5.1.1-2. The lifting force results in a bending moment producing compression and tension zones in the base plate and the mounting bolts. Shear stress is effectively eliminated from the mounting bolts by the tight fit of the trunnion base plate in its corresponding pocket in the top forging.

Each secondary lifting trunnion is attached to the upper forging by 12 bolts 1 1/8-12 UNF-2A.

The location of the neutral axis in the section (see Figure 2.5.1.1-2) is computed by equating the area moments of the tension and compression zones.

The area moment of the tension zone, S_{xyt}, is

$$S_{xyt} = (2)(0.856)\left(4.47 + \bar{y} + 3.27 + \bar{y} + 1.2 + \bar{y} + \bar{y} + 1.2\right)$$

The area moment of the compression zone, S_{xyc}, is

$$S_{xyc} = A_{cs}\left(y_G - \bar{y}\right) - \frac{2\pi}{4}\left(1.17^2\right)\left(4.47 - \bar{y} + 3.27 - \bar{y}\right)$$

where, the area of the circular segment, A_{cs}, is

$$A_{cs} = R^2(\alpha - \sin\alpha\cos\alpha)$$

and, the center of gravity of the circular segment, y_G, is

$$y_G = \frac{2R\sin^3\alpha}{3(\alpha - \sin\alpha\cos\alpha)}$$

$$y = R\cos\alpha$$

By iteration of the equation $S_{xyt} = S_{xyc}$,

$$\alpha = 1.12025 \text{ rad} = 64.1856 \text{ degrees}$$

The moment of inertia, I_{NA}, of the section about the neutral axis, is due to:

(1) The moment of inertia of the bolts, I_b

$$I_b = 2\left(\frac{4\pi D_b^4}{64} + \frac{\pi D_b^2}{4}\left(\Delta_1^2 + \Delta_2^2 + \Delta_3^2 + \Delta_4^2\right)\right) = 173.931 \text{in.}^4$$

where D_b = effective bolt diameter, 1.044 in.

$$\Delta_1 = 4.47 + \bar{y}$$

$$\Delta_2 = 3.27 + \bar{y}$$

$$\Delta_3 = 1.20 + \bar{y}$$

$$\Delta_4 = \bar{y} + 1.20$$

$$\bar{y} = R\cos\alpha = 6\cos(1.12025) = 2.613 \text{ in.}$$

(2) The moment of inertia of the circular segment about the neutral axis, I_{cs}

$$I_{cs} = I_{csG} + A_{cs}\left(y_G - \bar{y}\right)^2 = 71.84 \text{ in}^4$$

where, I_{csG} is the moment of inertia of the circular segment about its horizontal axis at the center of gravity:

$$I_{csG} = \frac{R^4}{4}\left(\alpha - \sin\alpha\cos\alpha + 2\sin^3\alpha\cos\alpha - \frac{16\sin^6\alpha}{9(\alpha - \sin\alpha\cos\alpha)}\right)$$

(3) The moment of inertia of the bolt holes in the compression zone (subtractive), I_h, is

$$I_h = 2\left(\frac{2\pi D_h^4}{64} + \frac{\pi D_h^2}{4}\right)\left(\left(4.47 - \bar{y}\right)^2 + \left(3.27 - \bar{y}\right)^2\right)$$

D_h = bolt hole diameter = 1.17 in.

$$I_{NA} = I_b + I_{cs} - I_h = 237.061 \text{ in}^4$$

The bolt (#1) most distant from the neutral axis is selected for calculation of stresses.

YIELD STRENGTH CRITERIA

Tension stress on bolt #1 due to the bending moment, M_{by}, is

$$\sigma_{bly} = \frac{M_{by} y_1'}{I_{NA}} = \frac{(1{,}600{,}000)(7.083)}{237.061} = 46{,}610.3 \text{ psi}$$

where $M_{by} = (F_y)_s \cdot D = (390{,}000)(1.5 + 2.5) = 1{,}560{,}000 \text{ in} \cdot \text{lb.}$

$$y_1' = 7.083 \text{ in.}$$

The bolt maximum pre-load torque (T_{max}) is 510(12) in-lb, which produces a tensile stress (σ_i) in addition to the bending stress:

$$\sigma_i = \frac{F_{imax}}{A_t} = \frac{36{,}267}{0.856} = 42{,}368 \text{ psi}$$

Where:

At = 0.856 in.^{2} (1 1/8-in. bolt tensile area)

$$F_{imax} = \frac{T_{max}}{kd} = \frac{510(12)}{0.15(1.125)} = 36{,}267 \text{ lbs}$$

k = 0.15 for lubricated threads

d = 1.125 in. (nominal bolt diameter)

Shear stresses on the bolts do not show up due to the presence of the trunnion base plate. The total tensile stress (σ_T) in bolt #1 is then:

$$\sigma_T = \sigma_{bly} + \sigma_i = 46{,}610.3 + 42{,}368 \cong 88{,}978 \text{ psi}$$

The allowable stress, S_y, at 350°F is 139,500 psi.

The margin of safety is

$$M.S._Y = \frac{S_y}{\sigma_T} - 1 = \frac{139{,}500 \text{ psi}}{88{,}978 \text{ psi}} - 1 = +0.57$$

ULTIMATE STRENGTH CRITERIA

Tension stress on bolt #1 due to the bending moment, M_{bu}, is

$$\sigma_{blu} = \frac{M_{bu} y_1'}{I_{NA}} = \frac{(2{,}600{,}000)(7.083)}{237.061} = 77{,}684.0 \text{ psi}$$

where $M_{bu} = F_u \cdot D = (650{,}000)(1.5 + 2.5) = 2{,}600{,}000 \text{ in} \cdot \text{lb}$

$y_1' = 7.083$ in.

The total tensile stress (σ_T) in bolt #1 is then

$$\sigma_T = \sigma_{blu} + \sigma_i = 77{,}684 + 42{,}368 = 120{,}052 \text{ psi}$$

The allowable stress, S_u, at 350°F is 172,100 psi.

The margin of safety is

$$M.S._u = \frac{S_u}{\sigma_T} - 1 = \frac{172{,}100 \text{ psi}}{120{,}052 \text{ psi}} - 1 = +0.43$$

In the upper bolts, where the trunnion flange is in compression, the compressive force (F_c) is:

$$F_c = \frac{4.47 - \bar{y}}{4.47 + \bar{y}}(F_t) = \frac{1.857}{7.083}(66{,}498) = 17{,}434 \text{ lb}$$

where

$$F_t = \sigma_T(A_t) = 77{,}684 \times 0.856 = 66{,}498 \text{ lb}$$

The minimum tensile force (F_{imin}) is

$$F_{imin} = \frac{T_{min}}{kd} = \frac{490(12)}{0.15(1.125)} = 34{,}844 \text{ lb}$$

Because a positive margin of safety is demonstrated for the bolts in the tension-loaded region under maximum-specified pre-load, and because the compressive force (17,434 lb) in the compression-loaded region is less than the minimum pre-load tensile force (34,844 lb), an adequate amount of pre-load is present in the bolts under the lifting condition.

Secondary Lifting Trunnion Shank

Per ANSI N14.6, the shear stress is taken as an average value over the cross section.

YIELD STRENGTH CRITERIA

The shear stress is $$\tau_{sy} = \frac{(F_y)_s}{A} = \frac{390{,}000}{(\pi/4)(6.50)^2} = 11{,}747\,\text{psi}$$

By applying the lifting force at the middle of the shank, the bending moment, M_{sy}, is

$$M_{sy} = 390{,}000 \times 1.5 = 585{,}000\ \text{in} \cdot \text{lb}$$

and, the bending stress is

$$\sigma_{sy} = \frac{M_y}{S} = \frac{585{,}000}{(\pi/32)(6.50)^3} = 21{,}699\ \text{psi}$$

The combined stress is

$$\sigma_{evy} = \left[\left(\sigma_{sy}^2\right) + \left(3\tau_{sy}^2\right)\right]^{0.5} = 29{,}750\ \text{psi}$$

The margin of safety is

$$MS = \frac{S_y}{\sigma_{evy}} - 1 = \frac{91{,}250}{29{,}750} - 1 = +2.07$$

ULTIMATE STRENGTH CRITERIA

The shear stress is $$\tau_{su} = \frac{(F_u)_s}{A} = \frac{650{,}000}{(\pi/4)(6.50)^2} = 19{,}578\ \text{psi}$$

By applying the lifting force at the middle of the shank, the bending moment, M_{su},

$$M_{su} = 650{,}000 \times 1.5 = 975{,}000\ \text{in} \cdot \text{lb}$$

and, the bending stress is

$$\tau_{su} = \frac{(F_u)_s}{A} = \frac{650{,}000}{(\pi/4)(6.50)^2} = 19{,}578\ \text{psi}$$

$$\sigma_{su} = \frac{M_u}{S} = \frac{975{,}000}{\left(\pi/32\right)(6.50)^3} = 36{,}165 \text{ psi}$$

The combined stress is

$$\sigma_{evu} = \left[\left(\sigma_{su}^2\right) + \left(3\tau_{su}^2\right)\right]^{0.5} = \boxed{49{,}628} \text{ psi}$$

The margin of safety is

$$MS = \frac{S_u}{\sigma_{evu}} - 1 = \frac{133{,}250}{\boxed{49{,}628}} - 1 = +1.68$$

Secondary Trunnion Base Plate

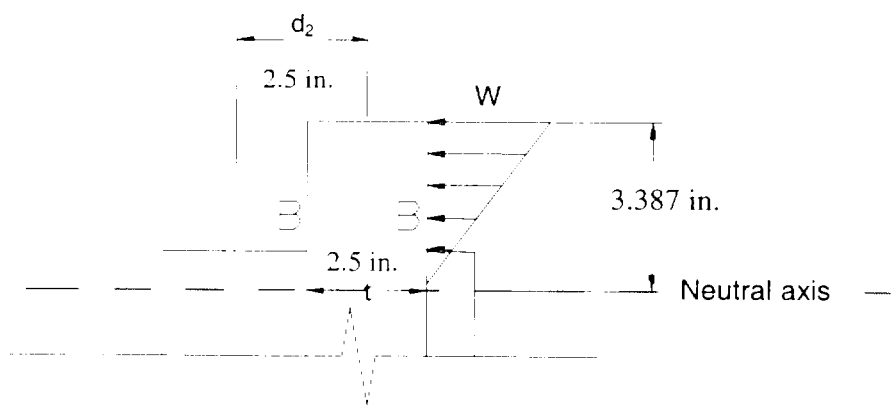

Two sections which are tangent to the upper and lower quadrants of the shank as depicted in Figure 2.5.1.1-2 are evaluated. The upper section is labeled Section B-B, and the lower section is labeled Section C-C. The following sketch illustrates the calculation procedure:

Section B-B

The bending stresses in the base plate cross-section at mid-thickness, σ_{bpi}, are:

$$\sigma_{bpi} = \frac{M_{bpi} \cdot y_i'}{I_{NA}} \text{ psi}$$

where $M_{bp} = F \cdot d_2$ in·lb.

y_i' = distance to bolt axis from neutral axis of section

$y_1' =$	7.083 in.	(Location 1)
$y_2' =$	5.883 in.	(Location 2)
$y_3' =$	3.813 in.	(Location 3)
$y_4' =$	1.413 in.	(Location 4)

To determine stresses, the linearly varying load distribution on the compression area of the base plate is determined. The total force, R_b, on the compression area is:

$$R_b = 2(T_1+T_2+T_3+T_4)$$

Where T_i (i = 1 to 4, corresponding to the locations shown in Figure 2.5.1.1-2) is $T_i = \sigma_{bpi}A_b$.

The maximum force per unit length, w, on the compression area is:

$$w = \frac{2R_b}{3.387}$$

and the value, w_B, on the section being considered is:

$$w_B = \frac{(0.5)(6.5) - \bar{y}}{3.387}(w)$$

The linearly varying distributed load produces a bending moment, M_{BB}, on Section B-B. The corresponding maximum normal stress (tension or compression) is:

$$\sigma_{BB} = \frac{6M_{BB}}{bt^2}$$

where $$M_{BB} = \frac{w_B l^2}{2} + \frac{(w - w_B)l}{2}\frac{2l}{3}$$

$$b = 2\left(\sqrt{6^2 - \left(\frac{6.5}{2}\right)^2} - 1.17\right) = 7.747 \text{ in.}$$

$$t = 2.5 \text{ in.}$$

The shear stress, τ_{BB}, is conservatively determined by

$$\tau_{BB} = \frac{R_b}{bt}$$

YIELD STRENGTH CRITERIA

T_{1y} = 27,431 lb.
T_{2y} = 22,784 lb
T_{3y} = 14,767 lb.
T_{4y} = 5,472 lb

$M_{byp} = F_y d_2$ = (390,000)(2.75) = 1,072,500 in·lb.

$R_{by} = 2(T_{1y} + T_{2y} + T_{3y} + T_{4y})$ = 140,908 lb.

w_y = 83,205 lb.

w_{By} = 15,649 lb/in.

M_{BBy} = 229,774 in·lb.

The normal stress is:

$$\sigma_{BBy} = \frac{6M_{BBy}}{bt^2} = \boxed{28{,}501 \text{ psi}}$$

The shear stress is:

$$\tau_{BBy} = \frac{R_{by}}{bt} = \boxed{7{,}280 \text{ psi}}$$

The evaluation stress and margin of safety are

$$\sigma_{evy} = \sqrt{\sigma_{BBy}^2 + 3\tau_{BBy}^2} = \boxed{31{,}270 \text{ psi}}$$

and $$MS = \frac{S_y}{\sigma_{evy}} - 1 = \boxed{\frac{91{,}250}{31{,}270} - 1 = +1.92}$$

ULTIMATE STRENGTH CRITERIA

Using the same method as for the yield strength criteria and substituting the loads and allowable stresses for the ultimate strength case:

T_{1u} = 45,718 lb.
T_{2u} = 37,973 lb
T_{3u} = 24,612 lb.
T_{4u} = 9120 lb

$M_{bpu} = F_u\, d_2 = (625{,}000)(2.75) = \boxed{1{,}787{,}500 \text{ in·lb}}$.
$R_{bu} = 2(T_{1u} + T_{2u} + T_{3u} + T_{4u}) = \boxed{234{,}846 \text{ lb.}}$
w_u = 138,677 lb.
w_{Bu} = 26,086 lb/in.
M_{BBu} = 382,537 in·lb.

The normal stress is

$$\sigma_{BBu} = \frac{6M_{BBu}}{bt^2} = \boxed{47{,}411 \text{ psi}}$$

The shear stess is

$$\tau_{BBu} = \frac{R_{bu}}{bt} = 12{,}126 \text{ psi}$$

The evaluation stress and margin of safety are

$$\sigma_{evu} = \sqrt{\sigma_{BBu}^2 + 3\tau_{BBu}^2} = 51{,}988 \text{ psi}$$

and

$$MS = \frac{S_u}{\sigma_{evu}} - 1 = \frac{133{,}250}{51{,}988} - 1 = +1.56$$

Section C-C

The bending moment at Section C-C, M_{CC}, is due to the tension force on the bolts at Location 1, see Figure 2.5.1.1-2.

$$M_{CC} = (2T_1)(4.47\text{-}3.27) = 2.4T_1$$

The normal stress, σ_{CC} , is

$$\sigma_{CC} = \frac{6M_{CC}}{bt^2}$$

The shear stress, τ_{CC}, is

$$\tau_{CC} = \frac{V}{bt}$$

where $V = 2(T_1 + T_2)$

YIELD STRENGTH CRITERIA

The normal stress is

$$\sigma_{CCy} = \frac{6M_{CCy}}{bt^2} = 8{,}166 \text{ psi}$$

where $M_{CCy} = 2.4T_{1y} = 65{,}834$ in·lb.

The shear stress is

$$\tau_{CCy} = \frac{V_y}{bt} = 5{,}186 \text{ psi}$$

where $V_y = 2(T_{1y} + T_{2y}) = 100{,}430 \text{ lb.}$

The evaluation stress and margin of safety are

$$\sigma_{evy} = \sqrt{\sigma_{CCy}^{\ 2} + 3\tau_{CCy}^2} = 12{,}180 \text{ psi.}$$

and

$$MS = \frac{S_y}{\sigma_{evy}} - 1 = \frac{91{,}250}{12{,}180} - 1 = +6.48$$

ULTIMATE STRENGTH CRITERIA

The normal stress is

$$\sigma_{CCu} = \frac{6M_{CCu}}{bt^2} = 13{,}598 \text{ psi}$$

where $M_{CCu} = 2.4T_{1u} = 109{,}724 \text{ in·lb.}$

The shear stress is

$$\tau_{CCu} = \frac{V_u}{bt} = 8{,}643 \text{ psi}$$

where $V_u = 2(T_{1u} + T_{2u}) = 167{,}382 \text{ lb.}$

The evaluation stress and margin of safety are

$$\sigma_{evu} = \sqrt{\sigma_{CCu}^{\ 2} + 3\tau_{CCu}^2} = 20{,}234 \text{ psi.}$$

and

$$MS = \frac{S_u}{\sigma_{evu}} - 1 = \frac{133{,}250}{20{,}234} - 1 = +5.58$$

Minimum Length of Thread Engagement

To prevent damage to the top forging, enough thread engagement length must exist to ensure that the bolt will fail before stripping the threads in the top forging under overloading conditions.

When the unit tensile strength of the external thread material substantially exceeds that of the internal thread material, the minimum length of engagement, L_e, required to develop maximum strength may be determined as follows.

$$L_e = \frac{S_{st} 2A_s}{S_{nt} \cdot \pi \cdot n \cdot D_{smin}\left(\frac{1}{2n} + 0.57735\left(D_{smin} - E_{nmax}\right)\right)} = 1.094 \text{ in.}$$

where S_{st} = unit tensile strength of the external (bolt) thread = 172,100 psi

S_{nt} = unit tensile strength of the internal (top forging) thread = 60,750 psi

A_s = tensile stress area = 0.856 in^2

n = threads per inch = 12

D_{smin} = minimum major diameter of the bolt thread = 1.1118 in.

E_{nmax} = maximum pitch diameter of top forging thread = 1.0787 in.

For the internal (top forging) thread to develop the unit shear strength, the shear area required is

$$\tau = \frac{T_{1u}}{AS_n} \leq 0.5S_{nt}$$

For T_{1u} = **45,718** lb and S_{nt} = 60,750 psi, $AS_n \geq$ **1.505 in^2**.

The internal thread (forging) shear area is

$$AS_n = \pi \cdot n \cdot L_e \cdot D_{smin}\left(\frac{1}{2n} + 0.57735\left(D_{smin} - E_{nmax}\right)\right)$$

and, the corresponding length of engagement is, $L_e \geq$ **0.591 in.**

For the external (bolt) thread to develop the unit shear strength, the shear area required is

$$\tau = \frac{T_{1u}}{AS_s} \leq 0.5S_{st}$$

For T_{1u} = **45,718 lb** and S_{st} = 172,100 psi, $AS_s \geq$ **0.531 in²**.

The external thread shear area is

$$AS_s = \pi \cdot n \cdot L_e \cdot K_{n\,max}\left(\frac{1}{2n} + 0.57735\left(E_{smin} - K_{nmax}\right)\right)$$

where K_{nmax} = maximum minor diameter of the internal thread = 1.053 in.

E_{smin} = minimum pitch diameter of the external thread = 1.0631 in.

and, the corresponding length of engagement is, $L_e \geq$ **0.281 in.**

The required length of engagement based on the internal threads, L_e = 1.094, governs, and is less than the actual thread length of 2.25 in. ensuring that bolt failure will occur before damaging the top forging in an overload condition.

Figure 2.5.1.1-1 Primary Lifting Trunnion Geometry

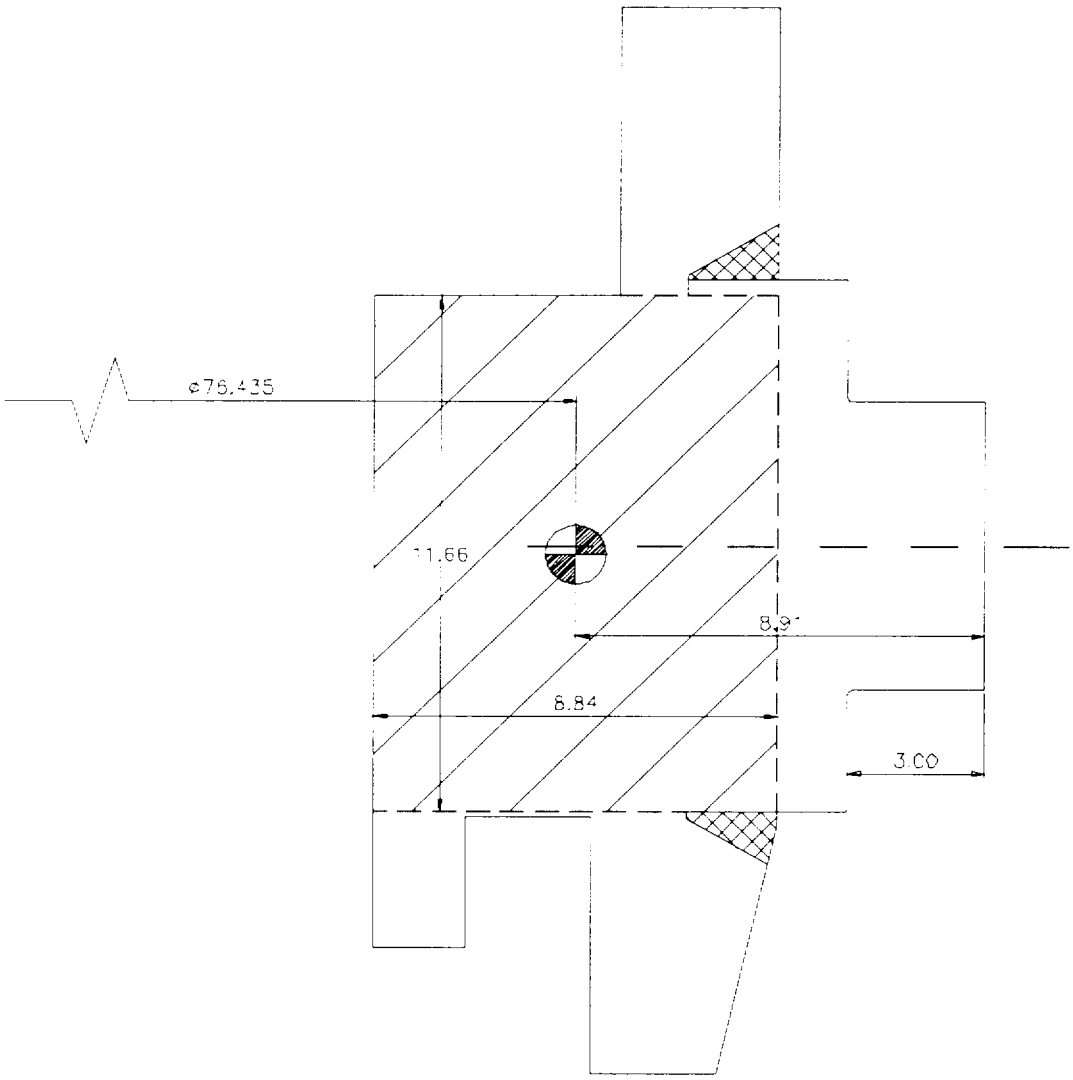

Figure 2.5.1.1-2 Secondary Lifting Trunnion Geometry

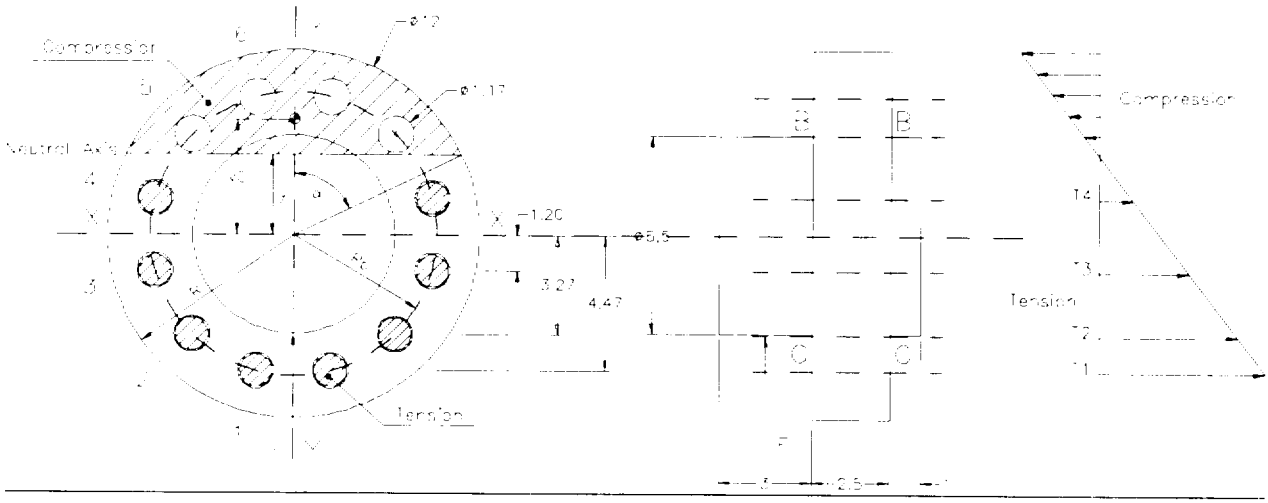

Table 2.5.1.1-1 Primary Trunnion/Top Forging Intersection Analysis Results

Angle (deg.)	Moment (in-lb)	Bending Stress (psi)	Twisting Moment (in-lb)	Shear Stress (psi)	SI (psi)	MS
0	-1,592,029	7,948	481,650	2,123	9,011	1.1
5	-1,332,095	6,650	609,232	2,685	8,547	1.3
10	-1,074,139	5,362	714,202	3,148	8,270	1.3
15	-820,125	4,094	796,819	3,512	8,130	1.4
20	-571,985	2,856	857,512	3,780	8,081	1.4
25	-331,609	1,655	896,875	3,953	8,077	1.4
30	-100,824	503	915,667	4,036	8,088	1.4
35	118,611	592	914,803	4,032	8,086	1.4
40	325,027	1,623	895,345	3,946	8,057	1.4
45	516,853	2,580	858,499	3,784	7,996	1.4
50	692,629	3,458	805,604	3,551	7,899	1.4
55	851,018	4,249	738,119	3,253	7,771	1.5
60	990,813	4,946	657,614	2,898	7,619	1.5
65	1,110,952	5,546	565,761	2,494	7,459	1.6
70	1,210,519	6,043	464,315	2,046	7,298	1.7
75	1,288,757	6,434	355,106	1,565	7,155	1.7
80	1,345,071	6,715	240,023	1,058	7,041	1.7
85	1,379,031	6,885	120,998	533	6,967	1.8
90	1,390,380	6,941	0	0	6,941	1.8

2.5.1.2 Cask Lid Lifting Analysis

The cask lid lifting system provides a mechanism to lift the cask lid and place it on the cask body. The cask lid is lifted by using a wire-rope sling that is load-rated for not less than the weight of the lid. Swivel hoist rings threaded into four equally spaced holes in the lid are used to attach the sling to the lid. These holes are clearly marked by engraved black painted letters on the top surface of the lid. The four slings attach to a strongback at two points, two slings at each point.

The lid-lifting system uses four equally spaced 1-8 UNC-3B threaded holes located on a 66.86-in. bolt circle. Helicoil thread inserts are used to increase the wear endurance. The lid material is SA-336, Type 304 stainless steel.

In accordance with the requirements of 10 CFR 71.45(a), a factor of safety of 3 against yielding is required of any lifting attachment that is a structural part of the package used to lift the package in the intended manner. Additionally, ANSI N14.6 requires that load-bearing members of a special lifting device must be capable of lifting 3 times the weight of the package without generating a combined shear stress or maximum tensile stress at any point in the device in excess of the minimum tensile yield strength of the materials. The load-bearing members must be capable of lifting 5 times the weight of the package without exceeding the ultimate tensile strength of the material. NUREG-0612 requires that dynamic loads must be considered when demonstrating compliance with ANSI N14.6.

The requirements of ANSI N14.6 are not applicable to the cask lid because the lid weighs less than 10,000 lb; however, since the requirements of ANSI N14.6 and NUREG-0612 envelope those of 10 CFR 71.45, the cask lid is evaluated to these requirements. Therefore, the shear stress generated in the bolt hole threads in the cask lid during lifting must maintain a factor of safety of 3 against yield stress and a factor of safety of 5 against ultimate stress.

The cask lid weighs 8,869 lb. Assuming the load on the hoist ring bolts is purely tensile results in a maximum shear stress on the cask lid bolt hole threads. Using a two-point lifting arrangement for a redundant load path, and using a dynamic load factor of an additional 10%, the load carried by each hoist ring bolt, F_y, is calculated as:

$$F_y = \frac{\text{Cask Lid Weight} \times \text{Dynamic Load}}{2 \text{ Lift Points}} = \frac{8{,}869 \times 1.1}{2} = 4{,}878 \text{ lb}$$

To carry the load at each lifting point, a swivel hoist ring load-rated at 10,000 lb is used. The hoist ring has 1-8 UNC-3A threads with a length of 1.54 in.

The shear area, A_n, in the cask lid bolt hole threads is calculated as:

$$A_n = 3.1416\ n\ L_e\ D_s\min\left[\frac{1}{2n} + 0.57735\left(D_s\min - E_n\max\right)\right] = 3.694\ \text{in}^2$$

where n = 8 (threads per inch)

L_e = 1.54 in. (bolt thread engagement length)

$D_s$min = 0.9850 in. (minimum major diameter of bolt threads)

$E_n$max = 0.9254 in. (maximum pitch diameter of lid threads)

The shear stress, τ, in the structural lid bolt hole threads is calculated as

$$\tau = \frac{F_y}{A_n} = \frac{4{,}878}{3.694} = 1{,}320.5\text{psi}$$

At a temperature of 300°F, which bounds all thermal conditions of the lid, SA336, Type 304 stainless steel has a yield strength of 22,500 psi and an ultimate strength of 61,500 psi. Thus, the shear stress of 1,303 psi produces the following factors of safety:

$$(FS)_{yield} = \frac{\text{yield strength}}{\text{shear stress}} = \frac{22{,}500}{1{,}320.5} = 17.04\ (>3)$$

$$(FS)_{ultimate} = \frac{\text{ultimate strength}}{\text{shear stress}} = \frac{61{,}500}{1{,}320.5} = 46.57\ (>5)$$

2.5.2 Tiedown Devices

The Universal Transport Cask is designed to satisfy the requirements of 10 CFR 71.45 (b) and the AAR Field Manual, Rule 88 [31], because rail is the most likely mode of transport. In this analysis, the cask is assumed to be supported horizontally on a railcar and subjected to the more limiting of either:

(1) A static force applied to the center of gravity of the package having a vertical component of 2 times the weight of the package, a horizontal component along the direction in which the vehicle travels of 10 times the weight of the package, and a horizontal component in the transverse direction of 5 times the weight of the package in accordance with 10 CFR 71.45 (b); or

(2) A 7.5-g longitudinal force, a 4-g vertical force, and a 1.8-g lateral force, in accordance with AAR Field Manual, Rule 88.

These loads are transferred to the rail supports by bearing on the rear rotation pockets, the front shear ring, and the tiedown assembly. Dynamic effects are negligible when considered in combination with the large applied load factors. In accordance with 10 CFR 71.45 (b), the structural components integral with the cask that are used for tiedown must be capable of withstanding the specified forces without generating stress in any material of the package in excess of its yield strength.

2.5.2.1 Tiedown Component Loading

The Universal Transport Cask is tied down to the transport vehicle by means of the following: (a) rotation pockets near the bottom at Point i (Figure 2.5.2.1-1); and (b) two 46° saddle supports, the tiedown assembly, and a shear ring near the top end at Point j (Figure 2.5.2.1-1). Longitudinal force towards the bottom of the cask is resisted by the rotation pockets. A shear ring welded to the cask top forging resists the longitudinal force towards the top end of the cask. A 0.70-in. gap between the shear ring and the saddle support accommodates any thermal expansion of the cask.

The resultant force on the shear ring is assumed to act at the centroid of the contact area between the shear ring and the saddle support. Referring to Figure 2.5.2.1-2, the distance of the centroid from the center of the cask is determined by calculating the centroid for q = 60° and subtract the contribution of the 14° arc.

For q = 60°, $`y_{60}$ = 36.148 in.

The centroid of the 14° arc is determined as `y 14 = 43.277 in.

The distance of the centroid from the center of the cask of the actual bearing area between
θ = 14° and 60° is calculated as $`y_{act}$ = 33.978 in.

The three loading cases for the tiedown components are vertical, longitudinal, and lateral loads. the reaction forces for each loading case are determined below by using the equations of equilibrium.

Vertical Loads Per 10 CFR 71.45 (b)

In the Downward Direction, using W = 260,000 lb., Fy = - 2W = - 520,000 lb.

By summing moments Mz about Point j, the reaction forces are determined to be

$R_{iy\ max}$ = 132,668 lb. $R_{iy\ min}$ = 126,772 lb.

By summing vertical forces, the reaction forces are determined to be $R_{jy\ max}$ = 266,456 lb. Note that $R_{ix} = R_{iy} = 0$ because of the gap provided in the shear ring.

In the Upward Direction, F_y = + 2W = 520,000 lb. Similarly, by summing moments M_z about point j:

$R_{iy\ max}$ = -132,668 lb. $R_{jy\ max}$ = -266,456 lb.

Note that the support saddle cannot carry any upward load. Hence the negative R_{jy} reaction force is resisted by the tiedown strap.

Longitudinal Load Per 10 CFR 71.45 (b)

In the Forward Direction, using Fx = + 10W = 2,600,000 lb. and summing horizontal forces, it is determined that R_{jx} = - 2,600,000 lb.

By summing moments about Point j, it determined that R_{iy} = - 250,433 lb.

By summing vertical forces, it is determined that R_{jy} = 500,866 lb.

In the Aft Direction, using F_x = - 10W = -2,600,000 lb. and summing horizontal forces, it is determined that R_{ix} = 1,300,000 lb.

By summing moments about j, it is determined that R_{iy} = - 22,111 lb.

By summing vertical forces, it is determined that R_{jy} = 44,222 lb.

Lateral Load Per 10 CFR 71.45 (b)

To find the reactions resisting the lateral load, F_x = 5W = 1,300,000 lb., the location of the bearing pressure between the support saddle and the cask surface must be found. The contact surface is one-half of the saddle, as shown in Figure 2.5.2-2.

For the 60° arc, `y = 30.231 in., and for the 14° arc, `y = 42.116 in.

The centroidal location of the resultant force acting on the support saddle between the 14° and the 60° angular distance from the vertical is determined as $`y_{act}$ = 30.04 in.

The horizontal distance from the center of the cask to the support point (Figure 2.5.2.1-2) is
d = 46.05 in.

By summing the moments, the reaction forces are determined to be $R'_{iz\ max}$ = - 663,341 lb and $R'_{iz\ min}$ = - 633,859 lb.

By summing forces along the Z-axis, the reaction force is determined to be $R_{jz\ max}$ = - 666,141 lb.

By summing forces along the Y-axis, it is determined that R_{iy} = - R'_{iy}.

By summing moments about the longitudinal axis of the cask, the reaction forces are determined to be

$$- R'_{iy}\ max = 196{,}626\ lb \qquad \text{and} \qquad R_{iy}\ max = - 196{,}626\ lb.$$

For the Opposite Lateral Load, the reactions for this case are opposite to those for the previous case, and

$$F_z = -5W = -1{,}300{,}000 \text{ lb}$$

Therefore, $R'_{iz\,max} = 663{,}341$ lb

$R_{jz\,max} = 666{,}141$ lb

$R'_{iy\,max} = 196{,}626$ lb.

Vertical Loads Per AAR Field Manual, Rule 88

In the Downward Direction, $F_y = -4W = -1{,}040{,}000$ lb. By summing moments M_z about Point j, the reaction forces are determined as:

$R_{iy\,max} = 265{,}336$ lb $\qquad$ $R_{iy\,min} = 253{,}543$ lb.

By summing vertical forces, the reaction force is determined as $R_{jy\,max} = 532{,}914$ lb.

(Note that $R_{ix} = R_{jx} = 0$ because of the gap provided in the shear ring.)

In the Upward Direction, $F_y = +4W = 1{,}040{,}000$ lb. Similarly, by summing moments M_z about Point j:

$R_{iy\,max} = -265{,}336$ lb $\qquad$ $R_{jy\,max} = -532{,}914$ lb.

Note that the support saddle cannot carry any upward load. Hence the negative R_{jy} is resisted by the tiedown strap.

Longitudinal Load Per AAR Field Manual, Rule 88

In the Forward Direction, $F_x = +7.5W = 1{,}950{,}000$ lb. By summing horizontal forces, it is determined that $R_{jx} = -1{,}950{,}000$ lb.

By summing moments about Point j, R_{iy} = - 187,825 lb.

By summing vertical forces, R_{jy} = 375,650 lb.

In the Aft Direction, F_x = - 7.5W = - 1,950,000 lb. By summing horizontal forces, it is determined that R_{ix} = 975,000 lb.

By summing moments about Point j, it is determined that R_{iy} = - 16,902 lb.

By summing vertical forces, it is determined that R_{jy} = 33,805 lb.

Lateral Load Per AAR Field Manual, Rule 88

The lateral load is F_x = 1.8W = 468,000 lb. By summing the moments, the reaction forces are determined to be $R'_{iz\,max}$ = - 238,803 lb and $R'_{iz\,min}$ = - 228,190 lb.

By summing forces along the Z-axis, the reaction force is determined to be $R_{jz\,max}$ = - 239,810 lb.

By summing forces along the Y-axis, it is determined that R_{iy} = - R'_{iy}.

By summing moments about the longitudinal axis of the cask, the reaction forces are determined to be R_{iy} = - 70,785 lb and - R'_{iy} = 70,785 lb.

For the Opposite Lateral Load, F_z = - 1.8W = - 468,000 lb. The reactions for this case are opposite to the previous case:

$R'_{iz\,max}$ = 238,803 lb $\qquad$ $R_{jz\,max}$ = 239,810 lb

R_{iy} = 70,785 lb $\qquad$ - R'_{iy} = - 70,785 lb.

Loads Summary

The results of all the loading cases are summarized in Tables 2.5.2.1-1 and 2.5.2.1-2.

Figure 2.5.2.1-1 Front Support and Tiedown Geometry

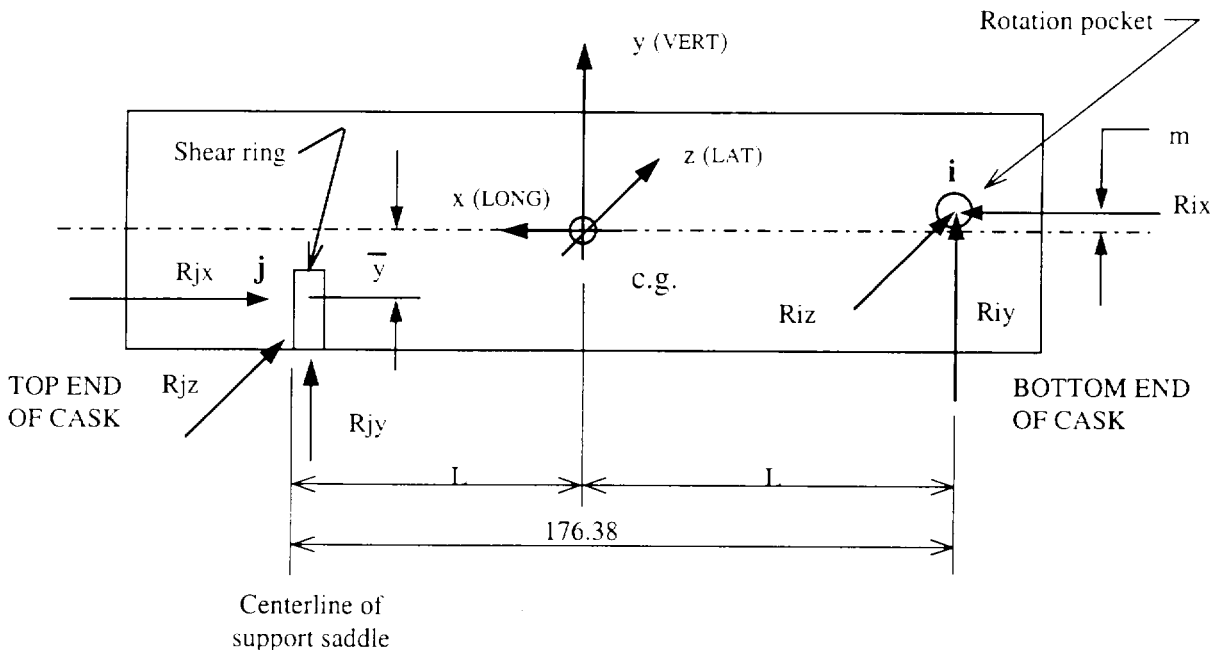

Figure 2.5.2.1-2 Shear Ring Geometry

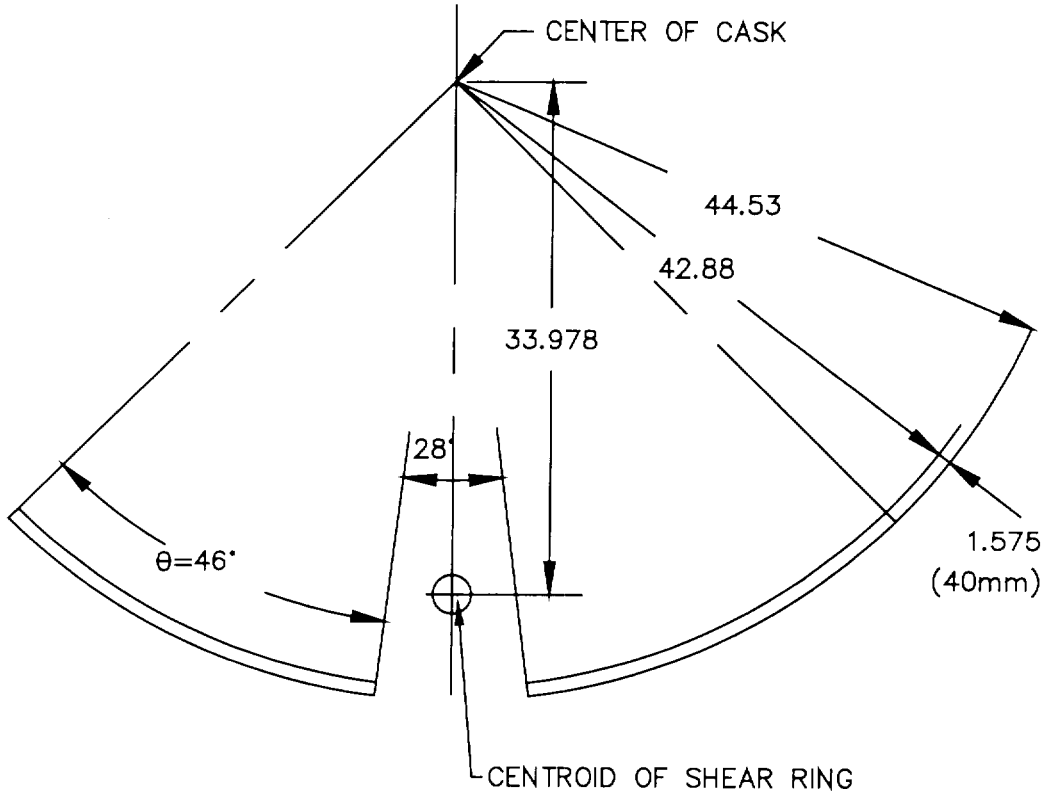

Figure 2.5.2.1-3 Free-Body Diagram of Cask Subjected to Lateral Load

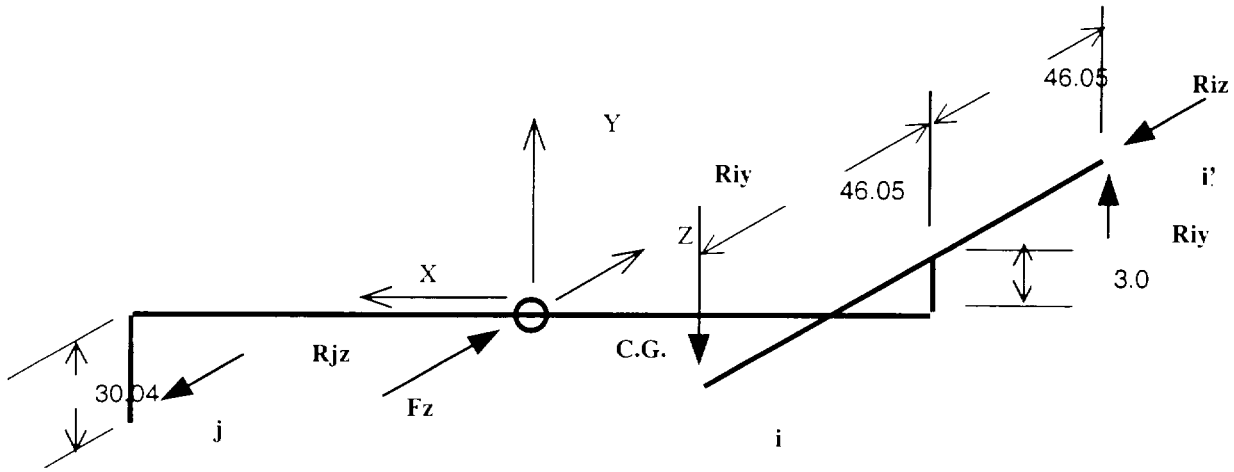

Table 2.5.2.1-1 Reactions Caused by Tiedown Devices (from 10 CFR 71.45 (b))

Reactions (lb)							
Load Case	**Load (lb)**	R_{jx}	R_{jy}	R_{jz}	R_{ix}	R_{iy}	R_{iz}
A1	F_y = -520,000	0	266,456	0	0	132,668	0
A2	F_y = 520,000	0	-266,456	0	0	-132,668	0
B1	F_x = 2,600,000	-2,600,000	500,866	0	0	-250,433	0
B2	F_x = -2,600,000	0	44,222	0	1,300,000	-22,111	0
C1	F_z = 1,300,000	0	0	-666,141	0	-196,626	-663,341
C2	F_z = -1,300,000	0	0	666,141	0	196,626	663,341
Combined Reactions (lb)							
A1 + B1 + C1		-2,600,000	767,322	-666,141	0	-314,391	-663,341
A1 + B1 + C2		-2,600,000	767,322	666,141	0	78,861	663,341
A1 + B2 + C1		0	310,678	-666,141	1,300,000	-86,069	-663,341
A1 + B2 + C2		0	310,678	666,141	1,300,000	307,183	663,341
A2 + B1 + C1		-2,600,000	234,410	-666,141	0	-579,727	-663,341
A2 + B1 + C2		-2,600,000	234,410	666,141	0	-186,475	663,341
A2 + B2 + C1		0	-222,234	-666,141	1,300,000	-351,405	-663,341
A2 + B2 + C2		0	-222,234	666,141	1,300,000	41,847	663,341

Table 2.5.2.1-2 Reactions Caused by Tiedown Devices (from AAR Field Manual Rule 88)

Reactions (lb)							
Load Case	**Load (lb)**	**R_{jx}**	**R_{jy}**	**R_{jz}**	**R_{ix}**	**R_{iy}**	**R_{iz}**
A1	F_y = -1,040,000	0	532,914	0	0	265,336	0
A2	F_y = 1,040,000	0	-532,914	0	0	-265,336	0
B1	F_x = 1,950,000	-1,950,000	375,650	0	0	-187,825	0
B2	F_x = -1,950,000	0	33,168	0	975,000	-16,584	0
C1	F_z = 468,000	0	0	-239,810	0	-70,785	-238,803
C2	F_z = -468,000	0	0	239,810	0	70,785	238,803
Combined Reactions (lb)							
A1 + B1 + C1		-1,950,000	908,564	-239,810	0	6,726	-238,803
A1 + B1 + C2		-1,950,000	908,564	239,810	0	148,296	238,803
A1 + B2 + C1		0	566,082	-229,810	975,000	177,967	-238,803
A1 + B2 + C2		0	566,082	239,810	975,000	319,537	238,803
A2 + B1 + C1		-1,950,000	-157,264	-239,810	0	-523,946	-238,803
A2 + B1 + C2		-1,950,000	-157,264	239,810	0	-382,376	238,803
A2 + B2 + C1		0	-499,746	-239,810	975,000	-352,705	-238,803
A2 + B2 + C2		0	-499,746	239,810	975,000	-211,135	238,803

2.5.2.2 Rear Support

The transport cask rear tiedown attachment is at the rotation pockets. The two rotation pockets are stainless steel forgings located near the bottom of the cask and spaced at approximately 180-degree positions in line with the two primary lifting trunnions.

2.5.2.2.1 Material Properties at 200°F

The yield strength of each material at 200°F is the allowable stress. The shear stress allowable for noncontainment structures is 0.6 S_y. The bearing stress allowable is equal to S_y. For the A-240 Type 304 Stainless Steel, Cask Outer Shell and Shear Ring:

S_y = 25.0 ksi S_u = 71.0 ksi.

For SA-336 Type 304 Stainless Steel, Cask Top Forging:

S_y = 25.0 ksi S_u = 66.2 ksi.

For Type XM-19 stainless steel forging, Rotation Pockets:

S_y = 47.0 ksi S_u = 99.5 ksi.

Loads

Examination of the load summaries in Tables 2.5.2.1-1 and 2.5.2.1-2 shows that the load conditions specified in 10 CFR 71.45 (b) produce the more critical loads on the rotation pockets.

Bearing Stress in Rotation Pocket

The Rotation Pocket diameter = 10 in., and the Trunnion Pin diameter = 8 in.

Inspection of the load combinations in Table 2.5.2.1-1 indicates that Case A2 + B2 + C1 is most critical for bearing stress on the rotation pockets:

$F_z = 670{,}000$ lb

$A_{br} = \pi(8.0)^2/4 = 50.26 \text{ in}^2$

$$S_{br} = \frac{F_z}{A_{br}} = 13{,}300 \text{ psi}$$

$$F_r = \sqrt{(F_x)^2 + (F_y)^2}\ 1 = 1{,}349{,}000 \text{ lb}$$

Where

$F_x = 1{,}300{,}000$ lb $\qquad F_y = -360{,}000$ lb.

Length of engagement, $a = 46.55 - 42.94 = 3.61$ in.

A clearance of 42.94 - 42.55 = 0.39 in. exists between the end of the pin and the rotation pocket. Consider that the cask is off center by this amount and the minimum engagement length is 3.61 - 0.39 = 3.22 in.:

$A_{br} = (10.0)(3.22) = 32.2 \text{ in}^2$

$$S_{br} = \frac{F_r}{A_{br}} = 41{,}894 \text{ psi} \qquad \text{and} \qquad MS = \frac{S_{bry}}{S_{br}} 2 - 1 = +0.12.$$

<u>Shear Stress In Rotation Pocket, Horizontal Loading: Double Shear:</u>

Inspection of the load combinations in Table 2.5.2.1-1 indicates that Case B2 is most critical for horizontal shear on the rotation pocket:

Minimum shear area, $A_s = 0.5(1{,}300{,}000)/(0.6)(47{,}000) = 23.05 \text{ in}^2$

Minimum edge distance from pocket centerline = 23.05/3.22 = 7.16 in.

Edge distance provided = 13.0 - 5.38 = 7.62 in.

MS = 7.62/7.16 - 1 = + 0.06.

The result is conservative; additional metal provided by the tapered portion of the rotation pocket is neglected.

Shear Stress In Rotation Pocket Vertical Loading: Single Shear

Inspection of the load combinations in Table 2.5.2.1-1 indicates that Case A2 + B1 + C1 is most critical for vertical shear stress on the rotation pocket where R_{iy} = 580,000 lb.

The minimum required projected bearing length in the vertical direction is

L_b = 580,000/ (3.22)(47,000) = 3.8 in.

Included angle = $\cos^{-1}$ (4.5/5) = 26°.

Bearing length provided = 2(5)sin 26 = 4.4 in. > 3.8 in.

MS = 4.4/3.8 - 1 = + 0.16.

The minimum shear area is

A_s = (580,000)/(0.6)(47,000) = 20.6 in^2

The minimum distance from rotation pocket centerline = 20.6/3.22 = 6.39 in. < 7 in.

MS = 7/6.39 - 1 = + 0.09.

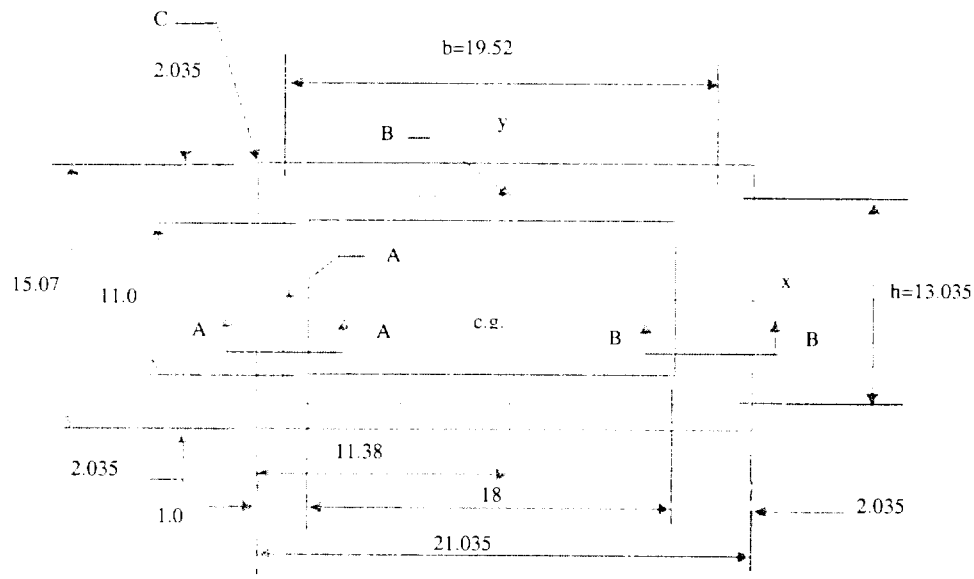

Stress in Weld at Interface with Rotation Pocket

Assume that the entire load is transferred to the cask outer shell through the weld at the base of the rotation pocket. The effective thickness of weld is

$$t_e = [(1.50)^2 + (1.375)^2]^{0.5} = 2.035 \text{ in. (Section B-B, 3 Sides).}$$

The section properties of weld group are

$$\text{Area } (A_w) = (21.035)(15.07) - (18.00)(11.00) = 119 \text{ in}^2$$

$$\bar{x} = \frac{15.07\ (21.035)^2/2\ -\ (11.00)(18.00)(1.0\ +\ 18.0/2)}{119.0} = 11.38 \text{ in}$$

$$I_x = \frac{(21.035)(15.07)^2}{12} - \frac{(18.0)(11.00)^3}{12} = 4003 \text{ in}^4$$

$$I_y = \frac{(15.07)(21.035)^3}{12} + 15.07(21.035)\left(\frac{21.035}{2} - 11.38\right)^2 - \frac{(11.0)(18.0)^3}{(12)} - 11.0(18.0)\left(\left(1.0 + \frac{18}{2}\right) - 11.38\right)^2 = 6201 \text{ in}^4$$

where

$b = 19.52$ in. $\qquad h = 13.035$ in.

$t_a = 1.0$ in. $\qquad t_b = 2.035$ in.

From Table 2.5.2.1-1, the loads for Case A2 + B2 + C1 are the highest combination loads on the weld group are $F_x = 1{,}300{,}000$ lb and $F_y = -360{,}000$ lb.

$$F_r = (F_x^2 + F_y^2)^{0.5} = 1{,}349{,}000 \text{ lb}$$

$$e_x = 11.38 - 5.38 = 6.0 \text{ in.} \qquad e_z = 5.25 - 3.22/2 = 3.64\text{in.};$$

conservatively use 3.9 in.

$$M_x = F_y\,(e_z) = 1{,}404{,}000 \text{ in-lb}$$

$$M_y = F_x\,(e_z) = 5{,}070{,}000 \text{ in-lb}$$

$$M_z = F_y\,(e_z) = 2{,}160{,}000 \text{ in-lb.}$$

The component stresses on the effective thickness weld group are:

$$S_{AC} = \frac{M_y c_x}{I_y} = \frac{(5{,}070{,}000)(11.38)}{(6201)} = 9{,}304 \text{ psi (bending stress at points A \& C)}$$

$$S_{BC} = \frac{M_x c_y}{I_x} = \frac{(1{,}404{,}000)(7.535)}{4003} = 2{,}643 \text{ psi (bending stress at points B \& C)}$$

$$S_s = \frac{F_R}{A_W} = \frac{1{,}349{,}000}{119.0} = 11{,}336 \text{ psi (resultant direct shear stress)}$$

$$(S_{ST})_A = \frac{M_Z}{2\,bht_A} = \frac{2{,}160{,}000}{(2)(19.52)(13.035)(1.0)} = 4245 \text{ psi (torsional shear stress at point A)}$$

$$(S_{ST})_B = \frac{M_Z}{2\,bht_B} = \frac{2{,}160{,}000}{(2)(19.52)(13.035)(2.035)} = 2086 \text{ psi}$$ (torsional shear stress at point B)

The von Mises equivalent stresses at points A, B, and C are

$$S_{EA} = \left[S_{AC}^2 + 3(S_S + (S_{ST})_A)^2\right]^{0.5} = 28{,}546 \text{ psi}$$

$$S_{EB} = \left[S_{BC}^2 + 3(S_S + (S_{ST})_B)^2\right]^{0.5} = 23{,}397 \text{ psi}$$

$$S_{EC} = \left[(S_{AC} + S_{BC})^2 + 3S_S^2\right]^{0.5} = 22{,}984 \text{ psi}.$$

The minimum margin of safety at the rotation pocket/weld interface is based on the yield strength of the XM-19 material, $S_y = 47.0$ ksi:

$$MS = \frac{47{,}000}{28{,}546} - 1 = +0.65.$$

Stress at Cask Body/Rotation Pocket Weld Interface

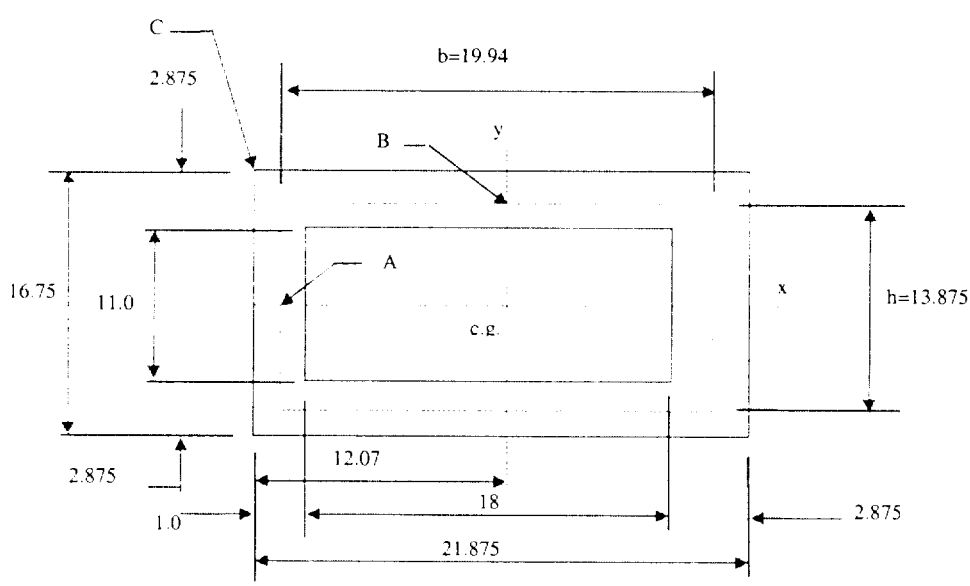

Section properties of weld/cask interface:

$$\text{Area } (A_w) = (21.875)(16.75) - (18.0)(11.0) = 168 \text{ in}^2$$

where $b = 19.94$ in. $h = 13.875$ in.

$t_A = 1.0$ in. $t_B = 2.875$ in.

$$\bar{x} = \frac{(16.75)(21.875)^2/2 - (11.0)(18.0)(1.0 + 18.0/2)}{168} = 12.07 \quad \text{in.}$$

$$I_x = \frac{(21.875)(16.75)^3}{12} - \frac{(18.0)(11.0)^3}{12} = 6570 \quad \text{in}^4 3$$

$$I_y = \frac{(16.75)(21.875)^3}{12} + 16.75(21.875)\left(\frac{21.875}{2} - 12.07\right)^2 - \frac{(11.0)(18.0)^3}{(12)} - 11.0(18.0)\left(\left(1.0 + \frac{18}{2}\right) - 12.07\right)^2 = 8{,}886 \text{ in}^4$$

Loads On Weld/Cask Interface

Inspection of the load combinations in Table 2.5.2.1-1, indicates that Case A2 + B2 + C1 is most critical for the rotation pocket recess are $F_x = 1{,}300{,}000$ lb and $F_y = -360{,}000$ lb.

$$F_r = (F_x^2 + F_y^2)^{0.5} = 1{,}349{,}000 \text{ lb}$$

$e_x = 12.07 - 5.38 = 6.7$ in. $e_z = 5.25 - 3.22/2 = 3.64$in.;

conservatively use 3.9 in.

$$M_x = F_y (e_z) = 1{,}404{,}000 \text{ in-lb}$$

$$M_y = F_x (e_z) = 5{,}070{,}000 \text{ in-lb}$$

$$M_z = F_y (e_z) = 2{,}412{,}000 \text{ in-lb.}$$

The component stresses on the effective thickness weld group are:

$$S_{AC} = \frac{M_y c_x}{I_y} = \frac{(5{,}167{,}500)(12.07)}{(8886)} = 6{,}887 \text{ psi (bending stress at points A \& C)}$$

$$S_{BC} = \frac{M_x c_y}{I_x} = \frac{(1{,}404{,}000)(8.375)}{6570} = 1{,}790 \text{ psi (bending stress at points B \& C)}$$

$$S_s = \frac{F_R}{A_W} = \frac{1{,}373{,}000}{168} = 8{,}030 \text{ psi (resultant direct shear stress)}$$

$$(S_{ST})_A = \frac{M_Z}{2bht_A} = \frac{2{,}412{,}000}{(2)(19.94)(13.875)(1.0)} = 4385 \text{ psi (torsional shear stress at point A)}$$

$$(S_{ST})_B = \frac{M_Z}{2bht_B} = \frac{2{,}412{,}000}{(2)(19.94)(13.875)(2.875)} = 1517 \text{ psi (torsional shear stress at point B)}$$

The Von Mises equivalent stresses at Points A, B, and C are:

$$S_{EA} = \left[S_{AC}^2 + 3(S_S{}^2 + (S_{ST}^2)_A)\right]^{0.5} = 17{,}279 \text{ psi}$$

$$S_{EB} = \left[S_{BC}^2 + 3(S_S{}^2 + (S_{ST}^2)_B)\right]^{0.5} = 14{,}267 \text{ psi}$$

$$S_{EC} = \left[(S_{AC} + S_{BC})^2 + 3S_S^2\right]^{0.5} = 16{,}393 \text{ psi}.$$

The minimum margin of safety at the weld/cask interface is based on the yield strength of cask material A-240, Type 304 stainless steel outer shell with S_y = 25 ksi and is:

$$MS = \frac{25{,}000}{17{,}279} - 1 = +0.45.$$

The positive margins of safety show that the rotation pockets satisfy the requirements of 10 CFR 71.45 (b).

2.5.2.3 Front Support

The longitudinal force toward the top end of the cask is resisted by a shear ring welded to the cask top forging. The shear ring bears on the shipping frame along two 46-degree arcs (Figure 2.5.2-1).

The load on the shear ring is R_{jx} = 2,600,000 lb.

Assuming that the neoprene cradle cushion compresses to 0.25 in. thick, the effective width of the ring in direct bearing against the side of the support frame is 1.65 in. The bearing pressure is

$$A_{brg} = (2)(92/360)(\pi)(42.88)(1.65) = 113.6 \text{ in}^2$$
$$S_{brg} = 2{,}600{,}000/113.6 = 22{,}887 \text{ psi.}$$

The allowable bearing stress on the surface of SA-336 Type 304 stainless steel is

$$(S_{brg})_{Allow} = 25{,}000 \text{ psi at a temperature of } 200°\text{F.}$$

The margin of safety for bearing is $MS = \frac{23{,}750}{22{,}887} 4 - 1 = +0.09.$

The shear stress across the weld is

$$S_s = R_{jx}/A_w = 2{,}600{,}000/185 = 14{,}054 \text{ psi}$$

where $A_w = \pi(0.5)(85.26 + 82.61)(92/360)(1.375)(2) = 185 \text{ in}^2.$

The margin of safety for shear is $MS = \frac{(0.6)(23{,}750)}{14{,}054} 5 - 1 = +0.07.$

2.5.2.4 Overload

According to 10 CFR 71.45 (b)(3), each tiedown device that is a structural part of a package must be designed so that failure of the device under excessive load would not impair the ability of the package to meet the other requirements of 10 CFR 71. For this reason, the shear capacity of the rotation pockets and shear ring welds is compared with the shear capacity of the outer shell.

2.5.2.4.1 Shear Capacities at Rotation Pockets

Rotation Pocket Weld

The effective shear area of the weld is 119 in^2 as shown in Section 2.5.2.2.1. The filler material used to weld the rotation pocket to the cask body is AWS E309, with an ultimate tensile strength of 80.0 ksi. Applying the von Mises failure criterion, the ultimate shear capacity of the weld is

$$F_w = (119)(0.577)(80{,}000) = 5{,}493{,}040 \text{ lb.}$$

Cask Body

The area of the interface between the weld and the cask body is 168 in^2. The cask body has a tensile strength of 71 ksi. The ultimate shear capacity of the cask body at the interfacing area with the weld is

$$F_{cb} = (168)(0.577)(71{,}000) = 6{,}882{,}456 \text{ lb} > 5{,}493{,}040 \text{ lb.}$$

Thus, the weld will fail in shear before the cask body, thereby ensuring that failure caused by excessive overload on the rotation trunnions will not impair the ability of the package to meet the other requirements of 10 CFR 71.

2.5.2.4.2 Shear Capacities at Shear Ring

Shear Ring Weld

The effective shear area of the weld is 185 in^2, as shown in Section 2.5.2.3. The filler material used to weld the shear ring to the cask body is AWS E316L with an ultimate tensile strength of 70.0 ksi. Applying the von Mises failure criterion, the ultimate shear capacity of the weld is:

$$F_w = (185)(0.577)(70{,}000) = 7{,}472{,}150 \text{ lb.}$$

Cask Top Forging

The area of the interface between the weld and the cask body is 185(1.423/1.375) = 191.5 in^2. The cask body has a tensile strength of 71 ksi. The ultimate shear capacity of the cask body at the interfacing area with the weld is

$$F_{cb} = (191.5)(0.577)(71{,}000) = 7{,}845{,}181 \text{ lb} > 7{,}472{,}150 \text{ lb.}$$

Thus, the weld will fail in shear before the cask body, ensuring that failure caused by excessive overload on the shear ring will not impair the ability of the package to meet the other requirements of 10 CFR 71.

2.6 Normal Conditions of Transport

This section presents the evaluation of the Universal Transport Cask for structural integrity for the normal conditions of transport.

10 CFR 71.71 requires that the Universal Transport Cask be structurally adequate for the following normal conditions of transport: (1) heat, (2) cold, (3) reduced external pressure, (4) increased external pressure, (5) vibration, (6) water spray, (7) free drop, (8) corner-drop, (9) compression, and (10) penetration. In the free-drop analyses, the cask impact orientation evaluated is the orientation that inflicts the maximum damage to the cask. The regulation requires that the cask be evaluated for the normal conditions of transport at the most unfavorable ambient temperature in the range from -40°F to +100°F.

The results of these evaluations demonstrate that the cask satisfies the requirements of 10 CFR 71.71 for normal conditions of transport.

2.6.1 Heat

The Universal Transport Cask is analyzed for structural adequacy in accordance with the requirements of 10 CFR 71.71(c)(1), "Heat (normal condition of transport)." The cask is loaded, ready for shipment, and supported in the horizontal position with an ambient temperature environment of 100°F, an internal pressure of 150 psig (from Section 3.4.4, the calculated pressures are 7.3 psig and 5.0 psig for casks containing PWR and BWR fuel, respectively), maximum decay heat load, maximum solar insolation, and still air.

The stress analysis of the cask is performed by using a three-dimensional finite element model and the ANSYS computer program [32]. The model considers thermal heat, internal pressure, bolt preload, gravity, and combined loading conditions. The finite element model is described in Appendix 2.10.2. The temperature-dependent material properties considered in the analysis are documented in Section 3.2.

The following categories of load on the cask are considered for the heat condition:

1. Closure lid bolt preload—The required total bolt preload on the lid bolts is 5.4×10^6 lb (111,680 lb/bolt for 48 bolts). Bolt preload is applied to the model by imposing initial strains to the bolt shafts.

2. Internal pressure—For analysis purposes, an internal pressure of 150 psig is applied on the interior surfaces of the cask cavity in the outward normal direction. On the basis of the calculated maximum normal operating cavity pressures for PWR and BWR casks (7.3 and 5.0 psig, respectively) use of 150 psig is conservative. The pressure loading region includes the mating surfaces of the lid and upper body forging outward to the lid seal centerline.

3. Thermal—The heat transfer analyses performed for maximum normal operating conditions determine the cask temperature distribution for the heat condition. For the heat condition, the cask is considered to be in the horizontal position subjected to an ambient temperature of 100°F, with maximum decay heat load and maximum solar insolation, in still air. The cask temperature distribution obtained for this heat condition is used as input to the ANSYS analysis to determine the stresses in the cask. The ANSYS analysis determines the stresses resulting from thermal expansion of the cask from its initial 70°F condition to its normal transport temperature condition. These stresses include the effects of the differential thermal growth within the components, which result from the temperature difference across the cask walls. The cask temperature distribution is also used in the ANSYS structural analysis to determine the values of the temperature-dependent material properties.

4. Gravity—The mechanical loads consist of gravity acting on the cask structure and its contents. The cask is assumed to be loaded and resting in the horizontal position on the front and rear cask supports. Mechanical loads resulting from a 1-g application of the cask structure and contents are imposed on the model. The weight of the cavity contents is imposed on the model as a contents pressure on the contact surface of the cask cavity.

5. Fabrication and Installation—The effects of stresses resulting from the processes used in fabrication and installation are negligible.

2.6.1.1 Summary of Pressures and Temperatures

The maximum normal condition temperatures are summarized in Table 2.6.1.1-1 for the various PWR and BWR cask components. Summaries of pressures for the PWR and BWR canister and cask configurations are listed in Tables 2.6.1.1-2 and 2.6.1.1-3, respectively. The Maximum Normal Operating Pressure (MNOP), as defined in NUREG-1617 [57], Table 4-1, is 7.3 psig (Section 3.4.4.1.2.1).

2.6.1.2 Thermal Expansion Evaluation

The differential thermal expansions between the basket disks and the canister and the canister and the cask are evaluated based on bounding results from the PWR thermal analyses. In performing the calculations, nominal dimensions of the various components are used. The data used in the evaluation are presented in Chapter 1.0.

All thermal expansions are calculated using the following relation:

$$\Delta l = l_0 \, \alpha \, \Delta T$$

where Δl is the resulting change in linear dimension, l_0 is the original dimension, α the material thermal expansion coefficient, and ΔT temperature differential. The original dimensions are expressed in terms of room temperature, so the calculated temperature differences are based on 70°F environment temperature.

2.6.1.2.1 Canister/Cask Radial Thermal Expansion

The maximum canister shell temperature is 398.7 °F. The thermal expansion coefficient of Type 304L stainless steel at 400 °F is 9.19E-6 in/in-°F [21]. The increase in diameter of the canister is then

$$\Delta d = d_0 \, \alpha \, \Delta T = 67.06 \, (9.19E\text{-}6 \text{ in/in-°F}) \, (398.7 - 70) = 0.203 \text{ in.}$$

The canister diameter increases to 67.06 + 0.203 = 67.263 in.

Since this diameter is smaller than the nominal diameter of the cask cavity (67.61 in.), a diametrical clearance of 67.61 - 67.263 = 0.347 in. is assured during normal operating conditions even without considering the thermal expansion of the cask inner shell.

2.6.1.2.2 Canister/Cask Axial Thermal Expansion

The maximum canister shell temperature is 398.7°F. This temperature is conservative to use for the axial expansion since a temperature gradient exists along the length of the canisters. The thermal expansion coefficient of Type 304L stainless steel at 400°F is 9.19E-6 in/in-°F. The longest canister configuration is PWR Class 3 with a length of 191.95 in. The increase in length of the canister is then

$$\Delta l = l_0 \, \alpha \, \Delta T = 191.95 \, (9.19E\text{-}6 \text{ in/in-°F}) \, (398.7 - 70) = 0.58 \text{ in.}$$

The canister length increases to 191.95 + 0.58 = 192.53 in.

The minimum cask shell temperature is conservatively assumed to be 150°F (bounding case since the minimum temperature in forging is 237.5°F). The thermal expansion coefficient of Type 304 stainless steel at 70°F is 8.46E-6 in/in-°F. The cask cavity is 192.5 in. in length. The increase in length of the cask cavity is then

$$\Delta l = 192.5 \, (8.46E\text{-}6 \text{ in/in-°F}) \, (150 - 70) = 0.13 \text{ in.}$$

The cask cavity length increases to 192.5 + 0.13 = 192.63 in. The resulting axial gap is 192.63 - 192.53 = 0.1 in. Therefore, the canister and cask will expand axially and not bind during normal transport conditions.

2.6.1.3 Stress Calculations and Comparison to Allowable Stresses

The stresses throughout the cask body are calculated for the individual and combined loading conditions . The loading conditions are: (1) 150 psig internal pressure (including bolt preload); (2) thermal heat (100°F) loads; and (3) gravity. Stress results for the individual loading case of 150 psig internal pressure (including bolt preload) are documented in Tables 2.6.1.3-1 and 2.6.1.3-2. Stress results for the thermal loading case are documented in Table 2.6.1.3-3. Stress results for the individual gravity cases are documented in Table 2.6.1.3-4 and 2.6.1.3-5. The conventions used for the stress summary tables are:

1. All stresses are in ksi.
2. Section stress locations are shown in Figures 2.10.2.2-1 through 2.10.2.2-4.
3. The stress intensities (SI) presented in the tables represent the maximum SI occurring at any circumferential location or the specified section. The stress components correspond to the section having the largest SI.
4. Angles shown in the tables are in degrees and they identify the circumferential location where the maximum stress intensity occurs. These angles are measured from the x-axis rotating about the y-axis.
5. Any stress component that is shown to be 0 ksi is defined as being less than 0.1 ksi.
6. The stress intensities shown in the tables are rounded to the nearest 0.1 ksi. The margins of safety are calculated prior to rounding the stress intensities.
7. "Heat(100°F)" refers to 100°F ambient temperature, maximum solar insolation and maximum decay heat applied to the cask in still air.
8. Stresses are reported in a cylindrical system and X, Y, Z correspond to radial, circumferential and axial respectively.

These tables document primary membrane (P_m), primary membrane plus primary bending (P_m + P_b), primary plus secondary (P + Q), and critical P_m, P_m + P_b, and P + Q stresses in accordance with the criteria presented in Regulatory Guide 7.6. As described in Section 2.6.7, procedures have been implemented to document the nodal and sectional stresses as well as to determine the critical stress summary for all cask components.

For the individual loading condition of internal pressure (including lid bolt preload), the maximum calculated primary membrane stress intensity is 10.9 ksi and the maximum calculated primary membrane plus bending stress intensity is 16.9 ksi . For the individual thermal loading condition, the secondary membrane stress is 13.9 ksi. For the individual gravity loading condition (including lid bolt preload), the maximum calculated primary membrane stress intensity is 1.8 ksi and the maximum calculated primary membrane plus bending stress intensity is 4.7 ksi in regions where bolt preload (Section 40) is not considered. Conservatively combining the maximum stresses without regard to location for the internal pressure and gravity load cases, the maximum calculated primary membrane stress intensity is 12.7 ksi, the maximum calculated primary membrane plus bending stress intensity is 21.6 ksi, and the maximum calculated primary plus secondary stress is 35.5 ksi.

To show that the Universal Transport Cask meets the requirements for normal conditions of transport, the calculated stress intensities are compared to the allowable stress criteria presented in Regulatory Guide 7.6. For normal conditions, the primary membrane, primary membrane plus bending, and primary membrane plus bending plus secondary stresses; are compared to the following stress allowables:

$P_m < S_m$

$P_m + P_b < 1.5\ S_m$

$P_m + P_b + Q < 3\ S_m$

Using the conservatively calculated stresses, the minimum margin of safety for the P_m, $P_m + P_b$, and P + Q stresses in the cask for the heat condition are:

Stress State	Max. Stress (ksi)	Allowable Stress (ksi)	Margin of Safety
P_m	12.7	20.0	+0.6
$P_m + P_b$	21.6	30.0	+0.4
P + Q	35.5	57.4	+0.6

Since the margins of safety are all positive, the Universal Transport Cask satisfies the requirements of 10 CFR 71.71(c)(1) for the heat (normal transport) condition.

Table 2.6.1.1-1 Maximum Component Temperatures—Normal Conditions of Transport, Maximum Decay Heat, Maximum Ambient Temperature

Component	Temperature (°F) Cask with PWR Fuel Canister		Temperature (°F) Cask with BWR Fuel Canister	
	Canister Gas: Air[6]	Canister Gas: Helium	Canister Gas: Air[6]	Canister Gas: Helium
Cask Lid O-Rings/Vent Port O-ring[1]	268	266	207	204
Lower Drain Port O-ring[4]	225	224	232	230
Cask Radial Outer Surface	279	266	267	256
Radial Neutron Shield	314	293	301	286
Lead Gamma Shield	328	306	315	298
Aluminum Disk Exterior	292	268	321	298
Aluminum Disk Interior	683	605	508	515
Support Disk Exterior	271	255	213	208
Support Disk Interior	686	608	610	512
Canister Shell	399	408	369	363
Canister Shield Lid	272	270	212	208
Canister Bottom Plate	325	324	264	262
Maximum Fuel Rod Cladding	808	673	670	548
Cask Bottom	218	217	229	228
Bottom Forging	225	224	232	230
Inner Shell	368	344	336	312
Outer Shell	323	301	309	293
Top Forging[2]	256	250	196	194
Cask Lid	268	266	207	204
Cask Lid Bolt[3]	268	266	207	204
Average Gas Temperature in the Canisters[5]	492	453	432	366

Conditions:
100°F ambient temperature
20 kW decay heat load, 1.1 peaking factor - PWR
16 kW decay heat load, 1.22 peaking factor - BWR
Solar insolation
Cask cavity gas: helium
Canister cavity gas: air or helium

1. Cask lid O-rings and vent port O-rings not explicitly modeled—taken to be the maximum cask lid temperature.
2. Average temperature.
3. Cask lid bolts not explicitly modeled—taken to be the maximum temperature of the cask lid.
4. Lower drain port O-ring not explicitly modeled - taken to be the maximum temperature of the bottom forging.
5. Calculated as a volumetric average.
6. The design basis cover gas in the canister is helium. Temperature results for air as the cover gas are provided as worst-case temperatures for structural evaluation.

Table 2.6.1.1-2 Summary of Canister Pressures During Normal Conditions of Transport

CONDITION	CANISTER INTERNAL PRESSURE(PWR)	CANISTER INTERNAL PRESSURE(BWR)
Normal (3% Rod Failure)	1.44 atm ≈ 21.20 psia ≈ 6.50 psig	1.33 atm ≈ 19.56 psia ≈ 4.87 psig
Pressure used for Canister Analysis	25 psig	25 psig

Table 2.6.1.1-3 Summary of Cask Pressures During Normal Conditions of Transport

Pressure Condition	Cask Cavity Internal Pressure (PWR)	Cask Cavity Internal Pressure (BWR)
Normal (3% Rod Failure)	1.50 atm ≈ 21.98 psia ≈ 7.3 psig	1.34 atm ≈ 19.74 psia ≈ 5.04 psig
Cask Lid Closure Analysis	80 psig	80 psig
Cask Body Finite Element Analysis	150 psig	150 psig

Table 2.6.1.3-1 P_m Stresses—150 psig Internal Pressure*, Heat (100°F)

Section	Angle	Cylindrical Stress Components (ksi) S_X	S_Y	S_Z	S_{XY}	S_{YZ}	S_{XZ}	SI (ksi)	Allowable Stress (ksi)	MS
1	180	-0.1	0.0	0.9	-0.2	0.0	0.0	1.2	20.0	15.43
2	180	0.0	0.0	1.1	-0.2	-0.1	0.0	1.3	20.0	14.89
3	105	0.3	0.5	0.6	0.4	-0.3	-0.5	1.4	20.0	13.74
4	20	-1.0	0.1	-1.7	-0.4	-0.3	-0.4	2.3	20.0	7.65
5	10	-0.5	-0.1	-1.5	0.0	0.0	0.0	1.4	20.0	13.13
6	0	-0.7	-0.1	-2.2	0.2	0.0	0.0	2.2	20.0	8.16
7	0	-1.0	2.7	-2.3	-0.1	0.1	0.0	5.1	20.0	2.95
8	0	2.5	0.0	-3.6	0.2	0.3	-0.4	6.2	20.0	2.22
9	0	-3.7	0.5	-5.6	1.5	0.3	-0.2	6.7	20.0	2.00
10	0	0.1	-7.8	-6.3	0.4	0.3	-0.4	8.1	19.1	1.37
11	0	-2.4	-11.7	-8.6	1.6	0.2	-0.4	9.9	19.1	0.93
12	0	-3.3	5.5	-3.6	0.5	0.3	0.1	9.1	19.1	1.09
13	0	-1.1	8.5	-2.3	0.8	0.3	0.1	10.9	19.1	0.75
14	0	-3.7	-0.6	-5.2	-1.2	0.1	-0.1	5.0	19.7	2.93
15	0	-0.5	0.0	-4.5	0.9	0.1	-0.3	5.3	19.7	2.73
16	50	0.4	0.4	0.2	1.4	1.2	0.3	3.7	19.7	4.34
17	0	-0.1	4.6	1.1	0.0	0.2	0.2	4.7	19.7	3.18
18	0	-0.1	5.4	0.9	0.0	0.1	0.2	5.6	19.7	2.53
19	0	-0.1	5.8	0.8	0.0	0.0	0.2	5.9	19.7	2.33
20	0	-0.1	5.6	0.9	0.0	-0.1	0.2	5.8	19.7	2.41
21	0	-0.1	5.0	1.1	-0.1	-0.1	0.2	5.1	19.7	2.88
22	0	-0.1	3.3	1.1	-0.2	-0.3	0.1	3.5	19.7	4.64
23	90	1.9	1.3	-0.1	1.3	0.0	0.0	3.0	19.1	5.29
24	0	-0.3	2.5	4.3	0.0	0.4	0.4	4.7	19.1	3.06
25	0	-0.3	4.8	3.7	0.0	0.2	0.4	5.1	19.1	2.72
26	0	-0.3	5.9	3.6	0.0	0.1	0.4	6.3	19.1	2.04
27	0	-0.3	6.4	3.7	0.0	0.0	0.4	6.7	19.1	1.85
28	0	-0.3	6.1	3.6	0.0	-0.1	0.4	6.4	19.1	1.98
29	0	-0.3	5.0	3.6	0.0	-0.2	0.4	5.4	19.1	2.56
30	0	-0.3	3.1	3.9	-0.1	-0.3	0.4	4.4	19.1	3.34
31	90	3.1	1.6	-0.1	-1.4	-0.1	0.0	4.0	19.1	3.73
32	70	1.4	-0.7	0.3	-1.2	-0.8	0.5	3.6	20.0	4.50
33	50	0.8	0.4	-0.9	-0.4	-0.5	0.6	2.5	20.0	7.08
34	60	2.8	1.6	1.4	-1.9	-1.4	1.4	5.2	20.0	2.82
35	90	1.7	0.3	0.2	-0.7	-0.3	0.0	2.2	20.0	8.28
36	180	-0.3	-0.5	3.9	-0.8	-0.1	-0.6	5.2	20.0	2.83
37	0	-0.8	-0.1	-0.4	-0.1	0.0	0.0	0.7	20.0	26.51
38	0	-0.8	-0.1	-0.6	-0.3	0.0	0.0	0.9	20.0	20.38
39	10	-0.8	-0.1	-0.7	-0.3	0.1	0.0	0.9	20.0	21.07
40	80	1.1	1.7	-0.2	-0.4	1.7	0.1	4.0	20.0	4.03
41	30	-1.2	0.0	-1.1	-0.1	-0.1	0.1	1.3	20.0	14.56

* Including cask lid bolt preload.

Table 2.6.1.3-2 $P_m + P_b$ Stresses—150 psig Internal Pressure*, Heat (100°F)

Section	Angle	Cylindrical Stress Components (ksi)						SI (ksi)	Allowable Stress (ksi)	MS
		S_X	S_Y	S_Z	S_{XY}	S_{YZ}	S_{XZ}			
1	180	1.8	0.1	4.4	-0.2	0.0	-0.1	4.3	30.0	6.00
2	180	0.0	0.0	3.1	-0.2	-0.1	-0.2	3.2	30.0	8.36
3	180	-0.9	-0.1	1.7	0.3	0.0	-0.2	2.8	30.0	9.72
4	20	-1.0	1.2	-1.4	-0.2	-0.3	-0.4	2.9	30.0	9.37
5	40	-2.3	-0.1	-4.5	0.0	0.0	0.0	4.3	30.0	5.91
6	0	-1.1	-0.2	-4.7	0.2	0.0	-0.1	4.6	30.0	5.59
7	0	2.5	6.6	-1.7	0.4	0.2	-0.1	8.4	30.0	2.57
8	0	5.8	10.9	0.5	0.4	0.4	-0.2	10.5	30.0	1.85
9	0	1.7	17.8	0.9	0.4	0.5	-0.1	16.9	30.0	0.77
10	0	2.6	-6.9	-5.1	-0.5	0.3	-0.5	9.7	28.7	1.97
11	0	4.9	-8.7	-5.3	1.0	0.3	-0.7	13.9	28.7	1.07
12	0	-6.6	4.7	-4.6	-0.1	0.2	0.2	11.3	28.7	1.55
13	0	-6.8	6.7	-4.4	0.8	0.4	0.3	13.6	28.7	1.11
14	0	-5.7	6.3	-3.9	-0.5	0.2	0.2	12.0	29.6	1.46
15	0	4.3	11.4	0.0	1.0	0.3	-0.2	11.6	29.6	1.54
16	40	0.9	1.1	0.9	2.0	2.5	0.9	6.4	29.6	3.59
17	0	-0.1	7.3	8.0	0.0	0.0	0.8	8.2	29.6	2.60
18	0	-0.1	2.2	-7.4	0.0	0.2	-0.5	9.7	29.6	2.05
19	0	-0.1	2.4	-7.9	0.0	0.0	-0.5	10.3	29.6	1.86
20	0	-0.1	2.5	-7.2	0.0	-0.2	-0.5	9.7	29.6	2.06
21	0	-0.1	7.6	7.5	0.0	0.1	0.7	7.8	29.6	2.80
22	40	0.8	1.3	0.9	-2.0	-2.6	0.9	6.6	29.6	3.48
23	0	-0.3	0.9	-2.6	0.8	0.9	-0.3	4.3	28.7	5.70
24	0	-0.2	4.9	8.7	0.0	0.1	0.8	9.0	28.7	2.19
25	0	-0.2	7.3	10.5	0.0	0.0	1.0	10.8	28.7	1.64
26	0	-0.2	9.1	12.0	0.0	0.0	1.1	12.4	28.7	1.31
27	0	-0.2	9.8	12.8	0.0	0.0	1.2	13.2	28.7	1.17
28	0	-0.2	9.3	12.5	0.0	0.0	1.2	12.9	28.7	1.22
29	0	-0.2	7.9	11.4	0.0	-0.1	1.1	11.9	28.7	1.42
30	0	-0.2	4.9	9.7	0.0	-0.1	0.9	10.1	28.7	1.85
31	0	-0.2	1.2	4.4	-0.5	-0.2	0.4	4.8	28.7	5.01
32	50	1.2	-1.0	0.8	-2.1	-2.0	0.9	6.5	30.0	3.60
33	50	1.1	-1.5	-2.5	-1.7	-1.7	0.7	6.2	30.0	3.83
34	0	-0.2	6.3	-2.0	0.6	-0.7	-0.3	8.5	30.0	2.54
35	0	1.0	-0.2	-3.0	0.6	-0.6	-0.3	4.4	30.0	5.82
36	180	-0.8	-0.6	3.6	-1.3	-0.4	-0.7	5.9	30.0	4.10
37	0	-6.9	-0.2	-8.1	-0.1	0.0	0.0	7.9	30.0	2.79
38	0	-4.6	-0.2	-7.2	-0.3	0.0	-0.1	7.0	30.0	3.28
39	0	-2.8	0.5	-6.2	-0.7	0.1	-0.1	6.9	30.0	3.36
40	80	5.1	6.7	1.7	-0.5	1.7	0.3	6.1	30.0	3.88
41	0	-2.4	-0.2	-1.3	0.2	0.0	0.1	2.2	30.0	12.37

* Including cask lid bolt preload.

Table 2.6.1.3-3 Thermal (Q) Stresses—Heat (100°F)

Section	Angle	Cylindrical Stress Components (ksi)						SI (ksi)
		S_X	S_Y	S_Z	S_{XY}	S_{YZ}	S_{XZ}	
1	80	4.5	2.9	0	0.3	0	0	4.6
2	0	3.4	4.2	0.1	-0.1	0.1	-0.1	4.1
3	180	7.3	5.3	7.3	-0.1	-0.3	3	6
4	0	7	-0.6	-4	0.3	0.7	-0.4	11.1
5	0	-5.3	-1.5	-0.3	-0.9	-0.2	0.2	5.3
6	0	-2.7	-1.5	-0.1	-0.1	0	0	2.6
7	0	-4.5	-2.2	-8.4	-0.2	-0.1	-1.8	6.9
8	0	-4.5	-2.2	-8.4	-0.2	-0.1	-1.8	6.9
9	0	-0.4	-1.4	-9.6	0.1	0	-0.9	9.3
10	70	-1	1.5	2.1	-0.8	0.3	-0.3	3.5
11	50	0.6	2.2	2.7	-1.1	1.3	-0.7	4.1
12	20	0	2.1	3.3	-0.4	0.5	-0.2	3.6
13	0	0.4	2.2	3.2	-0.3	0	0.4	3
14	20	0	2.1	3.3	-0.4	0.5	-0.2	3.6
5	0	0.4	2.2	3.2	-0.3	0	0.4	3
16	0	-0.1	3.3	1.9	-0.3	0.1	0.1	3.5
17	0	-0.1	4.7	3.5	-0.5	0.1	0	5
18	0	-0.2	5	3.5	-0.5	0	0	5.3
19	0	-0.2	5.1	3.4	-0.5	0	0	5.3
20	0	-0.2	5.2	3.5	-0.5	0	0	5.5
21	0	-0.2	5.1	3.4	-0.5	-0.1	0	5.4
22	0	-0.1	3.4	2.5	-0.3	-0.1	-0.1	3.6
23	0	-0.3	-1	-5.1	0.1	0.2	-0.2	4.9
24	0	-0.2	-3	-6	0.3	0.4	0	5.9
25	0	-0.1	-5.3	-12	0.5	0.2	0	11.9
26	0	-0.2	-5.6	-13.7	0.5	0.1	0	13.6
27	0	-0.1	-5.1	-13.8	0.5	0	0	13.8
28	0	-0.1	-5.4	-14	0.5	0	0	13.9
29	0	-0.3	-6.2	-14	0.6	-0.1	0	13.7
30	0	-0.3	-6.3	-12.3	0.6	-0.2	0	12
31	0	-1	-3.7	-8	0.3	-0.6	-0.1	7.2
32	10	-0.2	0.6	3.2	0	0.1	-0.2	3.4
33	10	3.7	2.5	5.7	-0.1	0	-1	3.6
34	0	0.2	-2	-4.4	0	-0.5	-0.5	4.8
35	0	0	-0.7	-2.5	0.1	-0.1	-0.1	2.5
36	0	-0.2	1.4	-1.4	-0.2	-0.1	0	2.9
37	150	-2.7	-2.9	0	0.8	0	0	3.6
38	180	-2.7	-2.6	0	0.1	0	0	2.7
39	120	0.4	-0.3	-2.9	-0.1	-0.1	0.2	3.4
40	180	-1.4	1.6	0.7	0.4	0.1	0.3	3.2
41	10	0	2.8	5.5	0	0.3	0.1	5.5

Table 2.6.1.3-4 P_m Stresses—1-*g* Gravity Load*, Heat (100°F)

Section	Angle	Cylindrical Stress Components (ksi)						SI (ksi)	Allowable Stress (ksi)	MS
		S_X	S_Y	S_Z	S_{XY}	S_{YZ}	S_{XZ}			
1	120	0	0	0	-0.1	0	0	0.1	20	171.86
2	10	-0.1	-0.1	0	0	0	0	0.1	20	159.51
3	105	0	0	0	-0.1	0	0	0.1	20	134.04
4	10	-0.2	-0.3	-0.1	0	0	-0.1	0.2	20	79.35
5	10	-0.1	-0.1	0	0	0	0	0.1	20	137.89
6	0	-0.2	-0.2	0	0	0	0	0.2	20	97.38
7	0	-0.2	-0.3	0.1	0	0	0	0.4	20	51.3
8	10	-0.2	-0.4	-0.1	0	0	-0.1	0.4	20	51.99
9	10	-0.3	-0.5	-0.1	0	0	0.1	0.4	20	48.43
10	0	-0.3	-0.6	-0.5	0	0	0	0.3	19.1	59.26
11	0	-0.3	-0.7	-0.7	0	0	0.1	0.5	19.1	39.49
12	10	-0.4	-0.4	0.4	0	0	0	0.8	19.1	22.75
13	0	-0.3	-0.3	0.6	0	0	0	0.9	19.1	20.64
14	10	-0.4	-0.5	-0.2	0	0	-0.1	0.4	19.7	46.2
15	0	-0.2	-0.5	-0.1	0	0	0.1	0.4	19.7	45.37
16	50	0	0.1	0.1	0	-0.2	0	0.4	19.7	51.63
17	0	0	0.1	0.3	0	0	0	0.3	19.7	65.82
18	0	0	0.1	0.4	0	0	0	0.4	19.7	50.07
19	0	0	0.1	0.4	0	0	0	0.4	19.7	44.87
20	0	0	0.1	0.4	0	0	0	0.4	19.7	44.76
21	0	0	0.1	0.4	0	0	0	0.4	19.7	51.02
22	40	0	0.3	0.1	0	0.1	0	0.4	19.7	48.46
23	40	0	-0.1	0	0	-0.2	0	0.4	19.1	46.8
24	50	0	0	0	0	-0.2	0	0.4	19.1	49.05
25	60	0	0	0	0	-0.1	0	0.3	19.1	73.8
26	0	0	0.1	0.3	0	0	0	0.3	19.1	56.11
27	0	0	0.1	0.4	0	0	0	0.4	19.1	50.04
28	0	0	0.1	0.3	0	0	0	0.4	19.1	52.47
29	0	0	0.1	0.3	0	0	0	0.3	19.1	65.85
30	60	0	0	0	0	0.2	0	0.3	19.1	55.47
31	50	0	0.5	0	0	0.2	0	0.7	19.1	26
32	60	0	0.6	0	0	0.2	0.1	0.7	20	25.92
33	60	-0.4	0.7	0.1	-0.1	0.1	0.1	1.1	20	17.42
34	60	0.3	1	-0.2	0	0.2	0.1	1.3	20	14.56
35	70	-0.2	0.7	-0.1	0	0.2	0.3	1.1	20	16.64
36	180	1	1.4	-0.3	0.1	0	0.3	1.8	20	10.21
37	0	-0.3	-0.2	0	0	0	0	0.3	20	58.15
38	120	-0.3	-0.3	0	0	0	0	0.3	20	58.7
39	80	-0.2	-0.4	-0.8	0.1	0	0	0.6	20	32.53
40	80	-1.6	-2	-3.3	0.1	0	-1.1	2.9	20	5.89
41	0	-0.2	-0.1	-0.1	0	0	0	0.2	20	118.62

* Including cask lid bolt preload.

Table 2.6.1.3-5 $P_m + P_b$ Stresses —1-g Gravity Load*, Heat (100°F)

Section	Angle	Cylindrical Stress Components (ksi) S_X	S_Y	S_Z	S_{XY}	S_{YZ}	S_{XZ}	SI (ksi)	Allowable Stress (ksi)	MS
1	165	0	0.1	0	0	0	0	0.1	30	205.04
2	180	0	0.2	0	0	0	0	0.2	30	169.16
3	90	0.1	0	0.1	-0.1	-0.1	0	0.3	30	116.23
4	10	-0.1	-0.3	0	0	0	0	0.3	30	108.33
5	40	-0.1	-0.2	0	0	0	0	0.2	30	170.82
6	0	-0.2	-0.3	0	0	0	0	0.3	30	117.62
7	0	-0.2	-0.4	0.2	0	0	0	0.5	30	53.59
8	0	-0.1	-0.3	0.4	0	0	-0.1	0.7	30	40.85
9	0	0.1	-0.1	0.8	0	0	0	0.9	30	31.38
10	0	-0.2	-0.5	-0.4	0	0	0	0.3	28.7	84.53
11	0	0	-0.5	-0.5	0	0	0.1	0.6	28.7	48.05
12	10	-0.5	-0.4	0.3	0	0	0	0.9	28.7	31.69
13	0	-0.6	-0.4	0.4	0	0	0	1	28.7	26.44
14	10	-0.5	-0.4	0.4	0	0	0	0.9	29.6	32.69
15	0	0.1	-0.1	0.8	0	0	0.1	1	29.6	29.72
16	50	0	0.1	0.1	0	-0.2	0	0.5	19.7	38.96
17	0	0	0.4	0.4	0	0	0	0.4	19.7	43.82
18	0	0	0.5	0.5	0	0	0	0.6	19.7	34.63
19	0	0	-0.4	0.2	0	0	0	0.6	19.7	31.28
20	0	0	0.5	0.6	0	0	0	0.6	19.7	31.84
21	0	0	0.4	0.5	0	0	0	0.5	19.7	36.74
22	40	0	0.4	0.3	0	0.2	0	0.6	29.6	48.36
23	40	0	-0.1	0	0	-0.3	0	0.6	28.7	47.05
24	40	0	0.1	0	0	-0.3	0	0.5	19.1	36.34
25	0	0	0.4	0.3	0	0	0	0.4	19.1	42.84
26	0	0	0.5	0.5	0	0	0	0.5	19.1	35.34
27	0	0	0.5	0.5	-0.1	0	0	0.6	19.1	32.61
28	0	0	0.5	0.5	-0.1	0	0	0.6	19.1	33.46
29	0	0	0.5	0.4	0	0	0	0.5	19.1	37.41
30	50	0	0.2	0.1	0	0.2	0	0.4	19.1	41.75
31	40	0	0.6	0.1	0	0.3	0	0.8	28.7	33.62
32	50	0	0.6	-0.3	0	0.2	0.1	1	30	29.8
33	70	-0.8	0.4	-0.7	-0.2	0.2	0.1	1.4	30	20.34
34	50	0	0.6	-1.4	0	0.3	-0.1	2.1	30	13.55
35	70	-0.3	0.5	-1.1	0	0.4	1.5	3.1	30	8.56
36	70	3.2	1.9	1	0.1	0.2	0.4	2.3	30	11.88
37	0	-3.7	-3.6	0	0	0	0	3.7	30	7.06
38	30	-3.9	-3.7	-0.1	0	0	0	3.8	30	6.82
39	70	3.6	2.7	-1.2	0	0	0	4.7	30	5.32
40	0	-3.1	-6.3	-9.8	0.2	-0.1	0.3	6.7	30	3.45
41	0	-0.3	-0.1	0	0	0	0	0.4	30	82.5

* Including cask lid bolt preload.

2.6.2 Cold

The Universal Transport Cask body and closure lid are analyzed for structural adequacy in accordance with the requirements of 10 CFR 71.71(c)(2), "Cold (normal condition of transport)." The cask is loaded and ready for shipment in the horizontal position, with an ambient temperature environment of -40°F, an analyzed internal pressure of 150 psig, no decay heat load, no solar insolation, and in still air and shade. Note that although the Cold condition is associated with the minimum internal pressure, an internal pressure of 150 psig, which corresponds to the maximum internal pressure, is conservatively used.

2.6.2.1 Summary of Pressures and Temperatures

The minimum normal condition temperatures are summarized in Table 2.6.2.1-1 for the various PWR and BWR cask components (Note that the temperatures in air are used only for structural calculations and are not intended to be used as thermal design basis). Maximum internal pressures generated in the canister and cask are listed in Table 2.6.1.1-2 and 2.6.1.1-3. Closure bolts are qualified for a maximum pressure of 80 psig (Section 2.6.7.6). The Maximum Normal Operating Pressure (MNOP), as defined by NUREG-1617 [57], Table 4-1, is 7.3 psig (Section 3.4.4.1.2.1).

2.6.2.2 Thermal Expansion Evaluation

The discussion presented in Section 2.6.1.2 bounds the worst differential thermal expansion conditions since the evaluation results in higher temperatures. According to Section 2.6.1.2, thermal expansion of Universal Transport Cask is less than the minimum clearance between components.

2.6.2.3 Stress Calculations and Comparison to Allowable Stresses

The stresses throughout the cask body are calculated for the individual and combined loading conditions . The loading conditions are: (1) 150 psig internal pressure (including bolt preload); (2) cold (-40°F) thermal loads; and (3) gravity. Stress results for the individual loading case of 150 psig internal pressure (including bolt preload) are documented in Tables 2.6.2.3-1 and 2.6.2.3-2. Stress results for the thermal loading case is documented in Table 2.6.2.3-3. Stress results for the individual gravity cases are documented in Table 2.6.2.3-4 and 2.6.2.3-5. The conventions used for the stress summary tables are:

1. All stresses are in ksi.
2. Section stress locations are shown in Figures 2.10.2.2-1 through 2.10.2.2-4
3. The stress intensities (SI) presented in the tables represent the maximum SI occurring at any circumferential location or the specified section. The stress components correspond to the section having the largest SI.
4. Angles shown in the tables are in degrees and they identify the circumferential location where the maximum stress intensity occurs. These angles are measured from the x-axis rotating about the y-axis.
5. Any stress component that is shown to be 0 ksi is defined as being less than 0.1 ksi.
6. The stress intensities shown in the tables are rounded to the nearest 0.1 ksi. The margins of safety are calculated prior to rounding the stress intensities.
7. "Cold (-40°F)" refers to -40°F ambient temperature, no solar insolation and no decay heat applied to the cask in still air.
8. Stresses are reported in a cylindrical system and X, Y, Z correspond to radial, circumferential and axial respectively.

These tables document the primary membrane (P_m), primary membrane plus primary bending ($P_m + P_b$), primary plus secondary stresses (P + Q), and critical P_m, $P_m + P_b$, and P + Q stresses in accordance with the criteria presented in Regulatory Guide 7.6. As described in Section 2.6.7, procedures have been implemented to document the nodal and sectional stresses as well as to determine the critical stress summary for all cask components.

For the individual loading condition of internal pressure, the maximum calculated primary membrane stress intensity is 10.9 ksi and the maximum calculated primary membrane plus bending stress intensity is 16.9 ksi, . For the individual thermal loading condition, the peak stress is 13.9 ksi. For the individual gravity loading condition (including cask lid bolt preload), the maximum calculated primary membrane stress intensity is 1.9 ksi and the maximum calculated primary membrane plus bending stress intensity is 4.7 ksi except in regions affected by bolt preload. Conservatively combining the maximum stress without regard to location for the internal pressure and gravity load cases, the maximum calculated primary membrane stress intensity is 12.8 ksi, the maximum calculated primary membrane plus primary bending stress intensity is 21.6 ksi, and the maximum calculated primary plus secondary stress is 35.5 ksi.

Using the conservatively calculated stresses, the minimum margin of safety for the P_m, $P_m + P_b$, and $P + Q$ stresses in the cask for the cold condition are:

Stress State	Max. Stress (ksi)	Allowable Stress (ksi)	Margin of Safety
P_m	12.8	20.0	+0.6
$P_m + P_b$	12.6	30.0	+0.4
$P + Q$	35.5	57.4	+0.6

Since the margins of safety are all positive, the Universal Transport Cask satisfies the requirements of 10 CFR 71.71(c)(2) for the cold condition.

Table 2.6.2.1-1 Minimum Component Temperatures - Normal Conditions of Transport, Maximum Decay Heat, Minimum Ambient Temperature (Thermal Cold)

Component	Temperature (°F) PWR Cask		Temperature (°F) BWR Cask	
	Canister Gas: Air*	Canister Gas: Helium	Canister Gas: Air*	Canister Gas: Helium
Lid O-Ring[1]	154	147	69	64
Cask Radial Outer Surface	160	152	149	133
Radial Neutron Shield	197	186	183	164
Lead Gamma Shield	211	199	198	176
Maximum Basket Web[2]	599	497	524	408
Canister Shell	281	283	242	241
Canister Shield Lid	148	147	74	68
Canister Bottom Plate	208	203	132	128
Maximum Fuel Rod Cladding	744	582	593	442

Conditions: -40°F ambient temperature
20 kW decay heat load, 1.1 peaking factor - PWR
16 kW decay heat load, 1.22 peaking factor - BWR
No insolance
Cask cavity gas: helium
Canister cavity gas: air or helium

[1]Cask lid O-ring not explicitly modeled—taken to be the greater of the maximum cask upper forging and the maximum cask lid temperatures.

[2]Taken to be the greater of the maximum support disk and the maximum aluminum heat transfer disk temperatures.

* Note that temperatures in air are to be used only for structural calculations and are not intended to be used as thermal design basis.

Table 2.6.2.3-1 P_m Stresses—150 psig Internal Pressure*; Cold (-40°F)

Section	Angle	Cylindrical Stress Components (ksi) S_X	S_Y	S_Z	S_{XY}	S_{YZ}	S_{XZ}	SI (ksi)	Allowable Stress (ksi)	MS
1	180	-0.1	0.0	0.9	-0.2	0.0	0.0	1.2	20.0	15.57
2	180	0.0	0.0	1.1	-0.2	-0.1	0.0	1.2	20.0	15.03
3	105	0.3	0.5	0.6	0.4	-0.3	-0.5	1.3	20.0	13.88
4	20	-1.0	0.1	-1.7	-0.4	-0.3	-0.4	2.3	20.0	7.69
5	10	-0.5	-0.1	-1.5	0.0	0.0	0.0	1.4	20.0	13.20
6	0	-0.7	-0.1	-2.2	0.2	0.0	0.0	2.2	20.0	8.17
7	0	-1.0	2.7	-2.3	-0.1	0.1	0.0	5.1	20.0	2.95
8	0	2.5	0.0	-3.6	0.2	0.3	-0.4	6.2	20.0	2.23
9	0	-3.7	0.5	-5.6	1.5	0.3	-0.2	6.7	20.0	2.00
10	0	0.1	-7.8	-6.3	0.4	0.3	-0.4	8.1	20.0	1.48
11	0	-2.5	-11.7	-8.6	1.6	0.2	-0.4	9.9	20.0	1.02
12	0	-3.3	5.5	-3.6	0.5	0.3	0.1	9.1	20.0	1.20
13	0	-1.1	8.5	-2.3	0.8	0.3	0.1	10.9	20.0	0.84
14	0	-3.7	-0.6	-5.2	-1.1	0.1	-0.1	5.0	20.0	2.99
15	0	-0.4	0.1	-4.5	0.9	0.1	-0.3	5.3	20.0	2.79
16	50	0.4	0.4	0.2	1.4	1.2	0.3	3.7	20.0	4.46
17	0	-0.1	4.6	1.0	0.0	0.2	0.2	4.7	20.0	3.25
18	0	-0.1	5.4	0.9	0.0	0.1	0.2	5.6	20.0	2.59
19	0	-0.1	5.7	0.8	0.0	0.0	0.2	5.9	20.0	2.39
20	0	-0.1	5.6	0.9	0.0	-0.1	0.2	5.8	20.0	2.46
21	0	-0.1	5.0	1.1	-0.1	-0.1	0.2	5.1	20.0	2.93
22	0	-0.1	3.4	1.1	-0.1	-0.3	0.1	3.5	20.0	4.69
23	90	1.9	1.3	-0.1	1.3	0.0	0.0	3.1	20.0	5.56
24	0	-0.3	2.5	4.3	0.0	0.4	0.4	4.7	20.0	3.22
25	0	-0.3	4.8	3.7	0.0	0.2	0.4	5.2	20.0	2.85
26	0	-0.3	6.0	3.6	0.0	0.1	0.4	6.4	20.0	2.15
27	0	-0.3	6.4	3.7	0.0	0.0	0.4	6.8	20.0	1.95
28	0	-0.3	6.1	3.6	0.0	-0.1	0.4	6.5	20.0	2.09
29	0	-0.3	5.1	3.6	0.0	-0.2	0.4	5.4	20.0	2.69
30	0	-0.3	3.1	4.0	-0.1	-0.4	0.4	4.4	20.0	3.51
31	90	3.1	1.7	-0.1	-1.4	-0.1	0.0	4.1	20.0	3.92
32	70	1.4	-0.7	0.3	-1.2	-0.8	0.5	3.6	20.0	4.51
33	50	0.8	0.4	-0.9	-0.4	-0.5	0.6	2.5	20.0	7.08
34	60	2.9	1.6	1.4	-1.9	-1.4	1.4	5.3	20.0	2.78
35	90	1.7	0.3	0.2	-0.7	-0.3	0.0	2.2	20.0	8.19
36	180	-0.3	-0.5	3.9	-0.8	-0.1	-0.6	5.3	20.0	2.79
37	0	-0.8	-0.1	-0.4	-0.1	0.0	0.0	0.7	20.0	26.30
38	0	-0.8	-0.1	-0.6	-0.3	0.0	0.0	0.9	20.0	20.32
39	10	-0.8	-0.1	-0.7	-0.3	0.1	0.0	0.9	20.0	21.09
40	80	1.2	1.8	-0.2	-0.4	1.7	0.1	4.1	20.0	3.90
41	30	-1.2	0.0	-1.1	-0.1	-0.1	0.1	1.3	20.0	14.69

* Including cask lid bolt preload.

Table 2.6.2.3-2 $P_m + P_b$ Stresses—150 psig Internal Pressure*; Cold (-40°F)

Section	Angle	Cylindrical Stress Components (ksi)						SI (ksi)	Allowable Stress (ksi)	MS
		S_X	S_Y	S_Z	S_{XY}	S_{YZ}	S_{XZ}			
1	180	1.8	0.1	4.3	-0.2	0.0	-0.1	4.3	30.0	6.06
2	180	0.0	0.0	3.0	-0.2	-0.1	-0.2	3.2	30.0	8.45
3	180	-0.9	-0.1	1.7	0.3	0.0	-0.2	2.8	30.0	9.83
4	20	-1.0	1.2	-1.4	-0.2	-0.3	-0.4	2.9	30.0	9.40
5	40	-2.3	-0.1	-4.5	0.0	0.0	0.0	4.3	30.0	5.93
6	0	-1.1	-0.2	-4.7	0.2	0.0	-0.1	4.5	30.0	5.61
7	0	2.5	6.6	-1.7	0.4	0.2	-0.1	8.4	30.0	2.57
8	0	5.8	10.9	0.5	0.3	0.4	-0.2	10.5	30.0	1.85
9	0	1.7	17.8	0.9	0.4	0.5	-0.1	16.9	30.0	0.77
10	0	2.6	-6.9	-5.1	-0.5	0.3	-0.5	9.7	30.0	2.10
11	0	4.9	-8.8	-5.3	1.0	0.3	-0.7	13.9	30.0	1.16
12	0	-6.6	4.6	-4.6	-0.1	0.2	0.2	11.2	30.0	1.67
13	0	-6.8	6.6	-4.4	0.8	0.4	0.3	13.6	30.0	1.21
14	0	-5.7	6.3	-3.9	-0.4	0.2	0.2	12.0	30.0	1.50
15	0	4.3	11.3	0.0	1.0	0.3	-0.2	11.6	30.0	1.60
16	40	0.9	1.1	0.9	2.0	2.5	0.9	6.4	30.0	3.70
17	0	-0.1	7.3	7.9	0.0	0.0	0.8	8.2	30.0	2.67
18	0	-0.1	2.2	-7.4	0.0	0.2	-0.5	9.7	30.0	2.10
19	0	-0.1	2.4	-7.9	0.0	0.0	-0.5	10.4	30.0	1.90
20	0	-0.1	2.5	-7.2	0.0	-0.2	-0.5	9.7	30.0	2.10
21	0	-0.1	7.6	7.5	0.0	0.1	0.7	7.8	30.0	2.86
22	40	0.8	1.3	0.9	-2.0	-2.5	0.9	6.5	30.0	3.59
23	0	-0.3	0.9	-2.6	0.8	0.9	-0.3	4.3	30.0	5.02
24	0	-0.2	5.0	8.7	0.0	0.1	0.8	9.0	30.0	2.32
25	0	-0.2	7.4	10.5	0.0	0.0	1.0	10.9	30.0	1.74
26	0	-0.2	9.2	12.1	0.0	0.0	1.1	12.5	30.0	1.39
27	0	-0.2	9.9	12.9	0.0	0.0	1.2	13.3	30.0	1.25
28	0	-0.2	9.4	12.6	0.0	0.0	1.2	13.0	30.0	1.30
29	0	-0.2	8.0	11.6	0.0	-0.1	1.1	12.0	30.0	1.51
30	0	-0.2	4.9	9.8	0.0	-0.2	0.9	10.1	30.0	1.96
31	0	-0.2	1.2	4.4	-0.5	-0.2	0.4	4.8	30.0	5.23
32	50	1.2	-1.1	0.8	-2.1	-2.0	0.9	6.5	30.0	3.63
33	50	1.1	-1.6	-2.5	-1.7	-1.7	0.8	6.2	30.0	3.84
34	0	-0.2	6.3	-2.0	0.6	-0.8	-0.3	8.5	30.0	2.54
35	90	3.3	0.6	0.6	-0.8	-1.4	-0.1	4.4	30.0	5.76
36	180	-0.8	-0.6	3.7	-1.3	-0.4	-0.7	5.9	30.0	4.05
37	0	-7.0	-0.2	-8.2	-0.1	0.0	0.0	8.0	30.0	2.74
38	0	-4.7	-0.2	-7.3	-0.3	0.0	-0.1	7.1	30.0	3.22
39	0	-2.9	0.5	-6.3	-0.7	0.1	-0.1	7.0	30.0	3.29
40	80	5.2	6.9	1.7	-0.5	1.7	0.3	6.3	30.0	3.78
41	0	-2.4	-0.2	-1.3	0.2	0.0	0.1	2.2	30.0	12.44

* Including cask lid bolt preload.

Table 2.6.2.3-3 Thermal (Q) Stresses— Cold (-40°F)

Section	Angle	Cylindrical Stress Components (ksi)						SI (ksi)	[redacted]	[redacted]
		S_X	S_Y	S_Z	S_{XY}	S_{YZ}	S_{XZ}			
1	10	-0.1	0.0	0.0	0.0	0.0	0.0	0.1	[redacted]	[redacted]
2	10	-0.1	0.0	-0.1	0.0	0.0	0.0	0.1	[redacted]	[redacted]
3	105	0.0	0.0	0.1	0.1	0.0	-0.1	0.2	[redacted]	[redacted]
4	90	0.0	0.0	0.0	0.1	0.0	-0.1	0.2	[redacted]	[redacted]
5	0	-0.2	0.0	-0.1	0.0	0.0	0.0	0.2	[redacted]	[redacted]
6	0	-0.2	0.0	-0.1	0.0	0.0	0.0	0.2	[redacted]	[redacted]
7	0	-0.3	0.0	-0.2	-0.1	0.0	0.0	0.3	[redacted]	[redacted]
8	0	-0.3	0.0	-0.2	-0.1	0.0	0.0	0.3	[redacted]	[redacted]
9	0	0.0	0.2	-0.1	0.0	0.0	0.0	0.3	[redacted]	[redacted]
10	105	0.0	0.0	0.0	0.1	0.0	-0.1	0.2	[redacted]	[redacted]
11	180	-0.1	0.0	0.0	0.1	0.0	0.0	0.2	[redacted]	[redacted]
12	10	-0.3	0.2	-0.2	0.0	0.0	0.0	0.5	[redacted]	[redacted]
13	0	-0.1	0.3	-0.1	0.0	0.0	0.0	0.4	[redacted]	[redacted]
14	10	-0.3	0.2	-0.2	0.0	0.0	0.0	0.5	[redacted]	[redacted]
15	0	-0.1	0.3	-0.1	0.0	0.0	0.0	0.4	[redacted]	[redacted]
16	90	0.0	0.0	0.0	0.1	0.0	0.0	0.2	[redacted]	[redacted]
17	90	0.0	0.0	0.0	0.1	0.0	0.0	0.2	[redacted]	[redacted]
18	180	0.0	-0.1	0.0	0.0	0.0	0.0	0.1	[redacted]	[redacted]
19	180	0.0	-0.1	0.0	0.0	0.0	0.0	0.1	[redacted]	[redacted]
20	180	0.0	-0.1	0.0	0.0	0.0	0.0	0.1	[redacted]	[redacted]
21	180	0.0	-0.1	-0.1	0.0	0.0	0.0	0.1	[redacted]	[redacted]
22	70	0.0	0.0	0.0	-0.1	0.0	0.0	0.2	[redacted]	[redacted]
23	0	0.0	-0.1	-0.2	0.0	0.0	0.0	0.2	[redacted]	[redacted]
24	90	0.0	0.0	0.0	0.1	0.0	0.0	0.1	[redacted]	[redacted]
25	90	0.0	0.0	0.0	0.1	0.0	0.0	0.1	[redacted]	[redacted]
26	90	0.0	0.0	0.0	0.0	0.0	0.0	0.1	[redacted]	[redacted]
27	180	0.0	-0.1	0.0	0.0	0.0	0.0	0.1	[redacted]	[redacted]
28	180	0.0	-0.1	0.0	0.0	0.0	0.0	0.1	[redacted]	[redacted]
29	180	0.0	-0.1	0.0	0.0	0.0	0.0	0.1	[redacted]	[redacted]
30	90	0.0	0.0	0.0	0.0	0.0	0.0	0.1	[redacted]	[redacted]
31	90	0.0	0.0	0.0	0.0	0.0	0.0	0.1	[redacted]	[redacted]
32	90	0.0	0.0	0.0	-0.1	0.0	0.0	0.2	[redacted]	[redacted]
33	105	-0.1	0.0	0.0	-0.1	0.0	-0.1	0.3	[redacted]	[redacted]
34	180	0.0	0.2	0.1	0.0	0.0	0.0	0.2	[redacted]	[redacted]
35	90	-0.1	0.0	0.0	-0.1	0.0	0.0	0.2	[redacted]	[redacted]
36	0	-0.1	0.1	-0.3	0.0	0.0	0.0	0.3	[redacted]	[redacted]
37	0	-0.2	0.0	0.0	0.0	0.0	0.0	0.2	[redacted]	[redacted]
38	0	-0.2	0.0	-0.1	0.0	0.0	0.0	0.2	[redacted]	[redacted]
39	0	0.1	0.0	-0.1	0.1	0.0	0.0	0.2	[redacted]	[redacted]
40	0	0.2	-0.2	-0.1	0.1	0.0	0.0	0.4	[redacted]	[redacted]
41	0	-0.1	0.1	-0.2	-0.1	0.0	0.0	0.3	[redacted]	[redacted]

Table 2.6.2.3-4 P_m Stresses—1-g Gravity Load*: Cold (-40°F)

Section	Angle	Cylindrical Stress Components (ksi)						SI (ksi)	Allowable Stress (ksi)	MS
		S_X	S_Y	S_Z	S_{XY}	S_{YZ}	S_{XZ}			
1	0	-0.1	0	0	0	0	0	0.1	20	174.28
2	0	-0.1	-0.1	0	0	0	0	0.1	20	159.51
3	30	-0.1	-0.2	0	0	0	0	0.2	20	127.21
4	10	-0.2	-0.3	-0.1	0	0	-0.1	0.3	20	71.02
5	0	-0.1	-0.1	0	0	0	0	0.1	20	141.45
6	0	-0.2	-0.2	0	0	0	0	0.2	20	94.15
7	0	-0.2	-0.3	0.1	0	0	0	0.4	20	48.19
8	10	-0.1	-0.4	0	0	0	-0.1	0.4	20	46.8
9	0	-0.3	-0.5	0	0	0	0.1	0.5	20	41.17
10	0	-0.2	-0.6	-0.4	0	0	0	0.3	19.1	56.8
11	0	-0.3	-0.7	-0.7	0	0	0.1	0.4	19.1	48.38
12	0	-0.4	-0.4	0.5	0	0	0	0.9	19.1	20.28
13	0	-0.3	-0.3	0.7	0	0	0.1	1	19.1	18.98
14	0	-0.4	-0.5	-0.1	0	0	-0.1	0.5	19.7	40.11
15	0	-0.2	-0.5	-0.1	0	0	0.1	0.5	19.7	39.56
16	60	0	0	0	0	-0.2	0	0.3	19.7	55.68
17	0	0	0.1	0.3	0	0	0	0.4	19.7	55.13
18	0	0	0.1	0.4	0	0	0	0.4	19.7	44.84
19	0	0	0.1	0.5	0	0	0	0.5	19.7	41.42
20	0	0	0.1	0.5	0	0	0	0.5	19.7	41.96
21	0	0	0.1	0.4	0	0	0	0.4	19.7	48.01
22	40	0	0.3	0.2	0	0.1	0	0.4	19.7	47.6
23	40	0	-0.1	0	0	-0.2	0	0.4	19.1	50.73
24	50	0	0	0	0	-0.2	0	0.4	19.1	52.56
25	0	0	0.1	0.3	0	0	0	0.3	19.1	63.23
26	0	0	0.1	0.4	0	0	0	0.4	19.1	49.04
27	0	0	0.1	0.4	0	0	0	0.4	19.1	45.45
28	0	0	0.1	0.4	0	0	0	0.4	19.1	48.69
29	0	0	0.1	0.3	0	0	0	0.3	19.1	62.06
30	60	0	0	0	0	0.2	0	0.4	19.1	51.33
31	50	0	0.5	0	0	0.3	0	0.7	19.1	25.22
32	60	0	0.6	0	0	0.2	0.1	0.7	20	25.85
33	60	-0.4	0.7	0.1	-0.1	0.1	0.1	1.1	20	17.26
34	60	0.3	1	-0.2	0	0.3	0.1	1.3	20	14.17
35	70	-0.2	0.7	-0.1	0	0.2	0.3	1.2	20	15.98
36	180	1.1	1.6	-0.2	0.1	0	0.3	1.9	20	9.43
37	0	-0.4	-0.3	0	0	0	0	0.4	20	51.41
38	180	-0.4	-0.3	0	0	0	0	0.4	20	51.53
39	80	-0.3	-0.4	-0.8	0.1	0	-0.1	0.6	20	33.72
40	80	-1.6	-2	-3.4	0.1	0	-1.2	3	20	6.64
41	0	-0.2	-0.1	0	0	0	0	0.2	20	96.75

* Including cask lid bolt preload.

Table 2.6.2.3-5 $P_m + P_b$ Stresses—1-g Gravity Load*; Cold (-40°F)

Section	Angle	Cylindrical Stress Components (ksi)						SI (ksi)	Allowable Stress (ksi)	MS
		S_X	S_Y	S_Z	S_{XY}	S_{YZ}	S_{XZ}			
1	180	-0.1	0.1	0	0	0	0	0.2	30	149.45
2	20	-0.2	-0.2	0	0	0	0	0.2	30	152.69
3	30	-0.2	-0.2	0	0	0	0	0.3	30	118
4	10	-0.3	-0.3	-0.1	0	0	-0.1	0.3	30	99.67
5	0	-0.2	-0.2	0	0	0	0	0.2	30	143.72
6	0	-0.2	-0.3	0	0	0	0	0.3	30	98.57
7	0	-0.2	-0.3	0.3	0	0	0	0.6	30	49.13
8	0	-0.1	-0.2	0.5	0	0	-0.1	0.8	30	38.62
9	0	0.1	-0.1	0.9	0	0	0	1	30	28.82
10	0	-0.1	-0.5	-0.4	0	0	-0.1	0.4	28.7	69.04
11	0	0.1	-0.5	-0.5	0	0	0	0.6	28.7	47.89
12	0	-0.6	-0.4	0.4	0	0	0	1	28.7	26.6
13	0	-0.7	-0.4	0.5	0	0	0	1.2	28.7	23.39
14	0	-0.5	-0.4	0.5	0	0	0	1.1	29.6	27.02
15	0	0.1	-0.1	0.9	0	0	0.1	1	29.6	27.73
16	50	0	0.2	0.1	0	-0.2	0	0.5	19.7	40.89
17	0	0	0.4	0.5	0	0	0	0.5	19.7	38.44
18	0	0	0.5	0.6	-0.1	0	0	0.6	19.7	31.52
19	0	0	-0.4	0.3	0	0	0	0.7	19.7	29.11
20	0	0	0.5	0.6	-0.1	0	0	0.6	19.7	30.07
21	0	0	0.4	0.5	0	0	0	0.6	19.7	34.83
22	40	0	0.4	0.3	0	0.2	0	0.6	29.6	47.38
23	30	0	-0.2	0.1	0	-0.3	0	0.6	28.7	48.69
24	40	0	0.1	0.1	0	-0.2	0	0.5	19.1	38.1
25	0	0	0.4	0.4	0	0	0	0.5	19.1	41.19
26	0	0	-0.4	0.2	0	0	0	0.6	19.1	33.53
27	0	0	-0.4	0.2	0	0	0	0.6	19.1	30.74
28	0	0	-0.4	0.2	0	0	0	0.6	19.1	32.46
29	0	0	0.5	0.4	0	0	0	0.5	19.1	36.7
30	50	0	0.2	0.1	0	0.2	0	0.5	19.1	39.29
31	40	0	0.6	0.1	0	0.4	0	0.9	28.7	32.45
32	50	0	0.6	-0.3	0	0.2	0	1	30	30.11
33	70	-0.8	0.4	-0.6	-0.2	0.3	0.1	1.4	30	20.07
34	50	0	0.6	-1.4	0	0.3	-0.1	2.1	30	13.3
35	70	-0.3	0.5	-1.1	0	0.4	1.5	3.2	30	8.25
36	180	-0.4	0.7	-2	0.1	0	0.1	2.7	30	10.21
37	0	-3.8	-3.6	0	0	0	0	3.8	30	6.92
38	30	-4	-3.8	-0.1	0	0	0	3.9	30	6.67
39	70	3.5	2.7	-1.1	0	0	0	4.7	30	5.41
40	0	-3.2	-6.4	-9.9	0.2	-0.1	0.4	6.7	30	3.49
41	0	-0.3	-0.2	0	0	0	0	0.3	30	109.17

* Including cask lid bolt preload.

2.6.3 Reduced External Pressure

The drop in atmospheric pressure to 3.5 psia, as specified in 10 CFR 71.71(c)(3), effectively results in an additional internal pressure in the cask of 11.2 psig (14.7 -3.5 = 11.2). However, stresses are conservatively calculated for a 150 psig internal pressure as presented in Section 2.6.1.3. The maximum stress intensities in the cask due to the 150 psig pressure plus gravity are calculated to be a primary membrane stress of 12.7 ksi with a margin of safety of +0.6 and a primary membrane plus bending stress of 21.6 ksi with a margin of safety of +0.4. Therefore, the requirements of 10 CFR 71.71(c)(3) are met.

2.6.4 Increased External Pressure

An increased external pressure of 20 psia (5.3 psig external pressure), as specified in 10 CFR 71.71(c)(4), has a negligible effect on the Universal Transport Cask because of the thick outer shell and end closures of the cask. Conservatively, applying a 20 psig external pressure to the neutron shield shell produces a compressive hoop stress. With a radius of 46.055 in. (cask outer radius of 82.61/2 plus 4.75 in. to outer neutron shell) and a thickness of 0.25 in., the calculated hoop stress is 3,685 psi. This stress is low compared to the material strength and will result in no adverse impact on the performance of the cask. Based on these observations, the requirements of 10 CFR 71.71 (c)(4) are met.

2.6.5 Vibration

The effect of vibrations normally incident to transportation is considered to be negligible for the Universal Transport Cask. This conclusion is based on the following factors:

1. The minimum natural frequency of the cask is conservatively calculated as 228 Hertz [28] (Table 36, Case 4a). The determination of this natural frequency is made considering only the stiffness of the cask outer shell and the total cask weight of 159,898 lb for the case of a free cylinder. The most significant periodic impulse load occurs as the two closest rail car wheels pass over a rail junction. A maximum speed for rail transportation of 140 miles/hour or 205 feet/second [56] is very conservatively assumed. The duration between pulses is 0.024 seconds, which corresponds to a frequency of 1/0.024 = 42 hertz. This is significantly below the fundamental frequency of the cask. Consequently vibrational excitation is considered to be insignificant.

2. The calculated stresses due to vibrations normally incident to transportation are much smaller than the calculated stresses for the normal transport 1-ft drop event.

The following analysis documents the second factor mentioned above.

It is conservatively assumed that the normal transport vibration acceleration is equal to the equivalent acceleration which will produce the normal vertical loading imposed on the tiedown devices by 10 CFR 71.45 (b)(1). This regulation specifies a load factor of 2.0 to be applied to the package weight; therefore, it is assumed that the tiedown devices and the cask must resist an imposed 2.0 g vibration acceleration. From the 1-*g* stress evaluation presented in Section 2.6.1.3, the peak stress produced in the cask is 6,700 psi. Scaling the stress for 2 *g*, the maximum stress intensity is 13,400 psi.

The maximum stress intensity range for normal transport vibration is obtained by multiplying the maximum stress intensity from the 1g normal condition by the acceleration values from vibration . Thus the maximum stress intensity in the cask for the 2 *g* loading is S_{max} = 13,400 psi and S_{min} = -13,400 psi. The allowable alternating stress intensity for austenitic stainless steel is determined as the 10^{11} cycle value from the ASME Boiler and Pressure Vessel Code, Section III, Appendices, Table I-9.2.2 [17]. This value is S_a = 23,700 psi; therefore, the margin of safety for the critical component of the Universal Transport Cask for normal transport vibration is:

$$MS = (S_a/S_{alt}) - 1 = (23{,}700/13{,}400) - 1 = +0.77$$

where S_{alt} = ½ of the total applied stress range.

The rotation pockets serve as the rear tiedown for the Universal Transport Cask during normal transport. The rotation pocket is the critical tiedown component for all three load axes; the front of the cask is supported in a cradle and restrained vertically by a band attached to the cradle. The critical component on the rotation pocket is the attachment weld between the pocket and the cask outer shell, which has a maximum shear stress of 28,546 psi. This shear stress is produced by the 10.2 *g* resultant from the combined longitudinal and vertical shock (10.0 *g* longitudinal and 2.0 *g* vertical) tiedown load components (Section 2.5.2).

The ratio of the normal transport vibration acceleration to the resultant acceleration for the combined longitudinal and vertical shock is used to ratio the stresses. The alternating shear stresses are S_{max} = (2.0/10.2)(28,546) = 5,597 psi and S_{min} = -(2.0/10.2)(28,546) = -5,597 psi. The margin of safety for the rotation pocket as a rear tiedown device for normal transport is:

$$MS = (S_a/S_{alt}) - 1 = (23,700/5,597) - 1 = +3.2$$

Therefore, the Universal Transport Cask satisfies the requirements for normal vibration incident to transportation as required by 10 CFR 71.71(c)(5).

2.6.6 Water Spray

Water causes negligible corrosion of the stainless shell of the Universal Transport Cask, and the cask contents are protected in the sealed cavity. A water spray as specified in 10 CFR 71.71(c)(6) has no adverse impact on the package. The cask surface temperature specified during the water spray is between 100°F and -20°F. Consequently, the induced thermal stress in the cask components is less than the thermal stresses that occur during the extreme temperature conditions for normal transport. Therefore, the requirements of 10 CFR 71.71(c)(6) are satisfied.

2.6.7 Free Drop (1-Foot): Cask Body Analysis

The free drop scenario outlined by 10 CFR 71.71(c)(7) requires the Universal Transport Cask to be structurally adequate for a 1-ft drop (normal conditions of transport) onto a flat, essentially unyielding horizontal surface in the orientation that inflicts the maximum damage to the cask. In the following subsections, the cask body, impact limiters, closure lid and bolts, neutron shield shell, and upper ring components are evaluated for the end, side, and corner-drop orientations.

Evaluation of each drop orientation is accomplished by using finite element analysis techniques. A complete description of the 3D model used to analyze the cask body is presented in Appendix 2.10.2. Appendix 2.10.2 also describes the loadings applied to the finite element model, the thermal conditions considered, and the locations of the sections on the cask body that are evaluated. The results of each drop orientation listed above are presented in this section. The impact limiters and the impact limiter attachments are evaluated in Section 2.6.7.5 for all loading conditions and orientations.

The analysis is performed using a 20g acceleration for the end and side drops. Using a 20g acceleration provides a bounding analysis, as it exceeds the calculated g-loads for the end and side drop events shown in Table 2.6.7.5-3.

For normal conditions, the one-ft drop is not a sufficient height to rotate the cask to an oblique orientation following a drop. Therefore, oblique drop orientations are not considered a credible event, and are not included in these analyses.

Only the analyses for enveloping structural conditions, representing the more restrictive of either the PWR or BWR fuel payload configuration are presented. Where necessary, a composite payload of the PWR configuration decay heat load and the BWR configuration weight is used for the cask body analysis. This composite configuration imposes larger impact loads on the cask components and raises the component temperatures, thereby lowering the material strength, resulting in a more restrictive loading configuration than either the PWR or BWR payload configurations would impose.

2.6.7.1 One-Foot End Drop

In accordance with the requirements of 10 CFR 71.71, the Universal Transport Cask is structurally evaluated for the normal condition of transport 1-ft end-drop. In this event, the cask (equipped with an impact limiter over each end) falls a distance of 1 ft onto a flat, unyielding, horizontal surface. The cask strikes the surface in a vertical position; consequently, an end impact on the bottom end or top end of the cask occurs. **The analysis is performed using a 20g acceleration, which provides a bounding analysis as it exceeds the calculated g-loads for the end drop event shown in Table 2.6.7.5-3.**

Stress results for the 1-ft top-and bottom-end-drop combined loading are documented in Tables 2.6.7.1-1 through 2.6.7.1-16. These tables document the primary membrane (P_m), primary membrane plus primary bending ($P_m + P_b$), primary membrane plus primary bending plus secondary peak stress (P + Q), and critical (P_m, $P_m + P_b$, and P + Q) stresses in accordance with the criteria presented in Regulatory Guide 7.6.

As shown in Tables 2.6.7.1-1 through 2.6.7.1-8, the margins of safety for the primary stress intensity category are positive for all of the 1-ft top-end-drop conditions. The most critically stressed component in the system is the top forging for the top-end-drop. The minimum margin of safety for P_m stress intensity for the top-end-drop condition is found to be 1.66 as documented in Table 2.6.7.1-5. The minimum margin of safety for $P_m + P_b$ stress intensity for the top-end-drop condition is found to be 1.17, as documented in Table 2.6.7.1-6. The minimum margin of safety for the P + Q stresses (2.43) occurs in the inner shell, as documented in Table 2.6.7.1-8.

As shown in Tables 2.6.7.1-9 through 2.6.7.1-16, the margins of safety for the primary stress intensity category are positive for all of the 1-ft bottom-end-drop conditions. The most critically stressed components in the system are the cask body ligaments for the bottom-end-drop. The minimum margin of safety for P_m stress intensity for the bottom end-drop condition is found to be **0.74**, as documented in Table 2.6.7.1-13. The minimum margin of safety for $P_m + P_b$ stress intensity for the bottom-end-drop condition is found to be **1.29**, as documented in Table 2.6.7.1-14. The minimum margin of safety for the P + Q stresses (**2.49**) occurs in the inner shell as documented in Table 2.6.7.1-16.

Because the margins of safety are all positive, the Universal Transport Cask satisfies the requirements of 10 CFR 71.71(c)(7) for the 1-ft end-drop (normal transport) condition.

Table 2.6.7.1-1 P_m Stresses—1-Foot Top End-Drop, Bolt Preload, Internal Pressure

Section	Angle	Cylindrical Stress Components (ksi)						SI (ksi)	Allowable Stress (ksi)	MS
		S_X	S_Y	S_Z	S_{XY}	S_{YZ}	S_{XZ}			
1	70	0.3	0.3	0	0	0	0.1	0.4	20	44.31
2	180	0.3	0.3	0	0	0	0.1	0.4	20	48.47
3	180	0.2	0.4	0.2	0	0	0.2	0.4	20	48.37
4	180	0.3	0.2	0.3	0	0	0.3	0.6	20	35.02
5	180	-0.1	-0.1	-0.2	0	0	0	0.1	20	157.23
6	80	-0.1	-0.1	-0.1	0	0	0.1	0.2	20	92.5
7	0	-0.1	0.1	0.5	0	0	0.1	0.7	20	28.2
8	180	1.1	0	-0.2	-0.1	0	0.4	1.5	20	12.06
9	105	-0.7	-0.6	-0.2	-0.1	0.1	0.4	0.9	20	21.26
10	135	0.8	-0.5	-1.6	-0.1	0	0.6	2.7	19.1	6.1
11	135	0.2	-1.1	-2.8	-0.1	0.1	0.6	3.3	19.1	4.85
12	80	0.2	0.1	0.8	-0.1	0	0	0.8	19.1	24.3
13	80	0.7	0.4	1.4	-0.1	-0.1	0.1	1	19.1	17.24
14	135	-0.2	-0.1	0.5	0	0	-0.2	0.8	19.7	24.06
15	80	0.6	0.1	0.5	-0.1	-0.1	0.1	0.6	19.7	33.05
16	0	0	1	0.1	-0.1	0	0	1	19.7	18.04
17	0	0	1.3	-0.1	-0.1	0	0	1.5	19.7	12.58
18	0	-0.1	1.6	-0.3	-0.2	0	0	1.9	19.7	9.33
19	0	-0.1	2	-0.5	-0.2	0	0	2.5	19.7	6.79
20	0	-0.1	2.8	-0.8	-0.3	0	0	3.7	19.7	4.39
21	0	-0.1	4.1	-1.2	-0.4	0	0	5.3	19.7	2.72
22	0	-0.2	5.6	-1.8	-0.6	0	0.1	7.4	19.7	1.66
23	105	-0.1	0.2	-0.6	0	0.2	0.2	1	19.1	18.69
24	120	-0.1	1.5	-0.7	0	0.1	0	2.2	19.1	7.59
25	0	-0.1	1.1	-0.9	-0.1	0	0	2	19.1	8.44
26	0	-0.2	0.9	-1.2	-0.1	0	0	2.1	19.1	8.06
27	0	-0.2	0.7	-1.5	0	0	0	2.2	19.1	7.82
28	0	-0.2	0	-1.7	0.1	0	0	1.7	19.1	10.23
29	10	-0.2	-1.2	-1.9	0	0	0	1.7	19.1	10.2
30	20	-0.2	-2.8	-1.9	0	-0.1	0	2.6	19.1	6.41
31	90	-0.4	-3	-1.7	0.1	-0.5	0.1	2.8	19.1	5.87
32	0	-0.3	4.3	-2	-0.5	0	-0.3	6.4	20	2.1
33	0	1.1	2.9	-1.9	-0.2	0	-0.6	5	20	3.02
34	0	3.4	3.3	-3.1	-0.1	0.1	1.2	7	20	1.87
35	180	-0.6	1.5	-2.1	0.3	-0.2	0.2	3.8	20	4.31
36	0	1.5	1	-3.2	0	0.3	0.1	4.8	20	3.18
37	0	-0.3	-0.2	-1.2	0	0.2	0.6	1.4	20	12.85
38	0	-0.3	-0.2	-1.1	0	0.2	0.5	1.3	20	14.86
39	0	-0.1	-0.5	-3.1	0	0.1	0.2	3	20	5.7
40	0	-2	-2	-6.2	0	-0.1	-1.2	4.8	20	3.15
41	135	-0.2	-0.2	-0.6	0	0	0.2	0.5	20	40.25

Table 2.6.7.1-2 $P_m + P_b$ Stresses—1-Foot Top End-Drop, Bolt Preload, Internal Pressure

Section	Angle	Cylindrical Stress Components (ksi)						SI (ksi)	Allowable Stress (ksi)	MS
		S_X	S_Y	S_Z	S_{XY}	S_{YZ}	S_{XZ}			
1	70	1.4	1.8	0	0	0	0.1	1.8	30	15.46
2	180	0.4	1	0	0.1	0	0.1	1.1	30	27.25
3	180	0.7	0.5	0.7	0	0	0.5	0.9	30	31.7
4	180	0.6	0.5	0.6	0	-0.1	0.5	1	30	27.87
5	180	1.3	1	-0.2	0	0	0	1.4	30	19.94
6	120	0.7	1	0	0	0	0.1	1.1	30	27.04
7	0	-1.8	-0.4	-0.3	-0.1	0	0.1	1.6	30	18.24
8	135	0.3	-0.9	-2.5	-0.1	0	0.4	3	30	8.96
9	135	0.3	0.7	3.4	0	0.1	0.1	3.1	30	8.58
10	135	1.6	0	-1	-0.1	0	0.5	2.8	28.7	9.25
11	135	2	-0.2	-2.1	-0.1	0	0.7	4.3	28.7	5.7
12	105	-0.7	-0.2	0.4	-0.1	0	-0.1	1.1	28.7	23.98
13	120	-0.6	-0.1	1	-0.1	0	0.1	1.6	28.7	16.74
14	180	-0.4	-0.1	0.7	0	0.1	-0.2	1.3	29.6	22.42
15	80	1.5	0.7	1.6	-0.1	-0.2	0.2	1.2	29.6	24.18
16	20	-0.1	1	0	0	-0.1	0	1.1	29.6	25.85
17	20	-0.1	1.5	-0.1	0	0	0	1.6	29.6	18.08
18	30	-0.1	1.8	-0.2	0	0	0	2	29.6	13.45
19	0	0	2.2	-0.5	-0.2	0	0	2.7	29.6	9.91
20	20	-0.2	3.2	-0.7	0	0	0	3.9	29.6	6.66
21	0	0	4.3	-1.2	-0.4	0	0	5.5	29.6	4.36
22	10	-0.3	5.1	-3.8	0	0.1	0.1	8.9	29.6	2.32
23	80	-0.1	0.3	-0.6	0	0.2	0.1	1	28.7	27.23
24	180	-0.2	1.7	-0.7	0.2	0	0	2.5	28.7	10.56
25	0	-0.2	1.5	-0.8	-0.1	0	0	2.3	28.7	11.71
26	0	-0.2	1.4	-1.1	-0.1	0	0	2.4	28.7	10.78
27	0	-0.2	1.3	-1.3	-0.1	0	0	2.6	28.7	9.99
28	0	-0.3	0.6	-1.5	0	0	0	2.2	28.7	12.27
29	0	-0.3	-1.9	-2.1	0.2	0	0	1.9	28.7	14.24
30	20	-0.1	-3.3	-2.3	0	-0.1	0	3.2	28.7	8.08
31	0	-0.6	-4.6	-6.3	0.4	0.1	0.2	5.8	28.7	3.95
32	0	-0.6	4	-3.2	-0.5	0	-0.2	7.2	30	3.14
33	0	-0.5	1.7	-4.2	-0.2	0	-0.4	6	30	4.04
34	0	-0.2	-0.9	-14	0	-0.1	-0.3	13.8	30	1.17
35	0	-1	1.4	-3.3	-0.2	0.2	1.2	5.3	30	4.63
36	0	-0.7	-0.3	-5.9	0	0.4	0.1	5.6	30	4.35
37	10	1	2.9	-0.8	0	0.1	0.6	3.8	30	6.91
38	0	2.7	0.1	-1.3	0.2	0.3	0.5	4.3	30	6.05
39	0	4.8	1.4	-2.9	0.2	0.2	-0.2	7.7	30	2.88
40	0	-4.6	-5.4	-13.4	0	0	-0.1	8.7	30	2.43
41	135	0.1	-0.3	-1.1	0	0	0.2	1.2	30	23.27

Table 2.6.7.1-3 $P_m + P_b + Q$ Stresses—1-Foot Top End-Drop, Bolt Preload, Internal Pressure, Thermal Hot

Section	Angle	Cylindrical Stress Components (ksi)							Allowable Stress	
		S_X	S_Y	S_Z	S_{XY}	S_{YZ}	S_{XZ}	SI (ksi)	(ksi)	MS
1	80	5.8	4.4	0	0.3	0	0	5.8	60	9.28
2	0	4	5.2	-0.1	-0.1	0.1	0	5.3	60	10.41
3	10	-3.2	3.2	-0.1	0.1	0	0.2	6.5	60	8.28
4	0	7	-0.9	-4.4	0.3	0.6	-0.5	11.6	60	4.15
5	0	-4.7	-1.8	-0.5	-0.9	0.2	-0.2	4.5	60	12.2
6	0	-1.8	-0.1	-0.3	-0.2	0	0.1	1.7	60	33.7
7	0	-1.7	-0.3	-3.4	-0.1	-0.1	-0.8	3.5	60	15.99
8	0	-1.7	-0.3	-3.4	-0.1	-0.1	-0.8	3.5	60	15.99
9	40	-1.3	-0.5	-3	-1	1.3	0.4	4.3	60	13.08
10	0	-0.8	0.1	-3.3	-0.2	-0.2	-0.1	3.5	57.4	15.38
11	40	-1.3	-0.5	-3	-1	1.3	0.4	4.3	57.4	12.46
12	0	-0.6	2	4.5	-0.3	0.1	-0.2	5.2	57.4	10.11
13	0	-0.7	1.3	2.1	-0.3	0.1	-0.2	2.9	57.4	19.05
14	0	-0.6	2	4.5	-0.3	0.1	-0.2	5.2	59.1	10.45
15	90	-0.1	1.8	2.6	-0.1	-0.3	0	2.8	59.1	20.38
16	0	-0.1	3.4	1.7	-0.3	0.1	0.1	3.6	59.1	15.5
17	0	-0.1	5.3	3	-0.5	0.1	0	5.5	59.1	9.66
18	0	-0.2	5.9	2.7	-0.6	0	0	6.2	59.1	8.48
19	0	-0.2	6.5	2.3	-0.7	0	0	6.8	59.1	7.74
20	0	-0.2	7.4	2.1	-0.7	0	0	7.7	59.1	6.64
21	0	-0.2	8.4	1.4	-0.8	0	0	8.8	59.1	5.75
22	0	-0.2	8.7	1.4	-0.8	-0.1	0	9	59.1	5.55
23	0	-0.2	0.1	-5	0	0.2	0	5.2	57.4	10.08
24	0	-0.9	0.8	-6.6	-0.1	0.5	0	7.5	57.4	6.63
25	0	-0.3	-3.1	-12.7	0.3	0.3	0	12.5	57.4	3.59
26	0	-0.4	-3.6	-14.8	0.4	0.1	0	14.4	57.4	2.97
27	0	-0.3	-3.2	-15.2	0.4	0.1	0	15	57.4	2.83
28	0	-0.3	-4	-15.5	0.4	0	0	15.3	57.4	2.76
29	0	-0.6	-5.8	-15.8	0.6	-0.1	0	15.3	57.4	2.75
30	0	-0.6	-7.4	-14.6	0.7	-0.2	0	14	57.4	3.1
31	0	-1.5	-7	-14.2	0.5	-0.5	0	12.8	57.4	3.48
32	0	-0.2	5.4	-2.4	-0.6	0.1	-0.7	8.1	60	6.37
33	0	0.3	3	-6	-0.3	-0.1	-0.6	9	60	5.66
34	0	0.4	-2.5	-16.8	0.2	-0.5	0.4	17.2	60	2.49
35	0	-0.2	-0.8	-12.4	0.1	0.1	0.6	12.3	60	3.86
36	0	5.7	4.1	-2.3	0.1	0.2	0.2	8	60	6.48
37	10	-3.1	-4.5	-0.8	-0.2	0.2	0.4	3.8	60	14.79
38	135	-5.8	-2.6	-0.7	0.3	0	0.2	5.1	60	10.67
39	0	1.3	-2.9	-15.7	0.4	0.3	0.5	17.1	60	2.5
40	0	0.1	-2.4	-13.8	0.3	0.2	0.1	13.9	60	3.3
41	0	-0.2	2.8	6.3	-0.3	0.2	0.1	6.6	60	8.13

Table 2.6.7.1-4 $P_m + P_b + Q$ Stresses—1-Foot Top End-Drop, Bolt Preload, Internal Pressure, Thermal Cold

		Cylindrical Stress Components (ksi)							Allowable Stress	
Section	Angle	S_X	S_Y	S_Z	S_{XY}	S_{YZ}	S_{XZ}	SI (ksi)	(ksi)	MS
1	0	0.7	3.4	-0.1	-0.4	-0.1	0.2	3.5	60	15.99
2	0	1.3	2.9	0	-0.1	0	0.1	3	60	19.28
3	10	-4.2	1.8	-0.4	0.3	0	0.4	6.1	60	8.9
4	0	11.6	-0.7	-1.2	0.5	1	-1.1	13.9	60	3.33
5	0	-3.3	-2.3	-0.3	-0.4	0.1	-0.1	3.2	60	17.77
6	135	-2.4	-2.3	-0.3	0.3	0	0	2.4	60	24.06
7	180	-2	0.5	-0.5	0.3	0	0.2	2.6	60	21.87
8	30	0.3	-0.9	-3.6	-0.7	0.6	1.7	5.4	60	10.05
9	40	-4.3	-3.4	-6.6	-1	1.4	1.1	5.1	60	10.79
10	30	0.3	-0.9	-3.6	-0.7	0.6	1.7	5.4	57.4	9.56
11	30	0.3	-0.9	-3.6	-0.7	0.6	1.7	5.4	57.4	9.56
12	10	-3.8	-0.1	1.5	-0.2	0.3	0.4	5.4	57.4	9.62
13	10	-0.2	1.1	2.5	-0.2	0.2	0.8	3.2	57.4	17.16
14	10	-3.8	-0.1	1.5	-0.2	0.3	0.4	5.4	59.1	9.95
15	40	4.2	2.5	4.1	-0.6	-0.3	0.6	2.6	59.1	21.39
16	0	-0.1	3.3	1.7	-0.3	0.1	0.1	3.5	59.1	16.08
17	0	-0.1	5.4	2.8	-0.5	0.1	0	5.6	59.1	9.58
18	0	-0.2	6.1	2.5	-0.6	0	0	6.4	59.1	8.3
19	0	-0.2	6.6	2.1	-0.7	0	0	6.9	59.1	7.57
20	0	-0.2	7.5	1.8	-0.7	0	0	7.8	59.1	6.58
21	0	-0.2	8.4	1.2	-0.8	-0.1	0	8.7	59.1	5.77
22	0	-0.5	4.2	-4.6	-0.5	0.1	-0.1	8.8	59.1	5.73
23	0	-0.2	-0.7	-5.5	0.1	0.3	0.1	5.3	57.4	9.9
24	0	-1	1.6	-6.7	-0.2	0.6	0	8.4	57.4	5.85
25	0	-0.3	-3.4	-14	0.3	0.3	0	13.8	57.4	3.17
26	0	-0.4	-3.9	-16.2	0.4	0.2	0	15.8	57.4	2.62
27	0	-0.2	-3.5	-16.6	0.4	0.1	0	16.4	57.4	2.5
28	0	-0.3	-4.3	-17	0.5	0	0	16.7	57.4	2.43
29	0	-0.6	-6	-17.3	0.6	-0.1	0	16.7	57.4	2.43
30	0	-0.7	-7.6	-15.9	0.7	-0.3	0	15.3	57.4	2.75
31	0	-1.5	-6.6	-14.5	0.5	-0.6	0	13	57.4	3.41
32	0	-0.2	5.1	-3	-0.6	0.1	-0.7	8.4	60	6.17
33	0	0.3	3	-6	-0.3	-0.1	-0.6	9.1	60	5.59
34	0	0.3	-2.3	-16	0.2	-0.6	0.4	16.3	60	2.68
35	0	-0.2	-0.7	-12.3	0.1	0.1	0.6	12.2	60	3.93
36	0	6	4.5	-1.8	0.1	0.2	0.4	7.9	60	6.61
37	10	-2.9	-4.2	-0.8	-0.1	0.2	0.4	3.5	60	16.04
38	135	-6	-2.9	-0.7	0.3	0	0.2	5.4	60	10.2
39	0	1.3	-2.4	-15.3	0.3	0.3	0.5	16.6	60	2.61
40	0	0	-2	-13.6	0.3	0.2	0	13.6	60	3.43
41	10	-0.7	1.6	3.2	0	0.3	0.3	4.0	60	13.86

Table 2.6.7.1-5 Critical P_m Stress Summary (ksi)—1-Foot Top End-Drop, Bolt Preload, Internal Pressure

Component	Section	Angle	SI (ksi)	Allowable Stress (ksi)	Margin of Safety
1	4	180	0.6	20	35.02
2	8	180	1.5	20.0	12.06
3	11	135	3.3	19.1	4.85
4	14	135	0.8	19.7	24.06
5	21	0	5.3	19.7	2.72
6	22	0	7.4	19.7	1.66
7	23	105	1	19.1	18.69
8	30	20	2.6	19.1	6.41
9	31	90	2.8	19.1	5.87
10	34	0	7	20	1.87
11	40	0	4.8	20	3.15
12	41	135	0.5	20	40.25

Table 2.6.7.1-6 Critical $P_m + P_b$ Stress Summary (ksi)—1-Foot Top End-Drop, Bolt Preload, Internal Pressure

Component	Section	Angle	SI (ksi)	Allowable Stress (ksi)	Margin of Safety
1	1	70	1.8	30	15.46
2	9	135	3.1	30	8.58
3	11	135	4.3	28.7	5.7
4	14	180	1.3	29.6	22.42
5	21	0	5.5	**29.6**	**4.36**
6	22	10	8.9	29.6	2.32
7	23	80	1	28.7	27.23
8	30	20	3.2	**28.7**	**8.08**
9	31	0	5.8	28.7	3.95
10	34	0	13.8	30	1.17
11	40	0	8.7	30	2.43
12	41	135	1.2	30	23.27

Table 2.6.7.1-7 Critical $P_m + P_b + Q$ Stress Summary (ksi)—1-Foot Top End-Drop, Bolt Preload, Internal Pressure, Impact, Thermal Hot

Component	Section	Angle	SI (ksi)	Allowable Stress (ksi)	Margin of Safety
1	4	0	11.6	60	4.15
2	5	0	4.5	60	12.2
3	12	0	5.2	57.4	10.11
4	14	0	5.2	59.1	10.45
5	21	0	8.8	59.1	5.75
6	22	0	9	59.1	5.55
7	23	0	5.2	57.4	10.08
8	29	0	15.3	57.4	2.75
9	31	0	12.8	57.4	3.48
10	34	0	17.2	60	2.49
11	39	0	17.1	60	2.5
12	41	0	6.6	60	8.13

Table 2.6.7.1-8 Critical $P_m + P_b + Q$ Stress Summary (ksi)—1-Foot Top End-Drop, Bolt Preload, Internal Pressure, Impact, Thermal Cold

Component	Section	Angle	SI (ksi)	Allowable Stress (ksi)	Margin of Safety
1	4	0	13.9	60	3.33
2	8	30	5.4	60	10.05
3	10	30	5.4	57.4	9.56
4	14	10	5.4	59.1	9.95
5	21	0	8.7	59.1	5.77
6	22	0	8.8	59.1	5.73
7	23	0	5.3	57.4	9.9
8	29	0	16.7	57.4	2.43
9	31	0	13	57.4	3.41
10	34	0	16.3	60	2.68
11	39	0	16.6	60	2.61
12	41	10	4	60	13.86

Table 2.6.7.1-9 P_m Stresses—1-Foot Bottom End-Drop, Bolt Preload, Internal Pressure

Section	Angle	Cylindrical Stress Components (ksi)						SI (ksi)	Allowable Stress (ksi)	Margin of Safety
		S_X	S_Y	S_Z	S_{XY}	S_{YZ}	S_{XZ}			
1	180	-0.3	-1	0.1	0.1	0	0	1.1	20	16.48
2	180	-0.1	-0.7	0.1	-0.2	0	0	0.8	20	23.91
3	180	0	-5	-1.1	-0.1	0.4	0	5	20	3
4	180	-1.1	-3.5	0	-0.2	0.5	-0.2	3.7	20	4.42
5	180	0.5	-0.9	0.7	0.6	0.3	0	2	20	9.13
6	0	0.6	-0.6	0.7	0	0.1	0	1.4	20	13.68
7	0	0.5	-1.5	0.4	0.7	0	0	2.5	20	7.03
8	180	1.2	-2.5	-0.1	-1.7	0	0.2	5	20	3
9	180	2.1	-2.9	-0.2	0.6	0.3	0.3	5.3	20	2.8
10	180	4	-2.5	0.8	-4.4	-0.2	0.5	11	19.1	0.74
11	180	6.2	-2.6	1.2	-0.3	0.3	0.7	8.9	19.1	1.14
12	180	3.3	-0.8	1.6	2.2	0.6	0.3	6.1	19.1	2.13
13	180	6.7	1.6	3.3	-0.8	0.4	0.5	5.5	19.1	2.49
14	180	0.8	-3.4	0.2	1.8	0.6	0.1	5.7	19.7	2.44
15	180	3.7	-3.4	1.1	-0.9	0.3	0.3	7.4	19.7	1.67
16	0	-0.1	-1.8	4	-0.1	0	0.4	5.8	19.7	2.38
17	0	-0.1	-1.5	2.6	0	0	0.3	4.1	19.7	3.82
18	0	-0.1	-1.3	1.8	0	0	0.2	3.1	19.7	5.33
19	0	0	-1.1	1.4	0	0	0.2	2.5	19.7	6.78
20	0	0	-1	1.2	0	0	0.1	2.2	19.7	7.95
21	0	0	-0.8	1	0	0	0.1	1.8	19.7	9.98
22	0	0	-0.6	1	0	0	0.1	1.6	19.7	11.1
23	90	-3	-1.7	-0.3	-0.4	0	0.1	2.8	19.1	5.9
24	0	-0.3	-2.1	-2.1	0	0	-0.2	1.9	19.1	9.06
25	0	-0.3	-2	-0.7	0	0	-0.1	1.8	19.1	9.74
26	0	-0.2	-1.9	0.3	0	0	0	2.2	19.1	7.8
27	0	-0.2	-1.7	0.9	0	0	0	2.6	19.1	6.33
28	0	-0.2	-1.5	1.1	0	0	0.1	2.6	19.1	6.47
29	0	-0.1	-1.3	1.2	0	0	0.1	2.5	19.1	6.76
30	0	-0.1	-1	1.4	0	0	0.1	2.4	19.1	6.96
31	0	-0.1	-0.8	2.1	0	0	0.2	2.9	19.1	5.6
32	0	0	-0.5	1.4	0.1	0	0.1	2	20	9.18
33	0	-0.6	-0.1	1.5	0.1	0	0.2	2.1	20	8.55
34	0	0	-0.8	2.1	0	0	0.2	2.9	20	5
35	0	0.1	-0.2	1.4	0.3	-0.1	0.1	1.8	20	9.86
36	80	1.2	-0.4	-0.1	0.1	-0.8	0.2	2.4	20	7.46
37	30	-0.2	0	-0.2	0.1	-0.1	0	0.4	20	56.13
38	70	-0.2	0	-0.2	0.1	-0.2	0	0.4	20	43.87
39	0	-0.2	-1.1	-0.4	0.2	0.1	0	1	20	19.91
40	80	0.9	1.6	-0.1	-0.4	1.7	0.1	3.9	20	4.06
41	180	-0.4	-4.8	-0.1	-0.4	0.1	-0.1	4.8	20	3.17

Table 2.6.7.1-10 $P_m + P_b$ Stresses—1-Foot Bottom End-Drop, Bolt Preload, Internal Pressure

Section	Angle	Cylindrical Stress Components (ksi)						SI (ksi)	Allowable Stress (ksi)	Margin of Safety
		S_X	S_Y	S_Z	S_{XY}	S_{YZ}	S_{XZ}			
1	180	0.1	-1.1	1.3	0	-0.1	-0.1	2.4	30	11.44
2	180	1.2	-0.7	1.6	-0.2	0	0.1	2.3	30	11.94
3	180	-2.1	-6.5	-1	-0.1	0.5	-0.2	5.6	30	4.32
4	180	-2.3	-6.6	-1.3	-0.1	0.5	-0.2	5.5	30	4.42
5	0	0.8	-0.5	4	-0.5	0.1	0.3	4.7	30	5.37
6	120	3.6	-0.4	4.4	0	0	1	5.5	30	4.46
7	0	1.9	-2.6	0.2	0.4	0	-0.1	4.6	30	5.57
8	180	1.6	-2.4	0	-3.3	-0.1	0.3	7.7	30	2.9
9	180	5	-1.3	1.1	1.2	0.3	0.5	6.9	30	3.36
10	180	5.8	0.4	2.3	-5.6	-0.2	0.5	12.5	28.7	1.29
11	180	5.2	-5.1	0.4	-2.6	0.3	0.7	11.6	28.7	1.47
12	180	2.9	-0.7	1.4	3.3	0.6	0.3	7.6	28.7	2.79
13	180	11.7	4	5.5	-2.4	0.4	0.8	9.3	28.7	2.08
14	0	-0.3	-6.9	-1.1	-0.9	0.3	-0.1	6.9	29.6	3.31
15	180	-1.8	-9.5	-2.2	0.3	0.2	0.1	7.8	29.6	2.79
16	20	0.3	-1.9	3.7	0	0.1	1.4	6.2	29.6	3.79
17	20	0.2	-1.3	2.5	0	0	1	4.3	29.6	5.95
18	20	0.1	-1.2	1.8	0	0	0.7	3.3	29.6	8.05
19	20	0.1	-1	1.4	0	0	0.6	2.7	29.6	10.11
20	20	0.1	-0.9	1.2	0	0	0.5	2.3	29.6	11.74
21	20	0.1	-0.7	1	0	0	0.4	1.9	29.6	14.74
22	0	0	-1	0.8	0	0	0.1	1.8	29.6	15.13
23	180	-0.6	-5.6	-4	0	0.3	0.5	5.1	28.7	4.59
24	0	-0.3	-2.1	-2.7	0	0	-0.3	2.5	28.7	10.67
25	180	-0.4	-1.4	0.7	0	0	0	2.1	28.7	12.94
26	0	-0.2	-1.7	0.9	0	0	0	2.6	28.7	9.97
27	0	-0.2	-1.6	1.5	0	0	0.1	3	28.7	8.47
28	0	-0.2	-1.3	1.5	0	0	0.1	2.9	28.7	8.92
29	0	-0.2	-1.1	1.6	0	0	0.1	2.7	28.7	9.51
30	0	-0.2	-0.9	1.7	0	0	0.1	2.6	28.7	10.12
31	0	-0.1	-1.1	2.1	0	0	0.2	3.3	28.7	7.78
32	0	0	-0.8	1.4	0.1	0	0.1	2.3	30	12.23
33	10	-1.3	-1.6	0.9	0.3	-0.1	0.4	2.7	30	9.94
34	0	-0.1	-1.6	1.9	-0.1	0	0.2	3.5	30	7.49
35	0	0.4	-1.8	1.3	1.7	-0.2	0.1	4.2	30	6.17
36	80	1.1	0.1	-0.7	0.3	-1.2	0.3	2.8	30	9.83
37	0	-2.1	0	-1.6	0.1	0	0	2.1	30	13.41
38	20	-3.4	-0.1	-2.7	0.1	0	0.3	3.4	30	7.77
39	0	3.8	-1.4	2.6	0	0.1	-0.2	5.3	30	4.68
40	10	1.7	7.2	4.3	-1.6	0.3	0.5	6.5	30	3.63
41	180	0.6	-6.4	-0.2	-0.9	0	0	7.3	30	3.14

Table 2.6.7.1-11 $P_m + P_b + Q$ Stresses—1-Foot Bottom End-Drop, Bolt Preload, Internal Pressure, Impact, Thermal Hot

Section	Angle	Cylindrical Stress Components (ksi)						SI (ksi)	Allowable Stress (ksi)	Margin of Safety
		S_X	S_Y	S_Z	S_{XY}	S_{YZ}	S_{XZ}			
1	0	-2.5	-1.2	3	-0.5	-0.3	1	5.9	60	9.09
2	180	0.2	-0.9	1.8	-0.1	0	-0.2	2.8	60	20.54
3	180	1.1	-5	1.8	-1	0.5	-0.2	7.1	60	7.48
4	0	-9.4	-0.8	3.9	1.3	1.1	0.7	13.8	60	3.34
5	0	-0.3	-1	6.2	-0.3	-0.3	1.2	7.5	60	6.97
6	180	-2.4	-0.7	1.6	0	-0.1	-0.5	4.1	60	13.77
7	0	-6.2	-14.7	-3.4	-2.4	0.2	0.3	12	60	1
8	0	-6.2	-14.7	-3.4	-2.4	0.2	0.3	12	60	1
9	0	-0.7	-17.6	-2.8	-1.5	0.2	-0.2	17.2	60	2.49
10	180	5.3	2.3	4.8	-4.1	0.3	-0.1	8.8	57.4	5.51
11	180	0.9	-2.2	2	-2.1	0.4	-0.2	5.6	57.4	9.27
12	180	2.1	0.3	3.4	2.1	0.4	-0.1	4.8	57.4	10.94
13	180	9.3	3.4	6.7	-2.1	0.6	0.1	7.4	57.4	6.77
14	0	0	-6.6	0.8	-0.8	0.2	0.1	7.5	59.1	6.93
15	0	-0.1	-8.4	0.5	0.2	0	0.1	8.9	59.1	5.67
16	0	-0.1	-0.4	6.5	0	-0.1	0.6	6.9	59.1	7.51
17	0	-0.2	1.4	6.6	0	0	0.7	6.9	59.1	7.55
18	0	-0.2	1.7	6.2	0	0	0.6	6.5	59.1	8.1
19	0	-0.2	1.8	5.8	0	0	0.6	6.1	59.1	8.67
20	0	-0.2	2	5.7	0	0	0.6	6	59.1	8.92
21	0	-0.2	2.2	5.2	0	0	0.5	5.4	59.1	9.89
22	0	-0.1	0.6	3.2	-0.2	0.1	0.3	3.4	59.1	16.42
23	0	-0.7	-9.8	-3.3	-0.3	0	-0.3	9.2	57.4	5.27
24	0	-0.4	-8.2	-3.5	0	-0.4	-0.4	7.9	57.4	6.29
25	0	-0.4	-13.9	-4.5	0	-0.2	-0.5	13.6	57.4	3.23
26	0	-0.4	-15.5	-4	0	-0.1	-0.4	15.1	57.4	2.8
27	0	-0.2	-15.4	-3	0	0	-0.3	15.2	57.4	2.78
28	0	-0.2	-15.3	-3.2	0	0	-0.3	15.1	57.4	2.81
29	0	-0.5	-15.1	-3.9	0	0.1	-0.4	14.7	57.4	2.91
30	0	-0.5	-13.1	-3.7	0	0.3	-0.3	12.7	57.4	3.51
31	0	-0.9	-7.7	-0.4	-0.1	0.6	0	7.4	57.4	6.72
32	0	-0.1	-1.4	1.9	-0.4	0	0.3	3.4	60	16.48
33	0	0.1	-1	2.5	0	0.1	0.2	3.5	60	16.02
34	0	-1	-5.8	-0.6	-0.9	0.4	0.2	5.5	60	9.94
35	0	0	-9.8	-0.9	0.5	0	-0.1	9.9	60	5.08
36	0	0	-1.6	2.9	0.4	-0.1	0.3	4.7	60	11.88
37	150	-3.6	0	-4.9	0	0	-0.4	5	60	11
38	70	-3.8	-0.1	-5.1	0.1	-0.1	0.7	5.3	60	10.4
39	0	-1.1	-1.6	2.9	-1.2	0.3	0.1	5.5	60	9.97
40	60	0.6	5.4	-3.2	-0.8	1.6	3.3	11.2	60	4.37
41	180	-0.2	-1.7	2.2	1.1	0.6	-0.3	4.8	60	11.57

Table 2.6.7.1-12 $P_m + P_b + Q$ Stresses—1-Foot Bottom End-Drop, Bolt Preload, Internal Pressure, Impact, Thermal Cold

Section	Angle	Cylindrical Stress Components (ksi)						SI (ksi)	Allowable Stress (ksi)	Margin of Safety
		S_X	S_Y	S_Z	S_{XY}	S_{YZ}	S_{XZ}			
1	180	0.3	-1	1.4	0	-0.1	0	2.5	60	23.23
2	180	1.3	-0.7	1.7	-0.2	0	0.1	2.4	60	23.9
3	180	-2.6	-7.1	-1.4	0	0.5	-0.2	5.8	60	9.36
4	180	-2.6	-7.1	-1.4	0	0.5	-0.2	5.8	60	9.36
5	0	1.2	-0.5	3.9	-0.1	0.1	0.1	4.4	60	12.67
6	120	3.7	-0.3	4.6	0	0	1	5.6	60	9.74
7	0	0.5	-3.9	-0.6	0.2	0	-0.1	4.5	60	12.48
8	180	2.8	-5.2	-0.5	-3.1	0.2	0.5	10.2	60	4.91
9	180	6.2	-1.2	1.4	1.4	0.1	0.6	8	60	6.51
10	180	5.9	1.5	2.5	-5.1	0	0.4	11.2	57.4	4.12
11	180	2.8	-5.2	-0.5	-3.1	0.2	0.5	10.2	57.4	4.65
12	180	2.9	-0.2	1.6	2.9	0.5	0.3	6.7	57.4	7.51
13	180	11.8	4	5.6	-2.4	0.6	0.7	9.5	57.4	5.04
14	0	-0.1	-7.1	-1.2	-1	0.3	-0.1	7.4	59.1	7.04
15	180	0	-9.5	-1.6	-0.2	0.2	0.2	9.6	59.1	5.17
16	20	0.3	-2	3.6	0	0.1	1.4	6.1	59.1	8.64
17	20	0.2	-1.4	2.5	0	0	1	4.2	59.1	13.04
18	30	0.4	-1.2	1.5	0	0	0.9	3.2	59.1	17.33
19	20	0.1	-1	1.4	0	0	0.5	2.6	59.1	21.65
20	20	0.1	-0.9	1.2	0	0	0.5	2.2	59.1	25.36
21	150	0.2	-0.8	0.7	0	0	-0.5	1.8	59.1	31.79
22	0	0	-1.1	0.7	0	0	0.1	1.8	59.1	32.29
23	180	-0.6	-5.5	-4	0	0.3	0.5	5.1	57.4	10.3
24	0	-0.3	-2.1	-2.6	0	0	-0.3	2.4	57.4	23.26
25	180	-0.4	-1.3	0.8	0	0	0	2.1	57.4	26.16
26	0	-0.2	-1.7	1	0	0	0.1	2.7	57.4	20.52
27	0	-0.2	-1.5	1.5	0	0	0.1	3.1	57.4	17.63
28	0	-0.2	-1.3	1.6	0	0	0.1	3	57.4	18.39
29	0	-0.2	-1.1	1.7	0	0	0.1	2.8	57.4	19.31
30	0	-0.1	-0.9	1.8	0	0	0.2	2.7	57.4	20.19
31	0	-0.1	-1.1	2.3	0	0	0.2	3.5	57.4	15.57
32	0	0	-0.8	1.4	0.1	0	0.1	2.2	60	26.09
33	10	-1.7	-2.1	0.6	0.4	-0.1	0.4	3.1	60	18.18
34	0	-0.1	-1.4	2	0	0	0.2	3.4	60	16.56
35	0	0.1	-7.9	-0.6	0.5	-0.1	-0.1	8.1	60	6.45
36	80	1.2	-1.2	0.2	0	-0.5	0.2	2.6	60	22.3
37	50	-2	0	-1.9	0.1	-0.1	0.3	2.2	60	25.8
38	20	-3.6	-0.1	-2.8	0.1	0	0.3	3.6	60	15.48
39	0	-0.6	-1.2	1.2	-1	0.2	0	3.2	60	18.01
40	10	-3.5	4.3	1.4	-1.4	0.3	0.9	8.4	60	6.14
41	180	0.6	4.3	1.9	-0.9	0.1	-0.2	4.2	60	13.45

Table 2.6.7.1-13 Critical P_m Stress Summary (ksi)—1-Foot Bottom End-Drop, Bolt Preload, Internal Pressure

Component	Section	Angle	SI (ksi)	Allowable Stress (ksi)	Margin of Safety
1	3	180	5.0	20	3.0
2	9	180	5.3	20	2.8
3	10	180	11.0	19.1	0.74
4	15	180	7.4	19.7	1.67
5	16	0	5.8	19.7	2.38
6	22	0	1.6	19.7	11.1
7	23	90	2.8	19.1	5.9
8	28	0	2.6	19.1	6.47
9	31	0	2.9	19.1	5.6
10	34	0	2.9	20	6.0
11	40	80	3.9	20	4.06
12	41	180	4.8	20	3.17

Table 2.6.7.1-14 Critical $P_m + P_b$ Stress Summary (ksi)—1-Foot Bottom End-Drop, Bolt Preload, Internal Pressure

Component	Section	Angle	SI (ksi)	Allowable Stress (ksi)	Margin of Safety
1	3	180	5.6	30	4.32
2	8	180	7.7	30	2.9
3	10	180	12.5	28.7	1.29
4	15	180	7.8	29.6	2.79
5	16	20	6.2	29.6	3.79
6	22	0	1.8	29.6	15.13
7	23	180	5.1	28.7	4.59
8	27	0	3.0	28.7	8.47
9	31	0	3.3	28.7	7.78
10	35	0	4.2	30	6.17
11	40	10	6.5	30	3.63
12	41	180	7.3	30	3.14

Table 2.6.7.1-15 Critical $P_m + P_b + Q$ Stress Summary (ksi)—1-Foot Bottom End-Drop, Bolt Preload, Internal Pressure, Thermal Hot

Component	Section	Angle	SI (ksi)	Allowable Stress (ksi)	Margin of Safety
1	4	0	13.8	60	3.34
2	9	0	17.2	60	2.49
3	10	180	8.8	57.4	5.51
4	15	0	8.9	59.1	5.67
5	16	0	6.9	59.1	7.51
6	22	0	3.4	59.1	16.42
7	23	0	9.2	57.4	5.27
8	27	0	15.2	57.4	2.78
9	31	0	7.4	57.4	6.72
10	35	0	9.9	60	5.08
11	40	60	11.2	60	4.37
12	41	180	4.8	60	11.57

Table 2.6.7.1-16 Critical $P_m + P_b + Q$ Stress Summary (ksi)—1-Foot Bottom End-Drop, Bolt Preload, Internal Pressure, Thermal Cold

Component	Section	Angle	SI (ksi)	Allowable Stress (ksi)	Margin of Safety
1	4	180	5.8	60	9.36
2	8	180	10.2	60	4.91
3	10	180	11.2	57.4	4.12
4	15	180	9.6	59.1	5.17
5	16	20	6.1	59.1	8.64
6	22	0	1.8	59.1	32.29
7	23	180	5.1	57.4	10.3
8	27	0	3.1	57.4	17.63
9	31	0	3.5	57.4	15.57
10	35	0	8.1	60	6.45
11	40	10	8.4	60	6.14
12	41	180	4.2	60	13.45

2.6.7.2 One-Foot Side Drop

In the 1-ft side-drop event, the cask (equipped with an impact limiter over each end) falls a distance of 1 foot onto a flat, unyielding, horizontal surface. The cask strikes the surface in a horizontal position, thereby resulting in a side impact on the cask. The types of loading involved in a side-drop event are closure lid bolt preload, internal pressure load, thermal load, and inertial body load. The analysis is performed using a 20g acceleration load, which provides a bounding analysis, since it exceeds the calculated g-loads for the one-foot side drop event shown in Table 2.6.7.5-3.

The same conditions evaluated for the end-drop are also used in the side drop evaluation. Stress results for the combined 1-ft side-impact loading condition are documented in Tables 2.6.7.2-1 through 2.6.7.2-8.

As shown in Tables 2.6.7.2-5 and 2.6.7.2-6, the margins of safety for the primary stress intensity category are positive for the 1-ft side-drop condition. The most critically stressed component in the system is the cask body ligament region. The minimum margin of safety is found to be +0.04 for primary membrane stress intensity, as documented in Table 2.6.7.2-5. The minimum margin of safety is found to be 0.4 for primary membrane plus bending stress intensity, as documented in Table 2.6.7.2-6.

As seen from the tables, the minimum margin of safety for primary plus secondary stress intensity for the 1-ft side-drop is 1.18 (Table 2.6.7.2-8).

Because the margins of safety are all positive, the Universal Transport Cask satisfies the requirements of 10 CFR 71.71(c)(7) for the 1-ft side-drop (normal transport) condition.

Table 2.6.7.2-1 P_m Stresses—1-Foot Side-Drop, Bolt Preload, Internal Pressure

		Cylindrical Stress Components (ksi)							Allowable Stress	
Section	Angle	S_X	S_Y	S_Z	S_{XY}	S_{YZ}	S_{XZ}	SI (ksi)	(ksi)	MS
1	180	-0.7	1.5	0.0	0.1	0.0	0.1	2.4	20.0	7.47
2	135	0.2	1.2	0.0	-1.1	0.0	0.2	2.6	20.0	6.79
3	105	0.5	1.1	1.1	-1.0	-1.0	0.3	3.0	20.0	5.72
4	10	-4.1	-6.2	-2.1	-0.1	-0.3	-1.3	4.8	20.0	3.14
5	10	-3.0	-2.4	-0.1	0.2	0.0	0.0	2.9	20.0	5.96
6	10	-3.5	-4.2	-0.1	0.0	0.0	0.1	4.1	20.0	3.87
7	0	-4.2	-6.1	2.5	0.1	-0.2	-0.3	8.5	20.0	1.35
8	10	-1.6	-7.8	-0.4	-0.2	-0.7	-0.8	8.0	20.0	1.50
9	10	-5.2	-9.2	-0.2	0.1	-0.9	1.5	9.7	20.0	1.07
10	0	-4.5	-11.6	-10.2	0.6	-0.4	0.4	7.3	19.1	1.62
11	0	-6.1	-14.0	-15.4	0.7	-0.3	2.2	10.3	19.1	0.85
12	0	-8.3	-7.7	8.8	-0.1	-0.5	0.6	17.5	19.1	0.09
13	0	-5.2	-5.9	13.0	0.0	-0.5	1.0	18.5	19.1	0.03
14	10	-7.4	-10.6	-2.8	0.1	-0.6	-2.5	9.0	19.7	1.18
15	0	-4.4	-10.2	-2.3	0.5	-0.3	2.0	9.1	19.7	1.16
16	50	0.0	1.5	1.3	-0.1	-3.7	-0.1	7.4	19.7	1.66
17	0	-0.1	2.0	6.2	-0.3	-0.3	0.1	6.4	19.7	2.09
18	0	-0.1	1.6	7.9	-0.3	-0.2	0.0	8.1	19.7	1.43
19	0	-0.1	1.6	8.6	-0.3	0.0	0.0	8.8	19.7	1.23
20	0	-0.1	1.7	8.5	-0.3	0.1	0.0	8.6	19.7	1.28
21	0	-0.1	2.2	7.4	-0.3	0.2	-0.1	7.5	19.7	1.63
22	60	0.0	2.1	0.7	0.0	3.2	0.2	6.6	19.7	2.00
23	40	-0.2	-2.1	1.2	0.0	-3.6	0.4	7.8	19.1	1.45
24	50	-0.1	3.1	1.5	0.0	-3.7	-0.1	7.5	19.1	1.55
25	0	-0.3	4.0	5.6	-0.4	-0.3	0.0	6.1	19.1	2.15
26	0	-0.3	4.1	7.6	-0.4	-0.2	0.0	7.9	19.1	1.42
27	0	-0.3	4.2	8.4	-0.4	0.0	0.0	8.7	19.1	1.19
28	0	-0.3	4.1	8.1	-0.4	0.1	0.0	8.5	19.1	1.24
29	0	-0.3	4.0	6.9	-0.4	0.2	0.0	7.2	19.1	1.66
30	60	0.0	2.8	0.9	0.0	3.1	0.0	6.4	19.1	2.00
31	50	-0.1	2.8	1.6	0.0	4.3	0.2	8.7	19.1	1.19
32	70	0.1	2.3	-0.1	0.1	3.4	0.4	7.2	20.0	1.78
33	80	-1.0	0.9	-0.1	-0.7	2.2	0.1	4.7	20.0	3.23
34	60	0.8	2.3	1.4	0.2	3.5	0.2	7.1	20.0	1.82
35	0	-1.1	-4.8	0.4	0.3	0.0	-0.9	5.6	20.0	2.54
36	180	1.4	6.8	-0.8	0.8	0.2	1.1	8.1	20.0	1.47
37	0	-3.2	-0.4	-0.1	0.0	0.0	-0.2	3.1	20.0	5.49
38	0	-3.4	-1.7	-0.1	0.0	0.0	-0.4	3.4	20.0	4.90
39	0	-3.5	-2.8	1.0	0.0	-0.1	-0.2	4.6	20.0	3.33
40	10	-3.7	-5.5	-3.2	0.1	-0.2	-0.5	2.7	20.0	6.49
41	0	-5.0	-2.8	-1.3	-0.2	0.0	0.6	3.9	20.0	4.12

Table 2.6.7.2-2 $P_m + P_b$ Stresses—1-Foot Side-Drop, Bolt Preload, Internal Pressure

		Cylindrical Stress Components (ksi)							Allowable Stress	
Section	Angle	S_X	S_Y	S_Z	S_{XY}	S_{YZ}	S_{XZ}	SI (ksi)	(ksi)	MS
1	180	1.8	5.3	0.1	0.1	0.0	0.1	5.2	30.0	4.73
2	180	1.0	4.9	0.1	0.2	-0.1	0.1	4.8	30.0	5.22
3	90	2.7	1.3	2.5	-1.5	-1.8	1.0	5.4	30.0	4.51
4	90	2.9	1.3	2.1	-1.6	-2.0	1.3	5.8	30.0	4.22
5	60	-4.3	-5.0	-0.1	-0.4	0.0	0.0	5.0	30.0	4.96
6	0	-4.3	-6.6	-0.2	0.1	0.0	0.1	6.4	30.0	3.71
7	0	-2.5	-6.1	6.3	0.1	-0.3	-0.4	12.3	30.0	1.43
8	0	1.0	-3.5	12.0	0.2	-0.5	-1.4	15.7	30.0	0.91
9	0	1.6	-1.1	20.8	0.3	-0.6	0.0	22.6	30.0	0.33
10	0	-2.7	-10.3	-8.4	0.6	-0.3	-0.8	7.9	30.0	2.80
11	0	1.3	-10.4	-11.5	0.9	-0.4	1.2	13.4	30.0	1.24
12	10	-11.3	-8.4	7.8	0.1	-0.5	0.1	19.5	30.0	0.54
13	0	-12.3	-8.8	9.9	-0.3	-0.6	0.8	22.6	30.0	0.33
14	10	-9.1	-7.4	9.7	0.1	-0.6	-0.9	18.5	29.6	0.60
15	0	2.5	-2.2	18.3	0.3	-0.4	1.2	20.5	29.6	0.44
16	50	0.0	3.3	1.4	-0.1	-4.8	-0.1	9.8	19.7	1.02
17	0	-0.1	8.6	8.9	-0.8	-0.1	0.1	9.1	19.7	1.16
18	0	-0.1	9.9	11.2	-1.0	-0.1	0.0	11.3	19.7	0.74
19	0	-0.1	10.2	12.1	-1.0	0.0	0.0	12.3	19.7	0.60
20	0	-0.1	9.9	11.9	-1.0	0.0	0.0	12.3	19.7	0.60
21	0	0.0	8.4	10.1	-0.8	0.0	-0.1	10.2	19.7	0.94
22	40	-0.1	2.7	1.3	-0.1	4.8	0.1	9.7	29.6	2.07
23	40	-0.2	-1.5	1.7	0.0	-5.5	0.4	11.3	28.7	1.54
24	40	-0.2	4.7	1.6	-0.1	-4.8	-0.1	10.2	19.1	0.88
25	0	-0.2	10.5	8.2	-0.9	-0.1	0.0	11.3	19.1	0.69
26	0	-0.2	12.2	10.8	-1.1	-0.1	0.0	12.3	19.1	0.55
27	0	-0.2	13.0	11.9	-1.2	0.0	0.0	13.4	19.1	0.43
28	0	-0.2	12.8	11.5	-1.2	0.1	0.0	13.4	19.1	0.43
29	0	-0.2	11.7	9.9	-1.0	0.1	0.0	12.3	19.1	0.55
30	0	-0.2	9.7	6.2	-0.9	0.2	-0.1	10.1	19.1	0.90
31	40	-0.2	2.9	0.2	-0.1	6.5	0.1	13.4	28.7	1.15
32	50	0.0	2.0	-1.7	0.0	4.7	0.1	10.2	30.0	1.95
33	60	-2.1	-0.3	-2.4	-2.1	3.6	0.2	8.5	30.0	2.52
34	50	-0.1	0.5	-2.4	0.1	4.7	-0.4	10.0	30.0	2.01
35	50	-0.4	-2.2	-0.1	0.1	3.8	1.1	8.2	30.0	2.65
36	180	-0.2	5.8	-2.5	0.8	0.2	0.7	8.6	30.0	2.48
37	90	-7.0	-8.5	-0.2	-0.3	0.0	-0.1	8.4	30.0	2.56
38	180	-6.3	-7.1	-0.2	-0.1	0.0	-0.3	7.0	30.0	3.30
39	0	-2.4	-6.3	2.5	0.2	0.0	-1.3	9.1	30.0	2.28
40	0	1.7	-6.6	-3.7	0.4	0.0	1.4	8.6	30.0	2.48
41	0	-6.6	-2.9	0.7	-0.2	-0.1	0.4	7.4	30.0	3.06

Table 2.6.7.2-3 $P_m + P_b + Q$ Stresses—1-Foot Side-Drop, Bolt Preload, Internal Pressure, Thermal Hot

		Cylindrical Stress Components (ksi)							Allowable Stress	
Section	Angle	S_X	S_Y	S_Z	S_{XY}	S_{YZ}	S_{XZ}	SI (ksi)	(ksi)	MS
1	90	8.2	4.3	0.1	0.1	0.0	0.1	8.1	60.0	6.40
2	180	3.2	8.3	0.0	0.3	-0.1	0.2	8.3	60.0	6.21
3	80	10.7	5.2	10.7	-0.6	-0.9	4.1	9.9	60.0	5.09
4	0	5.9	-5.6	-6.8	0.6	0.7	-1.2	13.2	60.0	3.53
5	20	-4.2	-8.9	0.2	-2.0	-0.1	0.1	9.8	60.0	5.15
6	20	-3.1	-7.6	-0.1	-2.1	0.0	0.1	8.3	60.0	6.21
7	20	1.4	-3.3	8.5	-2.7	-3.0	0.4	14.4	60.0	3.17
8	20	1.4	-3.3	8.5	-2.7	-3.0	0.4	14.4	60.0	3.17
9	10	-0.2	-3.1	15.6	-0.2	-1.5	0.5	18.9	60.0	2.18
10	0	1.0	-8.4	-9.9	0.1	-0.6	-0.6	11.2	60.0	4.36
11	0	-0.4	-10.0	-11.0	0.0	-0.4	1.5	11.2	60.0	4.36
12	0	-9.1	-5.3	13.8	-0.7	-0.2	-0.3	23.0	60.0	1.61
13	0	8.3	1.5	22.0	-0.1	-0.6	2.9	21.0	60.0	1.86
14	0	-9.1	-5.3	13.8	-0.7	-0.2	-0.3	23.0	59.1	1.57
15	0	8.3	1.5	22.0	-0.1	-0.6	2.9	21.0	59.1	1.82
16	0	-0.1	11.2	10.3	-1.1	-0.1	0.0	11.5	59.1	4.14
17	0	-0.2	14.0	14.0	-1.3	0.0	0.1	14.4	59.1	3.11
18	0	-0.2	15.2	15.8	-1.5	0.0	0.0	16.1	59.1	2.67
19	0	-0.2	15.5	16.3	-1.5	0.0	0.0	16.6	59.1	2.55
20	0	-0.2	15.3	15.9	-1.5	0.0	0.0	16.3	59.1	2.62
21	0	-0.2	13.9	13.9	-1.3	0.0	-0.1	14.3	59.1	3.14
22	0	-0.1	10.2	11.3	-1.0	0.0	-0.2	11.5	59.1	4.14
23	40	-0.2	-2.0	1.5	-0.1	-4.7	0.2	10.1	57.4	4.70
24	0	-1.1	7.8	0.3	-0.7	0.3	0.1	9.0	57.4	5.35
25	0	-2.3	11.0	1.3	-1.2	0.1	0.0	13.5	57.4	3.27
26	0	-2.5	13.2	2.1	-1.4	0.0	0.0	16.0	57.4	2.58
27	0	-2.6	14.2	2.3	-1.5	0.0	0.0	17.0	57.4	2.37
28	0	-2.6	13.7	1.6	-1.4	0.0	0.0	16.4	57.4	2.49
29	0	-2.5	12.0	0.4	-1.3	0.0	0.0	14.8	57.4	2.88
30	0	-2.2	9.2	-2.1	-1.0	0.0	0.0	11.7	57.4	3.90
31	40	-0.3	0.1	0.0	-0.1	5.9	0.0	11.8	57.4	3.86
32	50	-0.2	3.4	1.3	0.0	5.4	-0.1	11.1	60.0	4.41
33	40	2.7	1.8	5.8	-4.1	4.5	-1.0	13.0	60.0	3.60
34	60	0.1	1.1	-5.3	0.0	4.0	0.0	10.4	60.0	4.78
35	0	-0.1	-10.2	-6.4	0.8	0.6	0.1	10.3	60.0	4.84
36	180	5.0	9.0	0.0	0.7	0.0	1.7	9.8	60.0	5.15
37	150	-11.0	-11.3	-0.1	0.6	0.0	-0.1	11.5	60.0	4.22
38	180	-9.1	-10.0	-0.2	0.0	0.0	-0.1	9.8	60.0	5.15
39	0	0.6	-8.9	1.5	0.9	0.3	0.2	10.7	60.0	4.62
40	180	-1.1	4.7	-6.3	0.7	0.1	-0.3	11.1	60.0	4.41
41	10	-2.4	-2.0	15.2	0.0	0.1	-0.9	17.7	60.0	2.40

Table 2.6.7.2-4 $P_m + P_b + Q$ Stresses—1-Foot Side-Drop, Bolt Preload, Internal Pressure, Thermal Cold

Section	Angle	Cylindrical Stress Components (ksi)						SI (ksi)	Allowable Stress (ksi)	MS
		S_X	S_Y	S_Z	S_{XY}	S_{YZ}	S_{XZ}			
1	180	1.0	5.9	-0.1	0.3	0.0	0.2	6.1	60.0	8.90
2	180	0.4	5.9	0.0	0.3	-0.1	0.2	6.0	60.0	9.07
3	90	4.8	2.7	3.6	-1.5	-2.0	2.0	6.4	60.0	8.42
4	0	9.6	-6.4	-3.5	0.7	1.0	-2.1	16.7	60.0	2.58
5	20	-5.5	-7.8	0.0	-1.0	0.0	0.0	8.2	60.0	6.30
6	0	-4.9	-8.7	-0.1	0.0	0.0	0.0	8.6	60.0	5.96
7	0	0.9	-3.6	12.1	0.0	-0.4	0.1	15.8	60.0	2.79
8	0	0.9	-3.6	12.1	0.0	-0.4	0.1	15.8	60.0	2.79
9	0	-0.4	-2.0	21.9	0.1	-0.4	0.4	23.9	60.0	1.51
10	0	3.0	-8.0	-8.4	0.5	-0.5	-0.1	11.8	60.0	4.08
11	0	-2.4	-11.8	-12.5	0.3	-0.5	2.5	11.5	60.0	4.22
12	0	-15.0	-8.4	12.0	-0.8	-0.3	0.0	27.1	60.0	1.21
13	0	10.7	1.8	24.6	0.2	-0.5	3.1	23.4	60.0	1.56
14	0	-15.0	-8.4	12.0	-0.8	-0.3	0.0	27.1	59.1	1.18
15	0	10.7	1.8	24.6	0.2	-0.5	3.1	23.4	59.1	1.52
16	0	-0.1	10.5	9.6	-1.0	-0.1	0.1	10.7	59.1	4.53
17	0	-0.2	13.5	13.4	-1.3	0.0	0.1	14.0	59.1	3.23
18	0	-0.2	15.0	15.3	-1.5	0.0	0.0	15.7	59.1	2.76
19	0	-0.2	15.3	15.8	-1.5	0.0	0.0	16.2	59.1	2.64
20	0	-0.2	15.0	15.5	-1.4	0.0	0.0	15.9	59.1	2.71
21	0	-0.2	13.4	13.6	-1.3	0.0	-0.1	13.9	59.1	3.26
22	50	-0.2	4.1	2.5	-0.1	5.4	0.1	11.1	59.1	4.33
23	30	-0.2	-3.8	1.8	-0.1	-4.2	0.5	10.3	57.4	4.59
24	0	-1.2	8.7	0.2	-0.8	0.3	0.1	10.2	57.4	4.65
25	0	-2.5	11.9	0.7	-1.3	0.2	0.0	14.7	57.4	2.91
26	0	-2.8	14.2	1.3	-1.5	0.1	0.0	17.3	57.4	2.33
27	0	-2.9	15.1	1.4	-1.6	0.0	0.0	18.3	57.4	2.14
28	0	-2.9	14.6	0.9	-1.6	0.0	0.0	17.8	57.4	2.23
29	0	-2.8	13.0	-0.3	-1.4	0.0	0.0	16.1	57.4	2.56
30	0	-2.4	10.4	-2.7	-1.1	0.0	0.0	13.2	57.4	3.33
31	40	-0.3	0.4	-0.5	-0.1	6.0	0.0	11.9	57.4	3.82
32	50	-0.1	2.8	0.9	0.0	5.4	0.0	11.0	60.0	4.46
33	40	1.6	1.0	4.6	-3.8	4.2	-0.8	12.0	60.0	3.99
34	0	-5.0	-10.0	-13.5	0.0	-0.5	-2.8	10.2	60.0	4.90
35	60	-0.1	-2.3	-5.3	0.0	4.5	0.6	9.7	60.0	5.22
36	180	5.1	9.4	0.2	0.8	0.0	2.0	10.0	60.0	5.02
37	180	-11.4	-11.2	-0.2	0.1	0.0	-0.1	11.2	60.0	4.36
38	180	-9.1	-10.0	-0.2	0.0	0.0	-0.1	9.8	60.0	5.15
39	0	0.5	-7.1	1.5	0.8	0.2	0.2	8.7	60.0	5.87
40	180	-0.7	5.2	-5.9	0.7	0.0	-0.2	11.2	60.0	4.36
41	0	-4.0	-4.0	11.6	-0.2	0.0	-1.2	15.9	60.0	2.77

Table 2.6.7.2-5 Critical P_m Stress Summary (ksi)—1-Foot Side Drop, Bolt Preload, Internal Pressure

Component	Section	Angle	SI (ksi)	Allowable Stress (ksi)	Margin of Safety
1	4	10	4.8	20	3.14
2	9	10	9.7	20	1.07
3	13	0	18.5	19.1	0.08
4	15	0	9.1	19.7	1.16
5	19	0	8.8	19.7	1.23
6	22	60	6.6	19.7	2.00
7	23	40	7.8	19.1	1.45
8	27	0	8.7	19.1	1.19
9	31	50	8.7	19.1	1.19
10	36	180	8.1	20	1.47
11	39	0	4.6	20	3.33
12	41	0	3.9	20	4.12

Table 2.6.7.2-6 Critical $P_m + P_b$ Stress Summary (ksi)—1-Foot Side-Drop, Bolt Preload, Internal Pressure

Component	Section	Angle	SI (ksi)	Allowable Stress (ksi)	Margin of Safety
1	4	90	5.8	30	4.22
2	9	0	22.6	30	0.33
3	13	0	22.6	28.7	0.33
4	15	0	20.5	29.6	0.44
5	19	0	12.3	29.6	1.40
6	22	40	9.7	29.6	2.07
7	23	40	11.3	28.7	1.54
8	27	0	13.4	28.7	1.15
9	31	40	13.4	28.7	1.15
10	32	50	10.2	30	1.95
11	39	0	9.1	30	2.28
12	41	0	7.4	30	3.06

Table 2.6.7.2-7 Critical $P_m + P_b + Q$ Stress Summary (ksi)—1-Foot Side-Drop, Bolt Preload, Internal Pressure, Thermal Hot

Component	Section	Angle	SI (ksi)	Allowable Stress (ksi)	Margin of Safety
1	4	0	12.9	60	3.66
2	7	20	14	60	3.3
3	12	0	22.4	57.4	1.56
4	14	0	22.4	59.1	1.64
5	19	0	16.2	59.1	2.64
6	22	0	11.2	59.1	4.29
7	23	40	9.8	57.4	4.88
8	27	0	16.6	57.4	2.46
9	31	40	11.5	57.4	4.01
10	33	40	12.7	60	3.74
11	40	180	10.8	60	4.54
12	41	10	17.2	60	2.49

Table 2.6.7.2-8 Critical $P_m + P_b + Q$ Stress Summary (ksi)—1-Foot Side-Drop Bolt Preload, Internal Pressure, Thermal Cold

Component	Section	Angle	SI (ksi)	Allowable Stress (ksi)	Margin of Safety
1	4	0	16.3	60	2.68
2	7	0	15.4	60	2.9
3	12	0	26.4	57.4	1.18
4	14	0	26.4	59.1	1.24
5	19	0	15.8	59.1	2.74
6	22	50	10.8	59.1	4.48
7	23	30	10	57.4	4.74
8	27	0	17.8	57.4	2.22
9	31	40	11.6	57.4	3.94
10	33	40	11.7	60	4.14
11	37	180	10.9	60	4.5
12	41	0	15.5	60	2.87

2.6.7.3 One-Foot Corner Drop

In this event, the Universal Transport Cask (equipped with an impact limiter over each end) falls a distance of 1 foot onto a flat, unyielding, horizontal surface. The cask strikes the surface on its top or bottom corner. The cask center of gravity is considered to be directly above the initial point of impact for the corner-drop condition. For the cask, the orientation angle is 23° and 23.5° for the top and bottom corner-drops, respectively.

Results for the top corner and bottom corner 1-ft drop evaluations are presented in Tables 2.6.7.3-1 through 2.6.7.3-16. For the top-corner-drop loading case including impact, bolt preload, and internal pressures the minimum margin of safety resulting from calculated P_m stress intensity is 1.54 (Table 2.6.7.3-5) and the minimum calculated $P_m + P_b$ stress intensity margin of safety is 1.11 (Table 2.6.7.3-6). As seen from the tables, the minimum margin of safety for primary plus secondary stress intensity for the 1-ft top corner-drop is 2.32 (Table 2.6.7.3-8).

For the bottom-corner-drop loading case including impact, bolt preload, and internal pressures the minimum margin of safety resulting from calculated P_m stress intensity is 0.84 (Table 2.6.7.3-13) and the minimum margin of safety resulting from calculated $P_m + P_b$ stress intensity is 1.34 (Table 2.6.7.3-14). As seen from the tables, the minimum margin of safety for primary plus secondary stress intensity for the 1-ft bottom corner-drop is 2.14 (Table 2.6.7.3-16).

Because the margins of safety are all positive, the Universal Transport Cask satisfies the requirements of 10 CFR 71.71(c)(7) for the 1-ft corner-drop (normal transport) condition.

Table 2.6.7.3-1 P_m Stresses—1-Foot Top Corner-Drop, Bolt Preload, Internal Pressure

		Cylindrical Stress Components (ksi)							Allowable Stress	
Section	Angle	S_X	S_Y	S_Z	S_{XY}	S_{YZ}	S_{XZ}	SI (ksi)	(ksi)	MS
1	180	-0.1	0.6	-0.1	0	0	0.1	0.9	20	21.74
2	180	0	0.8	0	0	0	0.1	0.9	20	20.22
3	180	0.2	1	0.1	0.1	0	0.1	1	20	18.38
4	0	-1.2	-1.9	0	0.1	0	-0.2	2	20	9.24
5	10	-1.1	-0.9	-0.1	0.1	0	0	1	20	18.67
6	0	-1.3	-1.7	-0.1	0	0	0.1	1.6	20	11.48
7	0	-1.6	-2.1	2.2	0	-0.1	-0.2	4.3	20	3.66
8	0	0.2	-3.1	0	0.3	-0.2	-0.3	3.6	20	4.54
9	40	-2.6	-2.5	0.7	0.4	-1.7	1.5	5.8	20	2.44
10	0	-2.2	-5.6	-6.7	0.3	-0.2	-0.1	4.6	19.1	3.14
11	0	-4.8	-7.8	-10.9	0.3	-0.1	1.7	7.1	19.1	1.7
12	0	-3.8	-3.3	3.1	0	-0.1	0.4	6.9	19.1	1.75
13	0	-4.1	-3.5	3.3	0	-0.1	-0.4	7.5	19.1	1.54
14	0	-2.7	-3.8	0.1	0.1	-0.1	-0.6	4	19.7	3.91
15	0	-2.6	-4.1	0.1	0.2	0	0.1	4.2	19.7	3.67
16	60	0	0	-0.1	0	-1.3	0	2.6	19.7	6.53
17	70	0	0.4	-0.7	0	-1	0	2.3	19.7	7.66
18	90	0	0.5	-1.6	0	-0.5	0	2.3	19.7	7.48
19	105	0	0.7	-1.9	0	-0.2	0	2.6	19.7	6.44
20	105	0	1.2	-1.9	0	0.1	0	3.1	19.7	5.26
21	80	0	2.2	-1.3	0	0.8	0	3.9	19.7	4.1
22	60	-0.1	3.8	-0.9	0	1.6	0.1	5.6	19.7	2.5
23	50	0	1.1	0.1	0	-2.5	0.2	5	19.1	2.8
24	0	-0.1	4.8	0.9	-0.5	-0.3	0	5	19.1	2.82
25	80	0	2.4	-0.9	0	-0.7	0	3.5	19.1	4.4
26	90	-0.1	2	-1.4	0	-0.1	0	3.4	19.1	4.58
27	90	-0.1	1.8	-1.6	0	0.2	0	3.4	19.1	4.65
28	90	-0.1	1.4	-1.5	0	0.5	0	3.1	19.1	5.21
29	70	-0.1	0.8	-1.1	0	1	0	2.7	19.1	6.03
30	50	-0.2	-0.1	-0.9	0	1.3	0	2.7	19.1	6.02
31	40	-0.3	-0.6	-1.2	0	1.7	0.1	3.6	19.1	4.38
32	70	-0.1	3.2	-1.1	0.1	1.6	0	5.3	20	2.74
33	180	0.4	2.1	-1.8	0.2	0	-0.3	4	20	4.05
34	0	1.2	0.5	-3.6	0.1	0.3	0.5	5	20	2.99
35	180	-0.4	2.3	-1.6	0.4	-0.2	0.3	4	20	3.98
36	180	1.2	3.2	-2.3	0.3	-0.2	0.7	5.7	20	2.54
37	0	-1.5	-0.3	-0.9	0	0.2	0.5	1.6	20	11.85
38	10	-1.5	-0.8	-0.5	0.1	0.1	0.4	1.3	20	14.92
39	80	-0.1	-0.7	-1.9	0	0	-0.1	1.8	20	10.25
40	80	-1.7	-1.7	-4	0	0	-1.4	3.7	20	4.47
41	0	-1.7	-1.2	-0.3	0	0	0.3	1.5	20	12.18

Table 2.6.7.3-2 $P_m + P_b$ Stresses—1-Foot Top Corner-Drop, Bolt Preload, Internal Pressure

Section	Angle	Cylindrical Stress Components (ksi)						SI (ksi)	Allowable Stress (ksi)	MS
		S_X	S_Y	S_Z	S_{XY}	S_{YZ}	S_{XZ}			
1	180	1	2.6	0	0.1	0	0.1	2.6	30	10.39
2	180	0.1	1.9	0	0.1	0	0.1	2	30	14.23
3	90	1.1	0.5	0.6	-0.5	-0.6	0.4	1.8	30	15.22
4	90	1.1	0.5	0.4	-0.5	-0.6	0.5	2	30	13.82
5	20	-2.6	-2.5	-0.1	0	0	0	2.4	30	11.35
6	0	-2.1	-3.2	-0.1	0.1	0	0.1	3.1	30	8.69
7	0	0.2	-1.5	5.5	0	-0.1	0	7	30	3.31
8	0	3.1	0.6	9.6	0.1	-0.2	-0.3	9.1	30	2.31
9	0	1.5	1.8	15.6	0	-0.3	0.5	14.2	30	1.11
10	0	-0.7	-4.7	-5.5	0.4	-0.1	-1	5.3	28.7	4.46
11	0	0.7	-5.2	-7.9	0.5	-0.2	0.6	8.7	28.7	2.29
12	0	-4.5	-3.5	2.9	-0.1	-0.1	0.4	7.5	28.7	2.82
13	0	-6	-4	3.1	-0.1	-0.2	0.1	9.1	28.7	2.15
14	0	-3.5	-3.2	2.9	0	-0.1	0	6.4	29.6	3.61
15	0	-1.6	-2.4	4.8	0.1	-0.1	-0.7	7.3	29.6	3.04
16	50	0	0.7	0.1	0	-1.8	0	3.6	29.6	7.11
17	0	0	3.4	2.8	-0.3	-0.1	0	3.5	29.6	7.47
18	0	0	4.3	3.5	-0.4	0	0	4.4	29.6	5.67
19	0	0	4.8	3.5	-0.5	0	0	4.9	29.6	5.04
20	0	0	5.1	3.1	-0.5	0	0	5.3	29.6	4.63
21	0	0	5.3	1.8	-0.5	0	0	5.4	29.6	4.45
22	40	-0.2	3.8	-2.3	0	2.1	0.1	7.4	29.6	3.01
23	50	0	0.6	-1.4	-0.1	-3.4	0.2	7.2	28.7	3.01
24	0	0	6.6	2.3	-0.6	-0.2	0	6.7	28.7	3.30
25	0	-0.1	5.7	3	-0.5	0	0	5.9	28.7	3.85
26	0	-0.1	5.6	3.4	-0.5	0	0	5.8	28.7	3.91
27	0	-0.1	5.5	3.3	-0.5	0	0	5.7	28.7	4.03
28	0	-0.2	4.8	2.7	-0.4	0	0	5	28.7	4.74
29	60	-0.1	2.9	-0.2	0	1.1	0	3.9	28.7	6.45
30	50	-0.2	1.1	-0.5	0	1.6	0	3.7	28.7	6.86
31	40	-0.2	0.2	0.5	0	2.5	0.1	5.1	28.7	4.66
32	50	-0.3	2.9	-2.8	0	2	-0.1	7	30	3.29
33	70	0.3	2.1	-0.9	-0.9	1.6	-0.3	4.7	30	5.4
34	60	-0.1	-0.1	-8.4	0	1.7	-0.4	9	30	2.33
35	180	-0.6	2.3	-1.8	0.4	-0.3	1.1	4.9	30	5.17
36	180	-0.3	2.6	-2.9	0.4	-0.3	0.5	5.7	30	4.24
37	70	-0.5	-3	-0.8	0.4	0.1	0.6	3.1	30	8.75
38	80	3.7	0.3	-0.4	0.1	0	0.4	4.2	30	6.19
39	80	4.6	1.3	-1.6	-0.1	0	-0.3	6.3	30	3.78
40	0	-3.6	-5.6	-11.6	0.1	0	0.2	8	30	2.74
41	0	-2.5	-1.3	0.4	-0.1	0	0.3	2.9	30	9.31

Table 2.6.7.3-3 $P_m + P_b + Q$ Stresses—1-Foot Top Corner-Drop, Bolt Preload, Internal Pressure, Thermal Hot

		Cylindrical Stress Components (ksi)							Allowable Stress	
Section	Angle	S_X	S_Y	S_Z	S_{XY}	S_{YZ}	S_{XZ}	SI (ksi)	(ksi)	MS
1	90	5	3.7	0	0.3	0	0.1	5	60	10.93
2	180	2.4	4.7	0	0.2	-0.1	0.1	4.7	60	11.65
3	10	-3.2	2.8	-0.1	0.3	0	0.1	6	60	8.95
4	0	7	-1.5	-4.5	0.4	0.7	-0.6	11.7	60	4.15
5	20	-1.7	-4.6	0.1	-1.3	-0.1	0	5.2	60	10.56
6	40	-2.4	-2.2	-0.2	-1.7	0	0	3.8	60	14.94
7	40	-2.1	-0.8	0.8	-1.7	-1.6	-0.6	5.5	60	9.96
8	0	1.2	-2.1	-5.4	-0.2	-0.2	1.3	7.2	60	7.35
9	30	-4.6	-4.4	-7.1	-2.1	1.8	1.1	6.6	60	8.11
10	0	3.6	-0.8	-4.5	0	-0.3	0.5	8.2	57.4	5.95
11	0	1.2	-2.1	-5.4	-0.2	-0.2	1.3	7.2	57.4	6.98
12	0	-3.9	-0.8	3.9	-0.5	0	0.2	7.9	57.4	6.27
13	40	-0.3	0.6	4.8	-1.7	-1.7	0.1	7.3	57.4	6.85
14	0	-3.9	-0.8	3.9	-0.5	0	0.2	7.9	59.1	6.5
15	40	-0.3	0.6	4.8	-1.7	-1.7	0.1	7.3	59.1	7.09
16	0	-0.1	5.7	4.1	-0.6	0.1	0.1	5.9	59.1	9.01
17	0	-0.2	8.1	5.7	-0.8	0.1	0	8.4	59.1	6.07
18	0	-0.2	8.9	5.6	-0.9	0.1	0	9.3	59.1	5.38
19	0	-0.2	9.3	4.9	-0.9	0.1	0	9.7	59.1	5.12
20	0	-0.2	9.7	3.9	-1	0.1	0	10.1	59.1	4.85
21	0	-0.2	9.8	2	-1	0.1	0	10.2	59.1	4.79
22	40	-0.4	4.8	-3.2	0	3	0	9.9	59.1	4.94
23	0	-0.3	-0.3	-4.6	0	0.2	0.2	4.3	57.4	12.23
24	0	-0.9	4.3	-4	-0.4	0.5	0	8.4	57.4	5.85
25	0	-0.4	-4.8	-11.6	0.4	0.2	0	11.2	57.4	4.11
26	0	-0.4	-5.7	-13.5	0.5	0.1	0	13.1	57.4	3.38
27	0	-2.5	6.1	-7.9	-0.8	0.1	0	14.1	57.4	3.08
28	0	-0.4	-5.9	-15	0.6	0.2	0	14.7	57.4	2.9
29	0	-0.6	-6.8	-16.2	0.6	0.2	0	15.6	57.4	2.67
30	0	-0.7	-7.1	-16	0.7	0.1	0	15.4	57.4	2.73
31	0	-1.4	-4.2	-15.4	0.3	-0.3	-0.1	14.1	57.4	3.07
32	0	-0.2	4.9	-4.6	-0.8	0.3	-0.9	9.9	60	5.08
33	0	0.3	2.7	-6.6	-0.4	0.1	-0.7	9.4	60	5.37
34	0	0	-4.8	-15.5	0.4	-0.1	0.4	15.6	60	2.84
35	0	-0.2	-5.6	-13.9	0.5	0.5	0.4	13.8	60	3.34
36	0	4.6	-1.5	-5.3	0.6	0.3	-0.7	10	60	4.98
37	180	-5.6	-1.9	-0.6	0.4	-0.1	0.4	5.1	60	10.79
38	180	-8.8	-5.1	-0.7	0.4	-0.1	0.2	8.2	60	6.31
39	80	1.2	-3.8	-10.4	0.6	0.7	0.6	11.9	60	4.05
40	0	-2.4	-9.5	-15.1	0.8	0.3	-0.7	13	60	3.63
41	10	-0.3	1.1	5.7	0	0.1	0.2	6	60	8.95

Table 2.6.7.3-4 $P_m + P_b + Q$ Stresses—1-Foot Top Corner-Drop, Bolt Preload, Internal Pressure, Thermal Cold

		Cylindrical Stress Components (ksi)							Allowable Stress	
Section	Angle	S_X	S_Y	S_Z	S_{XY}	S_{YZ}	S_{XZ}	SI (ksi)	(ksi)	MS
1	0	1.2	3.5	0	-0.2	0	0.1	3.6	60	15.87
2	0	0.9	3.1	0	-0.1	0	0.1	3.1	60	18.42
3	10	-3.6	2.1	-0.4	0.4	0	0.5	5.8	60	9.35
4	0	11.1	-1.7	-1.1	0.5	1.1	-1.3	13.8	60	3.34
5	50	-3.6	-3	-0.1	-0.6	0	0	3.9	60	14.53
6	0	-2.4	-3.6	-0.1	0	0	0	3.4	60	16.56
7	10	0.4	-0.2	4.8	-0.1	-0.1	-0.1	5.1	60	10.83
8	0	-0.3	-3.8	-7	0.1	-0.2	1.9	7.7	60	6.78
9	0	-0.3	0.5	9.2	-0.1	0	0.1	9.4	60	5.36
10	0	-0.3	-3.8	-7	0.1	-0.2	1.9	7.7	57.4	6.43
11	0	-0.3	-3.8	-7	0.1	-0.2	1.9	7.7	57.4	6.43
12	0	-5.9	-2	4.4	-0.5	0	0	10.4	57.4	4.54
13	0	5.7	2.5	9.9	0	-0.1	1.2	7.7	57.4	6.45
14	0	-5.9	-2	4.4	-0.5	0	0	10.4	59.1	4.71
15	0	5.7	2.5	9.9	0	-0.1	1.2	7.7	59.1	6.68
16	0	-0.1	5.3	3.7	-0.5	0.1	0.1	5.5	59.1	9.79
17	0	-0.1	7.8	5.3	-0.8	0.1	0	8.2	59.1	6.25
18	0	-0.2	8.8	5.2	-0.9	0.1	0	9.2	59.1	5.44
19	0	-0.2	9.2	4.4	-0.9	0.1	0	9.6	59.1	5.16
20	0	-0.2	9.6	3.4	-1	0.1	0	10	59.1	4.93
21	0	-0.2	9.6	1.4	-0.9	0.1	0	10	59.1	4.93
22	30	-0.3	3.8	-4.4	0	2.8	0	9.9	59.1	4.96
23	0	-0.3	-1.3	-5.5	0.1	0.3	0.3	5.3	57.4	9.85
24	0	-1	4.7	-4.4	-0.5	0.5	0	9.2	57.4	5.21
25	0	-0.4	-4.7	-12.9	0.4	0.2	0	12.5	57.4	3.58
26	0	-0.5	-5.8	-15	0.5	0.1	0	14.6	57.4	2.93
27	0	-2.8	6.6	-9.1	-0.9	0.1	0	15.7	57.4	2.64
28	0	-0.4	-6	-16.6	0.6	0.2	0	16.3	57.4	2.51
29	0	-0.7	-6.9	-17.9	0.6	0.2	0	17.3	57.4	2.32
30	0	-0.7	-7	-17.6	0.6	0.1	0	16.9	57.4	2.39
31	0	-1.5	-4	-16.3	0.3	-0.3	-0.2	14.9	57.4	2.84
32	0	-0.3	4.2	-5.8	-0.7	0.3	-1	10.3	60	4.84
33	0	0.3	2.1	-7	-0.3	0.1	-0.8	9.2	60	5.55
34	0	0	-3.9	-15.1	0.4	-0.1	0.4	15.1	60	2.96
35	0	-0.2	-4.5	-14	0.4	0.5	0.3	13.8	60	3.35
36	0	4.7	-1.4	-6.2	0.6	0.4	-0.2	11.1	60	4.42
37	180	-6.2	-2.2	-0.6	0.3	-0.1	0.4	5.7	60	9.56
38	180	-9.4	-5.6	-0.6	0.4	-0.1	0.1	8.8	60	5.81
39	0	0.3	-7.1	-11.7	0.7	0.2	-0.2	12	60	3.98
40	0	-2.3	-8.4	-15.2	0.7	0.3	-0.7	13.1	60	3.58
41	10	-1.4	0.2	5	0	0.4	0	6.5	60	8.26

Table 2.6.7.3-5 Critical P_m Stress Summary (ksi)—1-Foot Top Corner-Drop, Bolt Preload, Internal Pressure

Component	Section	Angle	SI (ksi)	Allowable Stress (ksi)	Margin of Safety
1	4	0	2	20	9.24
2	9	40	5.8	20	2.44
3	13	0	7.5	19.1	1.54
4	15	0	4.2	19.7	3.67
5	21	80	3.9	19.7	4.1
6	22	60	5.6	19.7	2.5
7	23	50	5	19.1	2.8
8	24	0	5	19.1	2.82
9	31	40	3.6	19.1	4.38
10	36	180	5.7	20	2.54
11	40	80	3.7	20	4.47
12	41	0	1.5	20	12.18

Table 2.6.7.3-6 Critical $P_m + P_b$ Stress Summary (ksi)—1-Foot Top Corner-Drop, Bolt Preload, and Internal Pressure

Component	Section	Angle	SI (ksi)	Allowable Stress (ksi)	Margin of Safety
1	1	180	2.6	30	10.39
2	9	0	14.2	30	1.11
3	13	0	9.1	28.7	2.15
4	15	0	7.3	29.6	3.04
5	21	0	5.4	**29.6**	**4.45**
6	22	40	7.4	29.6	3.01
7	23	50	7.2	28.7	3.01
8	24	0	6.7	**28.7**	**3.30**
9	31	40	5.1	28.7	4.66
10	34	60	9	30	2.33
11	40	0	8	30	2.74
12	41	0	2.9	30	9.31

Table 2.6.7.3-7 Critical $P_m + P_b + Q$ Stress Summary (ksi)—1-Foot Top Corner-Drop, Bolt Preload, Internal Pressure, and Thermal Hot

Component	Section	Angle	SI (ksi)	Allowable Stress (ksi)	Margin of Safety
1	4	0	11.7	60	4.15
2	8	0	7.2	60	7.35
3	10	0	8.2	57.4	5.95
4	14	0	7.9	59.1	6.5
5	21	0	10.2	59.1	4.79
6	22	40	9.9	59.1	4.94
7	23	0	4.3	57.4	12.23
8	29	0	15.6	57.4	2.67
9	31	0	14.1	57.4	3.07
10	34	0	15.6	60	2.84
11	39	80	11.9	60	4.05
12	41	10	6	60	8.95

Table 2.6.7.3-8 Critical $P_m + P_b + Q$ Stress Summary (ksi)—1-Foot Top Corner-Drop, Bolt Preload, Internal Pressure, and Thermal Cold

Component	Section	Angle	SI (ksi)	Allowable Stress (ksi)	Margin of Safety
1	4	0	13.8	60	3.34
2	9	0	9.4	60	5.36
3	12	0	10.4	57.4	4.54
4	14	0	10.4	59.1	4.71
5	20	0	10	59.1	4.93
6	22	30	9.9	59.1	4.96
7	23	0	5.3	57.4	9.85
8	29	0	17.3	57.4	2.32
9	31	0	14.9	57.4	2.84
10	34	0	15.1	60	2.96
11	40	0	13.1	60	3.58
12	41	10	6.5	60	8.26

Table 2.6.7.3-9 P_m Stresses—1-Foot Bottom Corner-Drop, Bolt Preload, and Internal Pressure

Section	Angle	Cylindrical Stress Components (ksi)						SI (ksi)	Allowable Stress (ksi)	MS
		S_X	S_Y	S_Z	S_{XY}	S_{YZ}	S_{XZ}			
1	180	-0.7	0.6	-0.9	0.1	0	-0.1	1.5	20	11.93
2	180	-0.4	0.8	-0.5	0.1	0	0.1	1.4	20	13.27
3	0	-1.3	-3.2	-6.4	0	-0.5	-0.2	5.2	20	2.82
4	180	-0.8	0.9	-1.8	0.2	0.2	0.3	2.8	20	6.07
5	180	-0.4	0.6	-0.8	0	0.3	-0.6	1.9	20	9.6
6	180	-0.1	0.9	-0.5	0.1	0.1	0.1	1.4	20	12.89
7	10	-1	-2.1	-0.1	-0.1	-0.2	0.3	2.1	20	8.57
8	10	2.4	0.4	-0.3	-0.6	-0.9	1.2	4.2	20	3.78
9	0	-1.6	-4.1	-3.4	0.3	-0.3	0.4	2.8	20	6.09
10	0	0.5	-3.7	-4.9	0.4	-0.1	3.4	8.7	19.1	1.19
11	0	1.4	-4.5	-8	0.5	-0.2	2.2	10.4	19.1	0.84
12	10	-1.4	-1.9	2.6	0.1	-0.5	-1.2	5	19.1	2.8
13	10	1.7	-0.5	4.8	-0.1	-0.6	0.2	5.4	19.1	2.54
14	0	-2.6	-4.3	-4.8	0.2	-0.6	-2.4	5.4	19.7	2.65
15	0	-0.4	-3.8	-4.8	0.3	-0.3	1.2	5.1	19.7	2.85
16	50	0	2.3	-1.8	0	-1.6	-0.1	5.2	19.7	2.77
17	70	0	1.1	-1.9	0	-1.1	0	3.7	19.7	4.37
18	90	0	0.4	-2.3	0	-0.5	0	2.9	19.7	5.78
19	90	0	0.1	-2.3	0	-0.2	0	2.4	19.7	7.12
20	105	0	-0.1	-2.2	0	0.1	0	2.2	19.7	8.14
21	105	0	-0.2	-1.8	0	0.3	0	1.8	19.7	9.94
22	70	0	0.4	-0.8	0	0.9	0.1	2.1	19.7	8.41
23	20	-0.2	-3.1	-2.7	0	-1	0.4	3.8	19.1	4.03
24	40	-0.1	0.8	-1.5	0	-1.5	0	3.7	19.1	4.14
25	60	-0.1	1.5	-1.2	0	-1.2	0	3.6	19.1	4.28
26	80	-0.1	2	-1.5	0	-0.8	0	3.8	19.1	4.03
27	90	-0.1	2.3	-1.7	0	-0.4	0	4	19.1	3.74
28	90	-0.1	2.4	-1.6	0	0	0	4.1	19.1	3.7
29	80	0	2.5	-1.2	0	0.4	0	3.9	19.1	3.92
30	0	-0.1	3.8	1.2	-0.4	0.2	0	4	19.1	3.74
31	40	-0.1	2.9	-0.1	0	2	0	5	19.1	2.81
32	80	0.1	0.9	-0.8	0	0.9	0.2	2.6	20	6.72
33	80	-0.8	0.9	-0.3	-0.2	0.6	0.1	2.1	20	8.45
34	60	0	1.8	0.3	0.2	1.6	0	3.6	20	4.55
35	180	-0.1	1.8	0	0.3	0	0.1	2	20	8.91
36	180	1.1	3.1	-0.5	0.3	0	0.5	3.8	20	4.27
37	10	-1.1	-0.3	-0.1	0.2	0	0	1.1	20	17.94
38	0	-1.2	-0.7	-0.1	0	0	-0.2	1.2	20	16.26
39	0	-1.2	-1	0	0	-0.1	0	1.2	20	15.19
40	80	-1.3	-2	-3	0	0	-1	2.6	20	6.57
41	0	-1.8	-1	-5	-0.1	-0.1	0.5	4.2	20	3.82

Table 2.6.7.3-10 $P_m + P_b$ Stresses—1-Foot Bottom Corner-Drop, Bolt Preload, and Internal Pressure

		Cylindrical Stress Components (ksi)							Allowable Stress	
Section	Angle	S_X	S_Y	S_Z	S_{XY}	S_{YZ}	S_{XZ}	SI (ksi)	(ksi)	MS
1	180	-0.9	1.2	-1	0.1	-0.1	-0.1	2.2	30	12.48
2	10	-2.6	-1.9	-0.2	0.1	-0.1	0.1	2.4	30	11.36
3	0	1.9	-2.4	-4.6	0.1	-0.5	0.3	6.5	30	3.58
4	0	-4.8	-4.3	-8.1	-0.1	-0.7	-0.9	4.3	30	6
5	180	-2.2	2.1	-0.4	0.4	0.2	-0.5	4.5	30	5.66
6	120	4.5	2.9	-0.3	-0.3	0	0.1	4.8	30	5.2
7	150	-2.2	1.3	-0.5	-0.1	0	0.6	3.6	30	7.26
8	0	0.9	-4.2	-6.5	0.5	-0.1	2.9	9.4	30	2.18
9	0	-3.3	-7	-11.3	0.5	-0.2	1.3	8.5	30	2.53
10	0	-0.5	-4.5	-6.6	0.4	-0.1	3.4	9.2	28.7	2.13
11	0	4.6	-2.8	-5.9	0.6	-0.2	3.1	12.3	28.7	1.34
12	0	-3	-2.6	1.8	0.1	-0.5	-2.2	6.6	28.7	3.35
13	10	-2.6	-2.2	3.3	0.1	-0.6	-0.7	6.1	28.7	3.67
14	0	-2.6	-6.4	-12.3	0.3	-0.6	-2.3	10.9	29.6	1.72
15	0	-5.4	-8.4	-15.9	0.3	-0.2	1.2	10.7	29.6	1.75
16	50	-0.1	3	-1.8	0	-2	-0.1	6.3	29.6	3.67
17	60	0	2.8	-1	0	-1.3	0	4.6	29.6	5.39
18	0	0	4.1	2.1	-0.4	0	0	4.3	29.6	5.94
19	0	0	3.9	2.7	-0.4	0	0	4.1	29.6	6.29
20	0	0	3.5	2.8	-0.4	0	0	3.6	29.6	7.16
21	0	0	2.5	2.3	-0.3	0	0	2.6	29.6	10.45
22	50	0	0.9	0.1	0	1.3	0.1	2.8	29.6	9.66
23	0	-0.4	-3.9	-6.2	0.4	-0.2	0.4	5.9	28.7	3.83
24	40	-0.2	1.2	-1.7	-0.1	-1.9	0	4.9	28.7	4.89
25	60	-0.1	3.3	-0.6	0	-1.4	0	4.8	28.7	5.01
26	0	-0.1	5.3	1.9	-0.5	0	0	5.5	28.7	4.24
27	0	-0.1	6	2.7	-0.6	0	0	6.2	28.7	3.60
28	0	-0.1	6.2	3	-0.6	0	0	6.4	28.7	3.48
29	0	-0.1	6.2	2.9	-0.6	0	0	6.3	28.7	3.52
30	0	0	6.2	2.1	-0.6	0.1	0	6.4	28.7	3.52
31	40	-0.1	3	-1	0	3	0	7.3	28.7	2.94
32	60	0.1	1	-1.6	0	1.3	0.1	3.6	30	7.29
33	70	-1.9	0.1	-2.4	-0.6	1	0.4	3.7	30	7.21
34	50	-0.1	1.6	-0.3	0	2.1	-0.1	4.6	30	5.54
35	70	-0.3	0.5	-0.6	0	1.4	1.5	4.1	30	6.26
36	180	-0.3	2.3	-2	0.4	0	0.3	4.4	30	5.83
37	0	-5.7	-5.3	-0.1	0	0	0	5.5	30	4.45
38	0	-4.4	-5.3	-0.2	0	0	-0.2	5	30	4.94
39	0	-3.1	-4.6	1.3	0	0	-0.4	5.9	30	4.11
40	0	-1.4	-6.4	-7.5	0.3	0	0.8	6.3	30	3.79
41	0	-0.3	-1	-7.2	0	0	0.9	7.1	30	3.2

Table 2.6.7.3-11 $P_m + P_b + Q$ Stresses—1-Foot Bottom Corner-Drop, Bolt Preload, Internal Pressure, Thermal Hot

		Cylindrical Stress Components (ksi)							Allowable Stress	
Section	Angle	S_X	S_Y	S_Z	S_{XY}	S_{YZ}	S_{XZ}	SI (ksi)	(ksi)	MS
1	0	-1.9	1.9	-1.2	-1	0.3	-0.4	4.5	60	12.29
2	180	2.5	2.9	-0.7	0	0	-0.1	3.6	60	15.87
3	0	0.4	-0.1	-8.4	-0.1	-0.9	0.5	9	60	5.69
4	0	6.3	-0.1	-5	0.2	-0.2	-0.3	11.4	60	4.25
5	20	-4	-9.2	-0.6	-1.4	-0.1	-0.5	9	60	5.66
6	50	-4.1	0.2	-0.6	-1.9	0	-0.1	5.7	60	9.46
7	40	-10.1	-5.9	-9.6	-2.6	-2.5	-3	10	60	4.98
8	0	3.4	-0.5	-3.9	-0.2	-0.5	4.5	11.6	60	4.18
9	0	-0.8	-4.8	-12.6	0.3	-0.8	-1.4	12.3	60	3.88
10	0	8.3	2.6	1	0	-0.6	5.3	12.9	57.4	3.44
11	0	3.4	-0.5	-3.9	-0.2	-0.5	4.5	11.6	57.4	3.95
12	50	-5.5	-1	3	-0.9	-0.4	-0.6	8.8	57.4	5.5
13	40	4.4	3.4	7.9	-2.2	-2.8	1.5	9	57.4	5.38
14	0	-0.6	-2.9	-14.1	0.2	-0.5	-1.6	13.9	59.1	3.25
15	0	-1.3	-4	-17.6	0.2	-0.2	0.8	16.3	59.1	2.62
16	0	-0.1	9.2	0.1	-0.9	0	0	9.5	59.1	5.25
17	0	-0.2	9.8	3.1	-1	-0.1	0	10.2	59.1	4.82
18	0	-0.2	9.8	4.5	-1	-0.1	0	10.2	59.1	4.8
19	0	-0.2	9.6	5.3	-1	-0.1	0	10	59.1	4.92
20	0	-0.2	9.4	5.9	-0.9	-0.1	0	9.8	59.1	5.06
21	0	-0.2	8.5	5.8	-0.8	-0.1	0	8.8	59.1	5.71
22	0	-0.1	5.7	4	-0.6	-0.1	-0.2	6	59.1	8.89
23	0	-0.8	-5	-13	0.4	-0.1	0.1	12.2	57.4	3.69
24	0	-0.5	-4.5	-10.4	0.4	0.1	0	10	57.4	4.76
25	0	-0.5	-6.4	-14.4	0.6	0	0	14	57.4	3.1
26	0	-0.5	-6.6	-15.1	0.6	-0.1	0	14.7	57.4	2.9
27	0	-0.3	-5.9	-14.5	0.6	-0.1	0	14.3	57.4	3.02
28	0	-0.3	-6	-14.2	0.6	0	0	13.9	57.4	3.12
29	0	-0.5	-6.4	-14.1	0.6	0	0	13.6	57.4	3.21
30	0	-0.5	-5.4	-12.4	0.5	-0.1	0	11.9	57.4	3.81
31	0	-0.3	-3.6	-7.9	0.3	-0.1	-0.2	7.6	57.4	6.56
32	50	-0.1	2.5	2.2	0	1.8	-0.1	4.2	60	13.13
33	40	1.2	2.1	3.5	-2.1	1.8	-0.5	6.1	60	8.89
34	0	-3	-5	-8.9	-0.2	-0.6	-1.8	6.9	60	7.66
35	60	-0.1	1	-5.9	0	1.6	0.7	7.8	60	6.74
36	70	5	2.2	0.8	1	1.4	0.8	5.7	60	9.44
37	30	-7.8	-8.1	-0.1	-1.5	0	0	9.3	60	5.45
38	60	-7.9	-5.8	-0.2	-0.3	0	-0.1	7.7	60	6.75
39	0	-1.4	4.4	-1.7	-0.3	-0.3	-1.3	7.3	60	7.26
40	70	-2.2	-2.4	-8.5	0.9	0.3	-0.6	7.1	60	7.41
41	60	-2.2	0.3	1.6	0	-1.1	-1.1	5.1	60	10.82

Table 2.6.7.3-12 $P_m + P_b + Q$ Stresses—1-Foot Bottom Corner-Drop, Bolt Preload, Internal Pressure, Thermal Cold

		Cylindrical Stress Components (ksi)							Allowable Stress	
Section	Angle	S_X	S_Y	S_Z	S_{XY}	S_{YZ}	S_{XZ}	SI (ksi)	(ksi)	MS
1	180	-2.2	0.6	-1	0.3	0	-0.2	2.9	60	19.42
2	10	-3.4	-2.6	-0.3	-0.1	-0.1	0.2	3.1	60	18.13
3	0	-5.5	-3	-11.7	-0.1	-1	-1	9.1	60	5.6
4	0	10.1	-1.9	-4.5	0.4	0.1	-1.3	14.9	60	3.04
5	10	-3.8	-6	-0.6	-0.4	-0.1	-0.4	5.5	60	9.95
6	135	-6.6	-3.1	-0.5	-0.3	0	0	6.1	60	8.87
7	180	-2.5	2	-0.7	0.5	0	0.7	4.8	60	11.44
8	0	2.3	-3.5	-8.7	0.3	-0.4	6.1	16.4	60	2.66
9	0	-3.8	-7.8	-15.9	0.3	-0.1	1.9	12.7	60	3.73
10	0	2.3	-3.5	-8.7	0.3	-0.4	6.1	16.4	57.4	2.5
11	0	2.3	-3.5	-8.7	0.3	-0.4	6.1	16.4	57.4	2.5
12	20	-3.8	-1.7	3.1	-0.3	-0.5	-1.6	7.7	57.4	6.45
13	20	11.4	4.9	10.8	-1	-1.6	2.5	9.5	57.4	5.04
14	0	-2.2	-5.8	-16.6	0.3	-0.6	-2.4	15.2	59.1	2.9
15	0	-3.5	-7.9	-22.1	0.4	-0.3	1.3	18.8	59.1	2.14
16	0	-0.1	8.8	-0.7	-0.8	-0.1	0	9.6	59.1	5.19
17	0	-0.2	9.6	2.4	-1	-0.1	0	10	59.1	4.94
18	0	-0.2	9.8	4	-1	-0.1	0	10.1	59.1	4.83
19	0	-0.2	9.6	4.9	-1	-0.1	0	10	59.1	4.92
20	0	-0.2	9.3	5.5	-0.9	-0.1	0	9.7	59.1	5.09
21	0	-0.2	8.3	5.5	-0.8	-0.1	0	8.6	59.1	5.84
22	0	-0.1	5	3.4	-0.5	-0.1	-0.2	5.2	59.1	10.32
23	0	-0.8	-7.3	-15.3	0.7	0	0.3	14.6	57.4	2.94
24	0	-0.5	-3.8	-11.6	0.4	0.1	0	11.1	57.4	4.16
25	0	-0.5	-6.4	-16	0.6	0	0	15.6	57.4	2.68
26	0	-0.5	-6.7	-16.8	0.6	-0.1	0	16.4	57.4	2.51
27	0	-2.8	6.4	-9.4	-0.8	0	0	15.9	57.4	2.61
28	0	-2.7	6.6	-8.9	-0.8	-0.1	0	15.5	57.4	2.7
29	0	-0.6	-6.5	-15.6	0.6	0	0	15.1	57.4	2.8
30	0	-0.6	-5.4	-13.7	0.5	-0.1	0	13.1	57.4	3.37
31	0	-0.3	-3.1	-8.3	0.3	-0.2	-0.2	8	57.4	6.13
32	40	-0.1	1.5	2.5	0	1.7	-0.1	3.9	60	14.51
33	40	0.6	1.7	3	-1.7	1.5	-0.4	5.2	60	10.5
34	0	-3.9	-5.5	-10.5	-0.2	-0.6	-2.1	8	60	6.52
35	0	0	-4	-6.9	0.3	0.2	0.5	7	60	7.56
36	80	6.1	2.6	2.4	0.6	0.8	0.7	4.7	60	11.72
37	30	-7.7	-7.9	-0.2	-0.9	0	0	8.5	60	6.04
38	180	-6.5	-7.3	-0.2	0	0	-0.1	7.1	60	7.49
39	0	-0.9	4.5	-1.3	-0.2	-0.3	-1	6.7	60	7.98
40	80	-1.9	-2.7	-8.1	0.6	0.2	-0.6	6.7	60	8
41	50	-0.3	0.8	4.5	0	-0.3	0.9	5.2	60	10.51

Table 2.6.7.3-13 Critical P_m Stress Summary (ksi)—1-Foot Bottom Corner-Drop, Bolt Preload, Internal Pressure

Component	Section	Angle	SI (ksi)	Allowable Stress (ksi)	Margin of Safety
1	3	0	5.2	20	2.82
2	8	80	4.2	20	3.78
3	11	0	10.4	19.1	0.84
4	14	0	5.4	19.7	2.65
5	16	50	5.2	19.7	2.77
6	22	70	2.1	19.7	8.41
7	23	20	3.8	19.1	4.03
8	28	90	4.1	19.1	3.7
9	31	40	5	19.1	2.81
10	36	180	3.8	20	4.27
11	40	80	2.6	20	6.57
12	41	0	4.2	20	3.82

Table 2.6.7.3-14 Critical $P_m + P_b$ Stress Summary (ksi)—1-Foot Bottom Corner-Drop, Bolt Preload, Internal Pressure

Component	Section	Angle	SI (ksi)	Allowable Stress (ksi)	Margin of Safety
1	3	0	6.5	30	3.58
2	8	0	9.4	30	2.18
3	11	0	12.3	28.7	1.34
4	14	0	10.9	29.6	1.72
5	16	50	6.3	**29.6**	**3.67**
6	22	50	2.8	29.6	9.66
7	23	0	5.9	28.7	3.83
8	28	0	6.4	**28.7**	**3.52**
9	31	40	7.3	28.7	2.94
10	34	50	4.6	30	5.54
11	40	0	6.3	30	3.79
12	41	0	7.1	30	3.2

Table 2.6.7.3-15 Critical $P_m + P_b + Q$ Stress Summary (ksi)—1-Foot Bottom Corner-Drop, Bolt Preload, Internal Pressure, Thermal Hot

Component	Section	Angle	SI (ksi)	Allowable Stress (ksi)	Margin of Safety
1	4	0	11.4	60	4.25
2	8	0	11.6	60	4.18
3	10	0	12.9	57.4	3.44
4	15	0	16.3	59.1	2.62
5	18	0	10.2	59.1	4.8
6	22	0	6	59.1	8.89
7	23	0	12.2	57.4	3.69
8	26	0	14.7	57.4	2.9
9	31	0	7.6	57.4	6.56
10	35	60	7.8	60	6.74
11	37	30	9.3	60	5.45
12	41	60	5.1	60	10.82

Table 2.6.7.3-16 Critical $P_m + P_b + Q$ Stress Summary (ksi)—1-Foot Bottom Corner-Drop, Bolt Preload, Internal Pressure, Thermal Cold

Component	Section	Angle	SI (ksi)	Allowable Stress (ksi)	Margin of Safety
1	4	0	14.9	60	3.04
2	8	0	16.4	60	2.66
3	10	0	16.4	57.4	2.5
4	15	0	18.8	59.1	2.14
5	18	0	10.1	59.1	4.83
6	22	0	5.2	59.1	10.32
7	23	0	14.6	57.4	2.94
8	26	0	16.4	57.4	2.51
9	31	0	8	57.4	6.13
10	34	0	8	60	6.52
11	37	30	8.5	60	6.04
12	41	50	5.2	60	10.51

2.6.7.4 One-Foot Oblique Drop

One foot is not a sufficient height to rotate the cask to an oblique orientation following a drop. Therefore, one-foot drops at oblique orientations are not considered as a credible event, and are not included in these analyses.

2.6.7.5 Impact Limiters

The Universal Transport Cask design includes removable upper and lower impact limiters to ensure that the design impact loads on the cask are not exceeded for any of the defined impact load conditions. These impact load conditions include the cask falling 1-ft or 30-ft and landing (1) on its side so that both impact limiters are impacted simultaneously, (2) vertically on one impact limiter at either end, or (c) obliquely (including C.G. over the corner) on one impact limiter at either end.

The impact limiters decelerate the cask by applying a force in a direction opposite to the motion of the cask. The deceleration force is generated by crushing the redwood and balsa wood materials of the impact limiter between the cask and the unyielding surface. The energy absorbed during crushing is net force, the vector sum of the cask weight (downward) and the deceleration force (upward) multiplied by the distance crushed. The amount of energy an impact limiter can absorb is calculated for various cask impact orientations, from vertical (0°) to horizontal (90°).

The impact limiter analysis is based on the assumptions that the cask impacts upon an unyielding surface and that the impact limiter remains in position on the cask during all impact events (The qualification of the impact limiter attachment is presented in Section 2.6.7.5.7).

2.6.7.5.1 Description of Impact Limiters

Each of the impact limiters on the Universal Transport Cask consists of 2 energy-absorbing materials: (1) redwood and (2) balsa wood. The wood is enclosed in a thin stainless steel shell to maintain the wood orientation during an impact. Figures 2.6.7.5-1 and 2.6.7.5-2 show the locations on the cask and the primary dimensions of the impact limiters. Figure 2.6.7.5-2 shows the cross section of an impact limiter. The upper and lower impact limiters are configured similarly, except that the upper limiter has pockets for the lifting trunnions and a larger inside diameter. The lower (bottom) impact limiter 1-ft end drop analysis conservatively includes the effect of backing afforded by the neutron shield shell bottom plate. This results in a larger backed area for the lower impact limiter, even though the bottom end of the cask body has a smaller diameter than the top end. Consequently, there is a higher calculated g-load than would result from considering only the diameter of the bottom end of the cask. The approximate radius used for the backed area of the bottom impact limiter is 46.2 inches. The approximate radius of the backed area of the top impact limiter is 43.6 inches.

The outside diameter of the Universal Transport Cask upper and lower impact limiters is 124.0 in. and the height is 43.0 in. The overlap between the cask body and the impact limiters is 11.0 in. Sixteen retaining rods 1.0 in. diameter, attach each impact limiter to the end of the cask. The attachments are described in detail in Section 2.6.7.5.7. The height of the redwood in the end section of the impact limiter is 30.0 in. A ring of balsa wood forms part of the end section of the impact limiter. The ring dimensions are inside diameter of 99.2 in., an outside diameter of 123.75 in., and a height 21.6 in. The bottom region of the impact limiter is a 1.5 in. thick layer of balsa wood that absorbs most of the kinetic energy in a 1-ft end-drop impact and limits the impact force for normal conditions of transport (1-ft drop). The low crush strength is necessary because the impact area is considerably greater in a flat end impact than in any other drop orientation. The redwood and the balsa wood side ring absorb most of the energy in a corner impact and all of the energy in a side impact.

The different segments and sections comprising each limiter are bonded to each other with DAP-Weldwood resorcinol adhesive.

For each of the impact load conditions in this analysis, the impact limiters remain in position on the cask and absorb the energy of the impact; thus, they limit the impact loads to the calculated values presented in Tables 2.6.7.5-1 and 2.6.7.5-2 and summarized in Table 2.6.7.5-3.

2.6.7.5.2 Load Conditions

The specific loading conditions for the impact limiters are defined by 10 CFR 71.71(c)(7), 10 CFR 71.73(c)(1) and Regulatory Guide 7.8, as follows:

1. 1-ft drop of the cask impacting at any angle from vertical (flat end) to corner (cask center of gravity directly above point of impact).

2. 1-ft drop of the cask in a horizontal orientation (side impact).

3. 30-ft drop of the cask in an end, side, corner, or oblique orientation.

On the basis of these loading conditions, the Universal Transport Cask impact limiters are designed for the 30-ft cask drops but with consideration of the effect of a 1-ft vertical drop. The maximum impact forces and the maximum crush depth for the 1-ft and 30-ft cask drops are

obtained from the RBCUBED analyses of the impact limiters. RBCUBED [33] is a proprietary NAC computer program used to perform impact limiter analyses (Section 2.10.1.2).

2.6.7.5.3 Tests of Impact Limiter Specimens

To adequately specify the redwood crush strength and density and their relationship to each other, NAC International conducted compression tests of specimens taken from redwood purchased from a commercial supplier for the fabrication of scale-model impact limiters. Sixty parallel-to-the-grain-direction and 59 perpendicular-to-the-grain-direction specimens from separate redwood boards (one specimen was accidentally destroyed) were tested. A density versus crush strength (at 0.4 in/in strain) plot of the test data results was constructed for each of the two crush directions. A strain value of 0.4 in/in was selected for use throughout this evaluation of redwood crush strength because it is a representative location of significant strain on the apparent plateau of the stress–strain curves for all of the redwood specimens.

On the basis of the density versus crush strength parallel-to-the-grain direction plot, 13 specimens with the highest densities and 2 specimens with the lowest densities were discarded from the database because they showed a significant scatter in crush strength values and inconsistent force-deflection plots, when compared with the specimens that were within the density criteria. An acceptable range of density for redwood, 23.5 ± 3.5 lb/ft^3, was established and only redwood with a density within this range is used in the Universal Transport Cask impact limiters. For the remaining 45 parallel and 44 perpendicular-to-the-grain-direction "statistical" specimens, the force and deflection test data were converted to stress–strain data by dividing the measured force by the cross-sectional area of the specimen and the deflection by the length of the specimen.

A "least squares" straight-line fit was calculated for each of the crush direction data sets to establish the design relationship between density and crush strength. An average crush stress–strain curve for the parallel-to-the-grain direction was calculated by summing and averaging the test data values for the appropriate 45 statistical specimens. Similarly, an average crush stress–strain curve for the perpendicular-to-the-grain direction was calculated for the appropriate 44 statistical specimens. Figures 2.6.7.5-3 and 2.6.7.5-4 show the average, design maximum, and design minimum crush stress-strain curves for redwood in the parallel and perpendicular-to-the-grain directions, respectively.

The cold (-40°F) crush stress-strain curve for redwood in the parallel-to-the-grain-direction was conservatively obtained from the nominal room-temperature crush stress-strain curve by ratioing the temperature effect shown in Figure 8 of NUREG/CR-0322 [34]. The design maximum crush stress-strain curve for redwood in the parallel-to-the-grain direction was determined by ratioing the cold crush stress-strain curve by 1.10 to account for the positive fabrication tolerance on the average crush strength of the redwood. Similarly, the design minimum crush stress-strain curve (for redwood in the parallel-to-the-grain direction) was obtained by ratioing the nominal, room-temperature crush stress-strain curve based on the +152°F temperature effect shown in Figure 8 of NUREG/CR-0322 with a factor of 0.90 to account for the negative fabrication tolerance.

The design maximum and minimum crush stress-strain curves for redwood (in the parallel-to-the-grain-direction) are used as the basis for the bounding impact limiter analyses in the RBCUBED program. On the basis of Figure 9 of NUREG/CR-0322, a dynamic load factor of 1.058 is used for redwood. The design maximum and minimum crush stress-strain curves for redwood are based on quasi-static test results but are used directly in the RBCUBED program as dynamic crush stress-strain data. The 1.058 dynamic load factor is applied to the specified static test data crush strength of the redwood used for the Universal Transport Cask impact limiters.

The average static crush stress ± 10% is used in conjunction with the "least squares" straight line for the data set to read off the equivalent density limits. The average of the density limits is the density value specified for each 30-degree pie-shaped section of redwood in the impact limiters.

The curve for the crush strength in the perpendicular-to-the-grain direction (Figure 2.6.7.5-4) was obtained from the compression tests of 44 specimens of redwood that were matched with the specimens used for the parallel-to-the-grain direction compression tests (one perpendicular-to-the-grain-direction specimen was accidentally destroyed). The same procedure as outlined previously was followed to establish the design maximum and minimum crush stress–strain curves for redwood in the perpendicular-to-the-grain direction. These curves are also used as the basis for the bounding impact limiter analyses.

On the basis of Figure 16 of JPL Technical Report No. 32-944 [35], the average crush strength of the balsa wood in the parallel-to-the-grain direction at room temperature is 1,550 psi for a density of 10 lb/ft^3. The room temperature crush stress-strain curve for balsa wood (Figure 2.6.7.5-5) is

determined on the basis of Figure 6 of JPL Technical Report No. 32-1295 [36] and the NAC-STC Safety Analysis Report [37]. The -40°F cold and the +152°F hot crush stress–strain curves are obtained by ratioing on the basis of Figure 15 of JPL Technical Report No. 32-944.

To account for crush strength fabrication tolerances, the -40°F cold case comparison stresses are factored by 1.10 and the +152°F hot-case compression stresses are factored by 0.90. The resulting design maximum and minimum crush stress–strain curves for balsa wood are also presented in Figure 2.6.7.5-5.

The variation of crush strength of redwood and balsa wood as a function of the angle between the impact direction and the grain direction of the wood is shown in Figure 2.6.7.5-6.

2.6.7.5.4 Specification for Universal Transport Cask Impact Limiters

The redwood material used for the Universal Transport Cask impact limiters must meet density, crush strength (converted from the force-deflection curve) and moisture content specifications. The density of any single redwood board shall be 23.5 ± 3.5 lb/ft^3. The density of any 15° or 30° pie-shaped section of redwood shall be 22.3 ± 1.2 lb/ft^3. Each 15°, pie-shaped section of redwood in the side segment of the impact limiter shall have an average static crush strength value (in the parallel-to-the-grain direction) of 5,898 ± 620 psi at 0.4 in./in. strain and 70°F. Each 30-degree, pie-shaped section of redwood in the end segment of the impact limiter shall have an average crush strength value (in the perpendicular-to-the-grain direction), of 1,190 ± 130 psi at 0.4 in./in. strain and 70°F. The dynamic load factor of 1.058 for redwood, previously discussed, is included in the design specification of the redwood used in the Universal Transport Cask impact limiters as a reduction in the density specified for any 15° or 30° pie-shaped section. The moisture content of any single board shall be greater than 5% but less than 15%. The average moisture content for the lot of redwood shall be less than 12%.

The balsa wood to be used in the Universal Transport Cask impact limiters shall meet the specifications of MIL-S-7998A [38]: (1) density between 7 and 10 lb/ft^3, and (2) moisture content between 5 and 15% for any one piece with an average of not more than 12% for any lot of balsa wood.

2.6.7.5.5 Method of Impact Limiter Analysis

The primary areas of analytical evaluation required in an impact limiter analysis are (1) crush depth, (2) maximum crush force, and (3) attachment to the cask. The crush depth and maximum crush force are dependent on the crush strength of the crushable material, the area engaged in crushing, the geometry of the impact limiter, and the energy to be dissipated.

Deceleration forces for the impact limiters are directly related to the area crushing and the crush strength of the limiter materials. An end-drop impact illustrates the area engaged in crushing. The cask and the unyielding surface are rigid and undeformable compared with the redwood and balsa wood materials. The redwood and balsa wood materials are trapped in place between the cask and the impacted surface over the end area of the cask.

The layer of balsa wood located in the end of the impact limiters is designed to absorb the potential energy of the cask for a 1-ft drop impact. The redwood, which has a higher crush strength, structurally restrains or "backs" the balsa wood which has the lower crush strength than the redwood. The redwood absorbs the kinetic energy of the cask in a 30-ft drop impact. During an end impact, a force imbalance occurs in the impact limiter between the layer of balsa wood at the bottom end and the redwood during crushing. The balsa wood at the bottom will crush until lock-up occurs. When lock-up occurs, the crush strength of the balsa wood increases and exceeds that of the redwood and crushing then begins in the redwood beneath the cask.

The cask gains kinetic energy while falling prior to contact of the impact limiter with the unyielding surface (Section 2.6.7.5.6 describes the kinetic energy gain in more detail). Some kinetic energy is dissipated in crushing the balsa wood at the bottom of the impact limiter. The remaining energy is absorbed by crushing the higher strength redwood between the cask and the impacted surface. The cask backs the higher strength redwood.

A NAC proprietary computer program, RBCUBED [33], is used to analyze an impact limiter for an impact event to determine the dynamics of the event, the forces generated during that event, and the depth of crush. A detailed description of this program is provided in Section 2.10.1.2.

On the basis of results of previous eighth-scale compression tests of the impact limiters for the NAC-STC cask, the measured quasi-static compression force in an end-impact orientation is

higher than the RBCUBED calculated values. This is a result of shearing across the grain of the redwood. Shearing acts in a plane surrounding the shear area. In an end-impact crush, the plane is a thin ring with a diameter equal to the diameter of the cask. Because the crush force is proportional to the backed area, the size of which depends on the square of the cask diameter, shearing becomes a much less significant part of the maximum force for the full-scale impact limiter.

The sequence of crushing and the backed area concept are initiated as the lower crush strength balsa wood is crushed to stack height to the outer edge of the impact limiter. Higher crush strength redwood beneath the cask in the backed region is then crushed. The redwood on the "other side" of the shear plane in the "unbacked" region is essentially uncrushed.

On the basis of previous evaluations for the NAC-STC cask impact limiters, the combination of the accurate prediction of measured impact limiter crush forces and the visual evidence in the sectioned eighth-scale impact limiter after the quasi-static test shows that only the backed area of the redwood is crushed.

The cask orientation for a corner impact is defined by the angle from vertical of the cask's longitudinal axis when the cask center of gravity is vertically aligned with the impact point on the limiter. For the Universal Transport Cask, this angle can vary from 23.35° to 24°, depending upon the cask configuration, i.e., which canister (class of fuel) is being considered.

The RBCUBED computer program is run for various combinations of redwood and balsa wood in impact limiter designs until satisfactory results are obtained. Two runs are then made for each impact orientation. One run is made using the cold maximum crush strength stress-strain values of redwood and balsa wood plus 10% fabrication tolerance to determine the maximum impact limiter crush force on the cask. A second run, using the hot minimum crush strength values of redwood and balsa wood minus 10% fabrication tolerance, is also made to determine the maximum crush depth of the impact limiter.

2.6.7.5.6 Impact Limiter Analysis

2.6.7.5.6.1 Potential Energy and Cask Drop Impact Motion

According to 10 CFR 71, analyses must show that a spent-fuel shipping cask is capable of sustaining a normal condition 1-ft free drop. This normal condition could be followed by a hypothetical accident 30-ft free drop. To preclude the possibility of a drop onto a previously impacted limiter, the cask will not be used after drop until the impact limiters have been replaced or repaired as necessary and an evaluation of the cask and contents has been completed.

To ensure that the center of gravity translates a minimum of 30 feet before an impact limiter contacts the unyielding surface, the distance that the cask free falls is measured from the nearest point on the cask (impact limiter) to the unyielding surface. Additionally, the cask is assumed to seek a stable orientation on both impact limiters after contacting the unyielding surface. After an end-drop, for example, the cask is assumed to tip over and reach a stable horizontal orientation. When at rest horizontally on the unyielding surface (a datum surface), the cask is considered to have zero potential energy.

Potential energy is calculated by multiplying the weight of the cask by the height of the center of gravity of the cask above the datum surface. The design weight of the Universal Transport Cask, contents, and impact limiters is 260,000 lb. For these analyses, the center of gravity along the longitudinal centerline of the cask is determined. The center of gravity is a datum point at which all of the mass (weight) of the cask is considered to be located.

Translational Motion-Side Drop

Figure 2.6.7.5-7 shows the cask in the horizontal or side drop position. When released (in this orientation) from 30 feet (360 in), the cask has 9.36×10^7 in.-lb of potential energy. As shown in Figure 2.6.7.5-7, the cask translates in the vertical direction and impacts on an unyielding surface. The deceleration forces created by crushing the impact limiters oppose the translational motion of the cask. Impact limiter crushing continues until all of the potential energy of the cask is absorbed, thereby decelerating the cask to rest. Both impact limiters crush simultaneously in a side drop; therefore, the cask is in a stable orientation following a side drop event.

In a side drop, the cask experiences only translational motion in the vertical direction. If the energy stored elastically in the impact limiter during deceleration is ignored, the dissipated energy equals the initial potential energy of the cask. During the side drop, both impact limiters are simultaneously engaged in decelerating the cask; therefore, each impact limiter absorbs one-half of the total cask energy ($9.36 \times 10^7 / 2 \cong 4.68 \times 10^7$ in-lbs).

Translational and End-Rotational Motion - End Drop

Figure 2.6.7.5-8 shows the cask in the end-drop position. End drops are drop angles that range between 0° (end-drop) and 23.35–24° (corner-drop) and characteristically show translational and end-rotational motion. As in a side drop, a cask in the end-drop position translates through a vertical distance of 30 feet and decelerates as a result of an impact on the unyielding surface. Deceleration forces acting on the end of the cask are symmetric and uniform for a flat end-drop; therefore, the cask remains vertical during deceleration and after the cask has come to rest. The energy absorbed by one impact limiter, while decelerating the cask during an end impact, equals the change in potential energy of the cask during the drop. The cask comes to rest in the vertical position on the crushed impact limiter.

Translational and Rotational Motion-Oblique Drops

Figure 2.6.7.5-9 shows the cask in an oblique-drop orientation. Evaluation of the critical angle for slapdown concludes that the angle of drop resulting in the maximum acceleration imposed on the cask corresponds to the side drop. The 75° drop is bounded by the side drop for the NAC-UMS design.

The slapdown effect is associated with free drop angles in which the transport cask assumes a near horizontal position (shallow angle). The leading end of the transport cask impacts the ground first followed by a translational and rotational motion. The translational motion is a consequence of the crushing of the limiter at the leading end. The rotational motion is a result of the moment of the cask weight acting at the cask CG about the leading end. The moment results in an angular acceleration and, therefore, an increasing angular velocity as the trailing end of the cask rotates towards the ground. The trailing end of the cask has not impacted the ground during this time and, therefore, does not contribute to the moment about the leading end of the cask. As a result, the trailing end of the cask derives its velocity from two terms; the translational velocity of the leading end of the cask with the addition of the cask's instantaneous angular velocity

factored by the length of the cask. The slapdown effect is associated with the increasing velocity of the trailing end of the cask. Depending on the geometry, the trailing end velocity can be greater than, or lesser than, the leading end initial impact velocity. If the velocity increase due to the angular rotation, contribution is less than the velocity decrease due to the translational deceleration, the trailing end velocity would be less than the initial impact velocity of the leading end. Likewise, with the reverse condition of these two contributions, the trailing end initial impact velocity would be larger than the leading end impact velocity, giving rise to an increased deceleration at the trailing end of the cask, which is commonly associated with the slapdown effect.

The ratio of cask length (L) to radius of gyration (r) is identified as the most important geometrical parameter affecting slapdown severity [58]. In the absence of friction, a cask with L/r less than two will not experience slapdown effects.

During the time between initial impact of the leading end impact limiter and the initial impact of the trailing impact limiter, the only forces acting on the package are the crush force and gravity. The crush force is normal to the impact surface and acts vertically upward through the point of rotation. The package weight acts downward through the center of gravity.

The radius of gyration (r) for the NAC-UMS transport package (loaded cask with impact limiters attached) is:

$$r = \sqrt{\frac{I}{m}} = \sqrt{\frac{6.573\times10^9}{260{,}000}} = 159.0 \text{ in.}$$

where

$I = 6.573\times10^9$ lb-in.^{2}, the mass moment of inertia about the point of rotation

$m = 260{,}000$ lb, the cask design weight

The overall length (L) of the package is 273.3 in. The ratio $\frac{L}{r} = \frac{273.3}{159.0} = 1.7 < 2$

With the L/r ratio being less than 2, in the absence of frictional forces, the shallow angle drop is bounded by the side drop.

The NAC-STC package configuration has been shown to be similar to the NAC-UMS® package configuration with respect to the L/r ratio and the impact limiters are identical in construction with identical outer diameters. Comparing the NAC-STC side drop (cask axis 90° from vertical) and oblique drop (cask axis 75° from vertical) test results, no indication of friction effects are observed. The drop impact angles and corresponding accelerations for the upper and lower impact limiters are:

NAC-STC Quarter-Scale Model Drop Test Results		
Limiter	**Drop/impact angle**	**Maximum acceleration**
Upper	90° (side drop)	250 g
Lower	90° (side drop)	200 g
Upper	75° (oblique drop)	225 g
Lower	75° (oblique drop)	200 g

The Sandia analysis indicates that frictional forces, because their lines of action do not pass through the package CG, can have a significant effect on the angular acceleration of the package. This frictional effect could contribute to the vertical acceleration of both the "leading" and "trailing" impact limiter accelerations. The Sandia work demonstrates that normalized leading end accelerations for the cask, with L/r = 2 for the inelastic spring model, are less than the side drop accelerations. However, for impact angles less than 15° (with respect to the horizontal), the peak trailing end accelerations are predicted to exceed both the peak leading end and side drop accelerations. The report concludes that this acceleration increase is probably due to friction at the trailing end during secondary impact.

Accelerometer data from the NAC-STC oblique drop test are shown in Figure 2.6.7.5-10 and Figure 2.6.7.5-11 for the accelerometers at the bottom (leading end) and top (trailing end), respectively. Figure 2.6.7.5-10 (leading end accelerometer) indicates that from initial impact, t = 0 until t = 0.02 sec, the leading impact limiter experiences an initial negative acceleration peaking at approximately –60g and returning to zero near t=0.02 sec. At this time the trailing end impact limiter (still not in contact with the impact surface) experiences (as shown in Figure 2.6.7.5-11) a positive rotational acceleration peaking at less than 50g between t = 0.02 and t = 0.045. The trailing end then impacts and undergoes a sharp negative acceleration peaking at near -225 g and returning to 0 g at t = 0.052 sec. During this same time period (between t = 0.045 sec and t = 0.05 sec) the leading end acceleration peaks at approximately 65g and returns to 0g at t = 0.052. All significant acceleration excursions of both the leading and trailing impact limiters

have ended by t = 0.06 sec and the packaging reaches equilibrium at rest in the horizontal position by t = 0.10 sec.

The test results from the NAC-STC oblique drop (15° with respect to the horizontal) demonstrate that the peak accelerations measured by the upper and lower accelerometers do not differ significantly, indicating that any angular acceleration imparted to the package as a result of friction is insignificantly small. Furthermore, all peak accelerations of either the leading or the trailing impact limiter are less than the peak acceleration of the upper impact limiter in the side drop condition (-250g).

2.6.7.5.6.4 RBCUBED Calculated Force-Deflection Plots

The computer program RBCUBED (see Section 2.10.1 for a detailed description of the program) calculates an initial velocity (as the limiter touches the unyielding surface), a backed area engaged in crushing, a crush force, an energy absorbed for a crush increment, an elapsed crush time, and a cask velocity at the end of the crush increment. The computation cycle is repeated until all the kinetic energy is absorbed and the end of the cask is stopped. RBCUBED calculates the energy dissipation necessary to stop the translational motion of the end of the cask that first contacts the unyielding surface (both limiters in the side-drop drop).

Figures 2.6.7.5-12 through 2.6.7.5-18 show the deceleration force as a function of crush depth, calculated by using RBCUBED for the full-scale cask impact limiters. Each curve illustrates the plus and minus tolerance energy absorption profile for either the upper or lower impact limits. Quasi-static tests performed on eighth-scale models of NAC-STC impact limiters further substantiate the RBCUBED calculated values. For the oblique drops, only the 75° drop orientations are shown (Figures 2.6.7.5-14 and 2.6.7.5-17) since these orientations produce the highest lateral deceleration component.

2.6.7.5.6.5 Results

Tables 2.6.7.5-1 and 2.6.7.5-2 present the results of the impact limiter design analyses for 1-ft drops and 30-ft drops, respectively. The calculated *g*-loads in the tables are based on the cold crush strength of -40°F plus 10% fabrication tolerance and on the hot crush strength at 152°F minus the 10% fabrication tolerance of redwood and balsa wood (calculated impact limiter temperature is 135°F). The weight of design basis cask 260,000 lb is used.

The calculated (RBCUBED) force-deflection curves for the Universal Transport Cask impact limiters for all drop orientations are shown in Figures 2.6.7.5-12 through 2.6.7.5-18. To verify the results, the area under the curves is calculated by the trapezoidal method. This area represents the energy dissipated for each of the cases, i.e., $E_{max} = 9.74 \times 10^7$ in.-lb for the upper impact limiter at minimum strength and $E_{min} = 9.65 \times 10^7$ in.-lb for the upper impact limiter for the maximum crush strength condition. The potential energy to be dissipated is the cask weight (260,000 lb) multiplied by the distance the cask drops (360 in. + 14.9 in. crush depth), i.e., $E_p = (374.9)(260{,}000) = 9.74 \times 10^7$ in.-lb.

The calculated and actual values compare within 0.41%, which indicates that the proper amount of potential energy is dissipated in the RBCUBED analysis. Multiplying the total crush area (the maximum area backed by the cask) by the crush strength of the impact limiters to determine the reacting force provides another check. This hand-calculated value of the reaction force compares within 3.0% of the RBCUBED calculated value for the lower impact limiter and within 1.65% for the upper impact limiter. These results verify both the energy absorption and the reaction force calculations of RBCUBED for the impact limiters.

With both impact limiters at their minimum allowable crush strength (maximum crush depth case), clearance is maintained between the neutron shield and the unyielding surface for the 1-ft and 30-ft side impacts.

An evaluation of the displacements obtained from the RBCUBED runs is as follows:

1. The RBCUBED run for the 30-ft side-drop drop assumes that the cask is a rigid element and does not include the trunnions; therefore, the displacement from the 30-ft drop must be analyzed, by referring to Figure 2.6.7.5-2, as follows:

   The depth of crushable redwood around the side of the top of the cask is 18.68 in. The height of the lifting trunnion is 4.88 in., so that a height of 13.72 in. of crushable redwood outside of the lifting trunnions remains. The RBCUBED run for a 30-ft side-drop drop calculates a crush depth of 10.8 in. for the maximum crush strength condition and 13.3 in. for the minimum crush strength condition. For the maximum crush strength condition, the compression ratio of the redwood at the trunnion location is 10.8/13.72 = 0.79, which corresponds to a stress of 26,899 psi in the redwood. The compression ratio of the

redwood away from the trunnion location is 10.8/18.68 = 0.518 in/in, which corresponds to a crush stress of 9,582 psi. The increase in crush stress resulting from the presence of the trunnion is therefore 26,899 - 9,582 = 17,317 psi. The area of the trunnion covered by the impact limiter is 19.2 in^2. The increase in the deceleration force resulting from the presence of the trunnion is (19.2)(17,317) = 332,486 lb. The total deceleration force at the trunnion location increases from 1.32×10^7 lb to 1.35×10^7 lb, thereby producing a deceleration increase of 1.05 *g* (2.0%) from 50.95 *g* to 52 *g*.

For the minimum crush strength condition, the compression ratio of the redwood at the trunnion location is 13.3/13.72 = 0.97, corresponding to a stress of 31,100 psi in the redwood. The compression ratio of the redwood away from the trunnion location is 13.3/18.68 = 0.71, which corresponds to a stress of 12,960 psi in the redwood. The increase in deceleration force resulting from the presence of a trunnion is (19.2)(31,110 - 12,960) = 348,288 lb. The total deceleration force increases from 1.28×10^7 lb to 1.31×10^7 lb, thereby producing a deceleration increase of 1.03 *g* (2.0%) from 49.57 *g* to 50.6 *g*. Thus, a side impact of the cask over a lifting trunnion has a minimal effect on the deceleration force.

2. The 30-ft flat top-end-drop of the Universal Transport Cask produces a deformation of 14.9 in. in the redwood for the minimum crush strength condition with a compression ratio of 14.9/30 = 49.7%. This value corresponds to a stress of 2,085 psi in the redwood. Similarly, the deformation of the redwood for the maximum crush strength condition is 11.4 in., with a compression ratio of 11.4/30 = 38%. This value corresponds to 2,244 psi. Both stress values are well below lock-up stresses, which start at a compression ratio of 69%.

3. For a 30-ft corner-drop on the upper impact limiter, the maximum impact force occurs with the crushable material at hot condition. For this condition, the crush distance is 31.1 in. The cask impact limiter depth in the 45-degree corner-impact orientation is 33.4 in. The maximum compression ratio of the impact limiter is 31.1/33.4 = 93% for the upper impact limiter for the minimum crush strength condition. Thus, balsa wood lock-up occurs, but only in a very local region. The calculated average compression stress is 2,229 psi. Similarly, the crush depth for the maximum crush strength condition is 27.5 in. (82%) with a calculated average compression stress of 1,939 psi.

4. The cask analysis for these impact conditions is based on the maximum deceleration (*g*) derived from the RBCUBED results. Because of the higher crush strength of the redwood and balsa wood in the cold condition, the critical condition for maximum deceleration for any 1-ft drop is for the maximum crush strength condition. No lock-up occurs in the redwood and balsa wood for the minimum crush strength condition for a 1-ft drop. The critical deceleration condition for a bottom end impact is the maximum crush strength (cold) condition; the critical deceleration condition for a top end impact is also the maximum crush strength (cold) condition, where lock-up in the redwood occurs because of the high compression ratio. The critical deceleration condition for the bottom and top corner impacts is the minimum crush strength (hot) condition, in which local lock-up in the redwood and balsa wood occurs. The critical deceleration condition for a side-drop drop is the maximum crush strength (cold) condition.

The calculated *g*-load factors (deceleration values) determined by the RBCUBED analyses, which correspond to the bounding values for crush and acceleration, are summarized in Table 2.6.7.5-3. Acceleration values using wood properties at 70°F are shown in Table 2.6.7.5-4.

2.6.7.5.7 Impact Limiter Attachment Analysis

The following design criteria apply to the method of attaching the impact limiters to the cask body.

1. The impact limiters must remain attached to the cask body during normal handling and transport. Satisfaction of this criterion ensures that the limiters will be in a proper position to perform their impact-limiting function in the event of a free drop (normal or accident).

2. In a free drop (normal or accident), the limiter (or limiters) making initial contact with the unyielding surface must remain in position on the cask for the full duration of the initial impact. Satisfaction of this criterion ensures that the limiter(s) will be able to properly perform the impact-limiting function.

3. In a free drop (normal or accident) involving an initial impact on a single impact limiter, the limiter on the opposite end of the cask must remain attached to the cask during the initial impact. Satisfaction of this criterion ensures that the limiter will be

in a proper position to perform its impact-limiting function in a subsequent secondary impact following the initial impact.

Sections 2.6.7.5.7.1 through 2.6.7.5.7.3 demonstrate that each of these criteria is satisfied.

2.6.7.5.7.1 Impact Limiter Attachment During Normal Handling and Transport

Attachment of the impact limiters to the cask body during normal handling and transport operations is ensured by demonstrating that the attachment hardware does not yield under normal handling and transport conditions. The worst-case loading associated with normal handling and transport is a 7.5-*g*-load corresponding to the peak longitudinal shock loading expected as the result of rail transport (as specified by the Field Manual of the AAR [31]).

The design load, P, on the attachment is P = (7.5)(8,846) = 66,345 lb, where 8,846 lb is the weight of each impact limiter.

Analysis of Retaining Rods

Sixteen 1.25-in. diameter retaining rods are equally spaced on a bolt circle diameter of 81.8 in. for the upper limiter and 71.0 in. for the lower limiter. The attachment geometry of the impact limiters is shown in Figure 2.6.7.5-19. The retaining rods are SA-193, Grade B8S stainless steel with a yield strength of 39.8 ksi and a design stress intensity (S_m) of 13.0 ksi at 200°F (Table 2.3.5-3).

The load on each retaining rod resulting from a longitudinal shock load of 7.5 *g* is given as

$$P = 66{,}345/16 = 4{,}147 \text{ lb per retaining rod.}$$

The retaining rod tensile area is 0.606 in^2 in the threaded region, resulting in a tensile stress of:

$$S_t = 4{,}147/0.97 = 4{,}275 \text{ psi}$$

Each retaining rod nut is torqued to 75 ± 5 ft-lbs, resulting in a preload of 2,560 lbs. Therefore, the preload stress is (2,560 lb/0.969 in^2 =) 2,642 psi. The total stress for the longitudinal shock load of 7.5g is, therefore, 4,275 + 2,642 = 6,920 psi (6.9 ksi). For the retaining rods, the allowable stress is twice S_m, or 2 x 13.0 = 26.0 ksi. The Margin of Safety (MS) is:

$$MS = (26/6.92) - 1 = +2.76$$

Analysis of Retaining Rod Anchorage

The nut of the retaining rod is bearing on a washer that has a diameter of 5.0 in. and a thickness of 0.50 in. The washer is bearing on the bearing plate portion of the impact limiter shell, which bears on the redwood material.

The load on each of the 16 retaining rods resulting from the normal transportation acceleration is 4,147 + 2,560 = 6,707 lb . The bearing area between the bearing plate and the redwood material is:

$$A = (\pi/4)(5.0^2 - 3.0^2) = 12.57 \text{ in}^2.$$

The bearing pressure is:

$$p = 6{,}707/12.57 = 534 \text{ psi}$$

The perpendicular-to-the-grain compressive stress in the redwood at 2.5% strain is 750 psi. The margin of safety for compression of the redwood is

$$MS = (750/534) - 1 = +0.41.$$

The washer is made of Type 304 stainless steel and has a 1.31-in.-diameter hole in the center. It is analyzed by assuming that it is simply supported along a circle having a diameter equal to the edge of the hole in the bearing plate (3.00 in.). The total load of 6,707 lb is distributed along the edge of the nut, which has an average diameter of 1.939 in. From Roark, Table 24, Case 1a, [28], the stress on the washer is:

$$S_{max} = \left(\frac{12Wa^2}{\left(a - \frac{b^2}{a}\right)t^2}\right)\left[\frac{r_0}{a}\left\{\frac{1+\nu}{2}\ln\left(\frac{a}{r_0}\right) + \frac{1-\nu}{4}\left[1 - \left(\frac{r_0}{a}\right)^2\right]\right\}\right] = 24.4 \text{ ksi}$$

where:

$a = 1.50$ in.	$b = 0.655$ in.
$t = 0.50$ in.	$\nu = 0.31$
$r_0 = 0.9695$ in.	$W = (6{,}707/(2\pi \times 0.9695)) = 1{,}101$ lb/in.

The yield strength of Type 304 stainless steel is 25.0 ksi at 200°F. The margin of safety is calculated MS = 25.0/24.4 - 1 = + 0.02.

The positive margins of safety show that the attachment of the impact limiters is adequate during normal conditions of transport.

Evaluation of Impact Limiter Attachment for Vibration

During normal conditions of transport, the impact limiter attachment may be subjected to vibration induced from the combination of component natural frequency and a dynamic load forcing function dependent on the transport media. Design of the impact limiter attachment eliminates the potential for the postulated vibration loading to loosen the impact limiter attachment. Lock nuts are installed in back of each of the retaining rod attachment nuts to prevent them from becoming loose. Locking wires installed between sets of two retaining rods eliminate rotation of the impact limiter retaining rods relative to their anchorage. The combination of these two design features eliminates the potential for the impact limiter attachment to become loose as a result of postulated vibration loading during transport.

2.6.7.5.7.2 Response of Impacted Limiters During Initial Impact of Package with Ground

The second criterion applicable to the impact limiter attachments requires that the impact limiter making initial contact with the unyielding surface must remain in position on the cask for the full duration of the initial impact. To satisfy this criterion, the impact limiter(s) being crushed must not separate from the cask, although the attachment hardware (mounting plate and bolts) may fail during the impact event.

The ability of the NAC-STC impact limiter to remain in position during an impact was demonstrated with reference to several static compression tests of the NAC-STC, during which the only attachment mechanism was a strip of duct tape. All of the compression tests were performed by using eighth-scale models of the impact limiters. The results of these tests are applicable to the Universal Transport Cask.

Analytic evaluations are performed to further justify that the initially impacted Universal Transport Cask impact limiter remains in position during an impact event and properly perform its function. Results of evaluations indicate that the attachment hardware is not expected to fail

significant resistance to the applied separation moment exists as a result of a combination of crushing of the limiter at the cask interface and also as a result of frictional resistance that exists at the interface. This total resistance is calculated to be greater than the applied separation moment.

2.6.7.5.7.3 Response of Secondary Impact Limiter During Initial Imp-act of Package

The final criterion to be satisfied is that for a free drop (normal or accident) involving an initial impact on a single impact limiter. The limiter on the opposite end of the cask (secondary limiter) must remain attached to the cask during the initial impact, thus ensuring that the secondary limiter is in position to absorb the secondary impact. As discussed in Section 2.6.7.5.7.2, the secondary limiter remains in position for the full duration of the secondary impact and performs its impact-limiting function. Attachment is ensured by demonstrating that the attachment hardware (mounting plate and retaining rods) does not fail during the initial impact.

During a free drop of the cask (normal or accident) involving an initial impact on a single impact limiter, i.e., flat end, center of gravity over corner, or any oblique drop, the ground exerts an upward force on the impact limiter that strikes it. The impact limiter in turn exerts an upward force on the cask body, thus decelerating the cask body. The cask body exerts an upward force on the secondary impact limiter and decelerates it. This scenario is repeated during a rebound of the whole package: the ground exerts an upward force on the impact limiter that strikes it; the impact limiter that strikes the ground exerts an upward force on the cask body and the cask body exerts an upward force on the secondary impact limiter, thereby accelerating the whole package upwards. When the entire package is in the air, its components (the impact limiter, the cask body, and the secondary impact limiter) move with the same acceleration and velocity; no other force acts among them. Thus, it is evident that during a free-drop impact on the first impact limiter, no separation force exists between the cask body and the second impact limiter. The absence of separation forces ensures that the second impact limiter stays in position to absorb the second impact.

Analysis of the impact limiter mounting plate and retaining rods demonstrates that the impact limiter attachments provide significant resistance to any unspecified separation force on the impact limiter. This analysis provides further evidence that the secondary impact limiter will stay attached to the cask body to absorb the second impact.

Figure 2.6.7.5-1 Universal Transport Cask with Impact Limiters

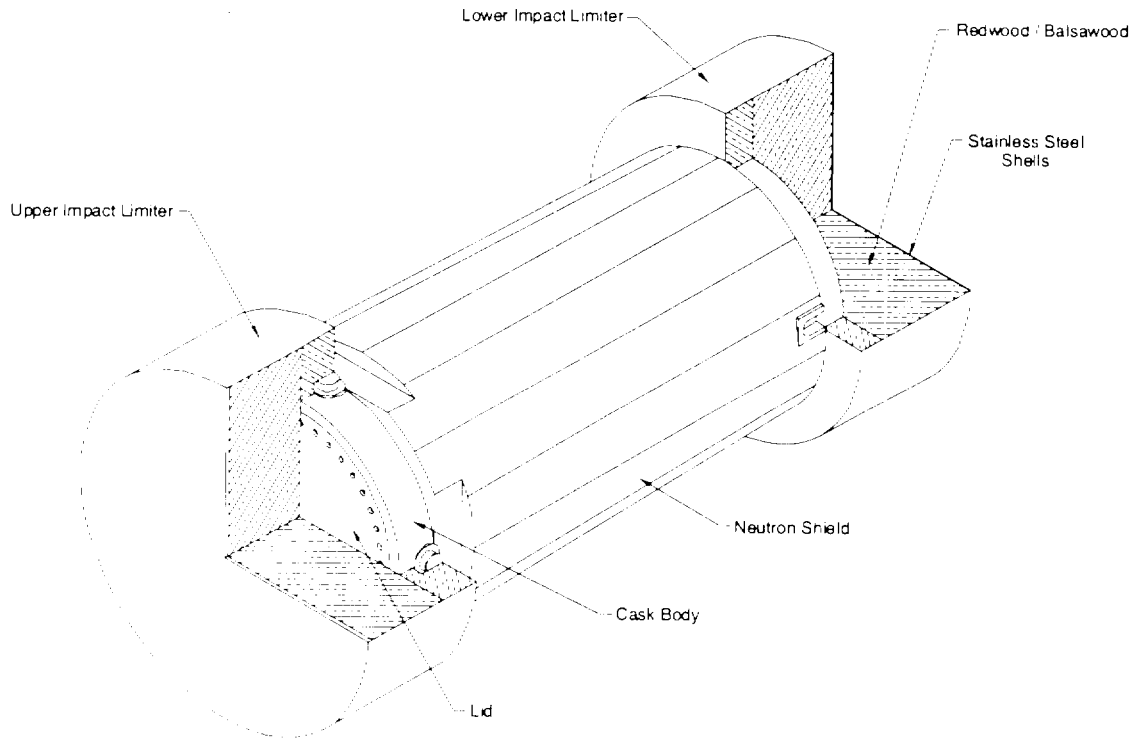

Figure 2.6.7.5-2 Cross Section of Lower Impact Limiter

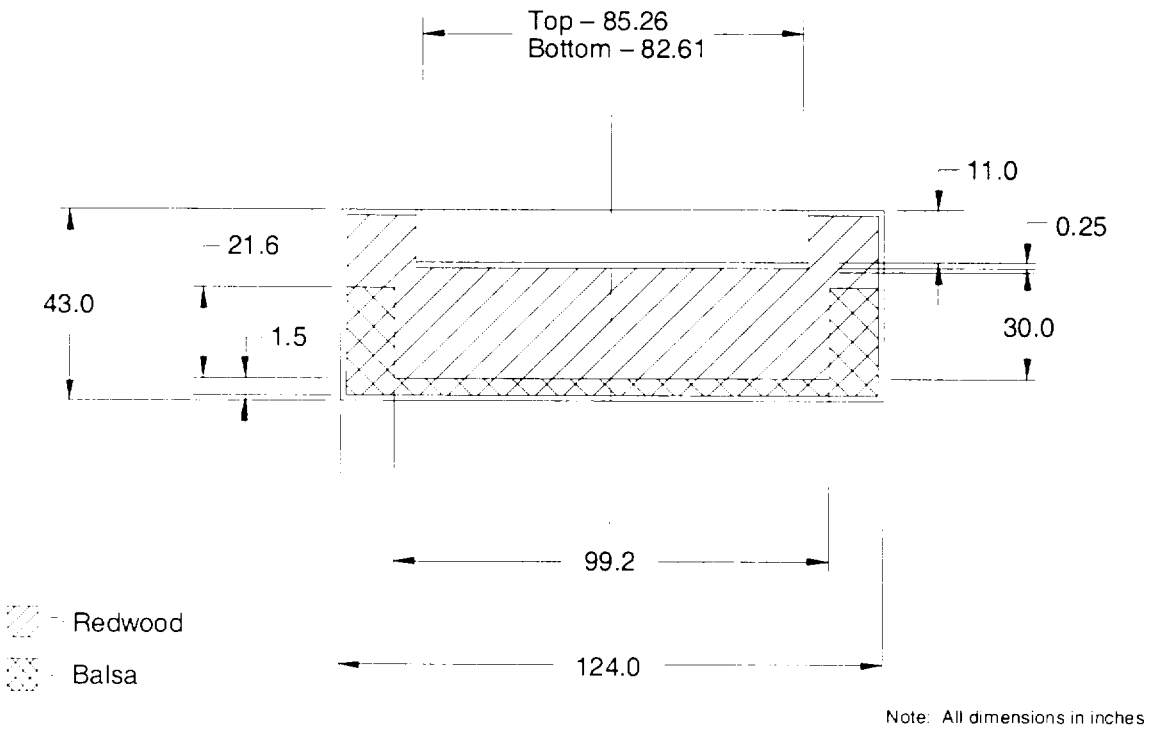

Figure 2.6.7.5-3 Crush Stress-Strain Curves for Redwood (Crush Strength Parallel to Grain)

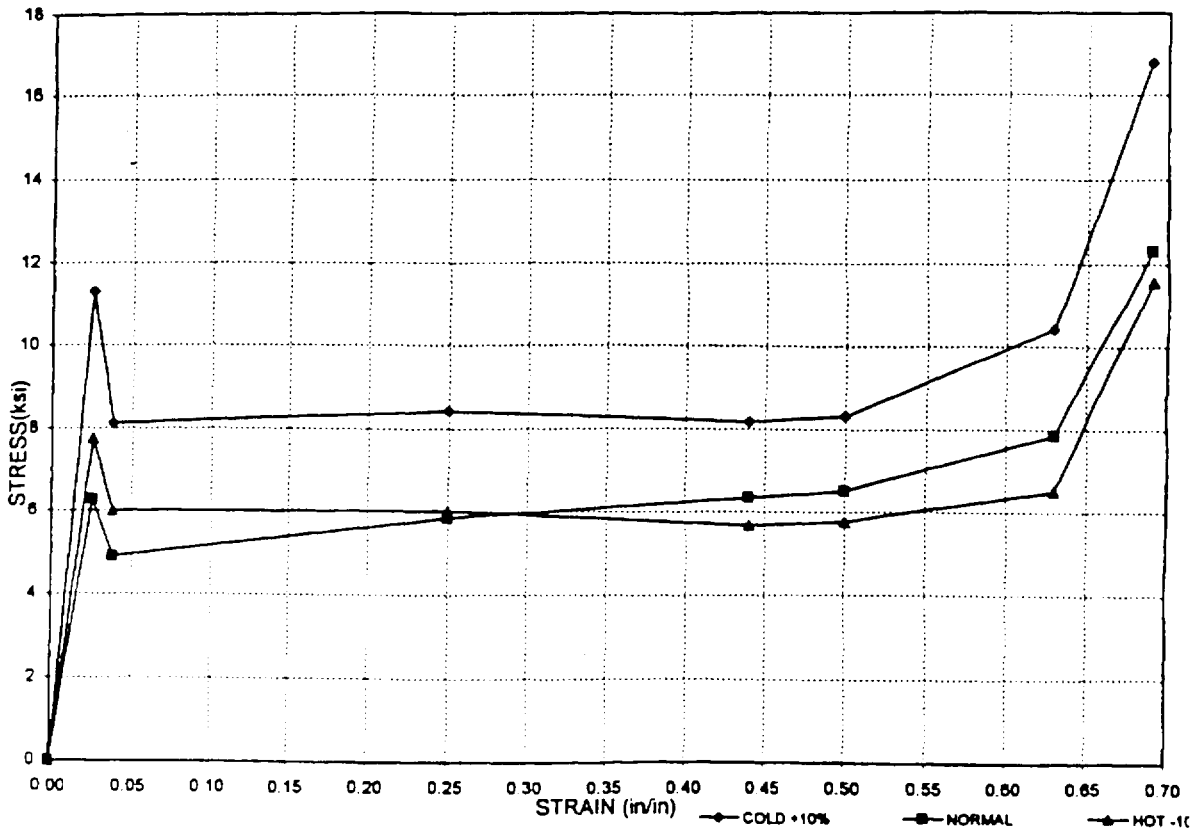

Figure 2.6.7.5-4 Crush Stress-Strain Curves for Redwood (Crush Strength Perpendicular to Grain)

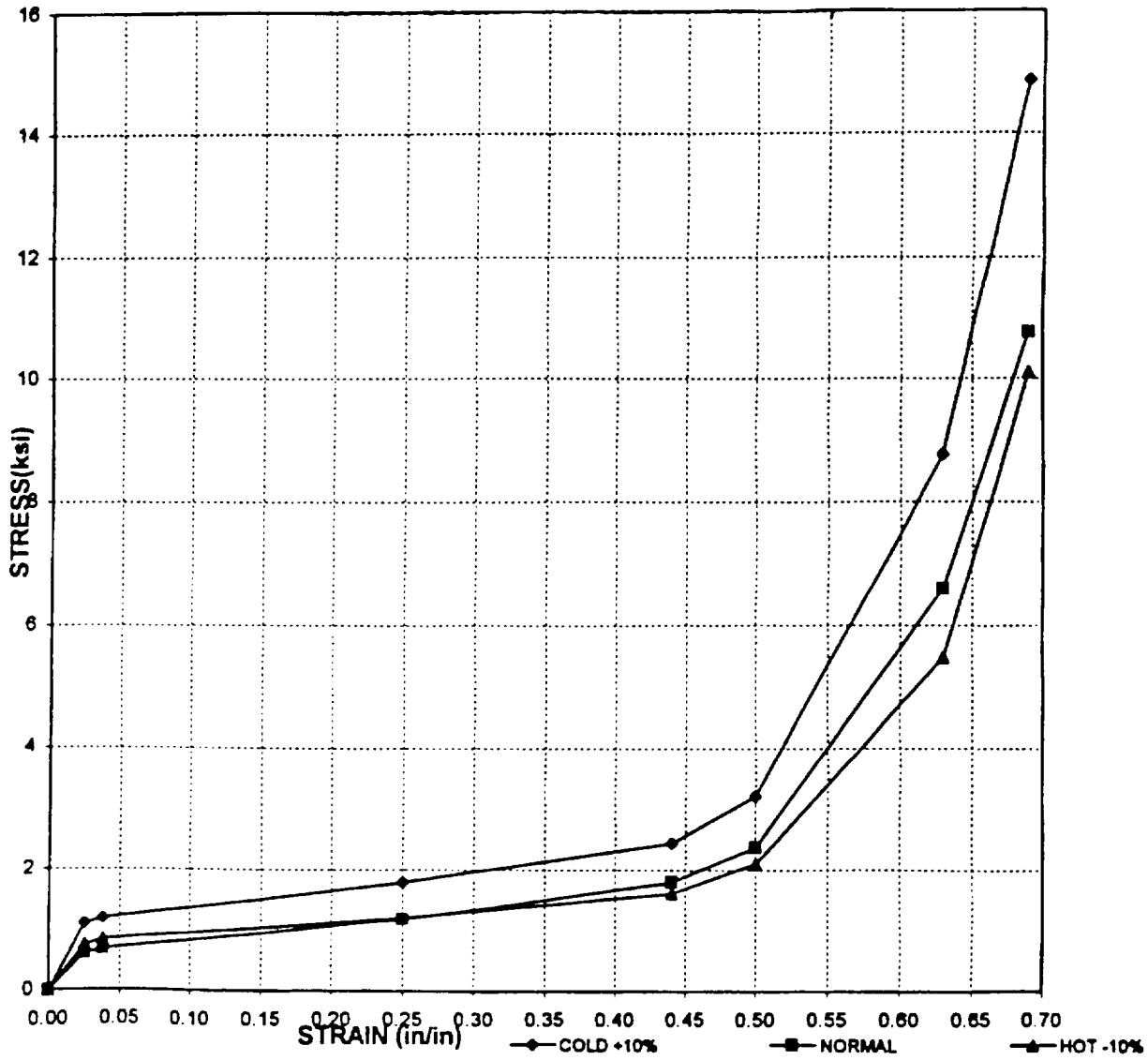

Figure 2.6.7.5-5 Crush Stress-Strain Curves for Balsa Wood (Crush Strength Parallel to Grain)

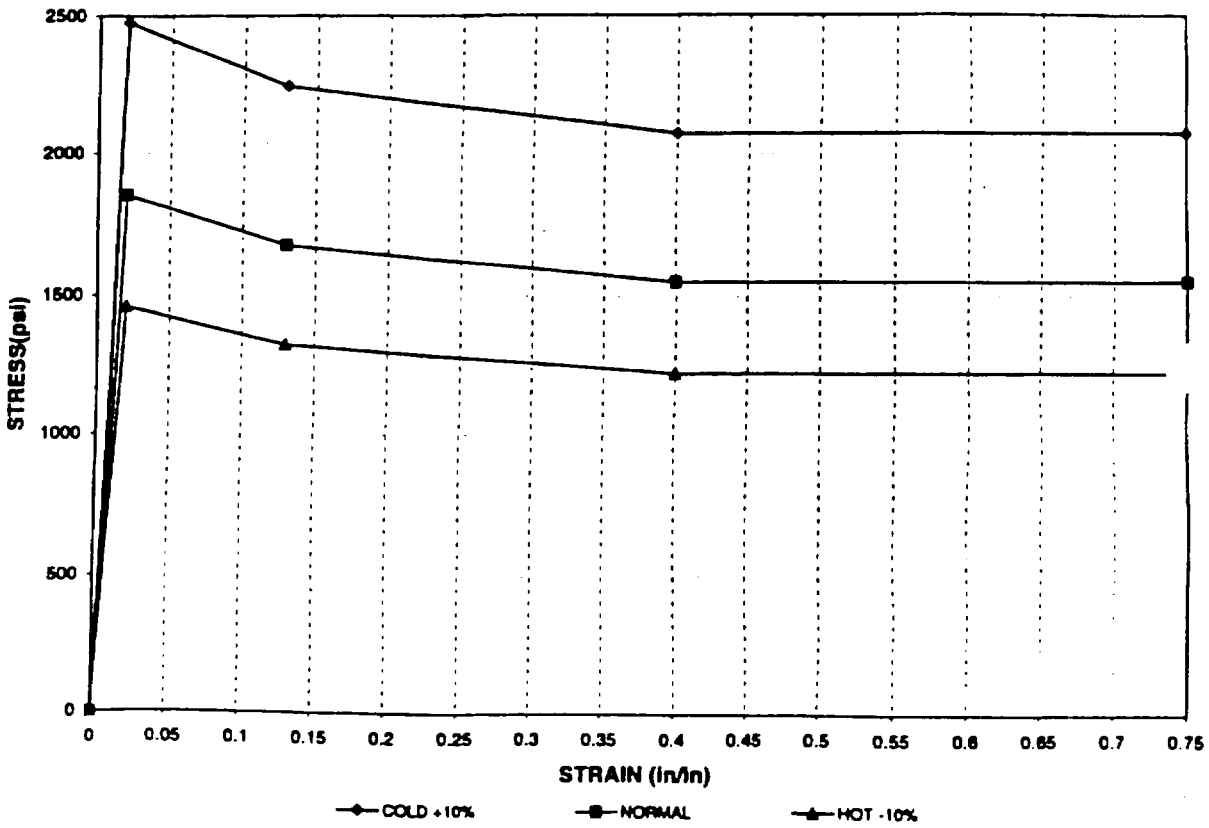

Figure 2.6.7.5-6 Variation of Crush Strength of Redwood and Balsa Wood with Impact Angle at 40 Percent Strain

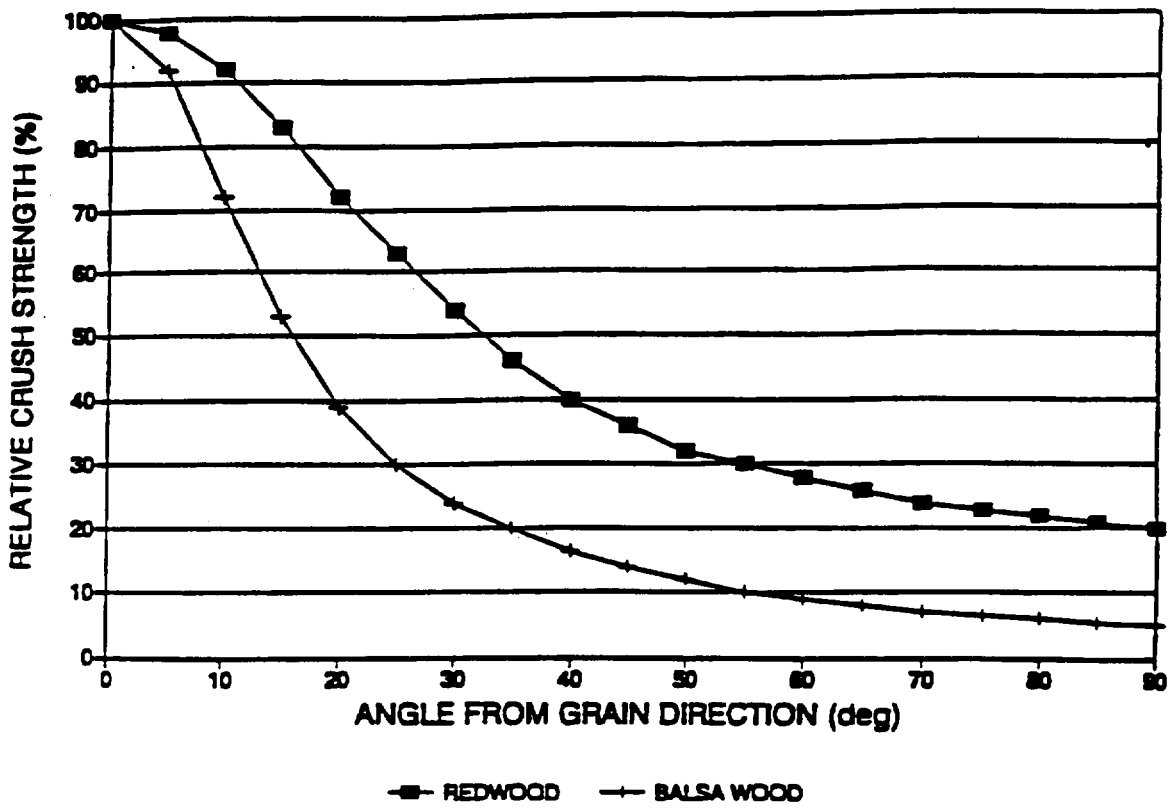

Figure 2.6.7.5-7 Cask Side-Drop Geometry

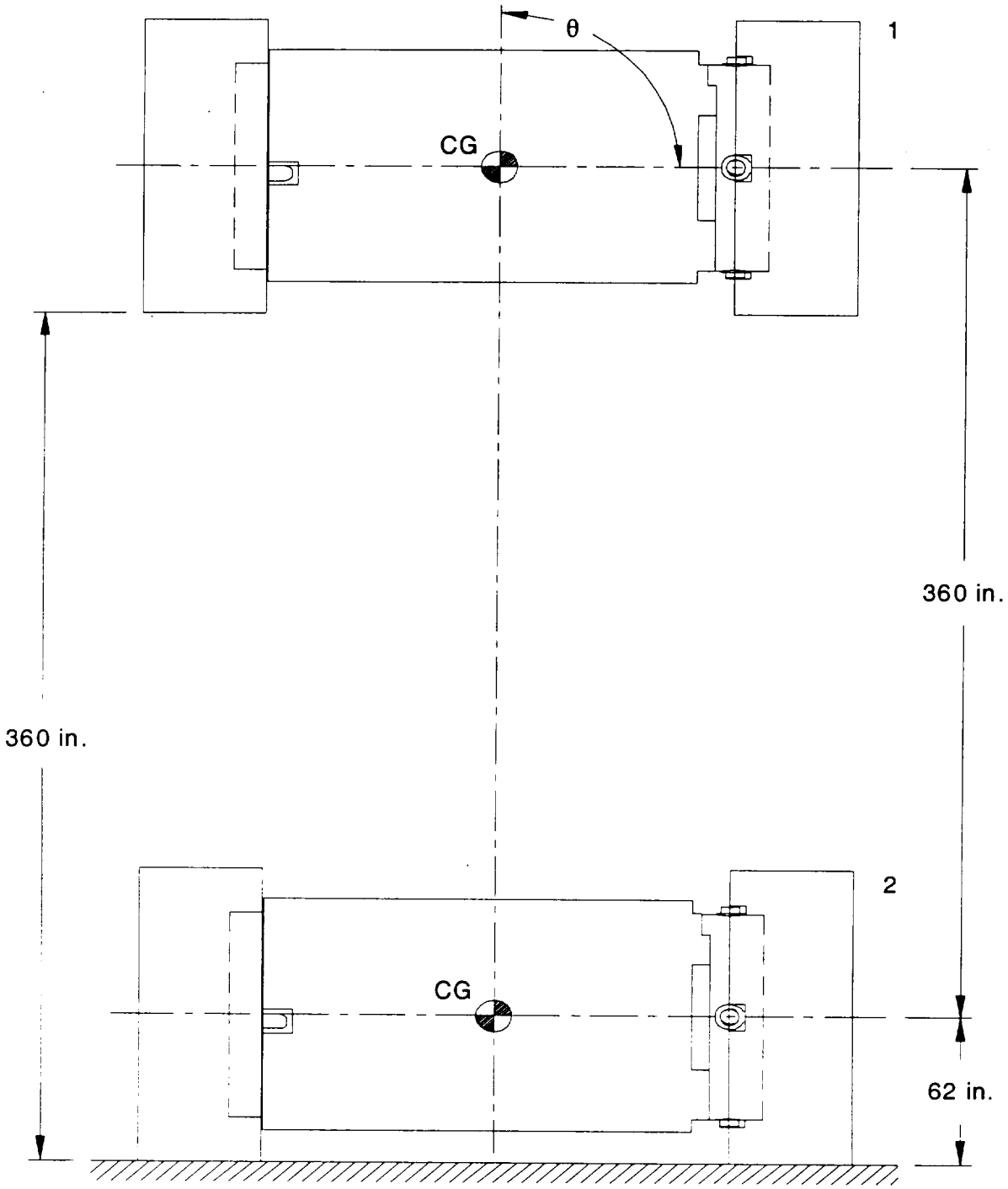

Figure 2.6.7.5-8 Cask End-Drop Geometry

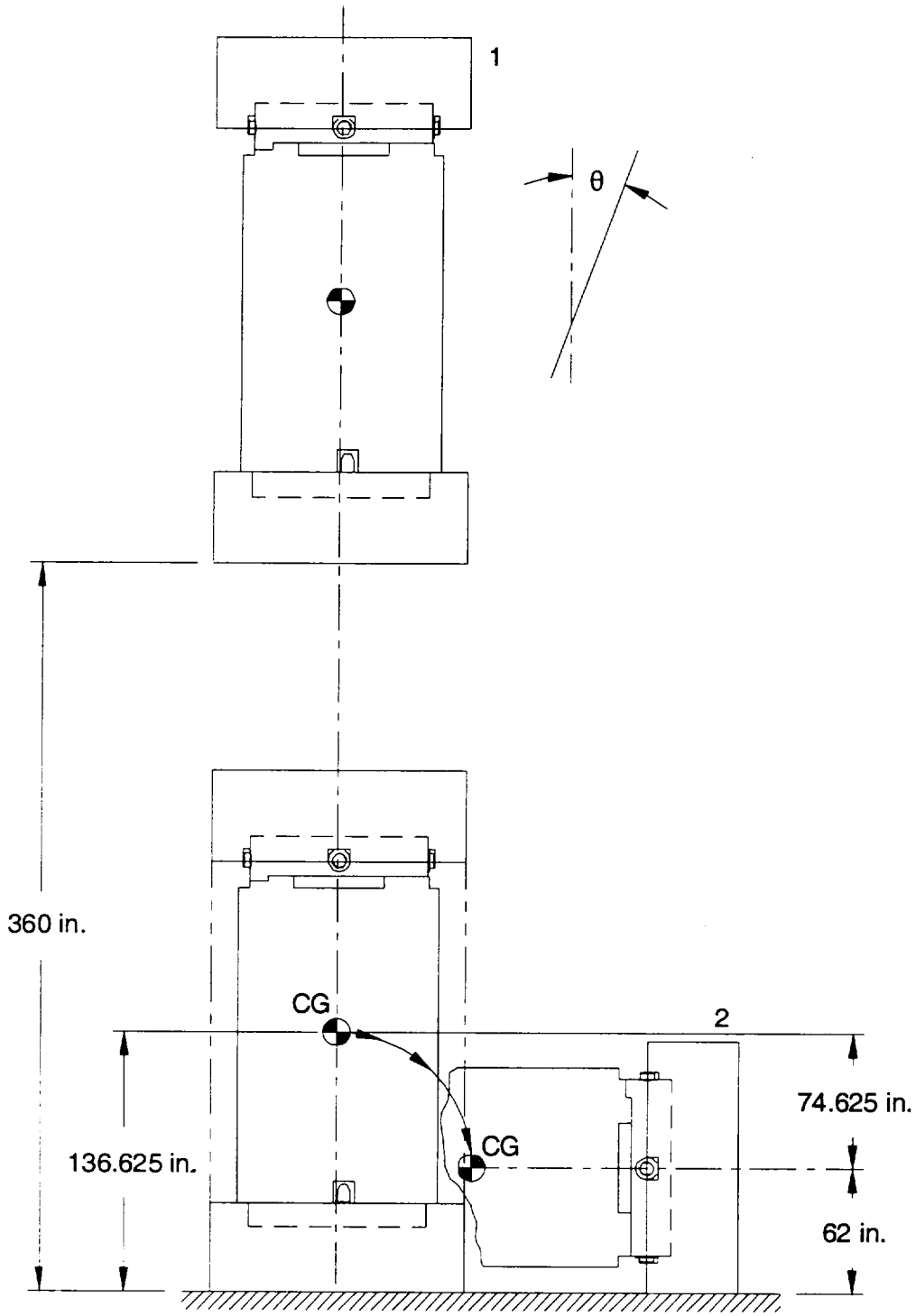

Figure 2.6.7.5-9 Cask Oblique-Drop Geometry

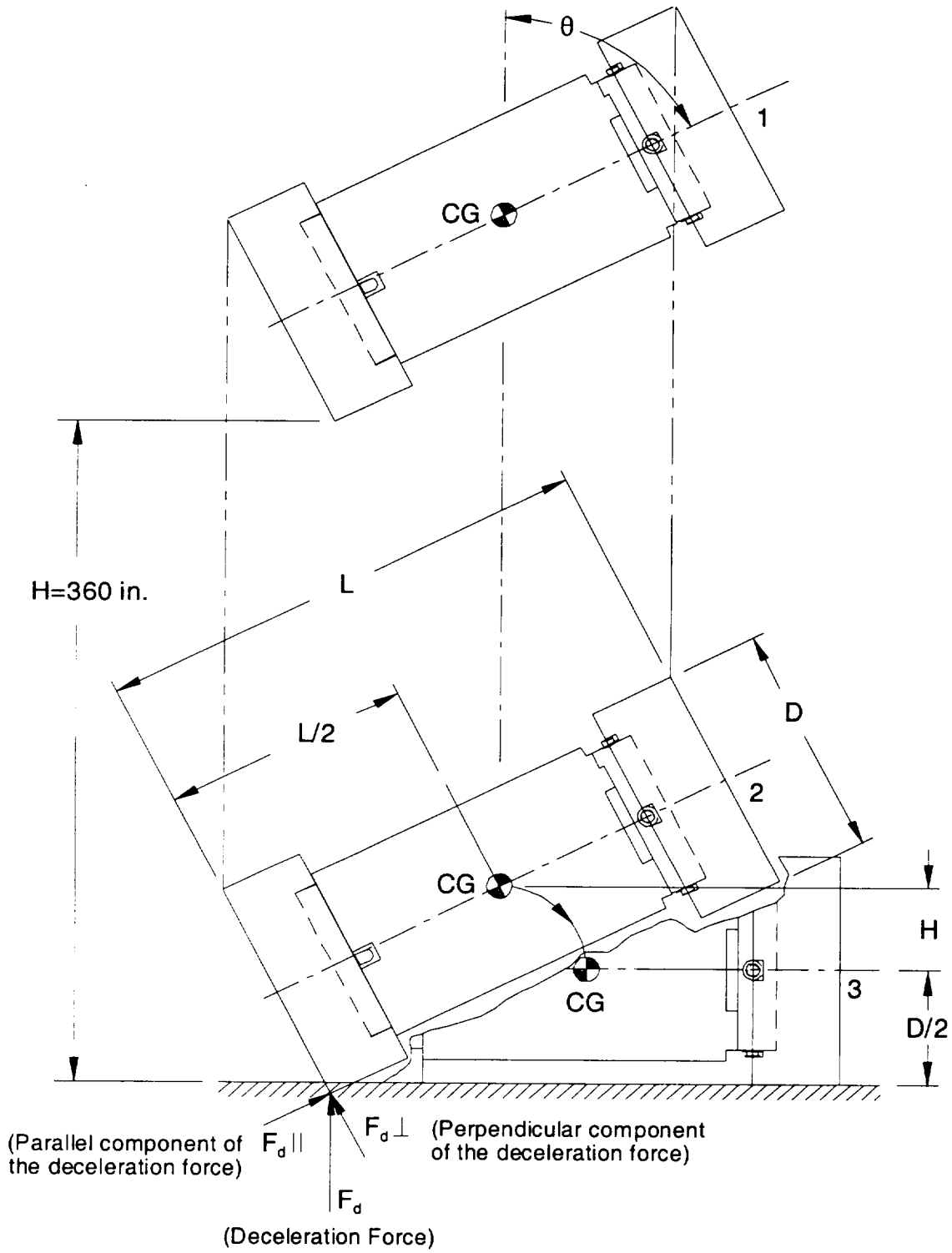

Figure 2.6.7.5-10 Accelerometer Time History at the Bottom of the NAC-STC 1/4-Scale Model Cask (75° Oblique Drop)

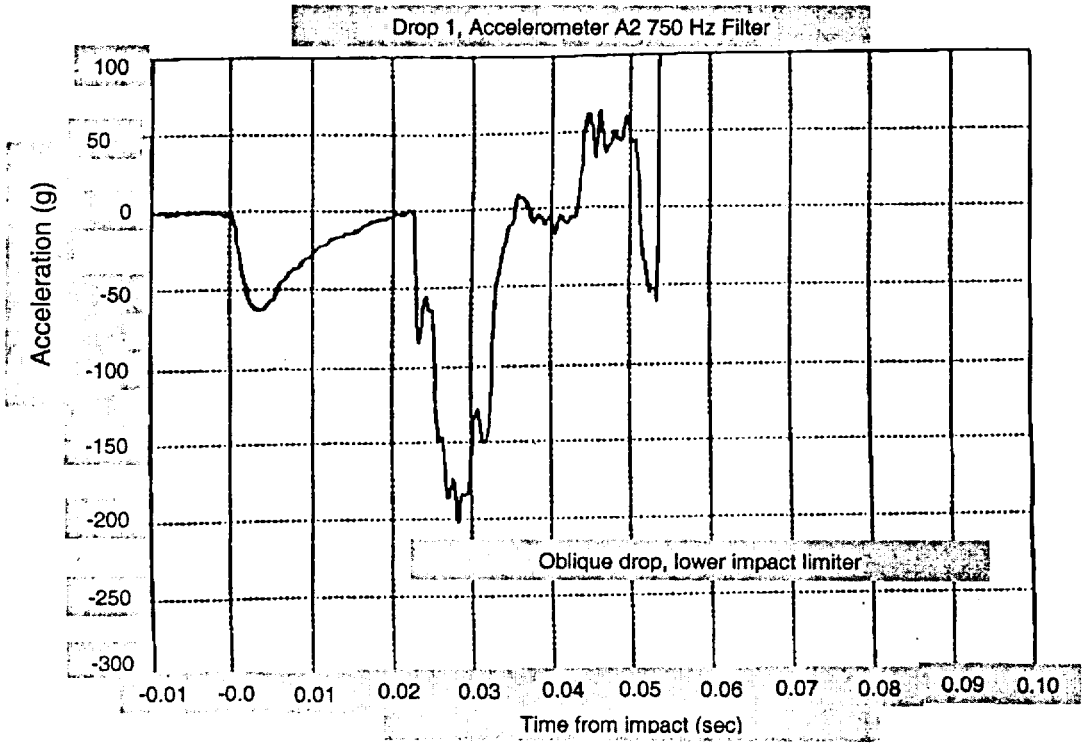

Figure 2.6.7.5-11 Accelerometer Time History at the Top of the NAC-STC 1/4-Scale Model Cask (75° Oblique Drop)

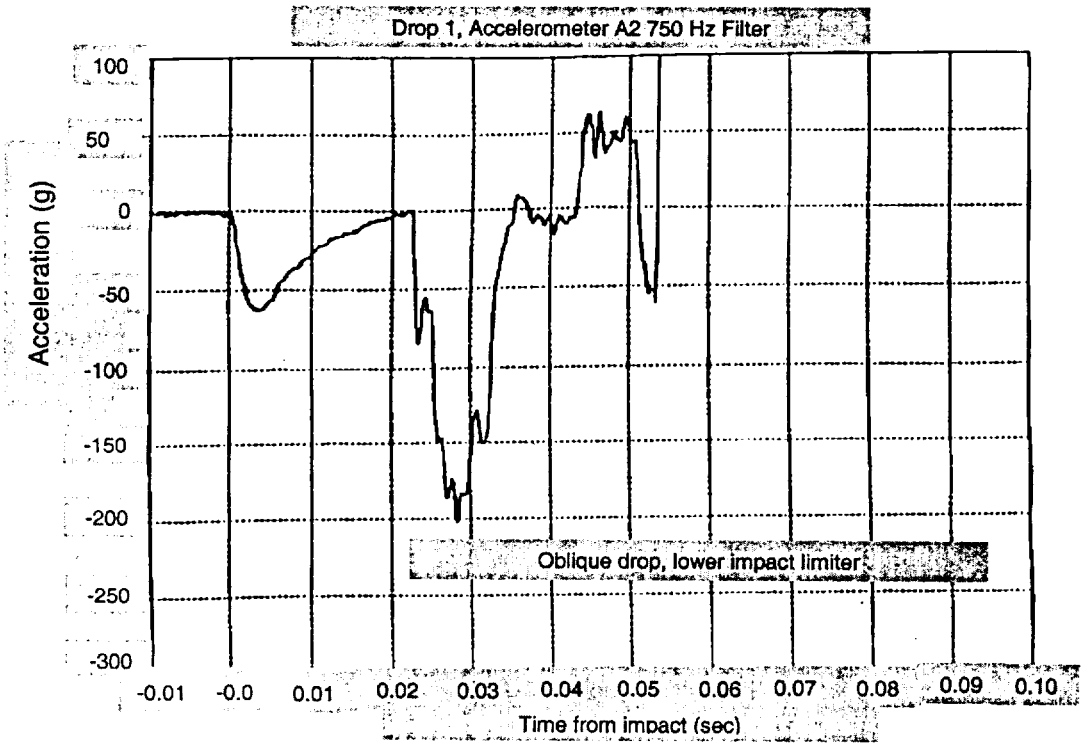

Figure 2.6.7.5-12 Force-Deformation Curve - Lower Impact Limiter (Bottom End Impact, 0 Degrees)

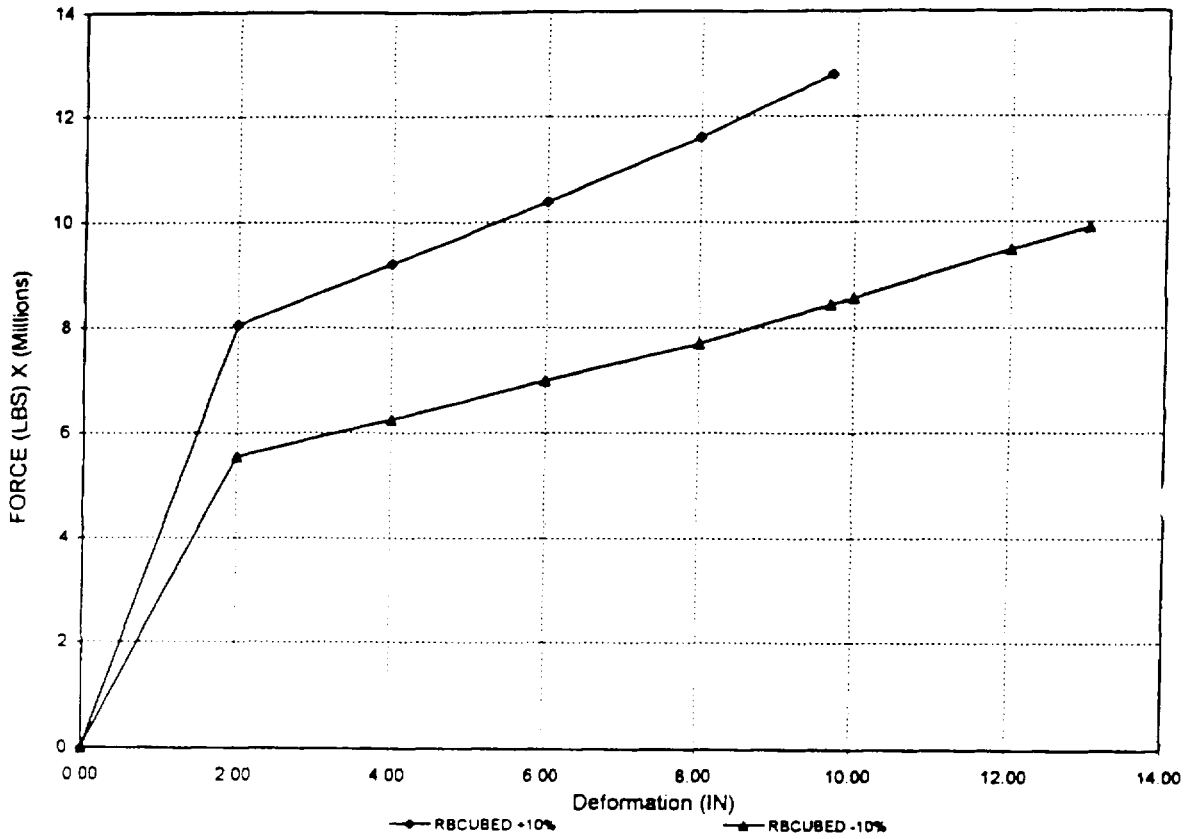

Figure 2.6.7.5-[redacted] Force-Deformation Curve - Lower Impact Limiter (Bottom Corner Impact, 24 Degrees)

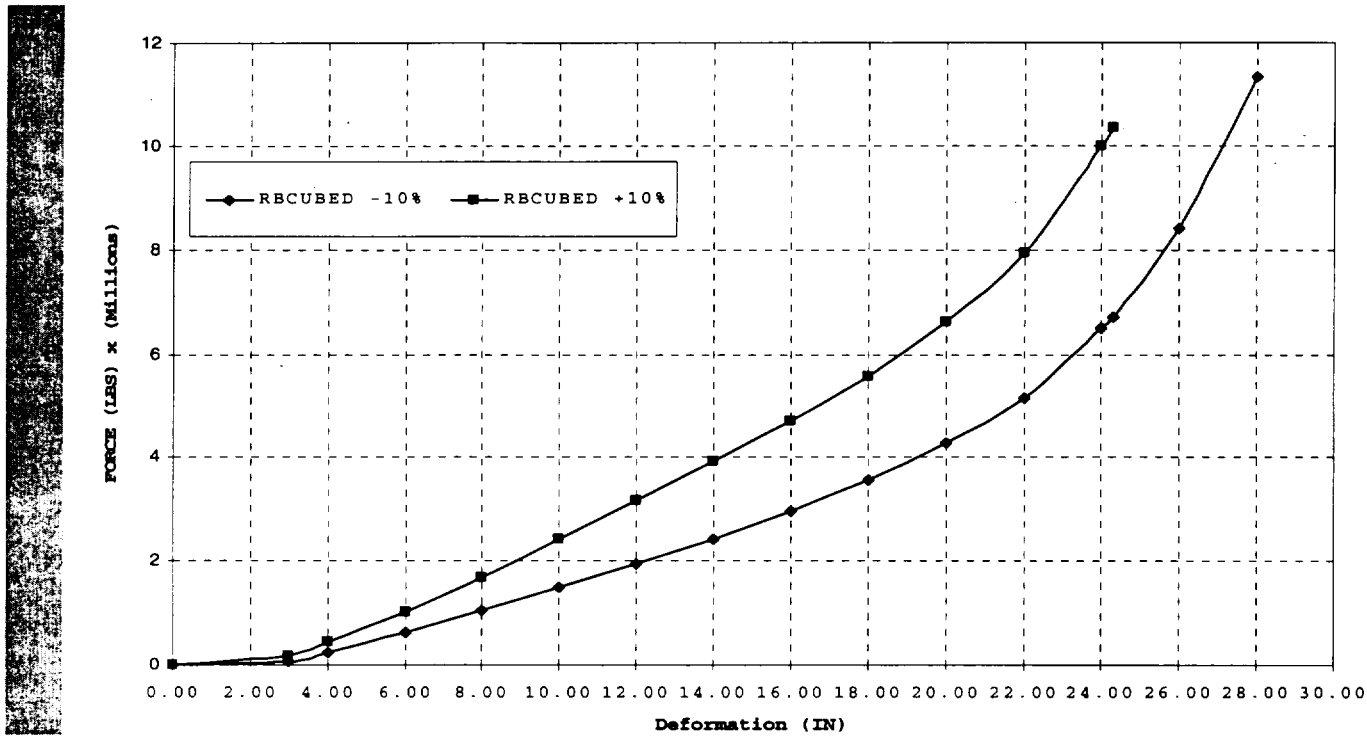

Figure 2.6.7.5-14 Force-Deformation Curve - Lower Impact Limiter (Bottom Oblique Impact, 75 Degrees)

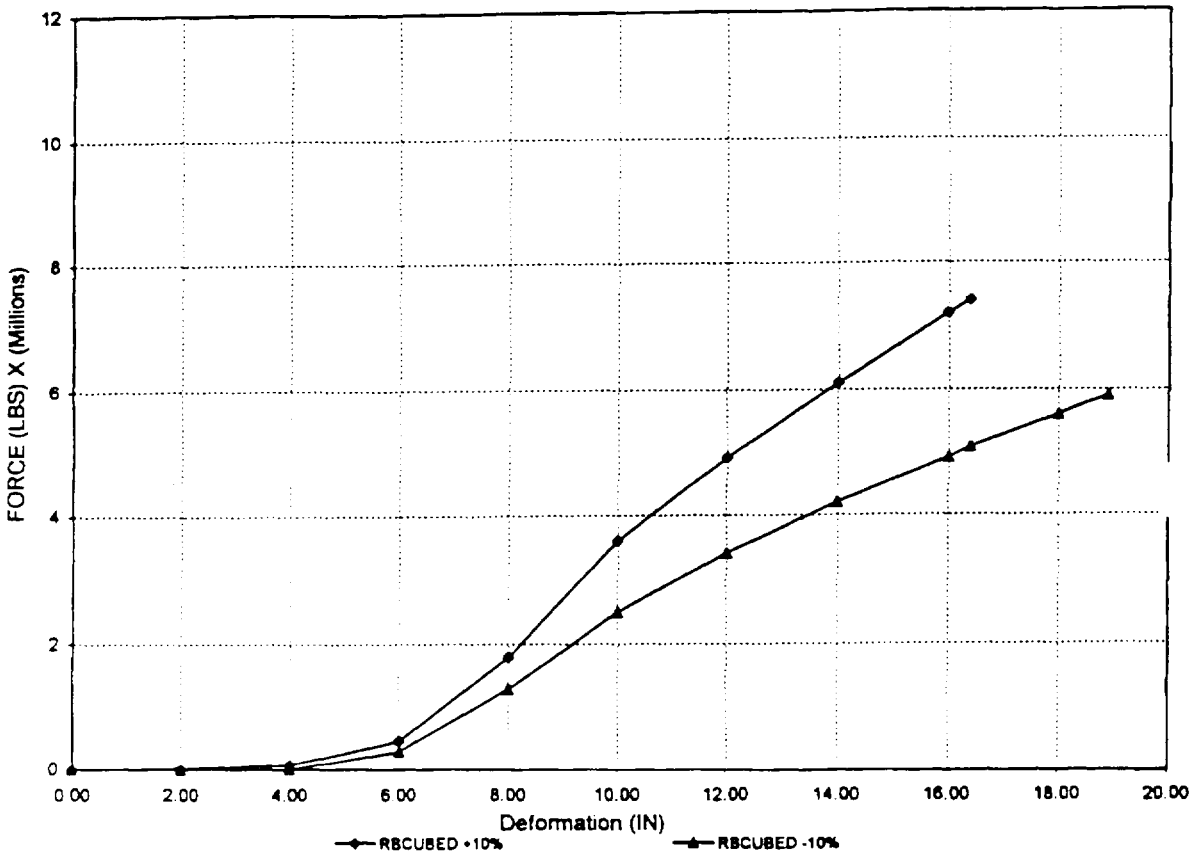

Figure 2.6.7.5-15 Force-Deformation Curve - Upper Impact Limiter (Top End Impact, 0 Degrees)

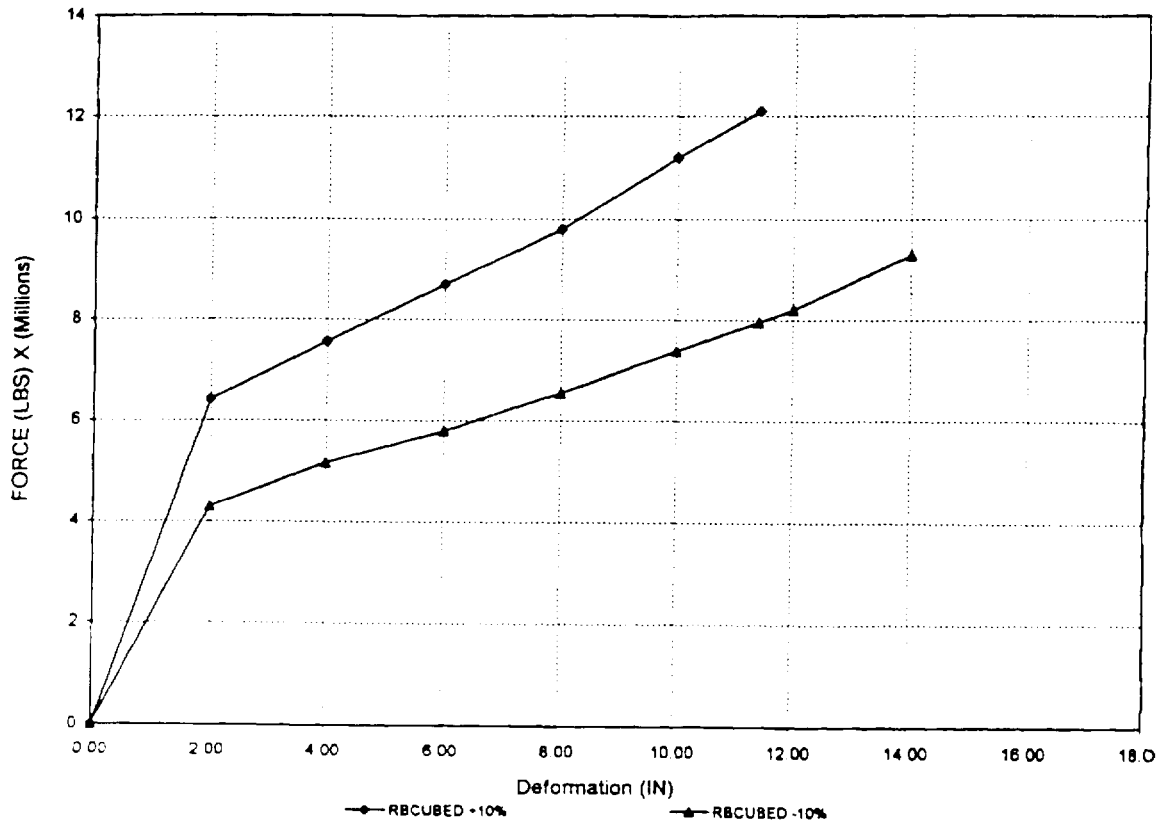

Figure 2.6.7.5-16 Force-Deformation Curve - Upper Impact Limiter (Top Corner Impact, 24 Degrees)

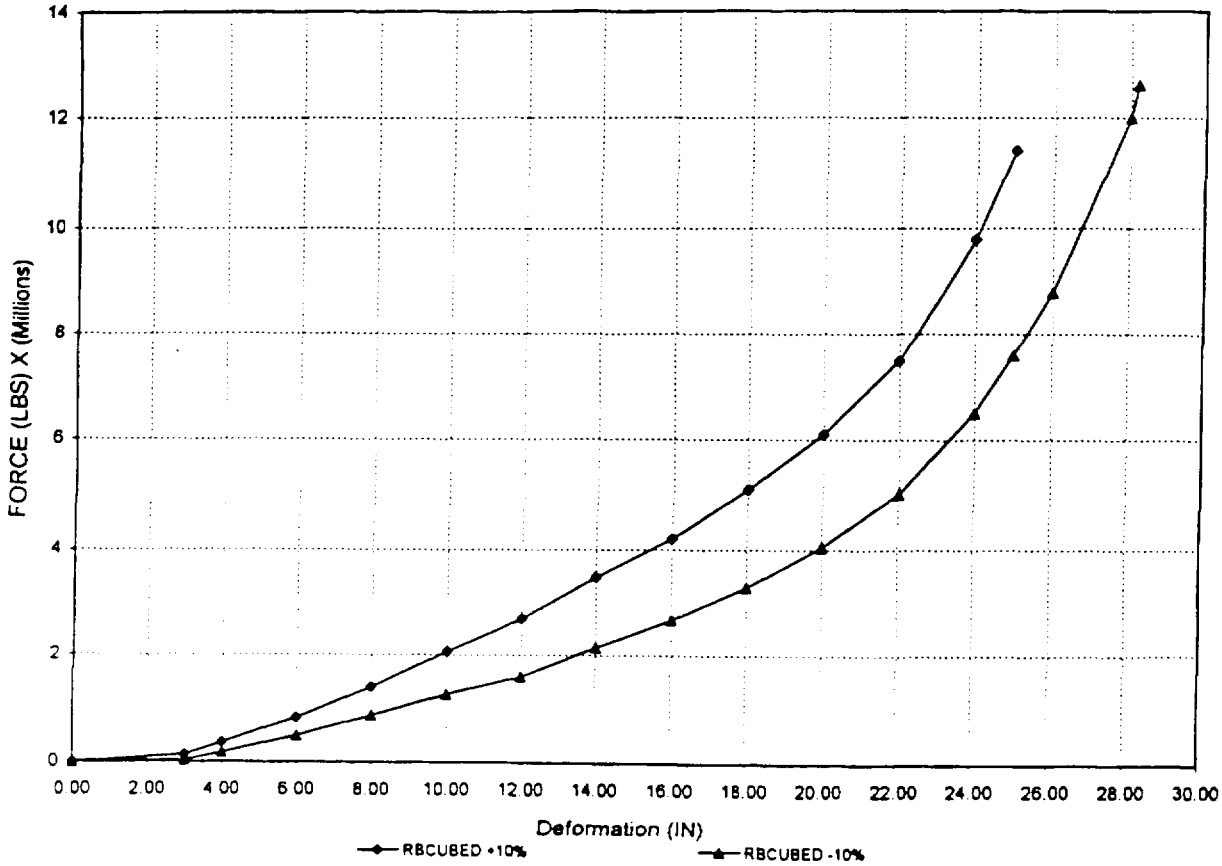

Figure 2.6.7.5-17 Force-Deformation Curve - Upper Impact Limiter (Top Oblique Impact, 75 Degrees)

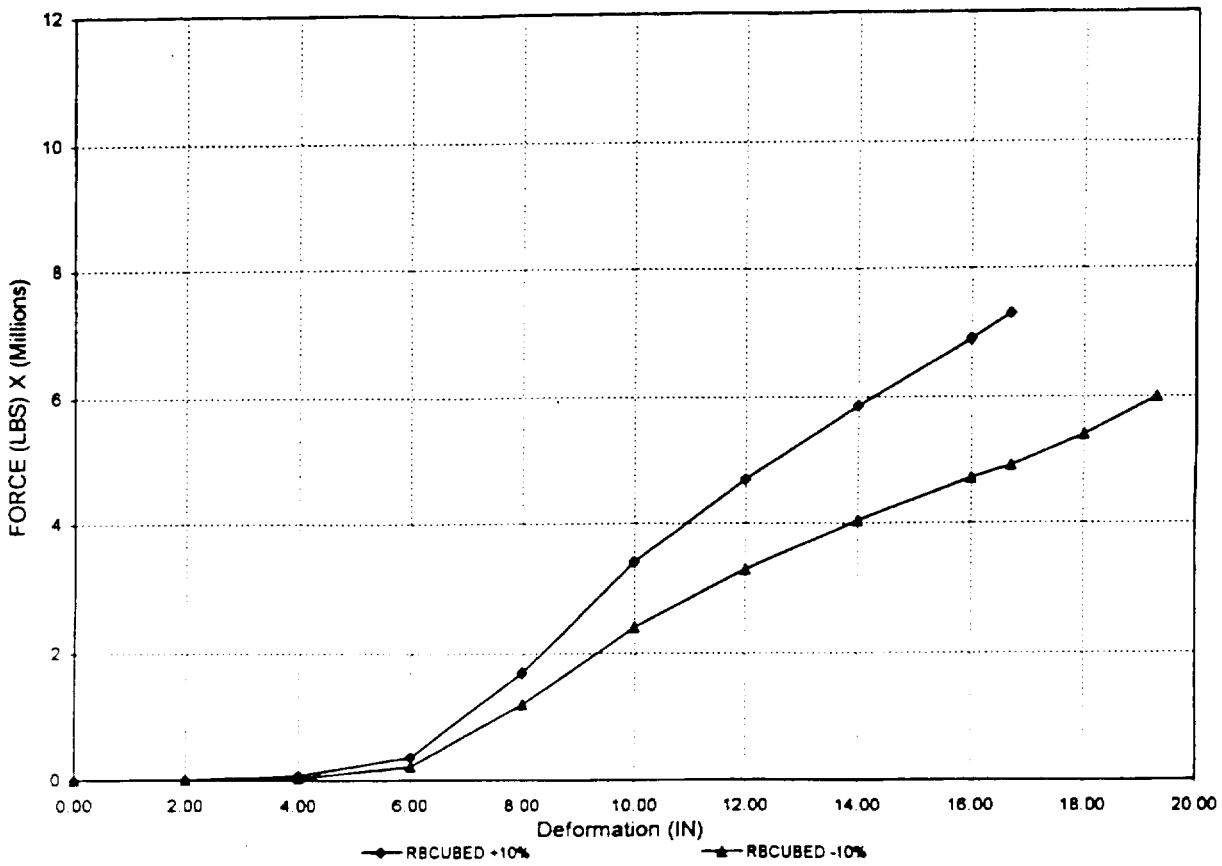

Figure 2.6.7.5-18 Force-Deformation Curve - Side Impact (90 Degrees)

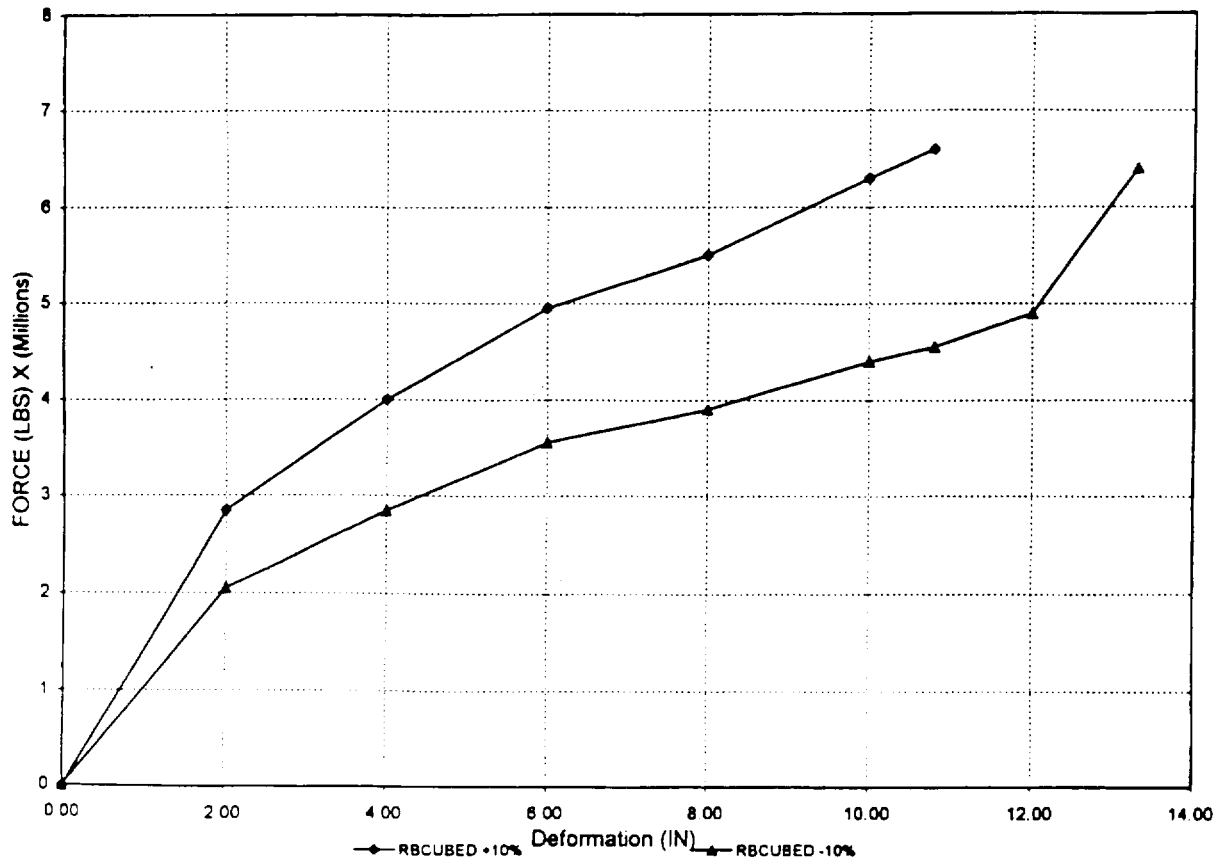

Figure 2.6.7.5-19 Impact Limiter Attachment Geometry

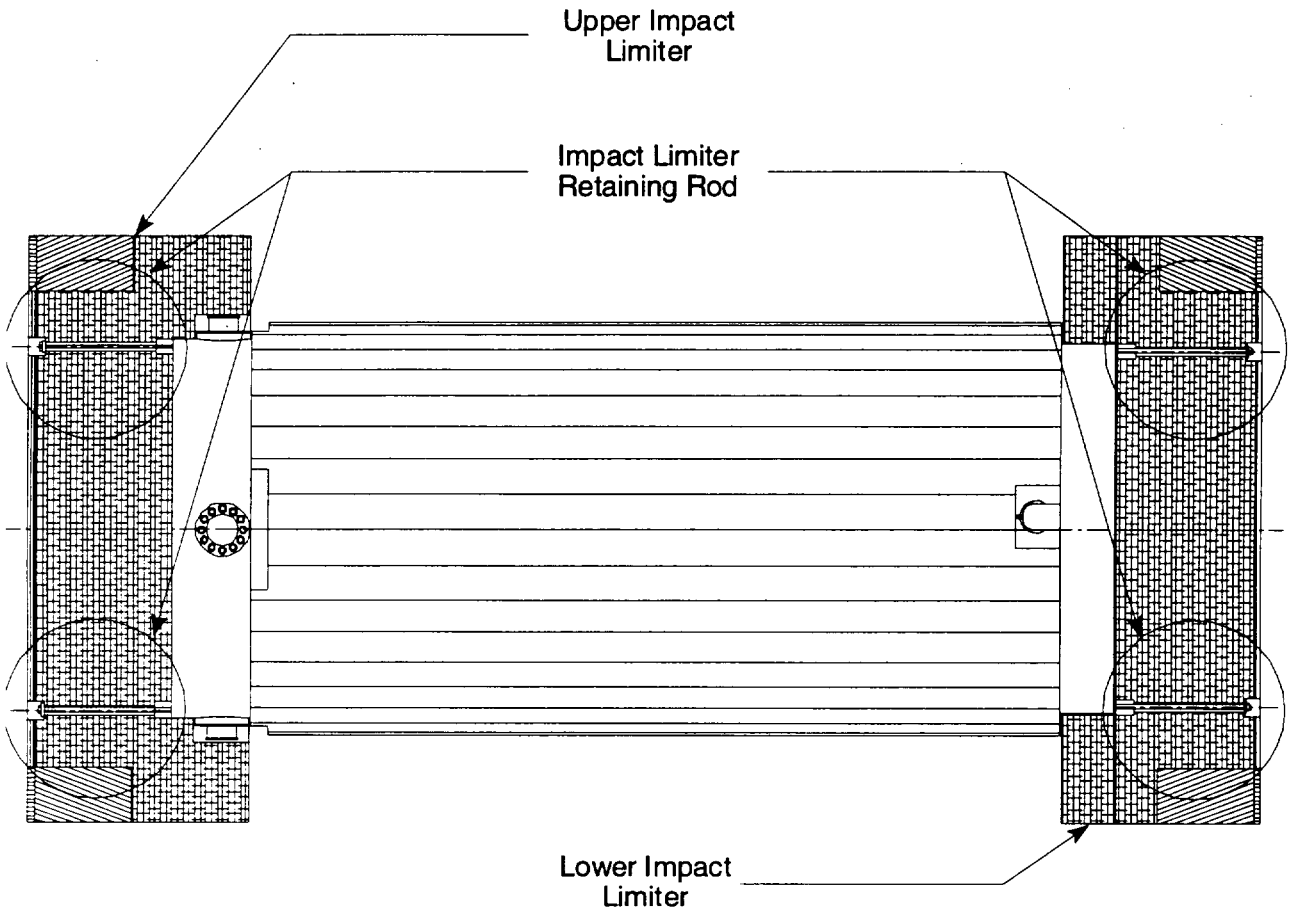

Table 2.6.7.5-1 Summary of Results-Impact Limiter Analysis for 1-Foot Free Drop

Analysis Description	Displacement (in.)	Force (lb)	Equivalent g-Load Factor*
End Impact			
Lower Impact Limiter (Max. Crush Strength)	1.00	4.44×10^6	17.10
Lower Impact Limiter (Min. Crush Strength)	1.50	2.58×10^6	9.93
Upper Impact Limiter (Max. Crush Strength)	1.00	3.99×10^6	15.36
Upper Impact Limiter (Min. Crush Strength)	1.70	3.82×10^6	14.71
Corner Impact			
Lower Impact Limiter (Max. Crush Strength)	6.20	1.45×10^6	5.59
Lower Impact Limiter (Min. Crush Strength)	7.40	1.22×10^6	4.70
Upper Impact Limiter (Max. Crush Strength)	7.50	1.31×10^6	5.06
Upper Impact Limiter (Min. Crush Strength)	9.10	1.09×10^6	4.19

* Equivalent g-load factor = force/260,000.

Table 2.6.7.5-1 Summary of Results-Impact Limiter Analysis for 1-Foot Free Drop (continued)

Analysis Description	Displacement (in.)	Force (lb)	Equivalent g-Load Factor*
Side Impact			
Lower Impact Limiter (Max. Crush Strength)	1.2	4.18×10^{6}**	16.07
Lower Impact Limiter (Min. Crush Strength)	1.5	3.54×10^{6}**	12.90
Upper Impact Limiter (Max. Crush Strength)	1.2	4.26×10^{6}**	16.40
Upper Impact Limiter (Min. Crush Strength)	1.4	3.53×10^{6}**	13.61

*Equivalent g-load factor = force/260,000.

**Total force for both impact limiters.

Table 2.6.7.5-2 Summary of Results-Impact Limiter Analysis for 30-Foot Free Drop

Analysis Description	Displacement (in.)	Force (lb)	Equivalent g-Load Factor*
End Impact			
Lower Impact Limiter (Max. Crush Strength)	9.8	1.29×10^7	49.70
Lower Impact Limiter (Min. Crush Strength)	13.1	9.96×10^6	38.30
Upper Impact Limiter (Max. Crush Strength)	11.4	1.21×10^7	46.75
Upper Impact Limiter (Min. Crush Strength)	14.9	1.06×10^7	41.10
Corner Impact			
Lower Impact Limiter (Max. Crush Strength)	24.2	1.06×10^7	40.85
Lower Impact Limiter (Min. Crush Strength)	28.0	1.13×10^7	43.60
Upper Impact Limiter (Max. Crush Strength)	24.7	1.14×10^7	43.94
Upper Impact Limiter (Min. Crush Strength)	28.1	1.25×10^7	48.90

* Equivalent g-load factor = force/260,000.

Table 2.6.7.5-2 Summary of Results—Impact Limiter Analysis for 30-Foot Free Drop (continued)

Analysis Description	Displacement (in.)	Force (lb)	Equivalent g-Load Factor*
Oblique Impact (30°)			
Lower Impact Limiter (Max. Crush Strength)	25.2	9.24×10^6	35.5
Lower Impact Limiter (Min. Crush Strength)	29.2	9.95×10^6	38.3
Upper Impact Limiter (Max. Crush Strength)	26.4	9.79×10^6	37.6
Upper Impact Limiter (Min. Crush Strength)	30	1.06×10^7	41
Side Impact			
Lower Impact Limiter (Max. Crush Strength)	11.2	$1.28 \times 10^{7**}$	49.3
Lower Impact Limiter (Min. Crush Strength)	14.0	$1.19 \times 10^{7**}$	45.87
Upper Impact Limiter (Max. Crush Strength)	10.8	$1.32 \times 10^{7**}$	50.95
Upper Impact Limiter (Min. Crush Strength)	13.3	$1.28 \times 10^{7**}$	49.57

*Equivalent g-load factor = force/260,000.

** Total force for both impact limiters.

Table 2.6.7.5-3 Summary of Cask Drop Equivalent *g*-Load Factors

Direction	Equivalent Load Factor[a]			
	1-Foot Drop	30-Foot Drop		
		Total	Axial Component[b]	Lateral Component[b]
Lateral (Side) (90°)	16.4	52.0	0.0	52.0[e]
Longitudinal (End) (0°)	171.	49.7	49.7	0.0
Corner(23.35° - 24°)	5.6	48.9	44.8	19.5
Oblique (30°)	c	41.0	35.6	20.6
Oblique (45°)	c	34.4	24.3	24.3
Oblique (60°)	c	31.9	16.0	27.6
Oblique (75°)	c	28.7	7.4	27.7
Slapdown Based on Oblique (75°)	c	54.9	0.0	54.9

a. Equivalent *g*-load factor = force/260,000 lb.

b. Axial component = total x cos θ

Lateral component = total x sin θ

where θ = 23.35°, 23.5°, 23.76°, 23.8°, 23.88°, 24, 30°, 45°, 60° or 75°.

c. Oblique orientations for 1-ft drop are not considered credible. Refer to Section 2.6.7.4.

d. Angles with highest *g*-loads.

e. Based on the addition of peak *g*-loads occurring at the trunnion.

Table 2.6.7.5-4 Summary of Results of RBCUBED Impact Limiter Analysis for 30-Foot Drop for Wood Properties at 70°F

Condition	Displacement (inch)	Equivalent g-Load Factor
End Impact		
Upper Impact Limiter	14.7	46.3
Corner Impact		
Upper Impact Limiter	27.7	47.8
Side Impact		
Lower Impact Limiter	13.7	48.6
Upper Impact Limiter	13.0	52.1

2.6.7.6 Closure Analysis

The Universal Transport Cask closure lid and the bolts are required to satisfy two criteria: (1) calculated maximum stresses must be less than the allowable stress limit (the material yield strength is conservatively selected), and (2) lid deformation or rotation at the O-rings must be less than the elastic rebound of the O-rings. Using consistently conservative assumptions, the NUREG/CR6007 [9] analysis of the cask closure system demonstrates that the cask closure assembly satisfies the performance and structural integrity requirements of 10 CFR 71.71(c)(7) for normal conditions of transport. The NUREG/CR-6007 analysis is summarized in the following paragraphs.

NUREG/CR-6007 provides formulas for calculating bolt forces generated by all regulatory (normal and hypothetical accident) transportation loading. Specifically, the report deals with the bolt stress analysis of a circular, cylindrical cask with a flat, circular, closure lid.

To ensure positive closure, the cask has 48 bolts 2–8 UN–2A socket head cap screws fabricated from SB-637, grade N07718. Material properties are taken at 275°F for the cask lid, closure bolts, and cask wall. A maximum temperature gradient of 3°F through the thickness of the cask lid is used as well. For evaluation purposes, a maximum internal pressure of 80 psi is used.

Accelerations are based on the impact limiter analysis for normal conditions of transport. Therefore, an acceleration of 20 g (1-foot drop) is taken to be the worst case. The 20 g load is also used for the vibration case. A factor of 1.1 is used for the dynamic load. The following calculations are a summary of the NUREG/CR-6007 evaluation based on the calculated preload of 111,680 lb/bolt.

The preload on the cask lid closure bolts considers the following factors: (1) an internal pressure force on the inner lid of 80 psi; (2) the O-ring compression force; and (3) the inertial weight of the lid, canister, basket, and fuel due to the 30-ft accident corner drop conditions. Based on the above considerations, a preload of 111,680 pounds/bolt is conservatively selected for the cask lid closure bolts. A minimum torque value of 3,738 foot-pounds, develops a tensile preload force of 111,680 pounds/bolt based on the following relationship:

$$T = F\left[\frac{L}{2\pi} + \frac{d_m \mu}{2\cos\alpha} + \frac{(d+b)\mu}{4}\right]$$ [46]

where:

T = applied torque in inch-pounds
F = preload force in pounds
d = bolt diameter = 2.0 in
b = bolt head diameter = 3.75 in. (at the bottom of the bolt head)
d_m = mean diameter of threads = 1.9188 in
α = one-half the thread angle = 30°
μ = coefficient of friction = 0.15
N = 8 threads per inch
$L = 1/N$

Therefore, the minimum torque, T, required to develop the preload of 111,680 pounds/bolt is determined as:

$$T = F(0.4017) \div 12$$

$$T = 3{,}738 \text{ foot-pounds}$$

An installation torque of 3,900 ±100 foot-pounds is specified to ensure that the minimum required torque of 3,739 foot-pounds is achieved.

Maximum stresses in the closure bolt result during the top-end corner drop (23.35° from axial plane of cask) assuming the closure bolts support the full weight of the cask lid and contents. This is conservative since during a top-end drop, the cask lid is fully supported by the impact limiter; thus, the closure bolts do not carry any weight. For the following evaluation, only worst case forces and stresses are reported.

The tensile force per bolt, F_{a_pt}, due to preload and thermal is:

$$F_{a_pt} = P_L + P_{th} = 134{,}877 \text{ pounds}$$

where P_L = 111,680 pounds, preload

P_{th} = 23,197 pounds resulting from thermal expansion

The tensile force per bolt, F_{a_al}, from all other credible loads is:

$$F_{a_al} = P_o + P_i + P_{20} + P_v = 59{,}573 \text{ pounds}$$

where P_o = 667 pounds, load resulting from O-ring compression and operation

P_i = 6,549 lb. load resulting from internal pressure

P_{20} = 48,662 lb. load due to 20 g top-end corner impact.

P_v = 3,695 pounds, load resulting from 20 g vibration.

Since F_{a_pt} is greater than F_{a_al}, the total tensile bolt load, F_a, is equal to F_{a_pt}:

$$F_a = 134{,}877 \text{ pounds}$$

The shear load is

$$F_s = |P_i + P_{th} + P_{20} + P_v| = 37{,}242 \text{ pounds}$$

where P_i = 15,245 pounds, load resulting from internal pressure

P_{th} = -57,647 pounds, load resulting from temperature difference between the cask lid and upper forging

P_{20} = 1,465 pounds, load resulting from 20 g top-end corner drop

P_v = 3,695 pounds, load resulting from 20 g side vibration load

The bending moment is

M_b = -675 inch-pounds, due to thermal load (other loads do not contribute due to cask lid design).

and the load resulting from torsion is

M_t = 22,440 inch-pounds.

These loads and moments translate into the following stresses:

The tensile stress in the bolt is:

$$\sigma_a = \frac{1.2732 F_a}{D^2} = 48{,}679 \text{ psi}$$

where D = 1.878 in., minimum bolt diameter. The shear stress is

$$\tau = \frac{1.2732 F_s}{D^2} = 13{,}441 \text{ psi}$$

Where D = 1.878 in., minimum bolt diameter.

The bending stress is

$$\sigma_b = \frac{10.186 M_b}{D^3} = 1{,}038 \text{ psi}$$

where D = 1.878 in., minimum bolt diameter.

The stress resulting from torsion is

$$\tau_t = \frac{5.093 M_t}{D^3} = 17{,}249 \text{ psi}$$

where D = 1.878 in., minimum bolt diameter.

For normal conditions, Table 6.1 of NUREG/CR-6007 requires that the average tensile stress is less than S_m (where $S_m = 2/3\ S_y$), or

$$\sigma_{t(ave)} = \sigma_a = 48{,}679 \text{ psi} < S_m = 94{,}350 \text{ psi.}$$

Table 6.1 also requires that the average shear, which is comprised of the average direct shear (τ) be less than 0.6 S_m. This is expressed as

$$\sigma_{s(ave)} = \tau = 13{,}441 \text{ psi} < 0.6\ S_m = 56{,}610 \text{ psi.}$$

For the combined state of stress that includes tension plus shear, the square of the computed average tensile stress divided by the allowable tensile stress plus the square of the average shear stress divided by the allowable shear stress must be less than 1. This is expressed as

$$\left(\frac{48{,}679}{94{,}350}\right)^2 + \left(\frac{13{,}441}{56{,}610}\right)^2 = 0.33 < 1.$$

For the combined state of stress that includes tensile, shear, and bending; the bolts must have a maximum stress intensity less than 1.35 S_m (when the minimum tensile strength is greater than 100,000 psi). Therefore, the maximum stress intensity is

$$\sigma_{total} = \sqrt{\left[\left(\sigma_a + \sigma_b\right)^2 + 4\left(\tau_t + \tau\right)^2\right]} = 78{,}989 \text{ psi} < 1.35\ S_m = 127{,}372 \text{ psi}.$$

The margin of safety for ASME SB-637, Grade N07718 closure bolts is 0.61.

2.6.7.6.1 Bolt Fatigue Evaluation

For the 2.00-inch closure bolts the fatigue life of 944 cycles is obtained from ASME Code Section III, Appendix I, Table I-9.1, Figure I-9.4 [17].

The maximum stress, S, on the cask closure bolts is:

$$S = \frac{4.0F}{A} = \frac{4.0(142{,}691)}{2.77} = 206{,}053 \text{ psi} \quad (206.053 \text{ ksi})$$

where:

$F = F_i + F_{th} = 119{,}494 + 23{,}197 = 142{,}691$ lb

$$F_i = \frac{12T}{\left(\frac{L}{2\pi} + \frac{d_2\mu_1}{2\cos\alpha} + \frac{(d+b)\mu_2}{4}\right)} = 119{,}494 \text{ lb (maximum preload force)}$$

$T = 4{,}000$ ft-lb (maximum initial torque, see Section 2.6.7.6)
$F_{th} = 23{,}197$ lb (thermal load, see Section 2.6.7.6)
$A = 2.77$ in^2, the cross-sectional tensile area of the bolt
4.0 = the stress reduction factor per NB-3232.3(c)

The number of cycles (N) is ([17], Table I-9.1):

$$N = N_i\left(\frac{N_j}{N_i}\right)^{\log\left(\frac{Si}{S}\right)} \Big/ \log\left(\frac{Si}{Sj}\right) \text{ or } N = 500\left(\frac{1000}{500}\right)^{\log\left(\frac{143}{103.03}\right)} \Big/ \log\left(\frac{143}{100}\right) = 944 \text{ cycles}$$

where

the maximum nominal stress (206.053 ksi) < $2.7S_m$ = 254.7 ksi, and the alternating stress (S_{alt}) is: (206.053 – 0)(0.5) = 103.027 ksi

N_i = 500 cycles

N_j = 1000 cycles

S_i = 143 ksi

S_j = 100 ksi

2.6.7.7 Neutron Shield Analysis

The Universal Transport Cask neutron shield is evaluated for two distributed-load conditions: a 1-foot end-drop event and a 1-foot side-drop event. For each of these conditions, the solid neutron shielding material applies a load on the neutron shield shell. The weights of the neutron shield shell and fins are included in the analysis. The neutron shield geometry is shown in Figure 2.6.7.7-1.

2.6.7.7.1 End Plate 1-Foot End-Drop Analysis

The primary loading on the neutron shield shell and end plates is the weight of the NS-4-FR neutron shielding material. The neutron shield is also evaluated for the impact loading of the NS-4-FR during a 1-foot bottom-end-drop event.

$$p = d_B L + d_p t, = 11 \text{ psi}$$

where:

d_B = 0.0607 lb/in^3, the density of NS-4-FR

L = 178.56 in, height of NS-4-FR material

d_p = 0.291 lb/in^3, density of Type 304 stainless steel

t = 0.5 in, plate thickness

The deceleration of the package during a 1-foot end-drop event is 20g. The impact load on the plate is calculated as PI = p(20) = 220 psi.

The material properties (conservatively taken at 300°F) for the Type 304 stainless steel shell, fins and bottom plate are:

S_u = 66,000 psi
S_y = 22,500 psi
$S_s = (0.5)S_y$ = 11,250 psi

Allowable Stresses

The allowable stress intensity for normal condition loading is (Regulatory Guide 7.6):

S_{allow} = Axial + Bending = 1.5 S_m = 30,000 psi,

Where S_m is equal to 20,000 psi for Type 304 stainless steel.

Calculated Stresses

From Table 26, Case 1 [28]:

$$S_s = \frac{\beta P b^2}{t^2} = 12{,}028 \text{ psi}$$

where:

$P = P_I$ = 220 psi
a = 11.49 inch and b = 4.5 inch
t = 0.5 inch
β= 0.675

The margin of safety is:

$$MS = \frac{30{,}000}{12{,}028} - 1 = +1.49$$

For the reaction in the welds, conservatively assuming all welds are quarter-inch fillets:

$$q_w = \frac{(P)(b)(a)}{(2)(b+a)} = \frac{(220)(4.5)(11.49)}{(2)(4.5+11.49)} = 356\,\text{lb/in}$$

The allowable shear/inch is (0.707)(0.25)(Ss), or 1,988 lb/in. Therefore the Margin of Safety is:

$$MS = \frac{1{,}988}{356} - 1 = 4.58$$

Figure 2.6.7.7-1 Neutron Shield Geometry

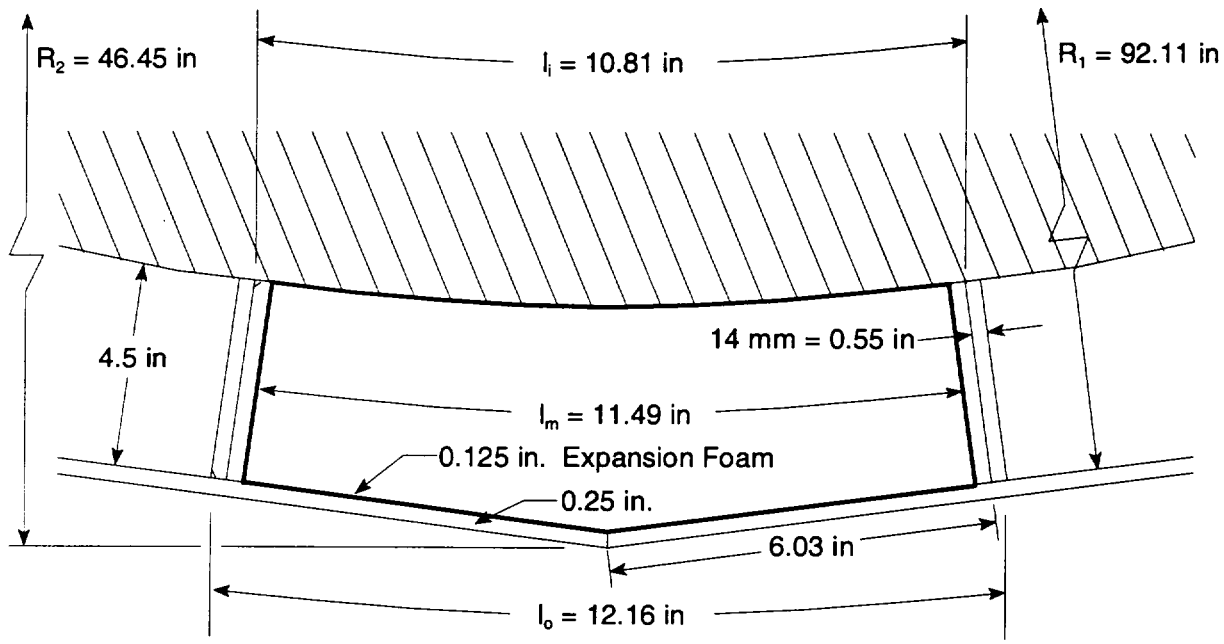

Neutron Shield Bottom Plate Attachment

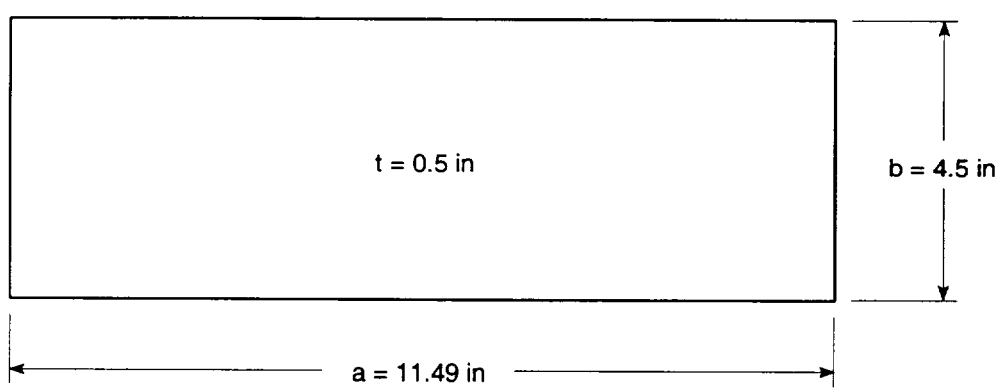

Equivalent Flat Plate Simply Supported

2.6.7.7.2 Side-Drop Analysis

This analysis assumes that the cask is subjected to a 1-foot side-drop event. The side-drop impact force is limited by the upper and lower impact limiters. For this analysis, an impact force equivalent to a 20-*g* side impact is used. The cask is stopped by the impact limiter before the neutron shield contacts the impacted surface. Therefore, the impact force is distributed through the cask body from the impact limiters. The impact deceleration force of the weight of the neutron shielding material is reacted by the neutron shield shell and fins, which transfer the load to the cask body. The NS-4-FR neutron shielding material is assumed to act as an internal pressure on the shell.

Because the structural function of the neutron shield shell and radial heat transfer fins is to support the NS-4-FR radial neutron shield, ASME Code Section III, Subsection NF [19] is used as the governing structural criterion for the evaluation of the welds connecting the radial heat transfer fins to the neutron shield shell and cask outer shell.

In addition to assuming the conservative load combination resulting from cold impact loads and discontinuity thermal expansion between the NS-4-FR and radial fin from hot, steady-state conditions, an additional 3-psi pressure is assumed to have been created from potential gas loss from the NS-4-FR subjected to extended service in a high end temperature environment.

Following the methodology of the ASME Code, Section III criteria and cask design practice, the load on the weld joints has been categorized into the following service-level conditions

Service Level B

1. Pressure developed on the neutron shield shell from differential radial thermal expansion of the NS-4-FR neutron shield is relative to the Type 304 stainless steel radial heat transfer fin. The thermal expansion is

$$T_E = (\alpha \times L \times \Delta T)_{NS-4-FR} - (\alpha \times L \times \Delta T)_{304SS}$$

$$= (4.72 \times 10^{-5})(11.49)(75) - (8.79 \times 10^{-6})(11.49)(75)$$

$$= 0.033 \text{ in.}$$

where

$\alpha_{NS\text{-}4\text{-}FR}$ = 4.72×10^{-5} in/in/°F, coefficient of thermal expansion at 158°F

α_{304SS} = 8.79×10^{-6} in/in/°F, coefficient of thermal expansion at 200°F

L = Length of the section

ΔT = 150 - 75 = 75°F, average temperature differential

Considering differential thermal expansion and 3% initial compression of the HT800 expansion foam on the inside surface of the neutron shield shell, a compressive load develops. The total compression is

$$\text{Compression} = 3\% \ (0.125) + 0.033 = 0.037 \text{ in}$$

The equivalent compression of the foam is

$$\% \ \text{Compression} = \frac{0.037}{0.125} \times 100 = 29.6\% \ .$$

Interpolating the manufacturer design information presented in Table 4.2-1, the equivalent pressure load developed on the neutron shield shell is 12.1 psi.

2. Potential pressure developed from extended service of the NS-4-FR neutron shield at high-end temperatures is defined as 3 psi for this evaluation.

Service Level C

1. Service Level B loads plus dynamic induced load from a postulated one foot side impact (20 *g*).

   Considering the mass of the neutron shield shell and NS-4-FR, the effective pressure load becomes

$$P = MA = (0.346)(20) = 6.9 \text{ psi}$$

where, from the dimensions provided in Fig. 2.6.7.7-1

M= [(4.5)(0.0607) + (0.25)(0.291)] x 1 = .346 lb, the mass of a 1 in^2 unit area,

A= 20 g, the acceleration during a side drop.

Service Level D

1. Service Level B loads plus dynamic induced load from a postulated 30-foot side impact (60 g). Considering the mass of the neutron shield shell and the NS-4-FR, the effective pressure load becomes

$$P = (0.346)(60) = 20.8 \text{ psi.}$$

The following evaluation is presented for two different load orientations of the fin welds. Case 1 represents the loads induced as a result of loading applied to the neutron shield and Case 2 represents loading applied to the radial heat transfer fin.

Case 1—Neutron Shield Shell Loading

Implementing the design criteria for noncontainment support structures presented in NF-3250, normal operation load service level stress in the weld region connecting the neutron shield shell to the radial heat transfer fin is evaluated using a conservative simplification of the plate and shell structure to that of a uniformly loaded beam having unit depth.

The maximum tension stress from Service Level B is:

$$S = \frac{6m}{t^2} \; 17{,}867 \text{ psi}$$

where $m = \frac{wl^2}{12} = 186.1 \text{ in.} - \text{lb}$

$t = 0.25 \text{ in.}$

and $w = 12.1 + 3 = 15.1 \text{ psi}$

$l = 12.16 \text{ in.}$

Allowable stress limits defined in NF-3256.2 and Table NF-3522 (b)-1 for full penetration groove welds define acceptable stress for this condition load as

$$S_{all} = 1.33 \times 1.5 \times 17{,}200 = 34{,}314 \text{ psi}$$

Thus, the margin of safety is

$$MS = \frac{34{,}314}{17{,}867} - 1 = +92.$$

The maximum tension stress for Service Level C load is:

$$S = \frac{6m}{t^2} \; 26{,}024 \text{ psi}$$

where $m = \frac{wl^2}{12} = 271.1 \text{ in.} - \text{lb}$

$t = 0.25 \text{ in.}$

and $w = 15.3 + 6.9 = 22.0 \text{ psi}$

$l = 12.16 \text{ in.}$

Allowable membrane plus bending stress limits defined in NF-3256.2 for Service Level C limits is

$$S_{all} = 1.5 \times 1.5 \times 17{,}200 = 38{,}700 \text{ psi}$$

Thus, the margin of safety is

$$MS = \frac{38{,}700}{26{,}024} - 1 = +0.49.$$

The maximum tension stress for Service Level D load is

$$S = \frac{6m}{t^2} = 31{,}850 \text{ psi}$$

As directed by NE-3256.2 for Service Level D, qualification of the structure is based on ASME Code Section III, Appendix F, [17] Paragraph F-1340, "Acceptance Criteria Using Plastic System Analysis."

Considering plastic failure of fixed-end beams with uniformly distributed load, the plastic moment then becomes (from [28] Table 15, Case 2d):

$$m = \frac{wl^2}{16} = 331.8 \text{ in.-lb}$$

where $w = 15.1 + 20.8 = 35.9$ psi

$l = 12.16$ inch

$t = 0.25$ inch

Paragraph F-1340 defines the allowable primary membrane plus primary bending stress intensity as the lesser of 1.5 ($2.4S_m$) and 1.5 ($0.7S_u$). Implementation of this criterion limits Service Level D stress to 68.8 ksi.

$$MS = \frac{68{,}800}{31{,}850.3} - 1 = +1.16 .$$

In addition to the evaluation of the maximum local bending stress in the weld region, shear stress is evaluated as follows:

Service Level	w (psi)	$S_s = \frac{wl}{2t}$ (psi)	Allowable Stress (psi)	MS
B	15.10	367	1.33 (.4S_y) = 12,700	+ Large
C	22.00	535	1.5 (.4S_y) = 14,000	+ Large
D	36.10	878	0.42 (S_u) = 28,900	+ Large

where $l = 12.16$

$t = 0.25$

Case 2—Heat Transfer Fin Loading

Following a similar method as used in the evaluation of the neutron shield shell, the heat transfer fin is evaluated by using a uniformly loaded beam with a fixed end at the cask outer shell surface and a simple support at the neutron shield shell. Because Level B load is developed from radial thermal growth of the NS-4-FR and postulated off gas pressure, Service Level B does not load the fin in the lateral direction. Tension stress developed in the fin from these radial loads is 70 psi, which is insignificant.

Lateral load from Service Level C produces the following stress:

$$S = \frac{6m}{t^2} = 2{,}135 \text{ psi}$$

where $m_{max} = \frac{wl^2}{8} = 35.3$ in.-lb

$w = (0.0607)(11.49)(20) = 13.95$ lb

$$l = \frac{92.11 - 82.61}{2} - 0.25 = 4.5 \text{ in.}$$

$$t = 0.315 \text{ in. (8 mm)}$$

From the preceding evaluation of the neutron shield shell, the service level C allowable is 38,925 psi. Therefore,

$$MS = \frac{38{,}925}{2{,}135} - 1 = \text{Large}.$$

Lateral load for Service Level D produces the following stress:

$$S = \frac{6m}{t^2} = 8{,}540 \text{ psi}$$

where $$m_{max} = \frac{wl^2}{6} = 141.23 \text{ in.-lb}$$

$$w = (0.0607)(11.49)(60) = 41.85 \text{ lb}$$

$$l = 4.5 \text{ in.}$$

$$t = 0.315 \text{ in. (8 mm).}$$

Using the acceptance criteria for an elastic system analysis provided in the ASME Code Section III, Appendix F, Paragraph F-1332.2, $(1.5 \times 1.2S_y \text{ or } 1.5 \times 1.55S_m < 1.5 \times .7S_u)$:

$$S_{All} = 45{,}000 \text{ psi}$$

$$MS = \frac{45{,}000}{8{,}540} - 1 = 4.27$$

In addition to the evaluation of the maximum local bending stress in the weld region, shear stress is evaluated as follows:

Service Level	w (psi)	$S_s = \frac{wl}{2t}$ (psi)	Allowable Stress (psi)	MS
C	13.95	6,126	14,400	+ Large
D	41.85	377	28,900	+ Large

where $l = 4.5$ in.

$t = 0.25$ in.

Therefore, the heat transfer load path through the welds connecting the neutron shield skin to the radial heat transfer fins is maintained for all transport package normal and accident condition loads.

2.6.7.8 Upper Ring/Outer Shell Intersection Analysis

When the cask is lifted at the lifting trunnions bending stresses are induced in the upper ring and outer shell intersection region of the cask body. These stresses are evaluated by means of a closed-form ring solution (from [29], pp. 390-393). The support provided by the bolted cask lid is conservatively neglected in this analysis.

The geometry and loading of the equivalent ring are defined as follows:

F = lifting force (not including weight of impact limiter)

$$= \frac{260{,}000}{2} = 130{,}000 \text{ lb}$$

q = dead weight load per unit length

W = width of equivalent ring = 3.45 in.

r = mean radius of the equivalent ring = 40.905 in.

$$a = \text{moment arm for the equivalent ring} = 45.63 - 40.905 = 4.725 \text{ in.}$$

On the basis of a total weight of 260,000 lb, q is calculated as:

$$q\,(\pi)(40.905)(2) = 260{,}000 \;\Rightarrow\; q = \boxed{1{,}011.6 \text{ lb/in}}.$$

The moment and torque on the equivalent ring are given by

$$M = \frac{T_o \sin\theta}{2} - qr^2\left(1 - \frac{\pi}{2}\sin\theta\right)$$

$$T = \frac{T_o \cos\theta}{2} - qr^2\left(\theta + \frac{\pi}{2}\cos\theta - \frac{\pi}{2}\right)$$

where theta, θ, is measured from the trunnion (θ = 0) in plane perpendicular to the centerline of the cask ($0 \le \theta \le 180$).

$$T_o = (F)(a) = (130{,}000)(4.725) = 611{,}997 \text{ in-lb.}$$

Substituting for T_o, q, and r,

$$M = 3.06 \times 10^5 \sin\theta - 1.693 \times 10^6\left(1 - \frac{\pi}{2}\sin\theta\right)$$

$$T = 3.06 \times 10^5 \cos\theta + 1.693 \times 10^6\left(\theta + \frac{\pi}{2}\cos\theta - \frac{\pi}{2}\right).$$

The normal stress is treated as bending resulting from the moment acting over a cross section.

$$\sigma = \frac{M(h/2)}{I} = 0.00511\,M$$

where $h = 18.44$ in

$$I = \frac{Wh^3}{12} = \frac{3.45 \times 18.44^3}{12} 14 = 1802.7 \text{ in}^4$$

The shear stress is (Roark's, 6th Edition, Table 20, Case 4)

$$\tau = \frac{3T}{8ab^2}\left[1 + 0.6095\frac{b}{a} + 0.8865\left(\frac{b}{a}\right)^2 - 1.8023\left(\frac{b}{a}\right)^3 + 0.9100\left(\frac{b}{a}\right)^4\right] = 0.0176T$$

where $a = \frac{h}{2} = \frac{18.44}{2} = 8.22$ in, length of longer side,

$b = \frac{w}{2} = \frac{3.45}{2} = 1.725$ in, length of shorter side.

The maximum stress intensity, where the moment and torque are functions of s, is calculated as

$$SI = 2\sqrt{\frac{\sigma^2}{4} + \tau^2} = 2\sqrt{(6.528 \times 10^{-6})M^2 + (3.10 \times 10^{-4})T^2}\ .$$

Resultant values of the stress intensity are evaluated in Table 2.6.7.8-1. The minimum margin of safety is

$$MS = \frac{30{,}000}{28{,}309} - 1 = +0.06$$

where $S_m = 20{,}000$ psi

$S_{allow} = 1.5\ S_m = 30{,}000$ psi.

Table 2.6.7.8-1 Resultant Stress Intensity Values in the Equivalent Ring

Angle [1] (degrees)	Moment (in-lb)	Torque (in-lb)	SI (psi)
0.0	$-1.693(10)^6$	$3.060(10)^5$	13,819
5.0	$-1.435(10)^6$	$4.425(10)^5$	17,219
10.0	$-1.178(10)^6$	$5.564(10)^5$	20,498
15.0	$-9.255(10)^5$	$6.482(10)^5$	23,310
20.0	$-6.788(10)^5$	$7.181(10)^5$	25,525
25.0	$-4.398(10)^5$	$7.669(10)^5$	27,098
30.0	$-2.103(10)^5$	$7.952(10)^5$	28,021
35.0	$7.860(10)^3$	$8.039(10)^5$	28,309
40.0	$2.131(10)^5$	$7.942(10)^5$	27,987
45.0	$4.038(10)^5$	$7.671(10)^5$	27,093
50.0	$5.786(10)^5$	$7.242(10)^5$	25,671
55.0	$7.361(10)^5$	$6.667(10)^5$	23,775
60.0	$8.751(10)^5$	$5.962(10)^5$	21,466
65.0	$9.945(10)^5$	$5.145(10)^5$	18,817
70.0	$1.094(10)^6$	$4.232(10)^5$	15,917
75.0	$1.171(10)^6$	$3.243(10)^5$	12,892
80.0	$1.227(10)^6$	$2.194(10)^5$	9,952
85.0	$1.261(10)^6$	$1.107(10)^5$	7,531
90.0	$1.272(10)^6$	0.0000	6,502

[1] The Angle is measured from the centerline of the trunnion.

2.6.8 Corner Drop

The Universal Transport Cask is composed of materials other than fiberboard or wood, and the weight of the package exceeds 220 lb (100 kg). Therefore, according to 10 CFR 71.71(c)(8), this test is not applicable to the Universal Transport Cask.

2.6.9 Compression

According to 10 CFR 71.71(c)(9), this test is not applicable to the Universal Transport Cask because the package weight is greater than 11,000 lb (5,000 kg).

2.6.10 Penetration

According to 10 CFR 71.71(c)(10), a penetration test involving a 13-lb (6-kg) penetration cylinder dropped from a height of 1 m is required for evaluation of packages during normal conditions of transport. However, Regulatory Guide 7.8 states that "the penetration test of 71.71 is not considered by the NRC staff to have structural significance for large shipping casks (except for unprotected valves and rupture disks) and will not be considered as a general requirement." Because the Universal Transport Cask has no unprotected valves or rupture disks that could be affected by normal conditions of transport, a penetration test is not performed.

2.6.11 Fabrication Stresses

The process of manufacturing the Universal Transport Cask can introduce thermal stresses in the inner and outer shells as a result of pouring molten lead between them. These thermal stresses are evaluated in this section to provide assurance that the manufacturing process does not adversely affect the normal operation of the cask or its ability to survive an accident. According to Regulatory Position 7 of Regulatory Guide 7.6, any residual stresses in the containment vessel shell resulting from inelastic strain associated with the secondary local bending stresses, which are due to the lead pour thermal gradient, must be considered in the total stress range for normal and accident load conditions. Residual stresses in the containment vessel and the outer shell induced by shrinkage of the lead shielding after the lead pouring operation are relieved early in the life of the cask because of the low creep strength of lead.

For the lead pour process, the initial temperature of the cask shells is controlled between 550°F and 650°F, and the lead temperature before pouring is between 698°F and 790°F. The cask is initially heated, at a rate not to exceed 90°F/hour, by using heaters inside the inner shell and heating rings around the outside of the outer shell. Heat-up is time-controlled consistent with uniform increases in shell temperatures. The heating procedures ensure that the cask surface temperature does not exceed 800°F during the molten lead pouring process. The shell temperatures are measured by thermocouples attached to the shell surfaces. A portable thermometer is also used to measure temperature at any location. To minimize the time that the cask is at elevated temperatures, cask heating begins only after all preparations have been completed.

The lead is poured after the cask reaches the specified temperatures. Molten lead is poured continuously through a filling tube with its open end maintained under the lead surface. The pouring time is kept as short as possible. During pouring, the interior heaters and exterior heating rings are continuously energized.

The cooling process consists of sequentially turning the exterior heating rings and interior heaters off, starting from the lowest point, and of spraying the cask with water from the outside. A layer of molten lead is maintained until the upper surface starts to solidify. This process allows the molten lead to fill the open space below it created by the lead shrinkage as it cools. The basic requirements and procedures for the Universal Transport Cask lead pour operations are described in Section 8.3.3.

2.6.11.1 Lead Pour

2.6.11.1.1 Cask Shell Geometry

At 70°F, the Type 304 stainless steel shell geometry is:

Inner Shell

Inside Diameter ($d_{i\text{-}70}$) = 67.61 in.

Outside Diameter ($d_{o\text{-}70}$) = 71.61 in.

Shell Thickness (t_i) = 2 in.

Outer Shell

Inside Diameter ($D_{i\text{-}70}$) = 77.11 in.

Outside Diameter ($D_{o\text{-}70}$) = 82.61 in.

Shell Thickness ($T_{o\text{-}70}$) = 2.75 in.

2.6.11.1.2 Stresses Resulting from Lead Pour

The hydrostatic pressure produced by the column of lead is:

$$q = \rho h = 73.8 \text{ psi}$$

where $\rho = 0.41$ lb/in^3 (lead density)

$h = 180$ in (maximum height of lead column)

For this analysis, it is assumed that the lead at a maximum temperature of 790°F, and the shell initially at 650°F, reach an equilibrium temperature of 750°F. At 750°F, key shell geometric dimensions are:

$$d_{o\text{-}750} = d_{o\text{-}70}\left(1 + \alpha \ \Delta T\right) = 72.09 \text{ in.}$$

$$D_{i\text{-}750} = D_{i\text{-}70}\left(1 + \alpha \ \Delta T\right) = 77.62 \text{ in.}$$

$$t_{i\text{-}750} = t_{i\text{-}70}\left(1 + \alpha \ \Delta T\right) = 2.01 \text{ in.}$$

where $\alpha = 9.76 \times 10^{-6}$ in/in/°F at 750°F (stainless steel)

$\Delta T = 750 - 70 = 680°F.$

The hydrostatic pressure of the molten lead subjects the inner shell to an external hydrostatic pressure, and the outer shell to an internal hydrostatic pressure. The hydrostatic pressure will vary from a maximum of 73.8 psi at the bottom of the inner shell to 0 psi at the top of the lead cylinder.

Using Reference [28] Table 29, Case 6, the deformation at the bottom of the inner shell, y_B, is found to be -1.955×10^{-3} in.

The maximum circumferential membrane stress in the inner shell is:

$$S_{\theta_{max}} = \frac{y_B E}{R} = -1323 \text{ psi}$$

where $E = 24.4\times10^{6}$ psi at 750°F

$R = 72.09/2 = 36.045$ in.

This stress will exist only as long as the lead is molten and will produce no plastic deformation of the inner shell. When the lead solidifies and begins to cool, it will shrink and exert a uniform external pressure on the inner shell because lead's coefficient of expansion is larger than that of stainless steel.

2.6.11.2 Cooldown

2.6.11.2.1 Hoop (Circumferential) Stresses

Lead decreases in volume during solidification. As the lower lead region solidifies, the molten lead above fills the shrinkage void between the solidifying lead and the inner and outer shells.

Using the coefficients of expansion for stainless steel and lead, the outer diameter of the steel shell and the inner diameter of the lead cylinder (assuming it is free to shrink) can be determined at 620°F (the melting point of lead) and at 70°F (normal conditions). Because the lead has a higher coefficient of expansion than stainless steel, a shrinkage force will develop between the steel shell outer surface and the lead inner surface. At 620°F, the outside diameter of the inner shell, and the inside diameter of the lead as it begins to solidify is:

$$d_{oshell620} = d_{oshell70}\left(1 + \alpha\ \Delta T\right) = 71.61\left(1 + 9.56 \times 10^{-6}(620 - 70)\right) = 71.98 \text{ in.}$$

where $d_{oshell70} = 71.61$ in.

$\alpha_{shell} = 9.56 \times 10^{-6}$ in./in./ °F (at 620°F)

If the lead were cooled without restraint to 70°F, the inner diameter of the lead cylinder would shrink to:

$$d_{ilead70} = d_{ilead620}\left(1 - \alpha\ \Delta T\right) = 71.98\left(1 - 20.2 \times 10^{-6}(620 - 70)\right) = 71.18 \text{ in.}$$

where

$d_{ilead620} = d_{oshell620} = 71.98$ in.

$\alpha_{lead} = 20.2 \times 10^{-6}$ in./in./°F

The interference between the lead cylinder and the inner shell is (71.61-71.18)/2 = 0.215 in. To fully accommodate this interference, the lead must be deformed 0.215 in.

For δ = 0.215 in., the maximum circumferential stress, $S_{\theta max}$, in the inner shell is:

$$S_{\theta max} = \frac{\delta\,(E)}{R} = 13.8 \text{ psi}$$

where $R = 71.18/2 = 35.6$ in.

$E = E_{lead70} = 2.28 \times 10^3$ psi

From Reference [28], Table 29, Case 12, the radial deformation of the inner shell under a uniform external radial pressure of 13.8 psi is determined for values of x, the distance from the open end of the inner shell, at 0.15 ft increments and the results are tabulated in Table 2.6.11.2-1. Examination of the data in Table 2.6.11.2-1 shows that the maximum radial deformation and circumferential stress, S_θ, occur at x = 13.65 ft.

The maximum circumferential membrane stress in the inner shell is:

$$S_{\theta_{max}} = \frac{yE}{R} = -255.3 \text{ psi}$$

where y = the radial deformation, -3.299×10^{-4} in.

$E = 28.3\times10^{6}$ psi

$R = 71.61/2 = 35.805$ in.

Axial Stresses

Axial stresses also develop in the lead shell and inner shell during fabrication as a result of the unequal shrinkage of the lead and steel shells. Assuming that the lead bonds to the inner shell during the cooldown process after completion of lead pouring, the strain in the lead, when cooled to 70°F, is:

$$M_{lead} = (\alpha_{lead} - \alpha_{shell})\Delta T = 0.0060 \text{ in/in.}$$

where $\alpha_{lead} = 20.2 \times 10^{-6}$ in/in/°F

$\alpha_{shell} = 9.56 \times 10^{-6}$ in/in/°F

$\Delta T = 620 - 70 = 550$°F

$$S_{lead} = \varepsilon E = 0.006 \times 2.28\times10^{6} = 13{,}680 \text{ psi}$$

The calculated stress is above the yield point of lead (ranging from 20 psi at 620°F to 640 psi at 70°F). The axial load placed on the steel inner shell by shrinkage of the lead is therefore limited by the yield strength of lead. The maximum load is:

$$P_{lead} = 640 \times (38.56^2 - 35.805^2)\pi = 411{,}930 \text{ lb.}$$

The corresponding compression stress in the inner shell to maintain equilibrium is:

$$S_{shell} = \frac{P}{A} = \frac{-411{,}930}{\pi\left((35.805)^2 - (33.805)^2\right)} = -942 \text{ psi}$$

This value is conservative because the yield strength of lead is very low at elevated temperatures (505 psi at 200°F; 380 psi at 300°F), therefore, the creep rate is high. Also, complete bonding of

the lead to the stainless steel inner shell is not expected to occur. Because it is based on the yield strength of lead at 70°F, this case bounds all others to be considered for axial loading.

2.6.11.2.3 Effects of Temperature Differential During Cooldown

The preceding analyses assume that the inner and outer shells and the lead are always at the same temperature at any time during the cooldown process. This assumption may not be true under actual conditions. However, because of the high thermal conductivity of the stainless steel and the lead, and because of the time-controlled cooldown process, the temperature differential between any two of the above shells is kept to a minimum. To determine the effect of temperature differential on the stresses in the shells, a temperature differential of 100°F is used.

If the inner shell is cooler than the lead, the interference between them as well as the corresponding interface pressure and hoop stresses are less than for the case of equal temperatures. Hence, the preceding analysis is conservative.

If the inner shell is hotter than the lead shell, an analysis is required. Assume the temperature of the inner shell to be 170°F and that of the lead to be 70°F. The inner radius of the stress-free lead shell at 70°F is 35.59 in.; the outer radius of the inner shell at 170°F is:

$$r_o = 35.805\,[1 + (8.54 \times 10^{-6})(100)] = 35.836 \text{ in.}$$

The interference between the inner shell and the lead is 35.836 - 35.59 = 0.246 in. To fully accommodate this interference, the lead must undergo a deformation of 0.246 in.

For $\delta = 0.246$ in., $S = \dfrac{\delta(E)}{R} = 15.6$ psi

where $R = 71.18/2$ in. $= 35.59$ in.

$E = 2.28\times10^3$ psi (at 70°F)

Using the same method as in the previous section, the radial deformation of the inner shell at x = 13.65 ft., the point of maximum deflection, is found to be -3.293×10^{-4} in.

The maximum circumferential membrane stress in the inner shell is:

$$S_{\theta_{max}} = \frac{yE}{R} = \frac{-3.293\times10^{-4}\left(27.8\times10^{6}\right)}{35.836} = -255.5 \text{ psi}$$

The axial stress in the inner shell also increases when the inner shell is 100°F hotter than the lead shell. As shown previously, the axial load on the inner shell is limited by the yield strength of the lead. Therefore, the previously computed axial load is the bounding case for this analysis.

Temperature differentials between the inner and outer shells are of no consequence, because the axial restraint between them is welded in place after cooldown, when the cask is at a uniform ambient temperature. Welding of the outer shell and the bottom inner forging to the bottom outer forging after cooldown is, therefore, a necessary fabrication step.

2.6.11.3 Lead Creep

As discussed in Section 2.6.11, cooling of the lead shell and inner shell introduces acceptably low hoop and axial stresses in the inner shell. Because lead demonstrates a significant creep rate at both room and elevated temperatures, these small stresses will be relieved early in the life of the cask, and will be further relieved during the thermal test of the cask.

Table 2.6.11.2-1 Stress Analysis Results for Uniform Pressure Loading of Inner Shell Due to Lead Pouring

X (ft)	Hoop stress, σ_2 (psi)	Radial Deflection, y (in.)
0.00	-247.1	-0.00031
0.15	-247.1	-0.00031
0.30	-247.1	-0.00031
0.45	-247.1	-0.00031
0.60	-247.1	-0.00031
0.75	-247.1	-0.00031
0.90	-247.1	-0.00031
1.05	-247.1	-0.00031
1.20	-247.1	-0.00031
1.35	-247.1	-0.00031
1.50	-247.1	-0.00031
1.65	-247.1	-0.00031
1.80	-247.1	-0.00031
1.95	-247.1	-0.00031
2.10	-247.1	-0.00031
2.25	-247.1	-0.00031
2.40	-247.1	-0.00031
2.55	-247.1	-0.00031
2.70	-247.1	-0.00031
2.85	-247.1	-0.00031
3.00	-247.1	-0.00031
3.15	-247.1	-0.00031
3.30	-247.1	-0.00031
3.45	-247.1	-0.00031
3.60	-247.1	-0.00031
3.75	-247.1	-0.00031
3.90	-247.1	-0.00031
4.05	-247.1	-0.00031
4.20	-247.1	-0.00031
4.35	-247.1	-0.00031
4.50	-247.1	-0.00031
4.65	-247.1	-0.00031
4.80	-247.1	-0.00031

Table 2.6.11.2-1 Stress Analysis Results for Uniform Pressure Loading of Inner Shell Due to Lead Pouring (Continued)

X (ft)	Hoop stress, σ_2 (psi)	Radial Deflection, y (in.)
4.95	-247.1	-0.00031
5.10	-247.1	-0.00031
5.25	-247.1	-0.00031
5.40	-247.1	-0.00031
5.55	-247.1	-0.00031
5.70	-247.1	-0.00031
5.85	-247.1	-0.00031
6.00	-247.1	-0.00031
6.15	-247.1	-0.00031
6.30	-247.1	-0.00031
6.45	-247.1	-0.00031
6.60	-247.1	-0.00031
6.75	-247.1	-0.00031
6.90	-247.1	-0.00031
7.05	-247.1	-0.00031
7.20	-247.1	-0.00031
7.35	-247.1	-0.00031
7.50	-247.1	-0.00031
7.65	-247.1	-0.00031
7.80	-247.1	-0.00031
7.95	-247.1	-0.00031
8.10	-247.1	-0.00031
8.25	-247.1	-0.00031
8.40	-247.1	-0.00031
8.55	-247.1	-0.00031
8.70	-247.1	-0.00031
8.85	-247.1	-0.00031
9.00	-247.1	-0.00031
9.15	-247.1	-0.00031
9.30	-247.1	-0.00031
9.45	-247.1	-0.00031
9.60	-247.1	-0.00031
9.75	-247.1	-0.00031

Table 2.6.11.2-1 Stress Analysis Results for Uniform Pressure Loading of Inner Shell Due to Lead Pouring (Continued)

X (ft)	Hoop stress, σ_2 (psi)	Radial Deflection, y (in.)
9.90	-247.1	-0.00031
10.05	-247.1	-0.00031
10.20	-247.1	-0.00031
10.35	-247.1	-0.00031
10.50	-247.1	-0.00031
10.65	-247.1	-0.00031
10.80	-247.1	-0.00031
10.95	-246.9	-0.00031
11.10	-246.9	-0.00031
11.25	-246.9	-0.00031
11.40	-246.9	-0.00031
11.55	-246.9	-0.00031
11.70	-246.7	-0.00031
11.85	-246.7	-0.00031
12.00	-246.7	-0.00031
12.15	-246.7	-0.00031
12.30	-246.9	-0.00031
12.45	-247.1	-0.00031
12.60	-247.6	-0.00031
12.75	-248.2	-0.00031
12.90	-249.1	-0.00032
13.05	-250.4	-0.00032
13.20	-251.7	-0.00032
13.35	-253.2	-0.00032
13.50	-254.5	-0.00032
13.65	-255.3	-0.00032
13.80	-255.1	-0.00032
13.95	-253.2	-0.00032
14.10	-248.6	-0.00031
14.25	-240.7	-0.0003
14.40	-227.9	-0.00029
14.55	-209.9	-0.00027
14.70	-185.9	-0.00024
14.85	-156.5	-0.0002
15.00	-123.5	-0.00016

2.6.12 PWR Transportable Storage Canister Analysis - Normal Conditions of Transport

In this section, the Transportable Storage Canister assembly containing PWR fuel is evaluated for the normal conditions of transport. The principal components of the canister assembly are the canister, the fuel basket assembly, the shield lid, and the structural lid. The canister and the canister shell, bottom plate, and lids are shown in Figures 2.6.12-1 and 2.6.12-2.

Spacers are used to properly locate the canisters containing Class 1 and 2 PWR fuel in the cask cavity. The analysis of the spacers is presented in Section 2.6.16. The geometries and materials of construction of the canister, baskets, and spacers are described in Section 1.2.1.2.

2.6.12.1 Analysis Description

The Transportable Storage Canister contains and confines the spent fuel in the fuel basket. The canister is the defined confinement boundary for its contents during transport and storage operations, but the canister is not considered to provide containment during transport operation; the Universal Transport Cask provides the containment boundary for transport. The canister in the transfer cask serves as the handling component for its basket and contents during loading, closure, and transfer from the pool to storage or to the transport vehicle.

Three canisters of varying lengths are designed to accommodate the three classes of PWR fuel. The design parameters of the canisters are provided in Table 1.2-3. For this analysis, the canister is modeled with the heaviest fuel (Class 2).

The structural design criteria for the canister is from the ASME Code Section III, Subsection NB. Consistent with this criterion, the structural components of the canister are shown to satisfy the allowable stress limits presented in Tables 2.1.2-2 and 2.1.2-3 as applicable. The allowable stresses used in this analysis are based on a temperature of 380°F for all locations in the canister, unless otherwise indicated. These allowables are conservative for all sections in the canister with the exception of Sections 5 and 6 (see Figure 2.6.12.3-1 for section locations).

For the canister structural lid weld (Section 13, Figure 2.6.12.3-1), base metal properties are used to define the allowable stress limits since the weld filler rod tensile properties are greater than the base metal. Also, the allowable stress is multiplied by a stress reduction factor of 0.8 per ISG-4 [49].

Figure 2.6.12-1 PWR Transportable Storage Canister

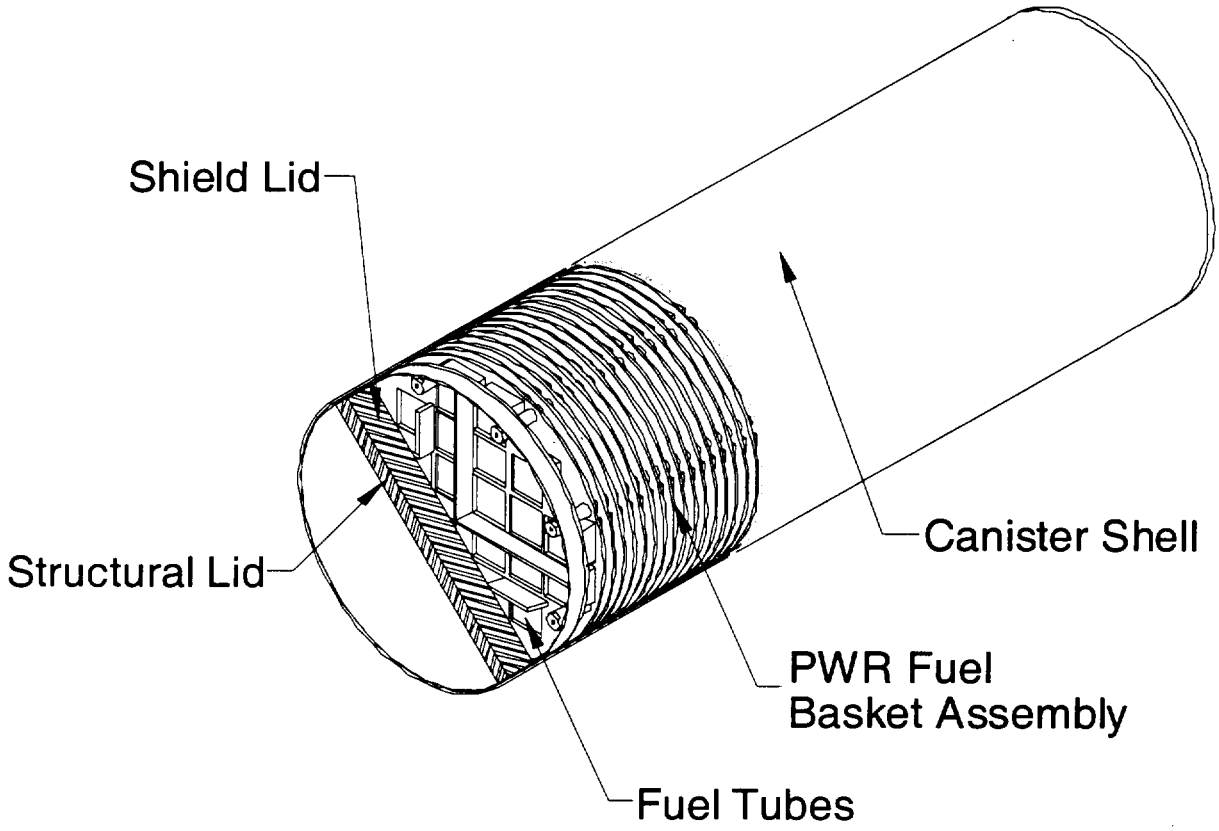

Figure 2.6.12-2 PWR Transportable Storage Canister Shell and Lids

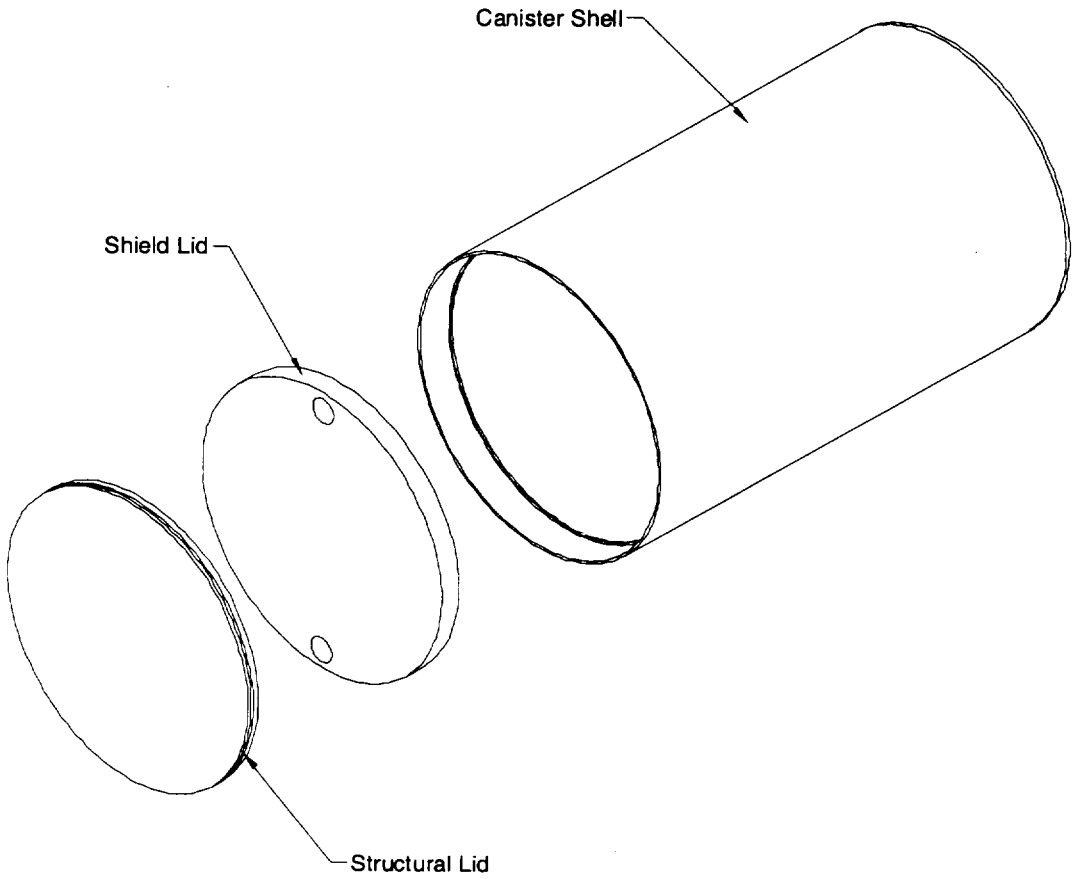

The maximum temperature in the canister shell central region is 399°F as determined in the thermal analysis presented in Section 3.4.2. This increase in temperature reduces the allowable S_m for Type 304L stainless steel from 16.0 ksi to 15.8 ksi. A review of the margins of safety for all cases evaluated indicates that the minimum margin for Sections 5 or 6 is 4.3 for the side-drop with pressure (Table 2.6.12.6-3). Using the allowable stress based on a temperature of 399°F reduces this minimum margin of safety to 4.23. Because this change in margin of safety is small, the increased peak temperature in the center of the canister has a negligible impact on the presented minimum margins.

The canister is analyzed by using the ANSYS [32] finite element computer program for the 1-ft free-drop condition in the top and bottom end, side, and top and bottom corner impact orientations. In addition, the effects of normal operating internal pressure and thermal stresses resulting from exposure of the cask to the hot (100°F ambient and solar insolance) and cold (-40°F ambient) normal conditions are evaluated. The worst-case stresses from these analyses are presented in Section 2.6.12.4.

2.6.12.2 Finite Element Model Description - PWR Canister

To evaluate the PWR Transportable Storage Canister for normal conditions of transport, ANSYS is used to construct and analyze a finite element model of the canister and its contents. The contents modeled consist of the fuel basket support disks and weldments. The fuel assemblies, fuel tubes, aluminum heat transfer disks, tie-rods, and related hardware are not explicitly modeled but rather are accounted for by applying pressure loads to the support disk slots as appropriate.

The finite element model of the canister is constructed by using ANSYS solid (SOLID45) elements. The model represents a one-half (180°) section of the canister and fuel basket. The basket support disks are modeled with three-dimensional shell (SHELL63) elements. The model uses gap-spring elements to simulate contact between adjacent components. Interaction between the basket and canister is accomplished by using three-dimensional gap elements (CONTAC52) along the periphery of the support disks. Contact between the canister and the cask inner shell is also modeled by using CONTAC52 gap elements. Contact between the canister structural lid and shield lid is modeled by using COMBIN40 combination elements in the axial degree of freedom. Simulation of the backing ring is accomplished by using a ring of COMBIN40 spring

gap elements connecting the shield lid and the canister in the axial direction at the lid lower outside radius. In addition, CONTAC52 elements are used to model interaction between the structural lid and canister shell and the shield lid and canister shell just below the respective lid weld joints. The size of the CONTAC52 gaps are determined from the nominal dimensions of contacting components. The COMBIN40 elements used between the structural and shield lids and for the backing ring are assigned small gap sizes of $1(10)^{-8}$ in. All gap-spring elements are assigned a stiffness of $1(10^{8})$ lb/in. Table 2.6.12.2-1 lists the element types assigned to specific gaps of the model. Table 2.6.12.2-2 lists the material properties used for the model.

Boundary conditions are applied to enforce symmetry at the cut boundary of the model. All nodes on the cask shell side of the canister-to-cask gap elements are fixed in all degrees of freedom. In addition, the axial and in-plane rotational degrees of freedom of the basket nodes are fixed.

Figure 2.6.12.2-1 is a plot of the entire canister finite element model including the support disks. An isolated view of the canister shield and structural lids portion of the model is presented in Figure 2.6.12.2-2, and an enlarged view of the model in the structural lid and shield lid weld regions is shown in Figure 2.6.12.2-3. The canister bottom plate portion of the model is shown in Figure 2.6.12.2-4.

The loading for the normal operating condition is based on 1-ft drops in conjunction with the internal pressure loading (to the canister). Drop orientations considered are the top and bottom end, side, and top and bottom corner-drops. In the end-drop orientation, the fuel contents load is transferred to the canister end and directly to the transport cask end through the cavity spacer. This corresponds to a compressive stress in the canister ends that is present in the finite element model. The canister shell is designed to be flush with the top surface of the structural lid with the worse case tolerance stack-up. This ensures that the content weight will be transferred through the lids to the transport cask during a top end or top corner drop condition. For the side-drop condition, the loads from the canister contents weight are transferred through the support disks into the canister wall, which is backed by the cask inner shell. Because the canister wall and the inner shell have different radii, a gap exists between the two surfaces. This gap results in the load passing only through regions in which the canister shell deflects to contact the inner shell. This load pattern is reflected in the side-drop analysis. For the corner-drop orientation, both the end-and side-load reactions with the cask inner shell are present.

The modeled contents weight includes 37,080 lb for all fuel assemblies (24 Class 1 PWR fuel assemblies), the fuel tube weight (3,417 lb), the aluminum heat transfer disk weight (1,946 lb), the disk spacer weight (1,879 lb), and the tie rod and nut and washer weights (783 + 94 lb). The weight of the support disks and weldments is accounted for by their being physically modeled. The PWR Class 1 configuration results in the largest load per support disk. The modeled canister length is 173.75 inches.

For the side and corner-drops, the weights of the fuel assemblies (W_{fuel}), aluminum heat transfer disks ($W_{ht\ disks}$), fuel tubes (W_{tubes}), tie rods (W_{rods}), nuts/washers (W_{nuts}), and spacers ($W_{spacers}$) are included in the model by applying a pressure load (F_{slot}) to the slot openings of the modeled support/weldment disks. This pressure load is calculated according to the following equation:

$$F_{slot} = \frac{W_{fuel} + W_{ht\ disks} + W_{tubes} + W_{rods} + W_{nuts} + W_{spacers}}{N_{slots} \times w_{slot} \times N_{disks}} \times g$$

where,

N_{slots} = number of slot openings in each support/weldment disk,
w_{slot} = width of each slot opening in each support/weldment disk,
N_{disks} = number of support/weldment disks, and
g = the associated g-loading for the drop height of interest.

For basket orientations other than 0°, the components of this resulting pressure load are applied to two faces of the slot opening. Additionally, for the corner-drops, the component resulting from accounting for the drop angle is used as the pressure load on the disk slot openings. For the PWR canister drop analyses, with 24 slot openings, a slot opening width of 9.272 inches, and a total of 34 support/weldment disks (32 support disks and 2 weldment disks), the resulting base pressure load used is:

$$F_{slot} = \frac{37{,}080 + 1{,}946 + 3{,}417 + 783 + 94 + 1{,}879}{24 \times 9.272 \times 34} \times g = 5.974 \times g$$

For the end drops, a uniform pressure representing the total weight of the fuel and fuel basket (52,369 lb) is applied to the canister shield lid (for top end-drop) or canister bottom plate (for

bottom end-drop). For the corner-drops, the component of this uniform pressure resulting from accounting for the drop angle is applied to the appropriate elements.

Changes were made to the fuel and fuel basket weight calculations after the finite element analyses were performed. These changes resulted in a total fuel and fuel basket weight of 52,565 lb. The total weight of the fuel and fuel basket analyzed in the PWR canister models is 52,369 lb. The revised calculations result in an increase in fuel and fuel basket weight of less than 1%; therefore, the modeled configuration will provide adequate stress results. Additionally, the length of the PWR Class 1 canister length was increased from 173.75 in. to 175.05 in. This is an increase of less than 1% and would also not sufficiently affect the results presented from these analyses.

The operational conditions also contain loads developed from the temperature distribution in the canister. These are included in the canister model analyses. The thermal analyses are described in Section 3.4.

The canister is analyzed for basket orientations of 0° and 45°. The angles describe the orientation of the basket elements with respect to the symmetry plane of the model. A value of 0° orients the ligaments in the basket elements parallel and perpendicular to the symmetry plane; a value of 45° orients the basket ligaments at +/- 45° from the symmetry plane. To accurately predict the canister response to impact, both orientations are run for the side, top-over-center-of-gravity, and bottom-over-center-of-gravity drop orientations. Top-end and bottom-end drops with varying basket orientations are not required since the basket disks are not included in these runs (their presence is accounted for by using applied pressure loads to the inner surface of the top or bottom).

Figure 2.6.12.2-1 PWR Canister Assembly Finite Element Model

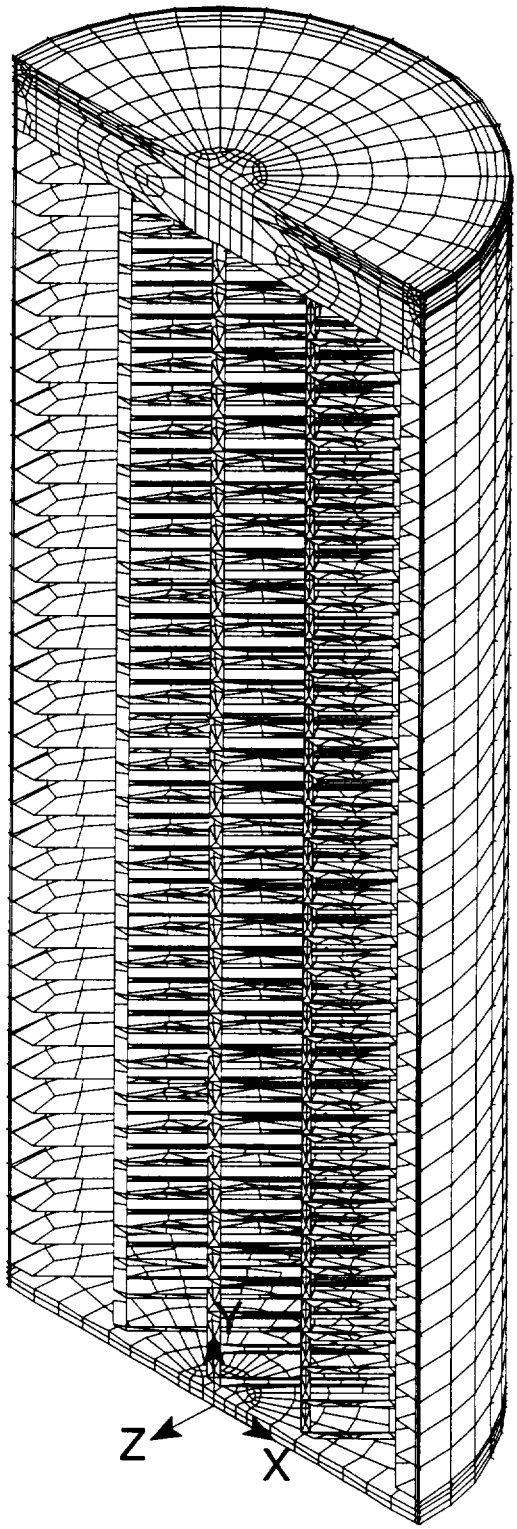

Figure 2.6.12.2-2 Canister Structural and Shield Lid Finite Element Mesh

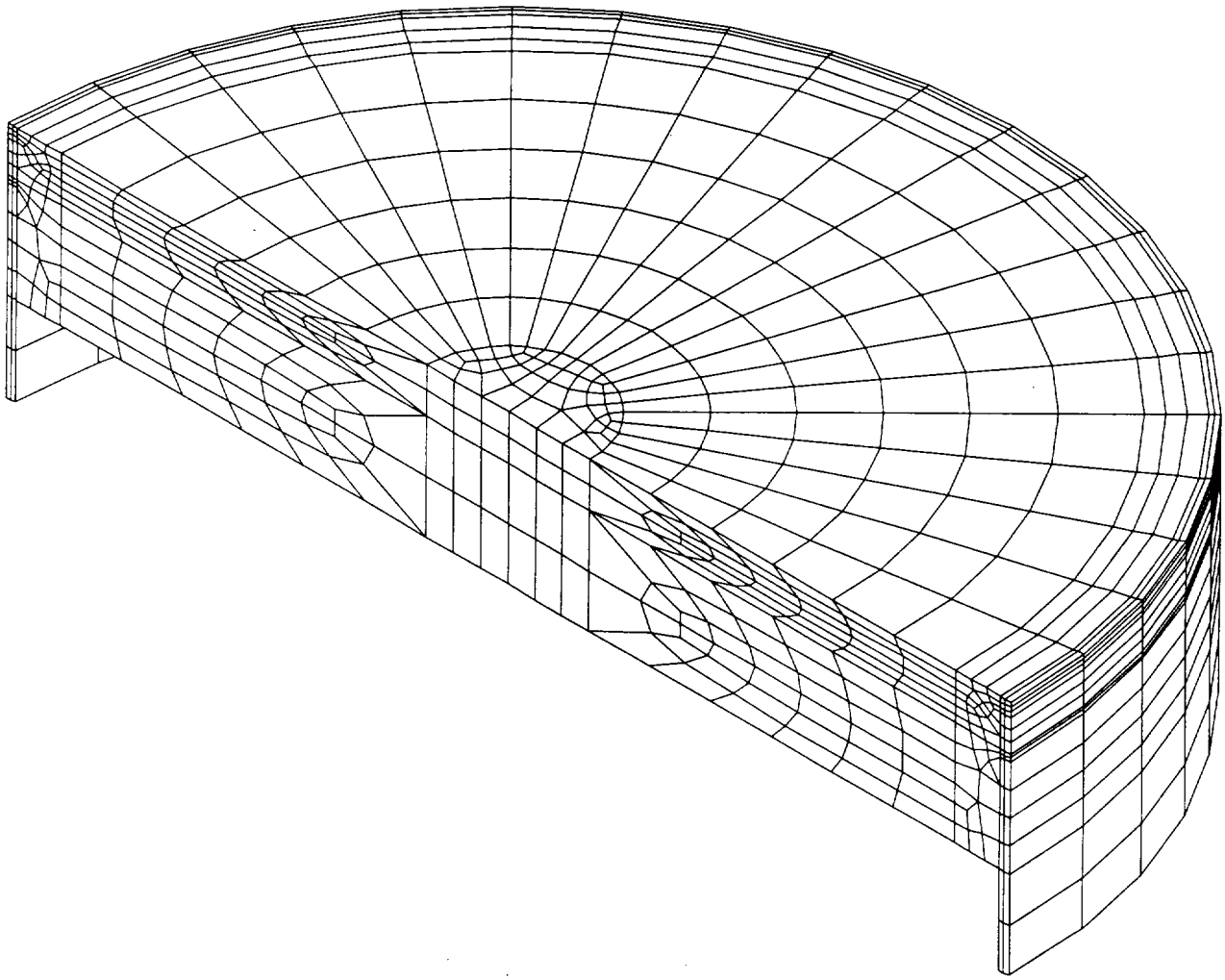

Figure 2.6.12.2-3 Structural and Shield Lid Weld Regions Finite Element Mesh

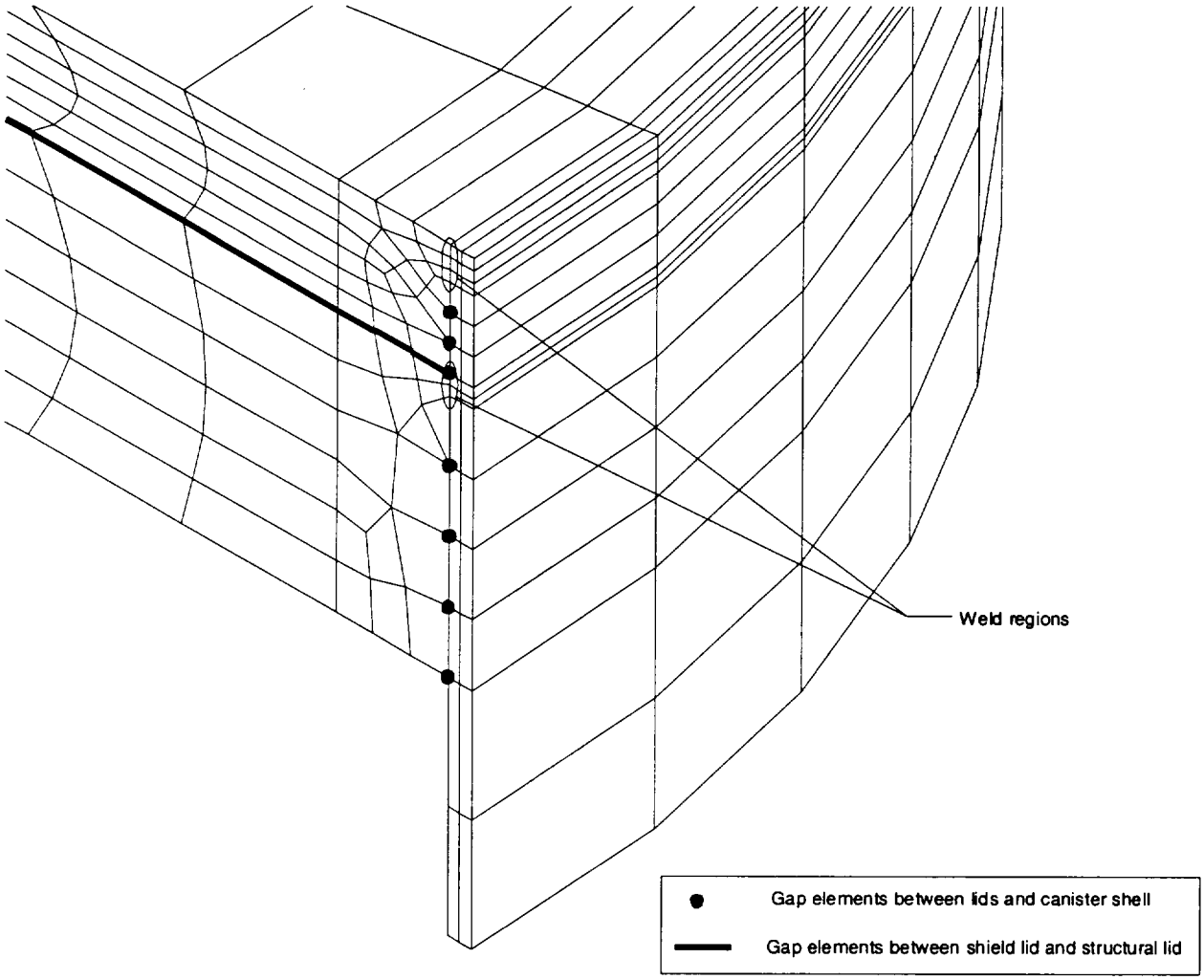

Figure 2.6.12.2-4 Canister Bottom Plate Finite Element Mesh

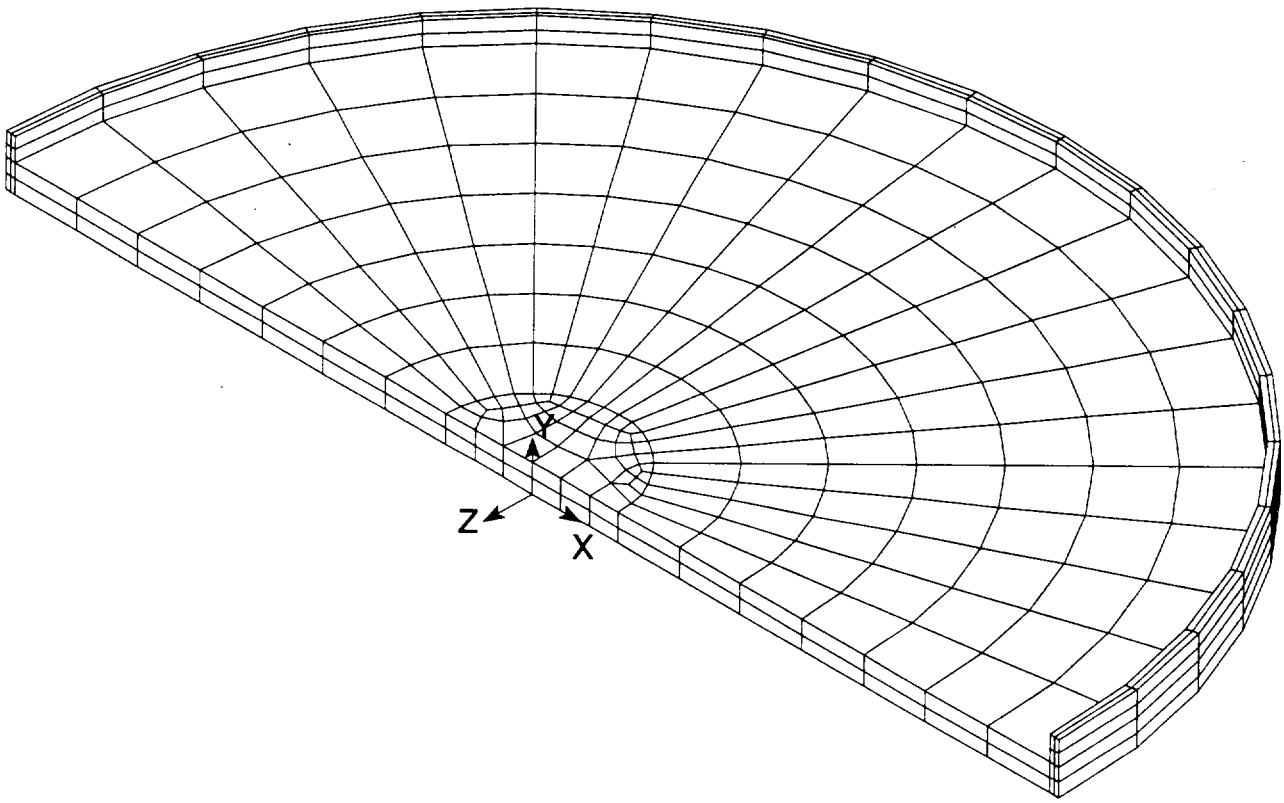

Table 2.6.12.2-1 Gap and Element Type Definition - Canister Model

Component
Axial Gaps from Canister Bottom Plate to Cask Shell (CONTAC52)
Radial Gaps from Canister Side to Cask Shell (CONTAC52)
Axial Gaps from Structural Lid Top to Cask Shell (CONTAC52)
Axial Gaps Between Structural and Shield Lid (COMBIN40)
Radial Gaps Between Shield Lid and Canister Inner Surface (CONTAC40)
Radial Gaps Between Shield Lid and Canister Inner Radius (CONTAC52)
Axial Gaps Between Shield Lid and Canister Wall to Simulate Backing Ring (COMBIN40)
Radial Gaps Between Basket and Canister Inner Surface (CONTAC52)

Table 2.6.12.2-2 Material Definition - Canister Model

Component	Material
Canister Shell and Structural Lid	304L Stainless Steel; ASME SA240
Top and Bottom Weldments	304 Stainless Steel; ASME SA240
Shield Lid	304 Stainless Steel; ASME SA240
Support disk	17-4 PH, ASME SA693 Type 630 Stainless Steel

2.6.12.3 Thermal Expansion and Thermal Stresses Evaluation of Canister for PWR Fuel

A thermal stress evaluation performed by using ANSYS determines the differential thermal expansion and the associated thermal stresses that result from a heat load of 20 kW. In assessing the thermal stresses, the following three extreme conditions are possible:

Condition	Ambient Temperature	Solar Insolance Applied to Cask Surface	20 kW Fuel Load
1	100°F	Yes	Yes
2	-40°F	No	Yes
3	-40°F	No	No

The temperatures employed in the thermal stress analysis are obtained by applying temperatures at 36 key locations on the canister shell and ends as thermal boundary conditions to the thermal equivalent model of the structural canister model. These temperatures are taken from the thermal evaluation described in Section 3.4. The structural finite element model described in Section 2.6.12.2 is used in this analysis. The equivalent thermal model is obtained by changing the structural element (SOLID45, which has three global displacements for degrees of freedom) to a SOLID70, which has temperature degrees of freedom at the individual nodes. The temperature-dependent thermal conductivity for the canister material is employed in the thermal conduction analysis. The temperatures generated in this analysis are used in the thermal stress analysis to evaluate the properties at temperature, as well as the stresses resulting from thermal expansion. Using this method, two separate cases: (Conditions 1 and 2) are evaluated: a hot case (100°F ambient with solar heat load and maximum decay heat) and a cold case (-40°F ambient and maximum decay heat). Condition 3 is not evaluated because the entire assembly would be at -40°F for the conditions described.

According to the ASME Code, Section III, Subsection NB, the allowable stress criteria are based on the evaluation of linearized stresses across critical cross sections through the canister wall. For the evaluation of the thermal stresses, the criteria for the stresses is based on peak stresses. The stress values taken from the analyses are the nodal stresses at the surface. The sections used in this evaluation are shown in Figure 2.6.12.3-1. Sections are evaluated every 9° around the circumference for each of the locations shown. The thermal stresses reported in Tables

2.6.12.3-1 and 2.6.12.3-2 correspond to the maximum stresses for any circumferential section, for each of the locations shown in Figure 2.6.12.3-1.

For Condition 1 or 2, the canister is hotter than the cask body and will undergo more thermal expansion than the cask body. To conservatively determine the minimum gap between the canister and the cask body resulting from thermal expansion, only expansion of the canister is considered. The canister is considered to be at 399°F (maximum shell temperature for thermal heat condition) and the cask inner shell temperature is assumed to be 70°F. Using the outer diameter of the canister of 67.06 in. and the coefficient of expansion for Type 304L stainless steel of 9.19 $(10)^{-6}$ at 400°F, the canister inner shell gap is reduced by (9.19 $(10)^{-6}$)(67.06 in.)(329°F) = 0.203 in. Because the nominal diametrical canister-inner shell gap is 67.61-67.06 = 0.55 in., the canister shell does not bind with the inner shell as a result of thermal expansion.

The maximum canister shell temperature is 399°F. This temperature is conservative to use for the axial expansion since a temperature gradient exists along the length of the canisters (i.e., the canister is cooler on the ends). The thermal expansion coefficient of Type 304L stainless steel at 400°F is 9.19 $(10)^{-6}$ in/in-°F. The longest canister configuration is PWR Class 3 with a length of 191.95 in. The increase in length of the canister is then

$$l = l_0 \, \alpha \, \Delta T$$

$$\Delta l = 191.95 \, (9.19 \, (10)^{-6} \text{ in/in-°F}) \, (399 - 70) = 0.58 \text{ in.}$$

The canister length increases to 191.95 + 0.58 = 192.53 in.

The minimum cask shell temperature is conservatively assumed to be 150°F (the peak inner shell temperature is 367.7°F; the upper forging minimum temperature is 237.5°F). The thermal expansion coefficient of Type 304 stainless steel at 70°F is conservatively used since the expansion coefficient increases with temperature 8.46 $(10)^{-6}$ in/in-°F. The cask cavity nominal length is 192.5 in. The increase in length of the cask cavity is then

$$\Delta l = 192.5 \, (8.46 \, (10)^{-6} \text{ in/in-°F}) \, (150 - 70) = 0.13 \text{ in.}$$

The cask cavity length increases to 192.5 + 0.13 = 192.63 in. The resulting axial gap is 192.63 - 192.53 = 0.1 in. Therefore, the canister and cask will expand axially and not bind during normal transport conditions.

Figure 2.6.12.3-1 Identification of Sections for Evaluating Linearized Stresses in Canister (in)

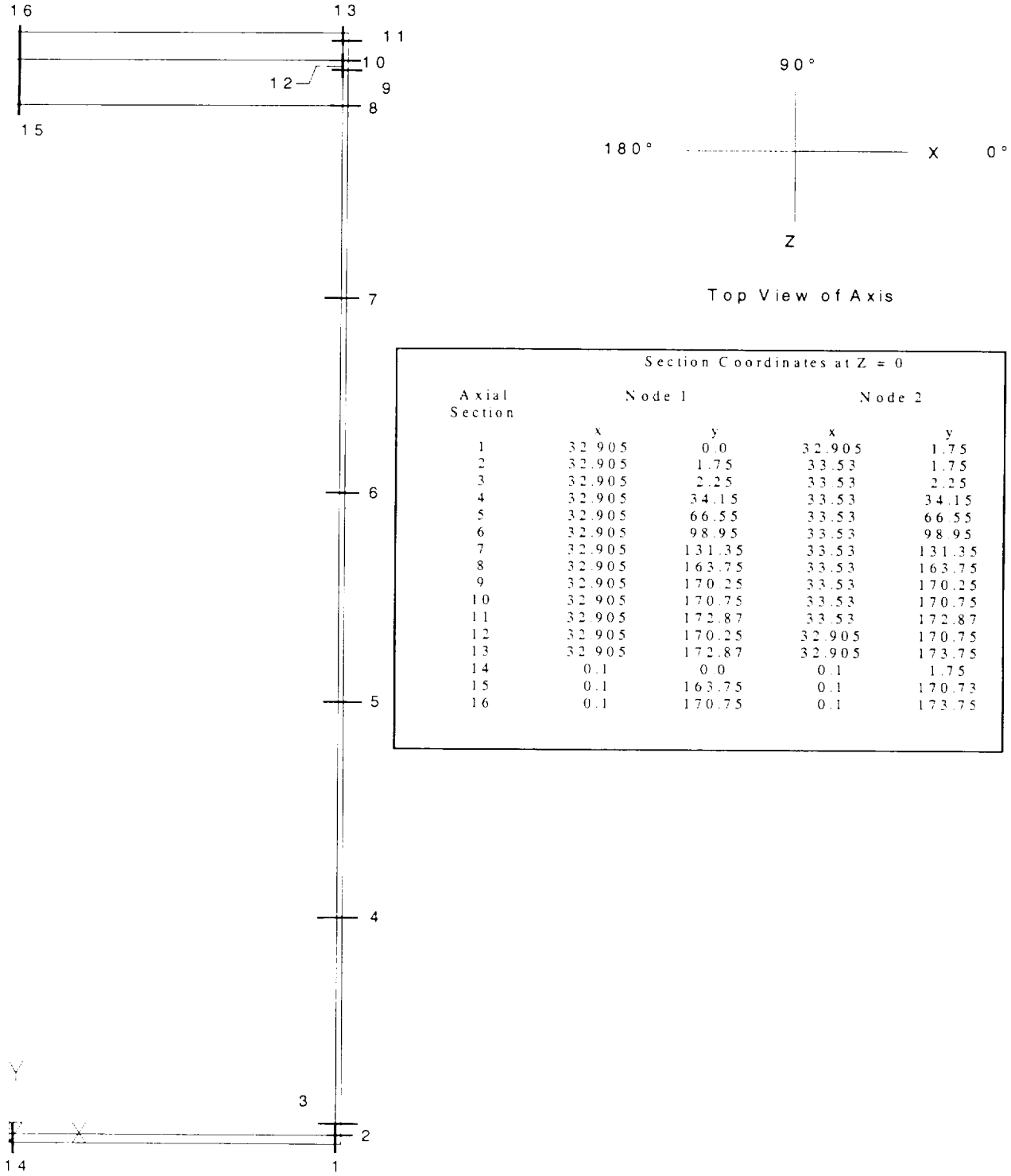

Section Coordinates at Z = 0				
Axial Section	Node 1		Node 2	
	x	y	x	y
1	32.905	0.0	32.905	1.75
2	32.905	1.75	33.53	1.75
3	32.905	2.25	33.53	2.25
4	32.905	34.15	33.53	34.15
5	32.905	66.55	33.53	66.55
6	32.905	98.95	33.53	98.95
7	32.905	131.35	33.53	131.35
8	32.905	163.75	33.53	163.75
9	32.905	170.25	33.53	170.25
10	32.905	170.75	33.53	170.75
11	32.905	172.87	33.53	172.87
12	32.905	170.25	32.905	170.75
13	32.905	172.87	32.905	173.75
14	0.1	0.0	0.1	1.75
15	0.1	163.75	0.1	170.73
16	0.1	170.75	0.1	173.75

Table 2.6.12.3-1 PWR Canister Linearized Q Stresses - Thermal Only (Hot 1)

Section Location	Angle of Peak Stress Location	Q Stresses (ksi)						SI (ksi)	[redacted]	[redacted]
		Sx	Sy	Sz	Sxy	Syz	Sxz			
1	180	0.2	0.1	2.1	-0.1	0	-0.1	2.2	[redacted]	[redacted]
2	9	-0.3	-1.2	0.7	-0.1	0	0.2	1.9	[redacted]	[redacted]
3	9	-0.1	-1.1	0.9	-0.1	0	0.2	1.9	[redacted]	[redacted]
4	0	0	-0.2	0.1	0	0	0	0.3	[redacted]	[redacted]
5	0	0	-0.8	0.7	0	-0.2	0	1.5	[redacted]	[redacted]
6	0	0	-0.6	0.3	0	0.1	0	0.9	[redacted]	[redacted]
7	0	0	-0.6	0.1	0	0	0	0.6	[redacted]	[redacted]
8	90	1	1.6	0	0	0	0	1.6	[redacted]	[redacted]
9	162	0.1	-1.6	-0.5	-0.1	0	0.2	1.7	[redacted]	[redacted]
10	90	0.3	1.7	-0.2	-0.2	0	0	1.9	[redacted]	[redacted]
11	81	-0.5	-1.4	0.2	-0.1	-0.1	-0.1	1.6	[redacted]	[redacted]
12	162	-0.3	0.6	-0.1	-0.1	0.1	-0.2	1.1	[redacted]	[redacted]
13	81	-0.4	0.1	-0.7	0	-0.1	0	0.8	[redacted]	[redacted]
14	0	-8.1	-1.4	-7.9	0.8	0.8	0.5	7.3	[redacted]	[redacted]
15	180	0.4	0	-0.1	-0.8	0	1.7	3.8	[redacted]	[redacted]
16	180	-0.2	0	0.1	-0.7	0	-1.2	2.7	[redacted]	[redacted]

Table 2.6.12.3-2 Linearized Stresses - Thermal Only (Cold 2)

Section Location	Angle of peak stress location	Q Stresses (ksi)						SI (ksi)		
		Sx	Sy	Sz	Sxy	Syz	Sxz			
1	180	0.2	0.1	2.4	-0.1	0	-0.2	2.4		
2	9	-0.3	-1.2	0.9	-0.1	0	0.2	2.1		
3	9	-0.1	-1.1	1	-0.1	0	0.2	2.1		
4	0	0	-0.3	0.1	0	0	0	0.4		
5	0	0	-0.9	0.8	0	-0.2	0	1.7		
6	0	0	-0.7	0.4	0	0.1	0	1.1		
7	0	0	-0.7	0.1	0	0	0	0.8		
8	90	1.1	1.8	0	0	0	0	1.8		
9	162	0.1	-1.6	-0.5	-0.1	0	0.2	1.7		
10	90	0.4	2	-0.2	-0.2	0	0	2.2		
11	81	-0.6	-1.5	0.2	-0.1	-0.1	-0.1	1.8		
12	162	-0.3	0.6	-0.1	-0.1	0.2	-0.2	1.1		
13	81	-0.5	0.1	-0.8	0	-0.1	0	0.9		
14	0	-9.1	-1.7	-8.8	0.7	0.9	0.5	8		
15	180	0.4	0	-0.1	-0.7	0	1.5	3.4		
16	180	-0.2	0	0.1	-0.6	0	-1	2.4		

2.6.12.4 Stress Evaluation of PWR Canister for 1-Foot End-Drop Load Condition

A structural analysis performed by using ANSYS evaluates the effect of a 1-ft end-drop impact for both the bottom and top-end orientations of the PWR canister. The ASME Code, Section III, Subsection NB requires that stresses arising from operational loads be assessed on the basis of the primary loads. The primary loads for the 1-ft drop result from the deceleration of the canister and its contents and the 25-psig pressure load internal to the canister. The applied deceleration is 20 *g* for both orientations. The inertial load of the canister is addressed by the deceleration factor applied to the canister density. The weight of the contents is represented by a pressure load on the inner end surface of the canister. Displacement constraints are applied to the plane of symmetry and the gap elements attached at the canister end to represent the top or bottom of the transport cask.

To determine the effect of the 25-psig pressure load, the top-end and bottom-end orientations with and without the pressure load are analyzed.

The locations of the linearized stresses are shown in Figure 2.6.12.3-1. The summary for P_m and $P_m + P_b$ stresses due to the internal pressure of 25 psig are summarized in Table 2.6.12.4-2 and 2.6.12.4-3, respectively. Results from the end-drops are summarized in Tables 2.6.12.4-4 through 2.6.12.4-7 for the conditions that produce the minimum margin of safety. Table 2.6.12.4-1 provides a summary of critical section stresses for the top and bottom end-drop conditions. The margins of safety in these tables are calculated as:

MS = (allowable stress/SI) -1.

Table 2.6.12.4-1 PWR Canister Critical Sections for the Pressure Only and 1-Foot End-Drop Load Condition

Condition	Stress	Critical Section	Table	Minimum Margin of Safety
Pressure (only)	P_m	2	2.6.12.4-2	+ 3.32
Pressure (only)	$P_m + P_b$	3	2.6.12.4-3	+ 0.71
Top-End Drop Inertia	P_m	2	2.6.12.4-4	+ 4.04
Top-End Drop Inertia	$P_m + P_b$	3	2.6.12.4-5	+ 1.1
Bottom-End Drop + Pressure	P_m	4	2.6.12.4-6	+ 4.33
Bottom-End Drop + Pressure	$P_m + P_b$	2	2.6.12.4-7	+ 5.71

Table 2.6.12.4-2 PWR Canister P_m Stresses - Internal Pressure

Section Location	Angle of Peak Stress Location	P_m Stresses (ksi)						SI (ksi)	Allowable Stress (ksi)	Margin of Safety
		Sx	Sy	Sz	Sxy	Syz	Sxz			
1	0	0.2	2.4	1	-0.3	0	0.1	2.4	16	5.75
2	0	1.6	-1.6	-2	-0.3	0	-0.2	3.7	16	3.32
3	0	0.3	0	-2.7	0.3	0	-0.2	3.3	16	3.83
4	0	0	0.6	1.3	0	0	0.1	1.3	16	10.98
5	0	0	0.6	1.3	0	0	0.1	1.3	16	11.02
6	0	0	0.6	1.3	0	0	0.1	1.3	16	11.02
7	0	0	0.6	1.3	0	0	0.1	1.3	16	11.02
8	0	0	0.6	0.7	0	0	0.1	0.7	16	22.64
9	180	0	0.5	0.3	-0.1	0	0	0.5	16	33.63
10	180	-0.3	0.3	0.2	0.1	0	0	0.6	16	25.71
11	0	0.3	-0.1	0.2	0	0	0	0.4	16	37.08
12	0	-0.1	-0.4	0	-0.1	0	0	0.5	16	33.99
13	9	0	0.3	0.2	0	0	0	0.3	12.8*	41.67
14	90	0.2	-0.2	0.2	-0.1	0.2	0	0.6	16	23.81
15	90	0	0	0	0	0	0	0	16	1025.99
16	0	0	0	0	0	0	0	0	16	365.18

* Allowable stress includes a stress reduction factor for weld: 0.8 x allowable stress.

Note: All of the allowable stress values presented in this table are based on SA240, Type 304L stainless steel at a temperature of 380°F unless otherwise stated. Localized peak temperatures in the central portion of the canister shell reach 399°F—resulting in slightly lower allowable stress values and subsequently slightly lower margins of safety for sections 5 and 6 than those presented in the table. However, this difference is negligible as discussed in Section 2.6.12.1.

Table 2.6.12.4-3 PWR Canister $P_m + P_b$ Stresses - Internal Pressure

Section Location	Angle of Peak Stress Location	$P_m + P_b$ Stresses (ksi)						SI (ksi)	Allowable Stress (ksi)	Margin of Safety
		Sx	Sy	Sz	Sxy	Syz	Sxz			
1	0	1.9	5.9	0.2	0	0	-0.1	5.7	24	3.24
2	0	0.8	-11.2	-5.1	-0.8	0	-0.4	12.2	24	0.97
3	0	0.7	-13.3	-6.5	0.1	0	-0.5	14	24	0.71
4	0	0	0.6	1.3	0	0	0.1	1.4	24	16.74
5	0	0	0.7	1.3	0	0	0.1	1.4	24	16.73
6	0	0	0.7	1.3	0	0	0.1	1.4	24	16.73
7	0	0	0.6	1.3	0	0	0.1	1.4	24	16.73
8	180	0	0.7	0.7	0	0	-0.1	0.7	24	31.59
9	180	0.1	0.9	0.5	-0.1	0	0	0.9	24	26.24
10	180	-0.1	1.4	0.6	0	0	-0.1	1.5	24	14.58
11	0	0.2	-1	-0.1	0.1	0	0	1.2	24	19.74
12	0	-0.4	-0.8	-0.1	-0.2	0	0	0.7	24	34.13
13	180	-0.4	0	0	-0.1	0	0	0.4	19.2*	47.00
14	90	7.6	-0.2	7.6	-0.1	0.2	0	7.8	24	2.06
15	90	-0.6	0	-0.6	0	0	0	0.6	24	40.86
16	81	0.3	0	0.3	0	0	0	0.3	24	74.05

* Allowable stress includes a stress reduction factor for weld: 0.8 x allowable stress.

Note: All of the allowable stress values presented in this table are based on SA240, Type 304L stainless steel at a temperature of 380°F unless otherwise stated. Localized peak temperatures in the central portion of the canister shell reach 399°F—resulting in slightly lower allowable stress values and subsequently slightly lower margins of safety for sections 5 and 6 than those presented in the table. However, this difference is negligible as discussed in Section 2.6.12.1.

Table 2.6.12.4-4 PWR Canister P_m Stresses - 1-Foot Top End-Drop

Section Location	Angle of Peak Stress Location	P_m Stresses (ksi)						SI (ksi)	Allowable Stress (ksi)	Margin of Safety
		Sx	Sy	Sz	Sxy	Syz	Sxz			
1	0	-0.1	-2	-0.7	0.3	0	0	1.9	16	7.31
2	0	-1.3	1.2	1.8	0.3	0	0.2	3.2	16	4.04
3	0	-0.3	0	2.5	-0.2	0	0.2	3	16	4.38
4	144	0	-0.7	0	0	0	0	0.7	16	20.58
5	153	0	-0.9	0	0	0	0	0.9	16	16.18
6	162	0	-1.1	0	0	0	0	1.1	16	13.28
7	180	0	-1.3	0	0	0	0	1.3	16	11.21
8	180	0	-1.2	0	0	0	0	1.3	16	11.57
9	180	0	-0.9	-0.2	0	0	0	1	16	15.82
10	144	-0.1	-0.9	-0.1	0	0	0.1	0.9	16	17.09
11	135	-0.1	-0.9	-0.1	0	0	0.1	0.9	16	17.3
12	144	0	-0.7	-0.1	0	0	0	0.7	16	21.43
13	180	0	-0.7	-0.1	0	0	0	0.7	12.8*	17.29
14	90	-0.2	0	-0.2	0.1	-0.1	0	0.4	16	44.06
15	144	0	-0.3	0	0	0	0	0.4	16	44.54
16	0	0	-0.4	0	0	0	0	0.4	16	40.07

* Allowable stress includes a stress reduction factor for weld: 0.8 x allowable stress.

Note: All of the allowable stress values presented in this table are based on SA240, Type 304L stainless steel at a temperature of 380°F unless otherwise stated. Localized peak temperatures in the central portion of the canister shell reach 399°F—resulting in slightly lower allowable stress values and subsequently slightly lower margins of safety for sections 5 and 6 than those presented in the table. However, this difference is negligible as discussed in Section 2.6.12.1.

Table 2.6.12.4-5 PWR Canister $P_m + P_b$ Stresses - 1-Foot Top End-Drop

Section Location	Angle of Peak Stress Location	$P_m + P_b$ Stresses (ksi)						SI (ksi)	Allowable Stress (ksi)	Margin of Safety
		Sx	Sy	Sz	Sxy	Syz	Sxz			
1	0	-1.4	-4.7	0.1	0	0	0.1	4.8	24	3.99
2	0	-0.6	9	4.3	0.7	0	0.4	9.8	24	1.45
3	0	-0.5	10.8	5.6	0	0	0.5	11.4	24	1.1
4	162	0	-0.8	0	0	0	0	0.8	24	30.8
5	162	0	-0.9	0	0	0	0	0.9	24	24.77
6	144	0	-1.1	0	0	0	0	1.1	24	20.42
7	171	0	-1.3	0	0	0	0	1.3	24	17.3
8	180	0.1	-1.2	0	-0.1	0	0	1.3	24	17.37
9	45	-0.1	-1.1	-0.1	0	0	-0.1	1.1	24	21.59
10	180	0	-1	-0.2	0	0	0	1	24	22.45
11	135	-0.1	-1	-0.1	0	0	0.1	1	24	23.42
12	180	0	-0.7	-0.1	-0.1	0	0	0.7	24	31.5
13	180	0	-0.8	-0.1	0	0	0	0.7	19.2*	26.43
14	90	-6.8	-0.1	-6.8	0.1	-0.1	0	6.7	24	2.57
15	81	0.1	-0.3	0.1	0	0	0	0.4	24	55.49
16	0	0	-0.4	0	0	0	0	0.4	24	59.08

* Allowable stress includes a stress reduction factor for weld: 0.8 x allowable stress.

Note: All of the allowable stress values presented in this table are based on SA240, Type 304L stainless steel at a temperature of 380°F unless otherwise stated. Localized peak temperatures in the central portion of the canister shell reach 399°F—resulting in slightly lower allowable stress values and subsequently slightly lower margins of safety for sections 5 and 6 than those presented in the table. However, this difference is negligible as discussed in Section 2.6.12.1.

Table 2.6.12.4-6 PWR Canister P_m Stresses - 1-Foot Bottom End-Drop, Internal Pressure

Section Location	Angle of Peak Stress Location	P_m Stresses (ksi)						SI (ksi)	Allowable Stress (ksi)	Margin of Safety
		Sx	Sy	Sz	Sxy	Syz	Sxz			
1	180	0	-0.6	0	0.1	0	0	0.6	16	24.4
2	180	0.3	-1.9	-0.3	0.1	0	0	2.2	16	6.24
3	180	0.1	-1.9	-0.3	-0.1	0	0	2	16	7.08
4	180	0	-1.7	1.3	0	0	-0.1	3	16	4.33
5	180	0	-1.5	1.3	0	0	-0.1	2.8	16	4.69
6	180	0	-1.3	1.3	0	0	-0.1	2.6	16	5.11
7	180	0	-1.1	1.3	0	0	-0.1	2.4	16	5.58
8	180	0	-0.7	0.7	0	0	-0.1	1.4	16	10.31
9	18	-0.1	-0.5	-0.4	-0.1	0	-0.1	0.4	16	36.52
10	180	0.4	-0.3	-0.2	-0.1	0	0	0.7	16	21.21
11	0	-0.5	0.1	-0.2	0	0	0	0.6	16	27.29
12	99	-0.1	0.5	0.1	0	-0.1	0	0.6	16	27.09
13	0	0	-0.5	-0.3	0	0	0	0.4	12.8*	31.00
14	0	0.1	-0.4	0.1	0	0	0	0.4	16	34.57
15	108	0	0	0	0	0	0	0.1	16	302.05
16	0	0	0	0	0	0	0	0.1	16	286.36

* Allowable stress includes a stress reduction factor for weld: 0.8 x allowable stress.

Note: All of the allowable stress values presented in this table are based on SA240, Type 304L stainless steel at a temperature of 380°F unless otherwise stated. Localized peak temperatures in the central portion of the canister shell reach 399°F—resulting in slightly lower allowable stress values and subsequently slightly lower margins of safety for sections 5 and 6 than those presented in the table. However, this difference is negligible as discussed in Section 2.6.12.1.

Table 2.6.12.4-7 PWR Canister $P_m + P_b$ Stresses - 1 Foot Bottom End-Drop, Internal Pressure

Section Location	Angle of Peak Stress Location	$P_m + P_b$ Stresses (ksi)						SI (ksi)	Allowable Stress (ksi)	Margin of Safety
		Sx	Sy	Sz	Sxy	Syz	Sxz			
1	180	0.2	-0.4	0.1	0.1	0	0	0.7	24	34.19
2	180	0.2	-3.4	-0.7	0.1	0	0.1	3.6	24	5.71
3	180	0.1	-3.3	-0.6	-0.1	0	0	3.3	24	6.16
4	0	0	-1.7	1.3	0	0	0.1	3	24	6.95
5	0	0	-1.5	1.3	0	0	0.1	2.8	24	7.5
6	0	0	-1.3	1.3	0	0	0.1	2.6	24	8.11
7	0	0	-1.1	1.3	0	0	0.1	2.4	24	8.82
8	27	0.2	-0.9	0.5	0	0	0.2	1.5	24	14.94
9	108	-0.5	-1.1	-0.1	0	0.1	0.1	1.1	24	21.15
10	99	-0.7	-1.6	0.1	0	0	0.1	1.8	24	12.44
11	0	-0.2	1.3	0.2	-0.1	0	0	1.5	24	14.78
12	99	0.2	0.9	0.5	0	-0.2	0.1	0.8	24	29.14
13	0	0.5	0	0	-0.1	0	0	0.5	19.2*	37.40
14	0	0.1	-0.4	0.1	0	0	0	0.5	24	49.26
15	90	0.8	0	0.8	0	0	0	0.8	24	28.07
16	0	-0.4	0	-0.4	0	0	0	0.4	24	56.39

* Allowable stress includes a stress reduction factor for weld: 0.8 x allowable stress.

Note: All of the allowable stress values presented in this table are based on SA240, Type 304L stainless steel at a temperature of 380°F unless otherwise stated. Localized peak temperatures in the central portion of the canister shell reach 399°F—resulting in slightly lower allowable stress values and subsequently slightly lower margins of safety for sections 5 and 6 than those presented in the table. However, this difference is negligible as discussed in Section 2.6.12.1.

2.6.12.5 Stress Evaluation of PWR Canister for Combined Thermal and 1-Foot End-Drop Load Condition

The thermal stress loads described in Section 2.6.12.3 are applied in conjunction with the primary loads in Section 2.6.12.4 to produce a combined thermal stress plus end-impact loading. The stress evaluation is performed according to the ASME Code, Section III, Subsection NB. The most critical sections are listed in Table 2.6.12.5-1. The stresses reported in this table correspond to the nodal stress at the surface. The minimum margin of safety is +2.44 when 3 S_m is used as the stress criterion. Tables 2.6.12.5-2 through 2.6.12.5-5 tabulate the peak stresses for both the hot and cold conditions for both the top-and bottom-end-drop cases for the conditions that result in the minimum margin of safety. For both top and bottom orientations, the minimum margins occur without the addition of pressure. The margins of safety are calculated as:

MS = (allowable stress/SI) -1.

Table 2.6.12.5-1 PWR Canister Critical Sections for the Combined 1-Foot-End-Drop and Thermal Load Condition

Condition	Stress	Critical Section	Table	Minimum Margin of Safety
Top-End Drop + Thermal (cold)	P + Q	14	2.6.12.5-2	+ 2.44
Top-End Drop + Thermal (hot)	P + Q	3	2.6.12.5-3	+ 2.6
Bottom-End Drop + Thermal (cold)	P + Q	14	2.6.12.5-4	+ 7.47
Bottom-End Drop + Thermal (hot)	P + Q	14	2.6.12.5-5	+ 8.44

Table 2.6.12.5-2 PWR Canister $P_m + P_b + Q$ Stresses - 1-Foot Top End-Drop, Thermal Cold

Section Location	Angle of Peak Stress Location	$P_m + P_b + Q$ Stresses (ksi)						SI (ksi)	Allowable Stress (ksi)	Margin of Safety
		Sx	Sy	Sz	Sxy	Syz	Sxz			
1	90	1.3	-5.8	-1.8	0	0	0	7.2	47.9	5.67
2	45	3.4	10.6	3.4	0.4	-0.6	3.5	10.8	47.9	3.46
3	9	-0.1	-10.9	0.8	-0.6	0	0.2	11.8	47.9	3.08
4	0	0	-1.2	0	0	0	0	1.2	47.9	37.94
5	0	0	-2.1	0.6	0	-0.2	0	2.8	47.9	16.12
6	0	0	-2.3	0.2	0	0	0	2.5	47.9	18.39
7	0	0	-2.6	0	0	0	0	2.6	47.9	17.46
8	9	-0.2	-3.4	-0.3	0	0.1	0	3.3	47.9	13.67
9	162	0.1	-3.1	-0.7	-0.2	-0.1	0.3	3.3	47.9	13.63
10	0	-0.1	-2	-0.5	0.1	0	0	1.8	47.9	25.05
11	171	0	-3.3	-0.8	0	0	0.1	3.3	47.9	13.51
12	0	0.4	-0.9	0	0.2	0	0	1.3	47.9	35.99
13	0	0.2	-1	-0.1	0	0	0	1.2	38.32*	30.93
14	0	-15.7	-1.8	-15.4	0.1	-1	0.1	14	47.9	2.44
15	81	0.1	-0.3	0.1	0	0	0	0.4	47.9	116.3
16	0	0.1	-0.5	0.1	0	0	0	0.6	47.9	85.61

* Allowable stress includes a stress reduction factor for weld: 0.8 x allowable stress.

Note: All of the allowable stress values presented in this table are based on SA240, Type 304L stainless steel at a temperature of 380°F unless otherwise stated. Localized peak temperatures in the central portion of the canister shell reach 399°F—resulting in slightly lower allowable stress values and subsequently slightly lower margins of safety for sections 5 and 6 than those presented in the table. However, this difference is negligible as discussed in Section 2.6.12.1.

Table 2.6.12.5-3 PWR Canister $P_m + P_b + Q$ Stresses-1-Foot Top End-Drop, Thermal Heat

Section Location	Angle of Peak Stress Location	$P_m + P_b + Q$ Stresses (ksi)						SI (ksi)	Allowable Stress (ksi)	Margin of Safety
		Sx	Sy	Sz	Sxy	Syz	Sxz			
1	90	1.2	-5.9	-1.8	0	0	0	7.1	47.9	5.77
2	45	3.3	10.5	3.3	0.4	-0.6	3.5	10.8	47.9	3.44
3	9	-0.1	-11	0.7	-0.6	0.1	0.1	11.8	47.9	3.08
4	0	0	-1.1	0	0	0	0	1.2	47.9	40.01
5	0	0	-2	0.5	0	-0.2	0	2.5	47.9	17.84
6	0	0	-2.1	0.2	0	0	0	2.3	47.9	20.04
7	0	0	-2.4	0	0	0	0	2.4	47.9	19.03
8	9	-0.2	-3.2	-0.3	0	0.1	0	3	47.9	14.85
9	162	0.1	-3	-0.7	-0.1	-0.1	0.3	3.2	47.9	14.01
10	162	-0.3	-2	-0.5	-0.2	-0.1	0.1	1.8	47.9	26.36
11	171	0	-3	-0.7	0	0	0.1	3	47.9	14.76
12	0	0.3	-0.9	-0.1	0.2	0	0	1.2	47.9	37.66
13	0	0.2	-0.9	-0.1	0	0	0	1.1	38.32*	33.84
14	0	-14.8	-1.6	-14.6	0.1	-0.9	0	13.3	47.9	2.6
15	81	0.1	-0.3	0.1	0	0	0	0.4	47.9	116.41
16	0	0.1	-0.5	0.1	0	0	0	0.5	47.9	87.74

* Allowable stress includes a stress reduction factor for weld: 0.8 x allowable stress.

Note: All of the allowable stress values presented in this table are based on SA240, Type 304L stainless steel at a temperature of 380°F unless otherwise stated. Localized peak temperatures in the central portion of the canister shell reach 399°F—resulting in slightly lower allowable stress values and subsequently slightly lower margins of safety for sections 5 and 6 than those presented in the table. However, this difference is negligible as discussed in Section 2.6.12.1.

Table 2.6.12.5-4 PWR Canister $P_m + P_b + Q$ Stresses -1-Foot Bottom End-Drop, Thermal Cold

Section Location	Angle of Peak Stress Location	$P_m + P_b + Q$ Stresses (ksi)						SI (ksi)	Allowable Stress (ksi)	Margin of Safety
		Sx	Sy	Sz	Sxy	Syz	Sxz			
1	9	0.1	-2.1	1.2	-0.3	0.1	0.2	3.4	47.9	13.23
2	9	-0.3	-4.5	0.3	-0.1	0.1	0.1	4.8	47.9	9.04
3	9	-0.1	-4	0.6	0	0.1	0.1	4.6	47.9	9.38
4	0	0	-3.2	0	0	0	0	3.2	47.9	14.02
5	0	0	-3.5	0.6	0	-0.2	0	4.1	47.9	10.6
6	0	0	-3	0.2	0	0.1	0	3.2	47.9	13.91
7	0	0	-2.6	0	0	0	0	2.7	47.9	17.02
8	9	-0.2	-2.7	-0.2	0	0.2	0	2.6	47.9	17.55
9	162	-0.2	-3.3	-1.4	0.1	0.1	0.4	3.3	47.9	13.69
10	0	0.4	-3.9	-1.5	0	0.1	-0.1	4.3	47.9	10.22
11	0	-0.5	2.7	0.7	-0.1	0.1	0.1	3.2	47.9	13.86
12	18	1.1	1.7	0.3	0.4	0.1	-0.1	1.6	47.9	28.65
13	0	-1.4	-2	-1	0.3	0	0	1.2	38.32*	30.93
14	0	-11.2	-5.5	-10.9	0	0.1	0.1	5.7	47.9	7.47
15	81	1.7	0	1.4	0	0	0	1.7	47.9	27.66
16	72	-0.7	0	-0.6	0	0	0	0.7	47.9	68.32

* Allowable stress includes a stress reduction factor for weld: 0.8 x allowable stress.

Note: All of the allowable stress values presented in this table are based on SA240, Type 304L stainless steel at a temperature of 380°F unless otherwise stated. Localized peak temperatures in the central portion of the canister shell reach 399°F—resulting in slightly lower allowable stress values and subsequently slightly lower margins of safety for sections 5 and 6 than those presented in the table. However, this difference is negligible as discussed in Section 2.6.12.1.

Table 2.6.12.5-5 PWR Canister $P_m + P_b + Q$ Stresses - 1-Foot Bottom End-Drop, Thermal Heat

Section Location	Angle of Peak Stress Location	$P_m + P_b + Q$ Stresses (ksi)						SI (ksi)	Allowable Stress (ksi)	Margin of Safety
		Sx	Sy	Sz	Sxy	Syz	Sxz			
1	9	0.1	-1.9	1.1	-0.3	0.1	0.2	3.1	47.9	14.36
2	9	-0.3	-4.5	0.1	-0.1	0.1	0.1	4.6	47.9	9.45
3	9	-0.1	-4	0.4	0	0.1	0.1	4.4	47.9	9.79
4	0	0	-3.1	0	0	0	0	3.1	47.9	14.64
5	0	0	-3.3	0.6	0	-0.2	0	3.9	47.9	11.41
6	0	0	-2.8	0.2	0	0.1	0	3	47.9	14.76
7	0	0	-2.5	0	0	0	0	2.5	47.9	17.96
8	9	-0.2	-2.6	-0.2	0	0.2	0	2.4	47.9	18.74
9	162	-0.2	-3.2	-1.3	0.1	0.1	0.4	3.1	47.9	14.46
10	162	0	-3.8	-1.4	-0.1	0.1	0.5	4	47.9	10.93
11	9	-0.5	2.5	0.5	-0.1	0.1	0.1	3.1	47.9	14.68
12	162	0.6	1.9	0.2	-0.4	0	0.1	1.8	47.9	25.24
13	0	1	-0.2	0.2	-0.1	0	-0.1	1.2	38.32*	30.93
14	0	-10	-4.9	-9.7	0	0.1	0	5.1	47.9	8.44
15	72	1.7	0	1.4	0	0	0	1.6	47.9	28.14
16	72	-0.7	-0.1	-0.6	0	0	0	0.7	47.9	68.12

* Allowable stress includes a stress reduction factor for weld: 0.8 x allowable stress.

Note: All of the allowable stress values presented in this table are based on SA240, Type 304L stainless steel at a temperature of 380°F unless otherwise stated. Localized peak temperatures in the central portion of the canister shell reach 399°F—resulting in slightly lower allowable stress values and subsequently slightly lower margins of safety for sections 5 and 6 than those presented in the table. However, this difference is negligible as discussed in Section 2.6.12.1.

2.6.12.6 Stress Evaluation of PWR Canister for 1-Foot Side-Drop-Load Condition

The stresses in the PWR canister that result from a 1-ft side-drop are determined by using ANSYS. In the local regions of the lids and bottom plate, the loads are transmitted through the canister shell into the cask body inner shell. Outside of the lid and bottom plate regions, stress develops in the canister shell as a result of the basket loading the canister wall. The difference in the radii of the basket, canister, and cask body implies that the contact angle between the components is dependent on the loading. For this reason, the finite element model described in Section 2.6.12.2 contains a half model of the basket. Gap elements between the basket and the canister allow the interface to be dependent on the loading. The interface between the canister and the cask body inner shell is also represented by gap elements.

The load resulting from the contents is applied to the basket by means of pressure acting in the plane of the disks. The weight is assumed to act over the effective width of 9.272 in., in which the disk is 0.5 in. thick. This weight is distributed over the 32 support disks plus two end weldments. A deceleration factor of 20 *g* applied to the weights provides the loading for the basket assembly. In addition to the contents load, a 25-psig pressure is applied to the inner surface of the canister.

Analyses of the canister are performed for basket orientations of 0° and 45°. The angles describe the orientation of the basket elements with respect to the symmetry plane of the model. A value of 0° orients the ligaments in the basket elements parallel and perpendicular to the symmetry plane, a value of 45°orients the basket ligaments at +/- 45° from the symmetry plane. To assess the impact of the basket orientation on the canister response during impact, both basket orientations are run for the side-impact loading.

The methodology used to evaluate the stresses for the side-drop are similar to that used for the end-drop (Section 2.6.12.4) with following exceptions. Sections 9, 10, and 11 at the 0° circumferential position (see Figure 2.6.12.3-1) are not included in the evaluation. These regions are characterized as a bearing stress since they result from the canister shell bearing against the cask inner shell. Section 2.6.12.11 provides an assessment of the canister shell bearing stresses. Sections 9, 10, and 11 at all other angular locations are included in the evaluation. Also, Sections 12 and 13 at 0° are treated as local membrane stresses. According to the ASME Code Section III, Paragraph NB-3213.10, a stressed region may be considered local if the distance over

which the membrane stress intensity exceeds 1.1 S_m does not extend more than 1.0 times the square root of RT in the meridional direction, where R is the minimum midsurface radius of curvature and T is the minimum thickness in the region considered. For Section 13, the minimum thickness is that of the canister shell (0.625 in.) and the midsurface radius of the shell is 33.2175 in. The resulting distance is 4.56 in. A section located 4.56 in. from Section 13 in the meridional direction results in a membrane stress intensity of 6.7 ksi, which is below S_m. This section conservatively encompasses Section 12 since it is located 1.56 in. from this section. The stresses at adjacent circumferential sections (i.e., at 9°) for Sections 12 and 13 are also included in the tables for comparison. The critical section stresses are reported in Table 2.6.12.6-1 for the P_m and $P_m + P_b$ stresses.

Results are calculated for 1-ft side-drop with internal pressure both the 0° and 45° basket orientations. Tables 2.6.12.6-2 and 2.6.12.6-3 present the worst-case margins for the side-drop which occurs with the conditions noted. The minimum margin occurs for membrane without pressure and with pressure for membrane plus bending. The minimum margin of safety for the PWR canister in the side-drop is +0.02, which occurs at Section 12 in Table 2.6.12.3-1. The margins of safety are calculated as:

$$MS = (\text{allowable stress}/SI) - 1.$$

Table 2.6.12.6-1 PWR Canister Critical Sections for the 1-Foot Side-Drop Load Condition

Condition	Stress	Critical Section	Table	Minimum Factor of Safety
Side Drop	Pm	1	2.6.12.6-2	+ 0.07
Side Drop + Pressure	$P_m + P_b$	12	2.6.12.6-3	+ 0.02

Table 2.6.12.6-2 PWR Canister: P_m Stresses - 1 Foot Side-Drop

Section Location	Angle of Peak Stress Location	P_m Stresses (ksi)						SI (ksi)	Allowable Stress (ksi)	Margin of Safety
		Sx	Sy	Sz	Sxy	Syz	Sxz			
1	0	-14.7	-0.2	-5.2	-0.4	-0.1	-2	14.9	16	0.07
2	0	-13	-0.8	-6.4	-0.8	-0.4	-1.2	12.5	16	0.28
3	0	-3.8	-0.6	-3.3	-0.3	-0.6	-1.3	4.5	16	2.55
4	81	0	-0.2	0	0.8	0.1	0	1.5	16	9.39
5	9	-0.7	0.9	0.2	0	0	0.2	1.6	16	9.23
6	9	-0.7	1	0.2	0	0	0.2	1.7	16	8.19
7	9	-0.8	1.1	0.3	0	-0.1	0.2	2	16	7.18
8	0	-0.7	2.5	-1.1	-0.1	0.5	-0.1	3.7	16	3.34
9	9	-0.4	2.6	-2.1	0.05	1.3	-1.0	5.8	16	1.76
10	9	1.5	1.7	-2.1	-0.3	1.0	-0.6	4.6	16	2.48
11	9	3.7	1.8	-1.2	0.7	1.2	-1.6	6.4	16	1.5
12***	0	-24.4	-5.4	-6.7	-4.5	1.2	-1	21.7	24***	0.11
12	9	-0.5	-0.1	-3.5	0.1	0.6	-1.9	4.9	16	2.27
13*	0-7.5	-11.66	-3.42	-4.02	0.05	1.1	-2.33	9.99	12.8**	0.28
[illegible]	[illegible]	[illegible]	[illegible]	[illegible]	[illegible]	[illegible]	[illegible]	[illegible]	[illegible]	[illegible]
14	0	-0.9	-0.1	0.3	0	0	0	1.2	16	11.92
15	0	-0.3	0	0.1	0	0	0	0.4	16	35.79
16	0	-0.5	0.1	0.2	0	0	0	0.7	16	22.61

* Stress evaluated over weld compression region

** Allowable stress includes a stress reduction factor for weld: 0.8 x allowable stress.

*** Stresses treated as a local membrane stress. Allowable for normal conditions is $1.5S_m = 24$ ksi for P_L and $P_L = P_B$

Note: All of the allowable stress values presented in this table are based on SA240, Type 304L stainless steel at a temperature of 380°F unless otherwise stated. Localized peak temperatures in the central portion of the canister shell reach 399°F—resulting in slightly lower allowable stress values and subsequently slightly lower margins of safety for sections 5 and 6 than those presented in the table. However, this difference is negligible as discussed in Section 2.6.12.1.

Table 2.6.12.6-3 PWR Canister $P_m + P_b$ Stresses - 1-Foot Side-Drop, Internal Pressure

Section Location	Angle of Peak Stress Location	$P_m + P_b$ Stresses (ksi)						SI (ksi)	Allowable Stress (ksi)	Margin of Safety
		Sx	Sy	Sz	Sxy	Syz	Sxz			
1	0	-23	-0.9	-7.6	0.6	0	-2	22.5	24	0.07
2	18	0.5	-12.7	-3.1	-0.2	0.2	-1.5	13.7	24	0.74
3	27	-0.6	-12.5	-4.6	0.1	-0.6	-2.3	13	24	0.85
4	9	-0.8	1.9	3.9	0	0.1	0.7	4.8	24	3.95
5	9	-0.6	2.3	3.7	0	0	0.7	4.5	24	4.3
6	9	-0.6	2.4	3.7	0	-0.1	0.7	4.5	24	4.33
7	9	-0.7	2.4	3.7	0	-0.1	0.7	4.7	24	4.12
8	0	-0.4	2.7	-2.4	-0.2	0.4	-0.2	5.1	24	3.66
9	9	1.2	6.3	-0.4	-0.1	1.5	0.1	7.4	24	2.24
10	0	-18.9	-2	-4.5	-5.3	1	-1.1	20.3	24	0.18
11	9	4.0	0.9	-1.4	0.8	1.3	2.7	8.2	24	1.93
12*	0	-28.6	-6.6	-8.2	-4.3	1.5	-0.7	24.5	25	0.02
13**	0-7.9	-16.65	-6.26	-6.48	-0.11	1.66	-1.98	12.49	20***	0.60
14	90	-0.8	0	0.4	0	0	0	1.2	24	18.27
15	90	-0.6	0	-0.2	0	0	0	0.6	24	39.77
16	0	-0.4	0	0.3	0	0	0	0.7	24	33.98

* The peak temperature as calculated in Section 3.4 is 265°F in the region of Sections 12 and 13. There the allowable stress for Type 304L stainless steel is 1.5 (16.7) = 25.05 ksi.

** The peak temperature as calculated in Section 3.4 is 265°F in the region of Sections 12 and 13. There the allowable stress for 304L stainless steel is 1.5 (16.7) = 25.05 ksi. Stress evaluated over weld compressing region.

*** Allowable stress includes a stress reduction factor for weld: 0.8 x allowable stress.

Note: All of the allowable stress values presented in this table are based on SA240, Type 304L stainless steel at a temperature of 380°F unless otherwise stated. Localized peak temperatures in the central portion of the canister shell reach 399°F—resulting in slightly lower allowable stress values and subsequently slightly lower margins of safety for sections 5 and 6 than those presented in the table. However, this difference is negligible as discussed in Section 2.6.12.1.

2.6.12.7 Stress Evaluation of PWR Canister for Combined Thermal and 1-Foot Side-Drop Load Condition

The thermal stress loads described in Section 2.6.12.3 are applied in conjunction with the primary loads in Section 2.6.12.6 to produce a combined thermal stress plus 1-ft side-drop loading. The stress evaluation is performed according to the ASME Code, Section III, Subsection NB. The most critical sections are listed in Table 2.6.12.7-1. Results from the side-drop plus thermal load cases for the configurations that result in the minimum margins are presented in Tables 2.6.12.7-2 and 2.6.12.7-3. The stresses reported in this table correspond to the nodal stress at the surface. The minimum margin is +0.41 at Section 9 (see Table 2.6.12.7-1) when 3 S_m is used as the stress criteria. The margins of safety are calculated as:

MS = (allowable stress/SI) -1.

Table 2.6.12.7-1 PWR Canister Critical Sections for Combined 1-Foot Side-Drop and Thermal Load Condition

Condition	Stress	Critical Section	Table	Minimum Margin of Safety
Side Drop + Thermal (cold)	$P_m + P_b + Q$	9	2.6.12.7-2	+ 0.41
Side Drop + Thermal (hot)	$P_m + P_b + Q$	9	2.6.12.7-3	+ 0.59

Table 2.6.12.7-2 PWR Canister $P_m + P_b + Q$ Stresses - 1-Foot Side Drop, Thermal Cold

Section Location	Angle of Peak Stress Location	$P_m + P_b + Q$ Stresses (ksi)						SI (ksi)	Allowable Stress (ksi)	Margin of Safety
		Sx	Sy	Sz	Sxy	Syz	Sxz			
1	0	-15.3	-0.4	-4	-0.1	0.1	-1.7	15.1	47.9	2.17
2	0	-11.7	-0.2	-2.2	-1.2	-0.4	-1.7	12.1	47.9	2.97
3	27	0.7	5.2	1.3	1.2	1.6	1.2	6.4	47.9	6.46
4	0	-0.4	1.1	2.9	0	-0.1	0.6	3.5	47.9	12.73
5	45	-1.2	1.5	-1.2	-0.4	-0.4	-1.3	4.2	47.9	10.41
6	45	-1	1.2	-1.1	0.3	0.3	-1.2	3.5	47.9	12.51
7	0	-0.4	1.1	2.6	0	0	0.5	3.1	47.9	14.33
8	0	0	2.7	-1.5	-0.1	0.6	-0.1	4.3	47.9	10.04
9	0	-26.6	6.9	-9.1	-2.1	1.7	0.2	34	47.9	0.41
10	0	-18.8	-2.6	-5	-4.5	0.9	-1.1	18.9	47.9	1.54
11	0	-26.3	3.3	-8.7	-0.3	1.8	-0.1	29.9	47.9	0.6
12	0	-26.4	-4.8	-7.9	-3.7	1.7	-0.6	23.5	47.9	1.04
13	0	-32.5	-9.8	-10.6	-1.2	2	-1.4	24.5	38.32*	0.56
14	180	-9.3	-2.5	-7.6	0.1	1.2	-0.1	7	47.9	5.8
15	0	-0.7	0	-0.1	0	0	0	0.7	47.9	69.76
16	0	-0.6	0.1	0.1	0	0	0	0.7	47.9	63.87

* Allowable stress includes a stress reduction factor for weld: 0.8 x allowable stress.

Note: All of the allowable stress values presented in this table are based on SA240, Type 304L stainless steel at a temperature of 380°F unless otherwise stated. Localized peak temperatures in the central portion of the canister shell reach 399°F—resulting in slightly lower allowable stress values and subsequently slightly lower margins of safety for sections 5 and 6 than those presented in the table. However, this difference is negligible as discussed in Section 2.6.12.1.

Table 2.6.12.7-3 PWR Canister $P_m + P_b + Q$ Stresses - 1-Foot Side-Drop, Thermal Heat

Section Location	Angle of Peak Stress Location	$P_m + P_b + Q$ Stresses (ksi)						SI (ksi)	Allowable Stress (ksi)	Margin of Safety
		Sx	Sy	Sz	Sxy	Syz	Sxz			
1	0	-13.4	-0.3	-3.8	-0.1	0.1	-1.4	13.2	47.9	2.62
2	0	-9.8	0	-2	-1	-0.3	-1.4	10.2	47.9	3.7
3	27	0.6	4.6	1.1	1	1.3	1	5.5	47.9	7.65
4	0	-0.4	0.8	2.4	0	-0.1	0.5	3	47.9	15.13
5	45	-1	1.2	-1.1	-0.4	-0.4	-1.2	3.6	47.9	12.17
6	45	-0.9	1.1	-0.9	0.3	0.3	-1	3.1	47.9	14.39
7	0	-0.4	1	2.1	0	0	0.4	2.7	47.9	16.98
8	0	0	2.6	-1.2	-0.1	0.5	-0.1	4	47.9	11.05
9	0	-23.3	6.4	-8.2	-1.8	1.4	0.3	30.1	47.9	0.59
10	0	-16.5	-2.1	-4.8	-3.9	0.8	-0.8	16.6	47.9	1.88
11	0	-22.8	3.2	-7.8	-0.2	1.5	0	26.1	47.9	0.83
12	0	-23.3	-4.1	-7.4	-3.2	1.5	-0.4	20.8	47.9	1.31
13	0	-28.2	-8.5	-9.6	-1	1.6	-1.1	21.1	38.32*	0.82
14	180	-8.8	-1.6	-7.1	0.1	0.8	-0.1	7.4	47.9	5.51
15	0	-0.6	0	0.1	0	0	0	0.7	47.9	69.62
16	0	-0.7	0	-0.1	0	0	0	0.8	47.9	61.85

* Allowable stress includes a stress reduction factor for weld: 0.8 x allowable stress.

Note: All of the allowable stress values presented in this table are based on SA240, Type 304L stainless steel at a temperature of 380°F unless otherwise stated. Localized peak temperatures in the central portion of the canister shell reach 399°F—resulting in slightly lower allowable stress values and subsequently slightly lower margins of safety for sections 5 and 6 than those presented in the table. However, this difference is negligible as discussed in Section 2.6.12.1.

2.6.12.8 Stress Evaluation of PWR Canister for 1-Foot Corner-Drop Load Condition

A structural analysis performed by using ANSYS to evaluate the effect of a 1-ft end-drop impact for both the top-and bottom-corner orientations of the PWR canister. The ASME Code, Section III, Subsection NB, requires that stresses arising from operational loads be assessed on the basis of the primary loads. The primary loads for the 1-ft corner-drop result from the deceleration of the canister and its contents and the 25-psig pressure load internal to the canister. The applied deceleration is 20 *g* for both orientations (Note—the actual deceleration is 5.6 *g*; therefore, the results presented in this section are conservative). The inertial load of the canister is addressed by the deceleration factor applied to the canister density. The contents weight is represented by a pressure load on the inner end surface of the canister and a pressure applied to the basket by means of pressure acting in the plane of the disks. Displacement constraints are applied to the plane of symmetry and the gap elements attached at the canister end to represent the top or bottom of the transport cask.

The locations of the linearized stresses are shown in Figure 2.6.12.3-1. The maximum stresses for P_m and $P_m + P_b$ are tabulated in Tables 2.6.12.8-2 through 2.6.12.8-5 for the conditions that result in the worst-case stresses. The critical sections for the pressure and the pressure plus the deceleration load, with reference to the section and the appropriate tables, are shown in Table 2.6.12.8-1. The margins of safety in these tables are calculated as:

$$MS = (\text{allowable stress}/SI)-1.$$

Table 2.6.12.8-1 PWR Canister Critical Sections for the 1-Foot Corner-Drop Load Condition

Condition	Stress	Critical Section	Table	Margin of Safety*
Top Corner Drop + Pressure	P_m	9	2.6.12.8-2	+ 0.08
Top Corner Drop Inertia	$P_m + P_b$	2	2.6.12.8-3	+ 0.02
Bottom Corner Drop + Pressure	P_m	9	2.6.12.8-4	**± 0.02**
Bottom Corner Drop + Inertia	$P_m + P_b$	11	2.6.12.8-5	+0.26

* Note: These margins of safety are based on stresses calculated for corner drops with a 20 g deceleration load. The actual deceleration load is 5.6 g; therefore, these margins of safety are conservative.

Table 2.6.12.8-2 PWR Canister P_m Stresses 1-Foot Top Corner-Drop, Internal Pressure

Section Location	Angle of Peak Stress Location	P_m Stresses (ksi)						SI (ksi)	Allowable Stress (ksi)	Margin of Safety
		Sx	Sy	Sz	Sxy	Syz	Sxz			
1	0	-5.9	0.3	-1.7	0.2	-0.1	-0.8	6.4	16	1.5
2	0	-1.6	0.3	-1.5	-0.1	-0.3	-0.4	2.4	16	5.75
3	0	-0.5	0.5	-0.9	0.2	-0.3	-0.3	1.7	16	8.18
4	0	-1.2	-0.1	1.5	0	0	0	2.7	16	4.89
5	0	-1.2	-0.2	1.4	0	0	0	2.6	16	5.14
6	0	-1.2	-0.4	1.4	0	0	0	2.6	16	5.12
7	0	-1.2	-0.8	1.5	0	-0.1	0	2.7	16	4.91
8	45	0.4	-0.8	0.3	-0.4	-0.4	0.4	1.9	16	7.39
9	0	-16.1	-2	-4.4	-1.8	0.5	-0.4	14.7	16	0.08
10	0	-11.1	-4.3	-3.3	-1.9	0.2	-0.8	8.6	16	0.86
11	0	-15.1	-6.6	-5.4	-0.7	0.4	-0.4	9.9	16	0.61
12	0	-14.1	-6.2	-3.3	-2.9	0.2	-1	12	16	0.33
13	0	-13.2	-8	-4	-0.8	0.2	-1	9.5	12.8*	0.35
14	0	-0.2	0	0.2	0	0	0	0.4	16	37.89
15	171	-0.1	-0.3	0	0	0	0	0.4	16	40.38
16	0	-0.2	-0.4	0.1	0	0	0	0.5	16	34.04

* Allowable stress includes a stress reduction factor for weld: 0.8 x allowable stress.

Note: All of the allowable stress values presented in this table are based on SA240, Type 304L stainless steel at a temperature of 380°F unless otherwise stated. Localized peak temperatures in the central portion of the canister shell reach 399°F—resulting in slightly lower allowable stress values and subsequently slightly lower margins of safety for sections 5 and 6 than those presented in the table. However, this difference is negligible as discussed in Section 2.6.12.1.

Table 2.6.12.8-3 PWR Canister $P_m + P_b$ Stresses - 1-Foot Top Corner-Drop

Section Location	Angle of Peak Stress Location	$P_m + P_b$ Stresses (ksi)						SI (ksi)	Allowable Stress (ksi)	Margin of Safety
		Sx	Sy	Sz	Sxy	Syz	Sxz			
1	0	-15.3	-6.5	-4.5	-3.9	-0.2	-1	12.4	24	0.93
2	0	-19.4	3.9	-4.4	-0.7	1.2	-0.1	23.5	24	0.02
3	180	-0.5	9.9	5.3	0	0	-0.4	10.4	24	1.3
4	0	-1.4	0	2.5	0	0	0.1	4	24	5.04
5	0	-1.4	-0.1	2.4	0	0	0.1	3.8	24	5.37
6	0	-1.4	-0.4	2.4	0	0	0.1	3.8	24	5.35
7	0	-1.4	-0.7	2.5	0	-0.1	0.1	3.9	24	5.09
8	36	0.1	-1.4	0.1	-0.4	-0.7	0.1	2.2	24	9.92
9	0	-16.9	0.2	-5.4	-1.3	0.5	-0.2	17.3	24	0.38
10	0	-11.9	-5.7	-2.9	-3.4	0.1	-1.1	10.9	24	1.21
11	0	-17	-8.9	-5.6	-1.2	0.5	-0.7	11.8	24	1.03
12	0	-15.4	-6.1	-3.7	-2.4	0.4	-0.9	12.6	24	0.91
13	0	-15.7	-10.2	-5.4	-1.4	0.4	-1	10.8	19.2*	0.78
14	90	-6.4	-0.1	-5.9	0.1	-0.1	0	6.3	24	2.78
15	81	0	-0.3	0.1	0	0	0	0.4	24	54.38
16	0	-0.2	-0.3	0.1	0	0	0	0.4	24	53.04

* Allowable stress includes a stress reduction factor for weld: 0.8 x allowable stress.

Note: All of the allowable stress values presented in this table are based on SA240, Type 304L stainless steel at a temperature of 380°F unless otherwise stated. Localized peak temperatures in the central portion of the canister shell reach 399°F—resulting in slightly lower allowable stress values and subsequently slightly lower margins of safety for sections 5 and 6 than those presented in the table. However, this difference is negligible as discussed in Section 2.6.12.1.

Table 2.6.12.8-4 PWR Canister P_m Stresses - 1-Foot Bottom Corner-Drop

Section Location	Angle of Peak Stress Location	P_m Stresses (ksi)						SI (ksi)	Allowable Stress (ksi)	Margin of Safety
		Sx	Sy	Sz	Sxy	Syz	Sxz			
1	0	-7	-1.9	-2.4	-0.3	0	-1	6	16	1.67
2	18	0.6	-3.3	-0.6	0.1	-0.1	-0.5	4	16	2.95
3	18	0	-3.1	-0.9	0.1	-0.2	-0.4	3.3	16	3.84
4	0	-1.2	-2.3	0.2	0	0	-0.1	2.8	16	4.75
5	180	0	-2.2	-0.1	0	0	0	2.3	16	5.07
6	180	0	-2.2	-0.1	0	0	0	2.2	16	6.36
7	180	0	-1.9	-0.1	0	0	0	1.9	16	7.27
8	45	0.1	-1.1	0	-0.3	-0.3	0	1.5	16	10.29
9	0	-15	0.2	-4.5	-1.4	0.9	-0.3	15.6	16	0.02
10	0	-7.5	-0.4	-2.5	-1.4	0.7	-0.7	7.9	16	1.03
11**	0	-17.6	-1.1	-5.1	-0.2	1.1	-0.3	16.8	24	0.43**
11	9	2.9	1.3	-0.5	0.3	0.6	-1.0	4.1	16	2.90
12	0	-11.7	-2.7	-2.8	-2	0.6	-0.8	10.5	16	0.53
13	0	-11.8	-3.4	-3.1	0.1	0.8	-1.2	9.6	12.8*	0.33
14	0	-0.4	-0.3	0.2	0	0	0	0.5	16	28.96
15	0	-0.1	0	0.1	0	0	0	0.2	16	104.27
16	0	-0.3	0	0	0	0	0	0.3	16	50.45

* Allowable stress includes a stress reduction factor for weld: 0.8 x allowable stress.

** Stresses treated as local membrane stress. Allowable for normal conditons is 1.5 S_m = 24 ksi for P_L and $P_L + P_B$.

Note: All of the allowable stress values presented in this table are based on SA240, Type 304L stainless steel at a temperature of 380°F unless otherwise stated. Localized peak temperatures in the central portion of the canister shell reach 399°F—resulting in slightly lower allowable stress values and subsequently slightly lower margins of safety for sections 5 and 6 than those presented in the table. However, this difference is negligible as discussed in Section 2.6.12.1.

Table 2.6.12.8-5 PWR Canister $P_m + P_b$ Stresses - 1-Foot Bottom Corner-Drop

Section Location	Angle of Peak Stress Location	$P_m + P_b$ Stresses (ksi)						SI (ksi)	Allowable Stress (ksi)	Margin of Safety
		Sx	Sy	Sz	Sxy	Syz	Sxz			
1	0	-7.5	-0.8	-2.5	0.3	0.1	-1	7	24	2.44
2	18	-0.2	-6.9	-1.4	-0.1	0	-0.5	6.9	24	2.46
3	18	-0.3	-6.1	-1.3	0.2	0	-0.5	6	24	3.02
4	0	-1.4	-1.9	2.5	0	0	0.1	4.4	24	4.39
5	0	-1.3	-1.4	2.4	0	0	0.1	3.9	24	5.21
6	0	-1.3	-1.1	2.4	0	0	0.1	3.7	24	5.4
7	0	-1.4	-0.8	2.4	0	0	0.1	3.8	24	5.27
8	18	0.3	-1.1	-0.9	0.3	0.4	-0.4	2	24	11.1
9	0	-15.2	2.9	-5	-1.2	0.9	-0.1	18.3	24	0.31
10	0	-7.9	-0.8	-1.5	-2.3	0.5	-0.9	8.9	24	1.7
11	0	-15.9	2.9	-4.4	-0.1	1	0	18.9	24	0.26
12	0	-14.6	-3.7	-3.9	-1.8	0.8	-0.7	12.2	24	0.96
13	0	-18	-6.8	-5.9	-0.2	1.1	-0.9	13	19.2*	0.48
14	0	-0.4	-0.3	0.2	0	0	0	0.5	24	43.89
15	72	1.3	0	1.4	0	0	0	1.4	24	15.9
16	18	-0.9	0	-0.6	0	0	0	0.9	24	25.01

* Allowable stress includes a stress reduction factor for weld: 0.8 x allowable stress.

Note: All of the allowable stress values presented in this table are based on SA240, Type 304L stainless steel at a temperature of 380°F unless otherwise stated. Localized peak temperatures in the central portion of the canister shell reach 399°F—resulting in slightly lower allowable stress values and subsequently slightly lower margins of safety for sections 5 and 6 than those presented in the table. However, this difference is negligible as discussed in Section 2.6.12.1.

2.6.12.9 Stress Evaluation of PWR Canister for Combined Thermal and 1-Foot Corner-Drop Load Conditions

The thermal stress loads described in Section 2.6.12.3 are applied in conjunction with the primary loads in Section 2.6.12.8 to produce a combined thermal stress plus corner impact loading. The stress evaluation is performed according to the ASME Code, Section III, Subsection NB. On the basis of the results in Section 2.6.12.8, the most critical sections are identified in Table 2.6.12.9-1. The stresses reported in this table correspond to the nodal stress at the surface. The minimum margin of safety is +1.14 when 3 S_m is used as the stress criterion. Tables 2.6.12.9-2 through 2.6.12.9-5 tabulate the results for top and bottom corner-drop with thermal results for the conditions that result in the minimum margins of safety. The stress intensity criterion of 3.0 S_m is satisfied. The margins of safety are calculated as:

MS = (allowable stress/SI)-1.

Table 2.6.12.9-1 PWR Canister Critical Sections for the Combined 1-Foot Corner Drop and Thermal Load Condition

Condition	Stress	Critical Section	Table	Minimum Margin of Safety
Top Corner Drop + Thermal (cold)	$P_m + P_b + Q$	2	2.6.12.9-2	+ 1.14
Top Corner Drop + Thermal (hot)	$P_m + P_b + Q$	2	2.6.12.9-3	+ 1.24
Bottom Corner Drop + Pressure + Thermal (cold)	$P_m + P_b + Q$	9	2.6.12.9-4	+1.96
Bottom Corner Drop + Pressure + Thermal (hot)	$P_m + P_b + Q$	9	2.6.12.9-5	+1.37

Table 2.6.12.9-2 PWR Canister $P_m + P_b + Q$ Stresses - 1-Foot Top Corner-Drop, Thermal Cold

Section Location	Angle of Peak Stress Location	$P_m + P_b + Q$ Stresses (ksi)						SI (ksi)	Allowable Stress (ksi)	Margin of Safety
		Sx	Sy	Sz	Sxy	Syz	Sxz			
1	0	-19.5	-7.1	-4.4	-3.7	-0.2	-1	16.3	47.9	1.95
2	0	-19.9	2.3	-3.3	-0.6	1.2	-0.3	22.4	47.9	1.14
3	126	0.4	-10.3	0.3	0.7	0.1	-0.5	11.2	47.9	3.3
4	0	-1.4	-0.6	2.4	0	-0.1	0	3.7	47.9	11.79
5	0	-0.8	-2.9	1.7	0	-0.4	-0.2	4.8	47.9	9.08
6	0	-1.1	-1.9	2.1	0	0.2	-0.2	4.1	47.9	10.72
7	0	-1.3	-0.7	2.3	0	0	0	3.5	47.9	12.54
8	171	-0.2	-3.6	-0.4	0	0.2	0	3.5	47.9	12.78
9	0	-12.6	0.1	-3.8	-1.1	0.5	-0.2	12.9	47.9	2.71
10	0	-10	-4.8	-2.4	-2.5	0.1	-1	9	47.9	4.35
11	0	-11.8	-6.9	-3.9	-0.9	0.4	-0.6	8.2	47.9	4.85
12	0	-11.8	-4.2	-2.8	-1.9	0.4	-0.7	9.8	47.9	3.87
13	0	-11.8	-6.9	-3.9	-0.9	0.4	-0.6	8.2	38.32*	3.67
14	0	-15.3	-1.8	-14.4	0	-1	0	13.6	47.9	2.52
15	81	-0.1	-0.3	0.1	0	0	0	0.4	47.9	116.04
16	0	-0.1	-0.4	0.1	0	0	0	0.6	47.9	82.56

* Allowable stress includes a stress reduction factor for weld: 0.8 x allowable stress.

Note: All of the allowable stress values presented in this table are based on SA240, Type 304L stainless steel at a temperature of 380°F unless otherwise stated. Localized peak temperatures in the central portion of the canister shell reach 399°F—resulting in slightly lower allowable stress values and subsequently slightly lower margins of safety for sections 5 and 6 than those presented in the table. However, this difference is negligible as discussed in Section 2.6.12.1.

Table 2.6.12.9-3 PWR Canister $P_m + P_b + Q$ Stresses - 1-Foot Top Corner-Drop, Thermal Heat

Section Location	Angle of Peak Stress Location	$P_m + P_b + Q$ Stresses (ksi)						SI (ksi)	Allowable Stress (ksi)	Margin of Safety
		Sx	Sy	Sz	Sxy	Syz	Sxz			
1	0	-18.3	-6.7	-4.4	-3.4	-0.2	-0.9	14.9	47.9	2.22
2	0	-18.7	2.5	-3.1	-0.7	1	-0.3	21.4	47.9	1.24
3	126	0.4	-10.2	0.2	0.7	0.1	-0.4	11	47.9	3.35
4	0	-1.1	-0.5	2	0	-0.1	0.1	3.1	47.9	14.7
5	0	-0.5	-2.4	1.7	0	-0.3	0.1	4.2	47.9	10.38
6	0	-0.6	-1.5	2.1	0	0.2	0.3	3.7	47.9	12.08
7	180	0	-2.9	0	0	0	0	2.9	47.9	15.69
8	171	-0.1	-3.6	-0.4	0	0.2	0	3.5	47.9	12.78
9	0	-12.8	0.4	-3.8	-1.1	0.5	-0.2	13.5	47.9	2.56
10	0	-10.2	-4.8	-2.4	-2.6	0.1	-1	9.1	47.9	4.27
11	0	-12	-6.9	-4	-1	0.4	-0.6	8.4	47.9	4.73
12	0	-11.9	-4.1	-2.8	-2.1	0.4	-0.7	10	47.9	3.81
13	0	-12	-6.9	-4	-1	0.4	-0.6	8.4	38.32*	3.56
14	0	-14.5	-1.6	-13.6	0.1	-0.9	0	13	47.9	2.69
15	90	-0.1	-0.3	0.1	0	0	0	0.4	47.9	116.24
16	0	-0.1	-0.4	0.1	0	0	0	0.6	47.9	84.45

* Allowable stress includes a stress reduction factor for weld: 0.8 x allowable stress.

Note: All of the allowable stress values presented in this table are based on SA240, Type 304L stainless steel at a temperature of 380°F unless otherwise stated. Localized peak temperatures in the central portion of the canister shell reach 399°F—resulting in slightly lower allowable stress values and subsequently slightly lower margins of safety for sections 5 and 6 than those presented in the table. However, this difference is negligible as discussed in Section 2.6.12.1.

Table 2.6.12.9-4 PWR Canister $P_m + P_b + Q$ Stresses - 1-Foot Bottom Corner-Drop, Internal Pressure, Thermal Cold

Section Location	Angle of Peak Stress Location	$P_m + P_b + Q$ Stresses (ksi)						SI (ksi)	Allowable Stress (ksi)	Margin of Safety
		Sx	Sy	Sz	Sxy	Syz	Sxz			
1	0	-6.3	-0.9	-1.9	0.1	0	-0.8	5.6	47.9	7.53
2	27	-0.2	-5	-1.4	-0.2	-0.1	-0.8	5.2	47.9	8.15
3	27	-0.2	-5.1	-1.3	0	-0.3	-0.6	5.2	47.9	8.20
4	0	-1	-1.5	2.8	0	0	-0.2	4.3	47.9	10.03
5	0	-1	-1.1	2.8	0	0	0.2	3.9	47.9	11.33
6	0	-0.9	-0.8	2.8	0	0	0.2	3.8	47.9	11.75
7	0	-0.9	-0.6	2.8	-0.2	0	0.2	3.7	47.9	11.81
8	0	-0.6	0.2	1.2	-1.1	0.4	0.1	2	47.9	22.65
9	0	-14.3	2.2	-4.5	-1.1	0.9	-0.2	16.7	47.9	1.86
10	0	-9	-1.5	-1.7	-2.2	0.5	-1	9.2	47.9	4.23
11	0	-14.2	1.1	-4.5	-0.2	1.9	-0.1	15.4	47.9	2.11
12	0	-13.6	-2.9	-3.5	-1.8	9	-0.7	11.9	47.9	3.02
13	0	-17.3	-5.6	-5.5	-0.5	1	-0.8	12.9	38.32*	1.97
14	0	-0.3	-0.4	0.2	0	0	0	0.6	47.9	85.16
15	81	0.7	0	0.9	0	0	0	0.9	47.9	51.95
16	45	-0.6	-0.1	-0.4	0	0	0	0.6	47.9	82.75

* Allowable stress includes a stress reduction factor for weld: 0.8 x allowable stress.

Note: All of the allowable stress values presented in this table are based on SA240, Type 304L stainless steel at a temperature of 380°F unless otherwise stated. Localized peak temperatures in the central portion of the canister shell reach 399°F—resulting in slightly lower allowable stress values and subsequently slightly lower margins of safety for sections 5 and 6 than those presented in the table. However, this difference is negligible as discussed in Section 2.6.12.1.

Table 2.6.12.9-5 PWR Canister $P_m + P_b + Q$ Stresses - 1-Foot Bottom Corner-Drop, Internal Pressure, Thermal Heat

Section Location	Angle of Peak Stress Location	$P_m + P_b + Q$ Stresses (ksi)						SI (ksi)	Allowable Stress (ksi)	Margin of Safety
		Sx	Sy	Sz	Sxy	Syz	Sxz			
1	0	-2.1	0	1.3	0	0.1	-0.1	3.5	47.9	12.79
2	162	0.1	-5.1	0.3	0.1	0	-0.1	5.4	47.9	7.87
3	162	0.1	-4.9	0.4	0	-0.1	-0.1	5.3	47.9	8.12
4	180	0	-3.7	1.2	0	0	-0.1	4.9	47.9	8.76
5	180	0	-3.8	1.5	0	-0.2	0	5.3	47.9	8.06
6	0	-0.5	-1.6	3.5	0	0.1	0.2	5.1	47.9	8.34
7	0	-0.9	-0.6	3.2	0	-0.1	0.3	4.1	47.9	10.82
8	0	-0.6	0.8	2	-0.1	0.6	0.3	2.9	47.9	15.7
9	0	-17	2.9	-5.3	-1.3	1.2	-0.3	20.2	47.9	1.37
10	0	-11.5	-1.9	-2.4	-2.7	0.6	-1.2	11.6	47.9	3.13
11	0	-16.7	1.4	-5.5	-0.2	1.1	-0.2	18.4	47.9	1.61
12	0	-16	-3.2	-4	-2.2	1	-0.9	14.3	47.9	2.36
13	0	-20.5	-6.3	-6.5	-0.7	1.3	-1	15.6	38.3*	1.46
14	0	-10	-4.9	-9.7	0	0.1	0	5.1	47.9	8.33
15	90	0.8	0	1	0	0	0	1	47.9	47.69
16	27	-0.6	-0.1	-0.3	0	0	0	0.6	47.9	79.93

* Allowable stress includes a stress reduction factor for weld: 0.8 x allowable stress.

Note: All of the allowable stress values presented in this table are based on SA240, Type 304L stainless steel at a temperature of 380°F unless otherwise stated. Localized peak temperatures in the central portion of the canister shell reach 399°F—resulting in slightly lower allowable stress values and subsequently slightly lower margins of safety for sections 5 and 6 than those presented in the table. However, this difference is negligible as discussed in Section 2.6.12.1.

2.6.12.10 Shear Stresses for 1-Foot Drops

The primary mechanism for shear loading in the canister drop analyses occurs for the bottom end-drop in the canister structural and shield lid welds. The maximum stress intensity for either Sections 12 or 13 during the bottom end-drop is 1.8 ksi for the bottom end-drop with thermal heat (Table 2.6.12.5-5). The maximum shear is 1.8/2 = 0.9 ksi. The allowable shear is 0.6 S_m per the ASME Code, Section III, Subsection NB-3227.2 for pure shear loading. The maximum canister shell temperature is 399°F and the margin of safety for pure shear is

$$MS = 0.6 \times 15.8 / 0.9 - 1 = 9.53$$

2.6.12.11 Canister Bearing Stresses for 1-Foot Side Drop

The average bearing stress on the canister wall is computed for the side-drop using the smallest length of canister and the maximum mass for either the PWR or BWR canisters. This results in a conservatively bounding value of the average bearing stress. The maximum canister plus contents mass is for the BWR Class 5 with a weight of 75,896 lb. For contact of the canister wall with the inner shell over an 18° arc (conservative), the projected bearing width is 10.54 in. The length of the shortest canister is 175.25 in. (PWR Class 1). The average bearing stress is

$$\text{Bearing Stress} = 75{,}896 \text{ lb} \times 20g/(175.25 \text{ in.} \times 10.54 \text{ in.}) = 822 \text{ psi}$$

Based on a yield strength of 17.5 ksi at 400°F, the margin of safety is

$$MS = (17.5 / 0.822) - 1 = +\text{Large}$$

Next, the bearing stress evaluation is presented in the regions under the shield lid and structural lid welds for the normal conditions side-drop (see Sections 9, 10, and 11 in Figure 2.6.12.3-1). Three separate regions are considered for the bearing evaluation; (1) the area beneath the structural lid weld from 0° to 9°, (2) area between the structural lid weld and shield lid weld from 0° to 9°, and (3) area below shield lid weld between 0° and 9°.

In order to calculate the bearing stresses in these regions, forces from the gap elements between the canister shell and the cask inner shell in these regions are examined. The forces from the gap elements act normal to the surface of the shell (i.e., radially), but are conservatively summed for each of the three regions described above. The following enveloping force summations are obtained from the PWR and BWR analysis results for each of the regions. The governing load case is also noted.

Region 1:	-45,373 lb	PWR Side Drop with no Internal Pressure
Region 2:	-43,935 lb	PWR Side Drop With Internal Pressure
Region 3:	-78,640 lb	BWR Side Drop with Internal Pressure

Gaps at both 0° and 9° are closed. Gaps at angular locations greater than 9° remain open in the regions of interest. The projected width conservatively based on 9° contact is 5.27 for the three regions. Region 1 has a length equal to the weld thickness (0.88 in.), Region 2 has a length of (3 - 0.88) 2.12 in., and Region 3 has a length of 0.5 in. equal to length of the shield lid weld. The corresponding bearing stresses for each region are

Region 1: 45,373/(5.27 x 0.88) = 9,784 psi

Region 2: 43,935/(5.27 x 2.12) = 3,932 psi

Region 3: 78,640/(5.27 x 0.5) = 29,844 psi

The peak temperature in the canister shell in the region of the lids is 266°F for the PWR canister (see Section 3.4). The yield strength is 19,950 psi based on this temperature for 304L stainless steel. The margins of safety for each region are presented below.

Region 1: 19,950 / 9,784 - 1 = 1.04

Region 2: 19.950 / 3.918 - 1 = 4.09

Region 3 is allowed 1.5 S_y since the width of application of the load is less than the distance to the free edge (0.5 < 3.0) and

Region 3: 1.5 x 19.950 / 29.844 - 1 = 0.0026

2.6.12.12 Canister Buckling Evaluation for 1-Foot End Drop

Code Case N-284-1 [12] of the ASME Boiler and Pressure Vessel Code is used to analyze the PWR canister for the normal condition 1-foot end drop (both top and bottom end drops). The evaluation requirements of Regulatory Guide 7.6, Paragraph C.5, are shown to be satisfied by the results of the buckling interaction equation calculations of Code Case N-284-1. The canister buckling design criteria are described in Section 2.1.2.5.3.

The data considered for the buckling evaluation includes shell geometry parameters, shell fabrication tolerances, shell material properties, theoretical elastic buckling stress values for the shell, and membrane stress components in the shell. The internal stress field that controls the buckling of a cylindrical shell consists of the longitudinal (axial) membrane, circumferential (hoop) membrane, and in-plane shear stresses. These stresses may exist singly or in combination, depending on the applied loading. Only these three stress components are considered in the buckling analysis.

A 20 g deceleration load was used for all the 1-ft drop canister analyses that are presented in Sections 2.6.12.4 through 2.6.12.9. The 20 g-load bounds all 1-ft deceleration loads for all other drop angles. The top- and bottom-end drops result in the largest potential for canister shell buckling and, therefore, are the two load cases presented here. The side drop load case is not considered a credible buckling mode of the canister shell and is, therefore, not presented here.

The stress results from the canister analysis are screened for the maximum values of the longitudinal compression, circumferential compression, or in-plane shear stresses for the 1-ft drop cases (top- and bottom-end drops) with and without pressure. For each loading case, the largest of each of the three stress components anywhere regardless of location within the PWR canister shell are combined. To these maximum stress components are added the maximum

stresses from the hot and cold thermal cases (Tables 2.6.12.3-1 and 2.6.12.3-2). Combining the maximum stress components in this way produces a conservative, bounding-case buckling evaluation of the PWR canister, one which envelopes all 1-ft PWR canister drop cases including those presented in Tables 2.6.12.4-4 and 2.6.12.4-6.

Consistent with the Code Case, the following are used:

- The symbols ϕ, θ, or $\phi\theta$ correspond to the longitudinal (axial) direction or stress component, circumferential (hoop) direction or stress component, and in-plane shear stress component, respectively.
- The formulas in the Code Case for cylindrical shells (unstiffened) are used.
- The factor of safety is 2.0 for Normal Conditions.

The analytical process used for the PWR canister is the same as that described in a step-by-step example presented in Section 2.7.12.3 (for the cask inner shell).

The geometry parameters used in the PWR canister evaluation are presented in Table 2.6.12.12-1.

The maximum stress components used in the evaluation and the buckling interaction ratios for the top- and bottom-end drop cases are provided in Table 2.6.12.12-2. The results of the buckling analysis show that all interaction equation ratios are less than 1.0. Therefore, the buckling criteria of Code Case N-284-1 are satisfied, thus demonstrating that buckling of the PWR canister does not occur.

Table 2.6.12.12-1 Geometry Parameters for the PWR Canister

Parameter	Value
t = thickness (in)	0.625
ID = inside diameter (in)	65.81
R = radius (in) = (ID+t)/2	33.22
R/t	53.15
$(Rt)^{0.5}$	4.56
Overall Length (in)	191.95
Bottom Thickness (in)	1.75
Structural Lid Thickness (in)	3.0
L_o = Length used in evaluation (in)*	187.2
$L_\theta = 2\pi R$ = circumference (in)	208.7
ν = Poisson's Ratio	0.275

L_o = Overall canister length - Bottom thickness - Structural lid thickness.

Table 2.6.12.12-2 Buckling Evaluation Results for the PWR Canister for 1-Foot End Drop

Load Condition	Longitudinal (Axial) Stress* S_ϕ (psi)	Circumferential (Hoop) Stress* S_θ (psi)	In-plane Shear Stress $S_{\phi\theta}$ (psi)	Elastic Buckling Interaction Equations				Plastic Buckling Interaction Equations			
				Q1	Q2	Q3	Q4	Q5	Q6	Q7	Q8
1-Ft Top End Drop	2400	300	400	.009	.077	.066	.009	.077	.065	.077	.066
1-Ft Bottom End Drop	3600	600	300	.063	.115	.131	.064	.115	.131	.115	.131

Component stresses include thermal stresses.

* Compressive stresses

2.6.13 PWR Basket Analysis - Normal Conditions of Transport

The Universal Transport Cask PWR basket is a right-cylinder structure fabricated with 24 square fuel tubes, a number of circular support disks, a number of heat transfer disks, eight tie rods with spacers, and two end weldment plates. The number of support disks and heat transfer disks varies depending upon the class of PWR fuel the basket is designed to contain. The basket components and their geometry are illustrated in Figure 2.6.13-1 and Figure 2.6.13-2. Figure 2.6.13-3 shows the details of the fuel tube with the encasing BORAL. The fuel tubes are open at each end; therefore, longitudinal fuel assembly loads are imparted to the canister shield lid or the bottom plate, and not the fuel basket structure. The fuel basket contains the fuel and is laterally supported by the canister shell.

The fuel assemblies together with the tubes are laterally supported in the holes in the stainless steel support disks. The aluminum heat transfer disks are located throughout the cavity to fully optimize the passive heat rejection from the package. They serve no structural function other than supporting their own weight. The dimensional differences between the heat transfer disk and the support disk accommodate the different rate of thermal growth between aluminum and stainless steel, thereby preventing interference between the tube, support disk, and heat transfer disks.

The primary function of the spacers and the threaded top nut is to locate and structurally assemble the support disks, heat transfer disks, and top and bottom weldment plates into an integral assembly. The spacers carry the inertial weight of the support disks, heat transfer disks, one end plate, and their own inertial weight for a normal transport condition 1-ft end-drop. The end-drop loading of the split spacers and tie rods represents a classical, closed-form structural analysis. The support disk requires a detailed finite element analysis for side-drop, end-drop, and oblique drops. The stainless steel fuel tubes are not considered to be a structural component with respect to the disks other than consideration of their mass contribution to loading.

The PWR fuel basket is evaluated for the normal transport loads in this section. End-drop, side-drop, oblique drop orientations are evaluated. The basket is evaluated for the hypothetical accident condition in Section 2.7.8.

Figure 2.6.13-1 PWR Fuel Assembly Basket

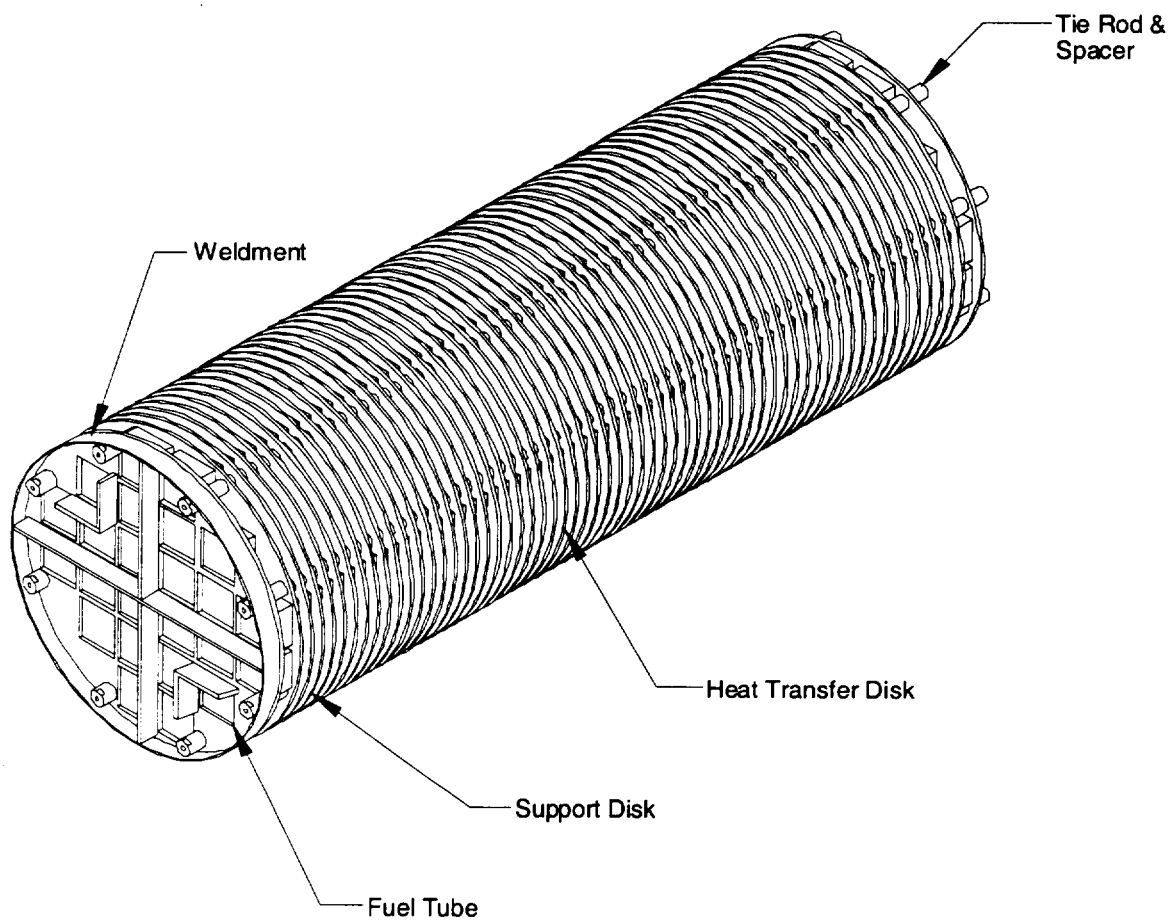

Figure 2.6.13-2 Support Disk Cross Section Configuration

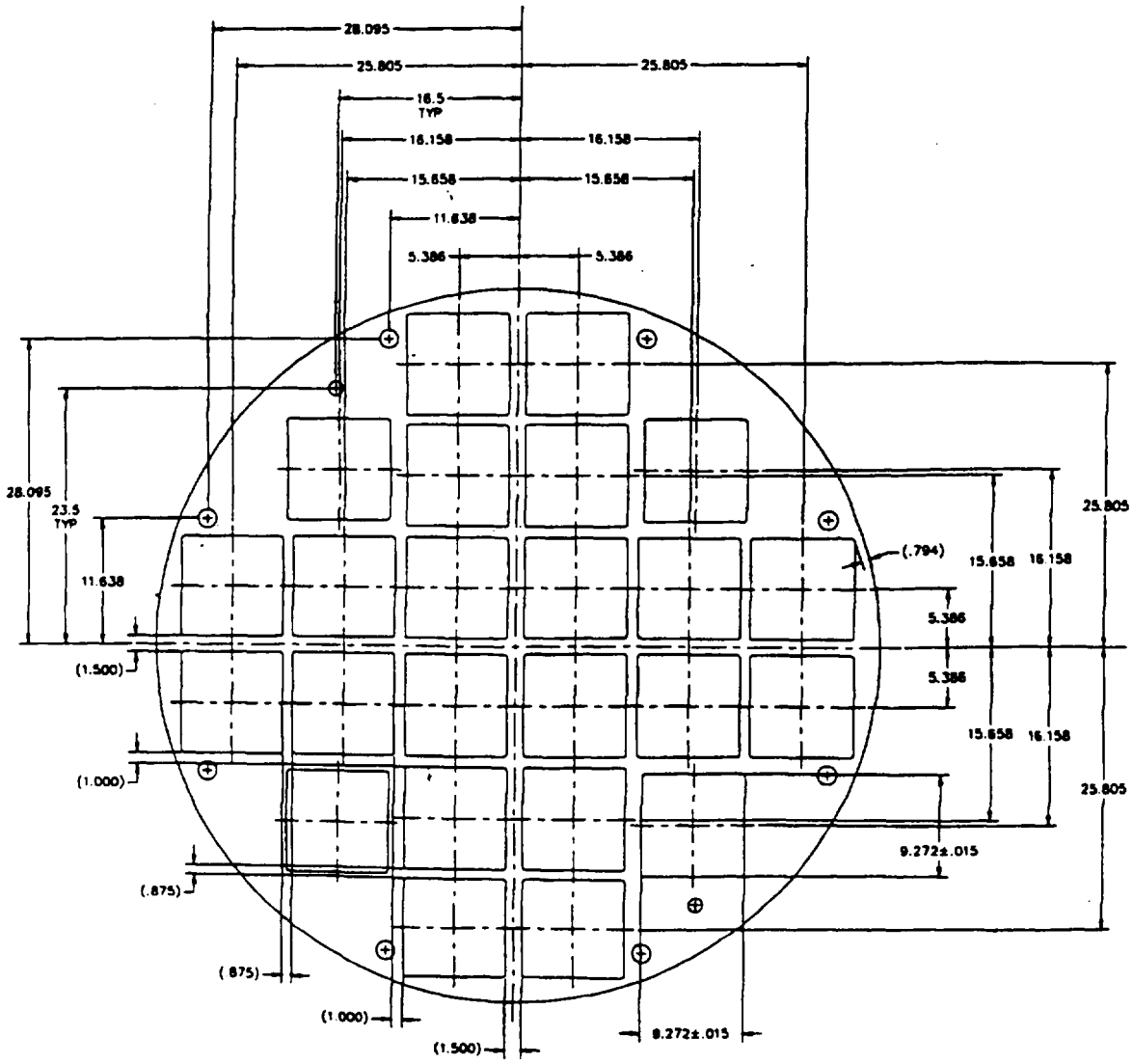

Note:

Engineering drawings provide appropriate tolerances for dimensions shown.

Figure 2.6.13-3 PWR Fuel Tube Configuration

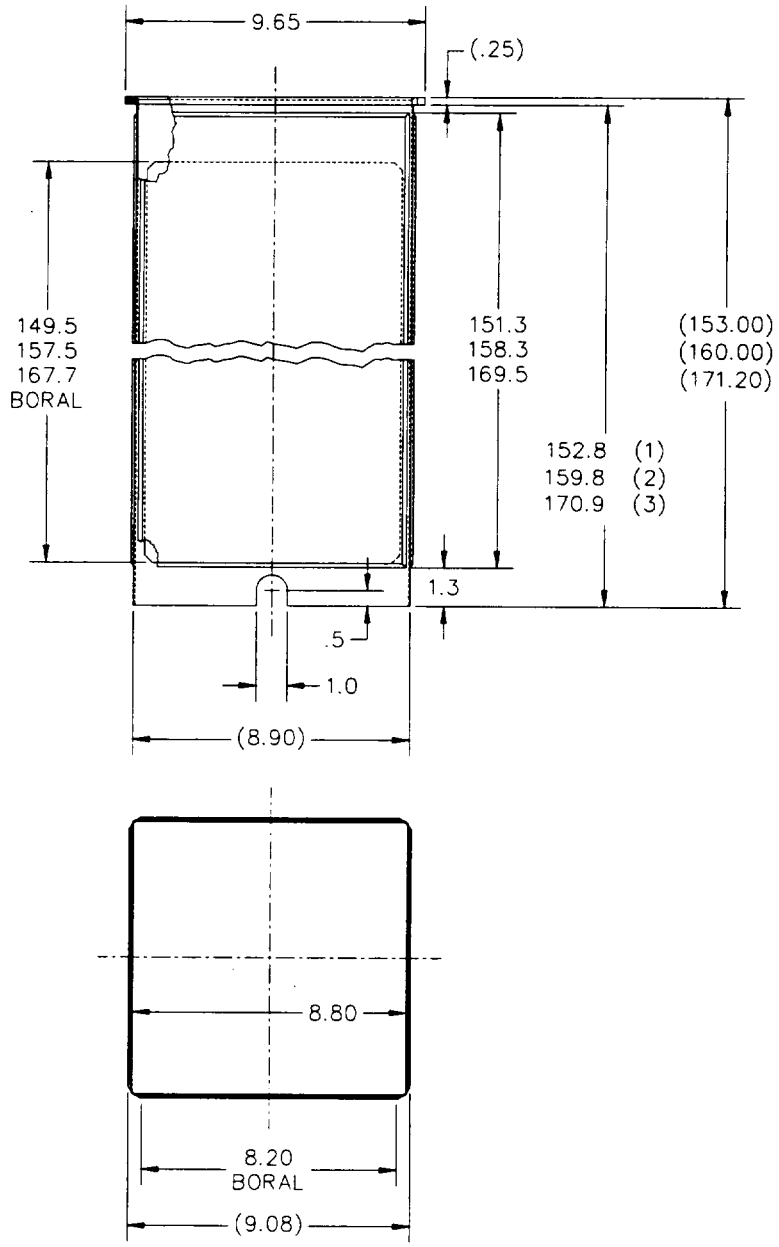

2.6.13.1 Analysis Description

On the basis of criticality control requirements, the PWR fuel basket design criteria require the maintenance of fuel support and control of spacing of the fuel assemblies for all load conditions. The structural design criteria for the structural components in the fuel basket is the ASME Code, Section III, Division 1, Subsection NG [15]. Consistent with this criterion, for any normal condition load and position orientation, the main structural component in the fuel basket, the stainless steel support disk, is shown to have a maximum primary membrane stress intensity and a primary membrane plus bending stress intensity in any disk. These are less than the design stress intensity value S_m and $1.5S_m$, respectively. The value of S_m is defined at the temperatures for the component being analyzed.

In the side-drop, the loads of the fuel assemblies are transferred into the plane of the support disks, from which they are transmitted to the canister shell. For the end-drop, the fuel basket components are loaded by their own inertial weight and do not experience load from the guided but freestanding fuel assemblies. Various cask drop angles and radial impact orientations of the support disk are evaluated. In addition to the load from inertial weight, the differential thermal expansion of the support disk is also evaluated.

2.6.13.2 Finite Element Model Description - PWR Basket

Two finite element models are generated to analyze the PWR fuel basket for the normal operating conditions: one for the end-drop, in which the loads are perpendicular to the plane of the disk, and one for the side-drop, in which the loads act in the plane of the disk. Both models accommodate thermal expansion effects by using the temperature distribution from the thermal analysis and the coefficient of thermal expansion. Off-angle (ϕ) drop results are calculated based on the component stresses from the end and side drop evaluation.

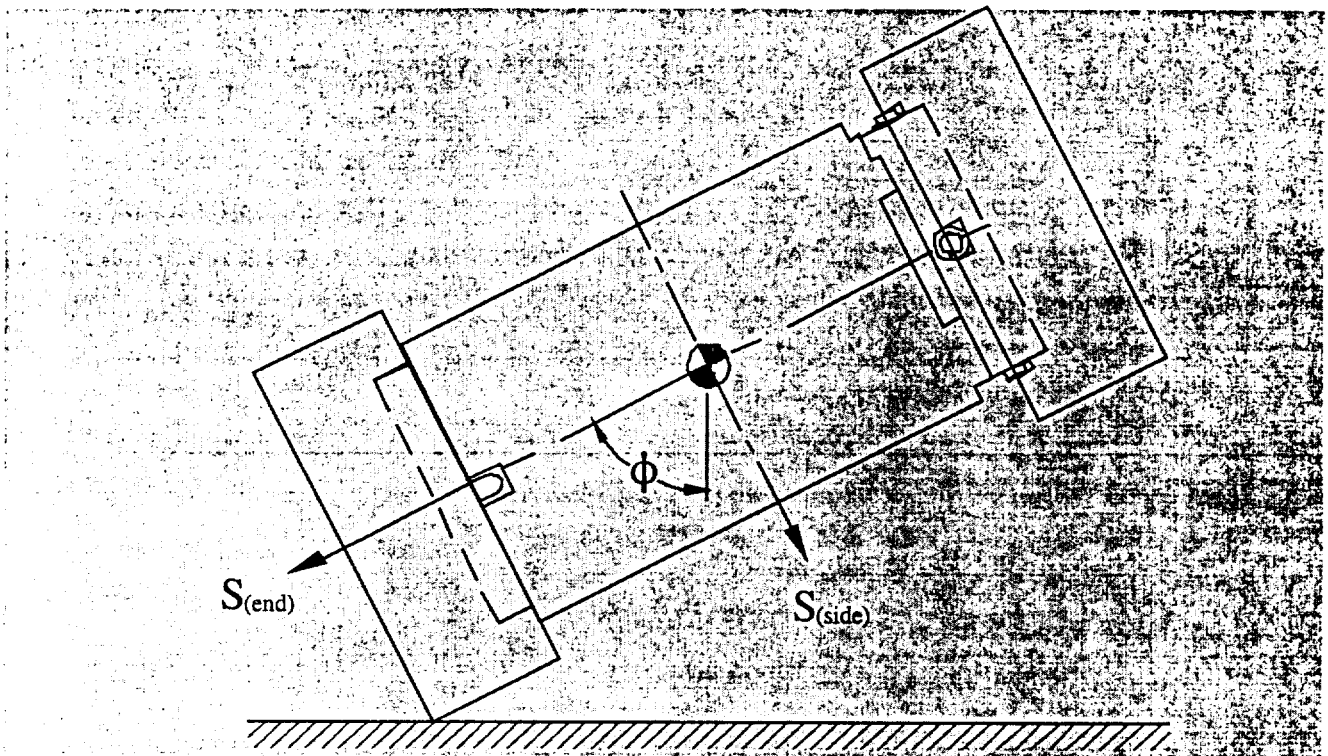

Oblique Drop

The finite element model for the side-drop is a two-dimensional model that includes the cross section of the canister shell. A complete basket support disk is modeled for the side impact evaluation (see Figure 2.6.13.2-1). ANSYS PLANE42 elements are used to model the support disk and canister. The PLANE42 is a two-dimensional element with four nodes. The PLANE42 elements correspond to plane stress and the thickness of the model for the disk is input as 0.5 in., which corresponds to the thickness of the support disk. For the canister shell, a thickness of 4 inches is used to approximate the center to center distance of support disks. For the end-drop, the PLANE42 elements are replaced with the SHELL63 elements and elements for canister shell are deleted. The nodal-element relationship is the same, with the exception of the change in the stiffness-displacement degree of freedoms. The shell elements accommodate the out-of-plane bending, which is present in the end-drop condition. The only loading in the out-of-plane direction is the inertial weight of the support disk.